



Engineering and
Physical Sciences
Research Council



University of
Salford
MANCHESTER

Considerations for optimising the design of rigid ankle-foot orthoses for children with cerebral palsy.

PhD Thesis Submission

Sean Donald

00604113

University of Salford

School of Health and Society

Supervisors: Professor Richard Jones, Julie Reay

Advisor: Professor Roozbeh Naemi

Contents

Publications and Presentations	5
Abbreviations	6
Abstracts	9
Introduction	11
1 Background	13
1.1 Cerebral Palsy (CP)	15
1.1.1 Overview	15
1.1.2 Primary impairments of the structure and function of the neurological systems	16
1.1.3 Secondary impairments of the structure and function of the musculoskeletal system	17
1.1.4 Tertiary impairments of gait	18
1.2 The management of gait impairments associated with CP using Ankle-Foot Orthoses (AFOs)	22
1.3 The biomechanical principles of AFO intervention	25
1.3.1 Direct biomechanical control	25
1.3.2 Indirect biomechanical control via shank alignment	26
1.3.3 The factors that influence rigid AFO stiffness	29
1.4 The Optimal segment kinematics and alignment approach to rehabilitation (OSKAR)	31
1.4.1 Overview	31

1.4.2	Determining the design of the ankle-foot orthosis-footwear combination (AFOFC) through classification of gait impairments . . .	33
1.4.3	Determining the ankle angle of the AFO	34
1.4.4	Tuning shank alignment	36
1.4.5	Normalisation of lever arm lengths	37
1.4.6	Challenges with implementing OSKAR in clinical practice.	38
2	Review of literature surrounding the clinical performance and mechanical properties of rigid AFOs.	40
2.1	The effects of rigid AFOs and AFOFC tuning on gait in paediatric neurological populations	42
2.1.1	Introduction	42
2.1.2	Identification of research questions	43
2.1.3	Identification of relevant studies	43
2.1.4	Study Selection	44
2.1.5	Charting Data	45
2.1.6	Summary of results	45
2.1.7	Discussion	57
2.1.8	Conclusions	60
2.2	The effects of rigid AFO design factors on the mechanical properties of the devices	61
2.2.1	Introduction	61
2.2.2	Identification of research questions	62
2.2.3	Search Strategy	62
2.2.4	Results	64
2.2.5	Discussion	68
2.2.6	Conclusion	70
2.3	Methods of quantifying AFO mechanical properties	71
2.3.1	Introduction	71
2.3.2	Functional Analysis	71
2.3.3	Bench Testing	72
2.3.4	Finite Element (FE) Analysis	76
2.3.5	Summary of findings	80

3	Understanding the stakeholder requirements related to rigid AFO design	82
3.1	Barriers and facilitators to the adherence of rigid AFOs in CP populations from the perspective of the user, parent/carer and clinician.	84
3.1.1	Introduction	84
3.1.2	Aims	84
3.1.3	Search Strategy	85
3.1.4	Results	86
3.1.5	Discussion	89
3.1.6	Conclusions	91
3.2	Gaining an insight into rigid AFO prescription: Semi-structured discussions with the clinical advisory group	92
3.2.1	Rationale for forming clinical advisory group	92
3.2.2	The demographics and role of the clinical advisory group	93
3.2.3	Structure of the PPIE Session	93
3.2.4	Summary of discussions with clinical advisory group	94
3.2.5	Interpretation of these discussions	96
3.3	Impact of the clinical advisory group discussion on future studies	97
4	Aims and objectives of the thesis	98
4.1	Aims and Objectives	99
4.2	Rational for the aims and objectives	99
4.3	Plan to deliver the aims of the thesis	103
5	Development of a FE model to measure AFO stiffness	105
5.1	AFO Manufacturing and Modelling Process	107
5.2	The repeatability of a test rig to measure the stiffness of rigid AFOs	111
5.2.1	Specifications for the test rig	111
5.2.2	Test rig design	112
5.2.3	Experimental procedure	115
5.2.4	Data Analysis	117
5.2.5	Results	120
5.2.6	Discussion	123
5.2.7	Conclusions	126

5.3	The validation of a FE model for measuring AFO stiffness	127
5.3.1	FE model Design	127
5.3.2	Experimental procedure	128
5.3.3	Data Analysis	130
5.3.4	Results	132
5.3.5	Discussion	138
5.3.6	Conclusions	141
6	The stiffness of clinically utilised rigid AFOs used for the management of gait impairments in children with CP.	142
6.1	Introduction	144
6.2	Aims	145
6.3	Methodology	145
6.3.1	Experimental procedure	145
6.3.2	Data Analysis	148
6.4	Results	150
6.5	Discussion	160
6.6	Conclusions	163
7	Development of a novel reinforcement to optimise the design of paediatric rigid AFOs	165
7.1	Introduction	167
7.2	Aims	168
7.3	Specifications for the design of an 'optimal' rigid AFO reinforcement . .	168
7.4	Development of a novel reinforcement for the 5-year-old-sized AFO . . .	171
7.4.1	The design process	171
7.4.2	Data Analysis	173
7.4.3	Stage 1: Rear Reinforcement	175
7.4.4	Stage 2: Distal to the malleoli reinforcements	179
7.4.5	Stage 3: Proximal to the malleoli reinforcements	182
7.4.6	Stage 4: X-Bar Optimisation	184
7.5	Scaling the reinforcement to the older paediatric ages.	190
7.5.1	Methodology	190

7.5.2	Scaled X-Bar Design	191
7.5.3	Stage 1: Determining the appropriate AFO and X-Bar thickness .	193
7.5.4	Stage 2: Optimising the Design of the X-Bar	196
7.6	Chapter Discussion	202
7.7	Conclusions	205
8	Thesis Discussion	206
8.1	Summary of main findings	208
8.2	Thesis Limitations	209
8.3	Future Work	211
8.4	Concluding Remarks	213
8.5	Clinical Implications	214
A	PPIE semi-structured interview questions	A
B	Test Rig ISPO World Congress 2023 Poster Presentation	C
C	AFO Transformation Matrices	E
D	The validity of measuring AFO thickness from 3D scans	G
D.1	Introduction	H
D.2	Methodology	I
D.2.1	Experimental Procedure	I
D.2.2	Data Analysis	J
D.3	Results	J
D.4	Discussion	J
D.5	Conclusion	K
E	Test rig Visual 3D marker model	L
F	Polypropylene Material Testing	N
F.1	Introduction	O
F.2	Methodology	O
F.2.1	Experimental Procedure	O
F.2.2	Data Analysis	P

F.2.3	Results	Q
G	Variation in manufactured AFO Thickness	R
G.1	5-year-old, 3mm, PPC AFO	R
G.2	5-year-old, 3mm, PPH AFO	S
G.3	10-year-old, 4.5mm, PPC AFO	S
G.4	10-year-old, 5mm, PPH AFO	T
G.5	15-year-old, 4.5mm, PPC AFO	T
G.6	5-year-old, 3mm, PPC AFO	U
H	Comparison of 15-year-old PPC 4.5mm thickness measured across repeat scans	V
I	The effects of ribbing placement on the mechanical properties of rigid AFOs	X
J	Calculation of AFO thinning during the vacuum-forming process	Z

List of Figures

1.1	The ICF model for characterising disability. Image reproduced from WHO, 2002[26]	15
1.2	The classification of atypical tone associated with cerebral palsy according to the surveillance for cerebral palsy in Europe[31].	17
1.3	The management paradigm for treating gait impairments in children with CP. (CP = Cerebral Palsy and SDR = Selective Dorsal Rhizotomy.)	22
1.4	Classification of bespoke thermoplastic AFOs designs. Reproduced from Eddison et al.[81]	25
1.5	Three-point force systems required to control ankle motion in all three planes. A) Sagittal control, red = plantar flexion, blue = dorsiflexion. B) Coronal control, red = pronation, blue = supination. C) Transverse control, red = external rotation, blue = internal rotation	26
1.6	Diagram showing the net sagittal moment acting on the knee in stance and the relationship between the external moment and ground reaction force (GRF) alignment. The spring represents the knee flexor muscles.	27
1.7	Typical GRF alignment with the joints of the lower limb throughout stance. Dashed line = The GRF. PF = Plantar Flexion. DF = Dorsiflexion.	28
1.8	Representation of how a rigid AFO can normalise ground reaction force alignment. Dashed line = The GRF. DF = Dorsiflexion.	28
1.9	The optimal segment kinematics and alignment approach to rehabilitation (OSKAR) algorithm for the biomechanical optimisation of rigid ankle-foot orthoses for children with cerebral palsy. Image reproduced from Owen, 2014[16].	32
1.10	Owen's system for classifying the gait of children with spastic cerebral palsy, based on shank kinematics. Image reproduced from Owen, 2014[16]	34

1.11	Owen’s clinical algorithm for determining the ankle angle of the AFO[106]	36
2.1	Flowchart for the link between the three literature reviews.	41
2.2	PRISMA flowchart of the screening process for the scoping review	45
2.3	PRISMA flowchart of the screening process for the scoping review	63
2.4	Examples of existing test rigs. Bregman et al.[92], and Ielapi et al.[248] (Left to right)	75
2.5	Types of FE models. A) 2-dimensional, shell model. B) 3-dimensional, solid model.	77
2.6	Examples of mesh elements used in FE analysis. Black dots = nodes. . .	78
3.1	Flowchart for the rationale of the stakeholder analysis.	83
3.2	PRISMA flowchart of the screening process for the scoping review	86
4.1	Plan to achieve the aims of the thesis. Green = Chapter 4. Turquoise = Chapter 5. Purple = Chapter 6. Red = Chapter 7	104
5.1	Process of developing and validating a FE model for quantifying AFO mechanical properties.	106
5.2	Flow chart of the AFO manufacturing and modelling process.	107
5.3	Process of modelling the adult AFO. A) Adult rectified positive mould. B) STL of the positive mould. C) Trim line definition. D) Adult AFO STL108	
5.4	AFO manufacturing and modelling process. A) Adult AFO. B) Scaled AFO STLs. C) AFO mould. D) 10-year-old AFO. E) 10-year-old AFO STL.	110
5.5	Evolution of the test rig design.	113
5.6	Final Test Rig Design	114
5.7	Marker array used to model the test rig. Green = AFO. Yellow = Test Rig. Blue = Steel Cable.	116
5.8	Structure of the rig repeatability study	120
5.9	Comparison of deflection measured using 3D MOCAP and a digital incli- nometer. Columns represent the mean of 3 repeats. Error bars represent \pm stdev. The star represents significance at $p < 0.05$	121

5.10	Comparison of force measured using force plates and the strain gauge. Columns represent the mean of 3 repeats. Error bars represent \pm stdev. The star represents significance at $p < 0.05$	122
5.11	Moment versus deflection curves and corresponding stiffness from both sessions. Columns represent the mean of 3 repeats. Error bars represent \pm stdev. The star represents significance at $p < 0.05$	123
5.12	Diagram of the Finite Element Model. F_x = Force in the x-direction, M_y = Moment about the Y-axis. d = Displacement along the axis symbolised by the dotted line.	128
5.13	Structure of the FE validation study	132
5.14	Mesh Convergence Analysis for the 5, 10 and 15-year-old FE models. . .	134
5.15	Effect of Poisson's ratio on computational stiffness	135
5.16	Computational versus Experimental Deflection-Curves	136
5.17	Computational versus Experimental AFO Stiffness	137
5.18	Experimental and computational behaviour of the 15-year-old, PPC, 4.5mm AFO.	139
6.1	Through the malleoli trim line definition	147
6.2	Clinical AFO designs for the 5-year-old AFO.	148
6.3	Computational bending behaviour of the clinically utilised AFO designs for the three age groups.	154
6.4	Computational mechanical properties of the clinically utilised AFO designs for the three age groups. Dashed line = Clinically significant deflection.	155
6.5	Von Mises stress distribution in the 5-year-old-sized 4mm PPH AFO with anterior trim lines. Von Mises stress measured in MPa.	156
6.6	Von Mises stress distribution in the 10-year-old-sized 4mm PPH AFO with anterior trim lines. Von Mises stress measured in MPa.	157
6.7	Von Mises stress distribution in the 15-year-old-sized 4mm PPH AFO with anterior trim lines. Von Mises stress measured in MPa.	157
6.8	Coronal deformation in the 5-, 10- and 15-year-old-sized, 4mm PPH AFO with anterior trim lines. Deformation measured in mm.	158

6.9	Change in Von Mises stress distribution with polypropylene type and thickness for the 5-year-old-sized AFO with anterior trim lines. Von Mises stress measured in MPa. The range of the colour bar has been manually adjusted.	158
6.10	Change in coronal deformation with polypropylene type and thickness for the 5-year-old-sized AFO with anterior trim lines. Deformation measured in mm. The range of the colour bar has been manually adjusted.	159
6.11	Change in Von Mises stress distribution with AFO design for the 5-year-old-sized 4mm PPH AFO. Von Mises stress measured in MPa. The range of the colour bar has been manually adjusted.	160
6.12	Change in coronal deformation with AFO design for the 5-year-old-sized 4mm PPH AFO. Deformation measured in mm. The range of the colour bar has been manually adjusted.	160
7.1	Decision matrix used during the development of the reinforcement	172
7.2	Rear Reinforcement Design	175
7.3	Effect of rear reinforcement width on AFO mechanical properties. Error bars denote the mechanical properties when the AFO thickness is reduced by 20%.	177
7.4	Effect of rear reinforcement height on AFO mechanical properties. Dark blue bars = mechanical properties at 100% thickness. Light blue bars = mechanical properties at 80% thickness.	178
7.5	Distal Reinforcement Design	180
7.6	Comparison of distal to the malleoli reinforcements. Dark blue bars = mechanical properties at 100% thickness. Light blue bars = mechanical properties at 80% thickness.	181
7.7	Proximal Reinforcement Design	183
7.8	Comparison of proximal to the malleoli reinforcements. Dark blue bars = mechanical properties at 100% thickness. Light blue bars = mechanical properties at 80% thickness.	184
7.9	X-Bar Reinforcement Design	185
7.10	Comparison of X-Bar Width. Dark blue bars = mechanical properties at 100% thickness. Light blue bars = mechanical properties at 80% thickness.	186

7.11	Comparison of each reinforcement design iteration. Dark blue bars = mechanical properties at 100% thickness. Light blue bars = mechanical properties at 80% thickness.	187
7.12	Comparison of the Von Mises stress distribution and coronal deformation for the reinforcement design iterations. The range of the colour bars has been manually adjusted.	188
7.13	10-year-old-sized AFO X-Bar Reinforcement Design	192
7.14	15-year-old-sized AFO X-Bar Reinforcement Design	193
7.15	Determining optimal AFO and X-Bar thickness for the 10-year-old-sized AFO. Dark blue bars = mechanical properties at 100% thickness. Light blue bars = mechanical properties at 80% thickness.	194
7.16	Determining optimal AFO and X-Bar thickness for the 15-year-old-sized AFO. Dark blue bars = mechanical properties at 100% thickness. Light blue bars = mechanical properties at 80% thickness.	195
7.17	Comparison of X-Bar arm width for the 10-year-old-sized AFO. Dark blue bars = mechanical properties at 100% thickness. Light blue bars = mechanical properties at 80% thickness.	197
7.18	Effect of the optimised X-Bar reinforcement on the Von Mises stress distribution in a 10-year-old-sized 4mm PPH AFO with anterior trim lines. Von Mises stress was measured in MPa. The range of the colour bar has been manually adjusted.	198
7.19	Effect of the optimised X-Bar reinforcement on the coronal plane deformation in a 10-year-old-sized 4mm PPH AFO with anterior trim lines. Deformation was measured in mm. The range of the colour bar has been manually adjusted.	198
7.20	Comparison of X-Bar arm widths for the 15-year-old-sized AFO. Dark blue bars = mechanical properties at 100% thickness. Light blue bars = mechanical properties at 80% thickness.	199
7.21	Effect of the optimised X-Bar reinforcement on the Von Mises stress distribution in a 15-year-old-sized 4mm PPH AFO with anterior trim lines. Von Mises stress was measured in MPa. The range of the colour bar has been manually adjusted.	200

7.22	Effect of the optimised X-Bar reinforcement on the coronal plane deformation in a 15-year-old-sized 4mm PPH AFO with anterior trim lines. Deformation was measured in mm. The range of the colour bar has been manually adjusted.	200
7.23	Comparisons of Von Mises stress distribution in the medial side of the non-reinforced, baseline AFOs for the three age groups. The range of the colour bar has been manually adjusted.	201
D.1	Change in AFO thickness and percentage measurement error with STL element size.	J
E.1	Marker array used to model the test rig. Green = AFO. Yellow = Test Rig. Blue = Steel Cable.	M
F.1	Dog Bone specimens used to determine the tensile properties of polypropylene	O
F.2	Tensile tester set-up	P
F.3	Stress-Strain curves for copolymer and homopolymer polypropylene . . .	Q
G.1	Variation in thickness of the 5-year-old, 3mm, PPC AFO manufactured for the rig repeatability and FE validity studies.	R
G.2	Variation in thickness of the 5-year-old, 3mm, PPH AFO manufactured for the rig repeatability and FE validity studies.	S
G.3	Variation in thickness of the 10-year-old, 4.5mm, PPC AFO manufactured for the rig repeatability and FE validity studies.	S
G.4	Variation in thickness of the 10-year-old, 5mm, PPh AFO manufactured for the rig repeatability and FE validity studies.	T
G.5	Variation in thickness of the 15-year-old, 4.5mm, PPC AFO manufactured for the rig repeatability and FE validity studies.	T
G.6	Variation in thickness of the 15-year-old, 5mm, PPH AFO manufactured for the rig repeatability and FE validity studies.	U
H.1	Scan 1: Variation in thickness of the 15-year-old, 4.5mm, PPC AFO . . .	V
H.2	Scan 2: Variation in thickness of the 15-year-old, 4.5mm, PPC AFO . . .	W

I.1 Comparison of 4mm PPH AFO mechanical properties between ribbing placement. Y

Acknowledgements

Firstly, I would like to acknowledge The UK Engineering and Physical Sciences Research Council (EPSRC) for funding this project through the Centre for Doctoral Training in Prosthetics and Orthotics (grant EP/S02249X/1) and the University of Salford for providing me with the equipment and facilities to conduct this research.

Then an immense thank you goes to Professor Richard Jones and Julie Reay. I owe a huge amount to the support and knowledge they have provided throughout the process. In particular, Julie has given valuable perspectives on the clinical aspects of the project, whilst Rich's experience as a PhD supervisor has been vital in shaping the thesis.

Next, I would like to recognise the contribution of Prof. Roozbeh Naemi, whose expertise played an influential role in the design of the test rig and validation of the finite element models. Furthermore, I extend my gratitude to Dr Anmin Liu, who was also consulted during this process, and the staff of the Maker's space, particularly George Dodgson and Aidan Dunbar, who assisted in the production of the rig and CAD modelling.

Meanwhile, James May, Bernie Noakes and Dan Fallon played critical roles in training and assisting me during ankle-foot orthoses manufacturing. Additionally, their generosity with their time and insights into the clinical and technical aspects of ankle-foot orthosis provision were crucial to the delivery of this thesis.

Furthermore, I am grateful to the staff involved with the Centre for Doctoral Training in Prosthetics and Orthotics, who allowed me the opportunity to complete this PhD and have assisted me in various ways. Moreover, the importance of the support provided

by my fellow PhD students at the University of Salford throughout this journey cannot be understated.

Finally, I would like to thank my friends and family who have supported me over the last four years. In particular, Emma has lived this experience through me and provided unwavering support throughout.

Publications and Presentations

Publications

On submission, none of the work in this thesis has been published. However, below is a list of planned publications

- The repeatability of a test rig to measure the stiffness of paediatric rigid AFOs using MOCAP
- The stiffness of clinically utilised rigid AFOs used to manage gait impairments in children with CP. A computational analysis.
- A novel, prototype reinforcement to optimise the design of paediatric rigid AFOs. a computational analysis.

Presentations

Elements of this work were presented at three conferences.

- 'Repeatability of a bespoke test rig for measuring the stiffness and mediolateral widening at the ankle of ankle-foot orthoses.', Poster Presentation, ISPO World Congres 2023
- 'The influence of material and design properties on the stiffness of rigid ankle-foot orthoses - Preliminary results.', Oral Presentation, The second P&O CDT Conference 2024
- 'Validation of a finite element model for measuring the stiffness of ankle-foot orthoses.', Poster presentation, The second P&O CDT Conference 2024

- 'Towards an optimised design for rigid ankle-foot orthosis for children with cerebral palsy', Poster Presentation, GCMAS Annual Meeting 2024

Abbreviations

AFO Ankle Foot Orthosis

AFOFC Ankle Foot Orthosis Footwear Combination

CP Cerebral Palsy

FE Finite Element

GMFCS Gross Motor Function Classification System

GRF Ground Reaction Force

ICC Intra-class Correlation Coefficient

ICF International Classification of Functioning, Disability and Health

MOCAP 3-Dimensional Motion Capture

OSKAR the Optimal Segment Kinematic Alignment Approach to Rehabilitation

PPC Copolymer Polypropylene

PPH Homopolymer Polypropylene

SEM Standard Error of Measurement

SDD Smallest Detectable Difference

SVA Shank to Vertical Angle

TMST Temporal Mid-Stance

Abstract

Cerebral Palsy (CP) is the leading cause of childhood motor disabilities, resulting in a variety of gait impairments. Ankle-foot Orthoses (AFOs) are key to managing these impairments, aiming to facilitate weight-bearing activities and normalise lower limb biomechanics. To optimise their performance, the Optimal Segment Kinematic Alignment Approach to Rehabilitation (OSKAR) has been recommended[1], [2], which focuses on manipulating shank kinematics, to normalise Ground Reaction Force (GRF) alignment and external joint moments. However, the ability to control and alter shank kinematics depends on the stiffness of a rigid Ankle Foot Orthosis (AFO), which is influenced by its design. Despite this, there are no clinical guidelines on how to tailor the design of rigid AFOs to the characteristics of the individual.

Therefore, this research aims to explore the impact of rigid AFO design factors on stiffness, before applying this knowledge to move towards an optimised rigid AFO design. To achieve these aims, Finite Element (FE) models, simulating the mechanical behaviour of AFOs designed for a 5-, 10- and 15-year-old child, were validated against data from a novel test rig. Then they were utilised in two primary research studies.

The first study investigated the mechanical properties of AFOs designed according to current practice, to determine the impact of thermoplastic rigidity and thickness, trim line design and ribbing on AFO stiffness. This demonstrated that AFO thickness and trim lines design had the biggest impact on AFO stiffness, whilst challenging some aspects of clinical practice, such as the placement of ribbing and the use of through the malleoli trim lines.

These findings were then applied to develop a novel reinforcement and move towards an

optimal rigid AFO design. This process was directed by design criteria which covered the mechanical, clinical and user requirements. It evaluated the effects of a prototype design, which has the potential to be applied clinically to stiffen rigid AFOs, whilst being more aligned to the needs of the user and clinician.

As a result, this thesis advanced the understanding of rigid AFO design for children with CP. Furthermore, by integrating FE analysis with mechanical and clinical design criteria, it outlined a new framework for rigid AFO design that links fundamental biomechanical principles to clinical applications, which with further refinement, could be used to optimise the design of rigid AFOs for clinical practice.

Introduction

Cerebral Palsy (CP) is the leading cause of motor disabilities in children, globally[3]–[5]. It is a neurological condition which results in a variety of complex gait impairments[6]–[9], which ultimately impact an individual’s participation in activities of daily living[10]–[13]. Central to managing these impairments are rigid Ankle-Foot Orthoses (AFOs), which are widely prescribed for children with CP to facilitate weight-bearing activities and improve the biomechanics of gait[14], [15].

To optimise their performance, it has been recommended that the Optimal Segment Kinematic Alignment Approach to Rehabilitation (OSKAR) is taken when prescribing a rigid AFO[1], [2]. OSKAR is an approach to AFO prescription, built on the theory that shank kinematics are central to maintaining typical Ground Reaction Force (GRF) alignment during gait. Therefore, AFOs can be used to control and tune shank alignment to normalise external moments in children with CP[16]–[19]. However, the success of OSKAR depends on the mechanical properties of rigid AFOs, which are dictated by their design. In particular, stiffness is critical, as it determines how effective the device is at immobilising the ankle and controlling shank kinematics[15]. Despite this, neither OSKAR nor wider literature, offers clinical guidance regarding the design of rigid AFOs to optimise their stiffness for individual patient characteristics.

Therefore, the thesis aims to address this issue by exploring the relationship between rigid AFO design factors, such as thermoplastic rigidity and thickness, trim line design, and reinforcements, and the stiffness of the device. This knowledge is then applied to move towards a more optimised rigid AFO design, which meets the desired mechanical, clinical and user requirements. To achieve this, Finite Element (FE) analysis, validated against experimental data from a novel test rig, was used to assess the mechanical be-

haviour of rigid AFOs. This allowed multiple design iterations to be evaluated across a range of paediatric-sized AFOs, without incurring costs and lead times associated with AFO manufacture. Therefore, the thesis also explores the viability of using computational analysis to direct the optimisation of rigid AFO design.

The thesis is structured into eight chapters. Chapter 1 introduces the key concepts regarding the management of gait impairments in children with CP, and establishes the scope of the thesis. Chapter 2 presents a comprehensive review of the literature related to the application and design of rigid AFOs, identifying the key areas for further research. After which, it evaluates the most appropriate method for quantifying AFO mechanical properties. Following this, Chapter 3 investigates the stakeholder requirements related to rigid AFO design, through a literature review and discussion with clinicians, before the findings of chapters two and three are collated and used to define the aims of the thesis in Chapter 4. After this, Chapter 5 details the development and validation of the FE models used to simulate the bending behaviour of AFOs for a 5-, 10- and 15-year-old. These were then applied to first evaluate how design factors influence mechanical properties of rigid AFOs which align with current clinical practice, and then to optimise the design of rigid AFOs, through the development of a novel reinforcement in Chapters 6 and 7, respectively. Finally, Chapter 8 discusses the main findings, limitations and clinical relevance before outlining directions for future research.

Chapter 1

Background

Chapter Overview

The opening chapter of this thesis introduces key concepts regarding the management of gait impairments in children with Cerebral Palsy (CP), using rigid Ankle-Foot Orthoses (AFOs), and establishes the scope of the thesis. It begins by discussing CP and its associated impairments that ultimately limit an individual's mobility, activity levels, and participation. Then it highlights how the condition is managed before focusing on rigid AFOs and their indications for use, function and therapeutic objectives. Finally, The Optimal Segment Kinematic Alignment Approach to Rehabilitation (OSKAR) is introduced, an approach to AFO prescription focused on optimising the biomechanical performance of rigid AFOs, and discusses the potential barriers to its clinical implementation, which form the focus of subsequent literature reviews.

1.1 Cerebral Palsy (CP)

1.1.1 Overview

Cerebral palsy (CP) is an umbrella term used to define “a group of permanent disorders of the development of movement and posture, causing activity limitation, that are attributed to non-progressive disturbances that occurred in the developing fetal or infant brain”[20]. It has a global prevalence of approximately 2-3 live births per 1000[3]–[5], making it the leading cause of childhood motor disability. Although its prevalence is relatively static[21], survival rates for premature births have increased and the life expectancy for less severe cases is now comparable to the general population[22]. Furthermore, although the primary cause of the condition is non-progressive, the severity of associated impairments can develop during growth[23]. As a result, the burden on rehabilitation services has increased.

Since 2001, the impairments associated with disabilities have been classified according to health domains, using the International Classification of Functioning, Disability and Health (ICF) framework[24]. Cerebral palsy (CP) is a hierarchical condition, stemming from a primary lesion or defect in the developing brain. In turn, the mechanical environment stimulating growth is altered, leading to secondary impairments of the musculoskeletal system. Together, these primary and secondary impairments result in tertiary motor impairments. As a result, the clinical presentation of the condition is highly heterogeneous, and associated impairments span all three domains of the ICF[25] (Figure 1.1).

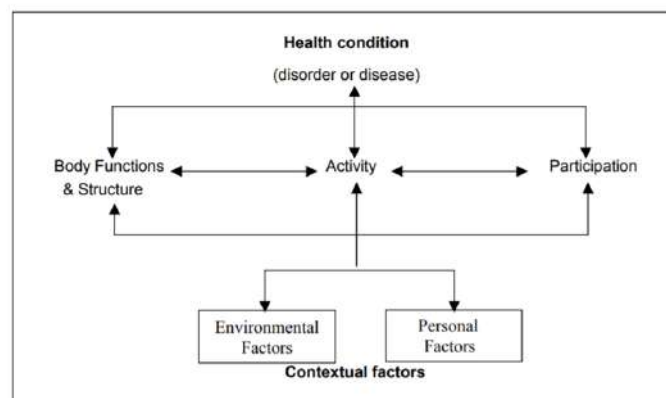


Figure 1.1: The ICF model for characterising disability. Image reproduced from WHO, 2002[26]

1.1.2 Primary impairments of the structure and function of the neurological systems

Primarily, CP has several congenital, neonatal and postnatal aetiologies, including brain haemorrhages, hypoxic and metabolic encephalopathies, infections, and trauma, which result in defects in the structure of the brain. The severity of the associated impairments depends on the aetiology, with congenital disturbances generally leading to more severe cases[23], [27]. Furthermore, damage to the brain disrupts typical neurological function, resulting in a loss of selective motor control, impaired balance and atypical tone, which are common across all cases.

The loss of selective motor control is defined as *“the ability of the body to isolate the activation of muscles in a selected pattern in response to demands of a voluntary posture of movement”*[28]. As a result, individuals with CP have limited control of bi-articular muscles, such as rectus femoris and gastrocnemius[23], and antagonistic activity patterns, such as during terminal swing where the knee is extended whilst the hip is flexed[29]. Furthermore, they may also experience weakness, as force generation depends on both the recruitment of motor units and the frequency of activation[30].

Balance refers to the ability of an individual to maintain a fixed, stable position in space. In addition to selective motor control, balance requires sensory feedback to regulate posture in response to environmental stimuli[23]. However, in CP, the mechanism for sensory feedback is disrupted, limiting an individual’s ability to respond to perturbations in gait, which restricts their dynamic stability and increases their risk of falling.

Finally, atypical tone results from pathological muscle activation and has been characterised based on the speed and type of motion produced, according to the surveillance for CP in Europe[31] (Figure 1.2). Dyskinesia refers to varied muscle tone caused by damage to the basal ganglia. It can be subdivided into dystonia, where movements are slow, torsional and usually localised to a single limb, and chorea/athetosis, characterised by jerky movements. Ataxia is characterised by impaired balance and the loss of coordination[23], [32]. Finally, spasticity refers to *“the resistance to externally imposed movement which increases with increasing speed of stretch and varies with the*

direction of joint movement” and/or “the resistance to externally imposed movement which increases rapidly beyond a threshold speed or joint angle.”[33]. This is symptomatic of a hyperactive stretch reflex, which is typically regulated by upper motor neuron control to maintain typical tone[34]. Although in practice, movement disorders often co-present[32], spasticity is the most prevalent, affecting 87% of patients with CP[35].

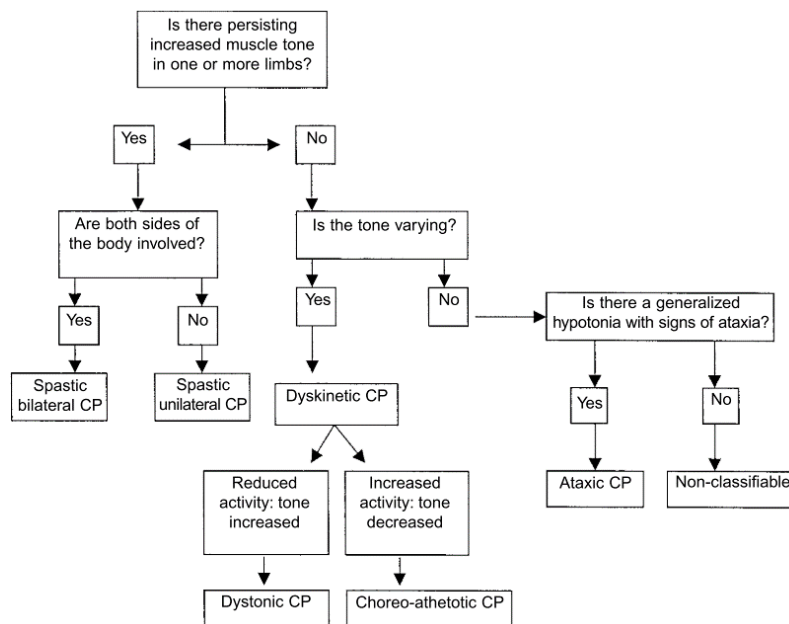


Figure 1.2: The classification of atypical tone associated with cerebral palsy according to the surveillance for cerebral palsy in Europe[31].

1.1.3 Secondary impairments of the structure and function of the musculoskeletal system

Typical musculoskeletal development occurs in response to mechanical stimuli exerted on the body during growth and weight-bearing activities. However, due to the primary neurological impairments, children with CP have delays in reaching motor milestones such as standing and walking by 10.8 and 12.0 months respectively, for the 50th percentile[36]. As a result, this has a critical effect on the functional development of the system[23].

Firstly, muscles undergo reduced stretching leading to atypical muscle architecture, sarcomere atrophy and a loss of elasticity due to stiffening of both the muscle fibres and

connective tissue. This results in muscle weakness and contractures, where the muscle appears functionally short, limiting force generation[30], [37], [38].

Secondly, delays in weight-bearing activities mean forces which stimulate skeletal remodelling are exerted later when bones have become more ossified and less malleable[39]. Meanwhile, spasticity exposes long bones to excessive, atypical torques. Together these limit the maturation of the infant skeleton, resulting in increased femoral anteversion and joint dysplasia, subluxation or dysfunction[38].

1.1.4 Tertiary impairments of gait

The primary function of typical gait is to advance the body whilst maintaining upright stability, and it is characterised by stability in stance, sufficient foot clearance during swing, pre-positioning of the foot in terminal swing, adequate step length and energy conservation[40]. However, collectively, the primary neurological and secondary musculoskeletal impairments associated with CP, lead to a loss of typical gait function and characteristics.

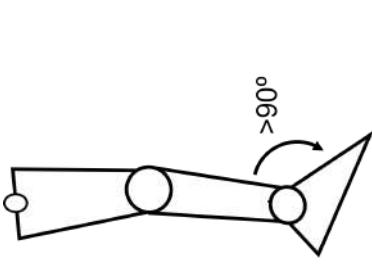
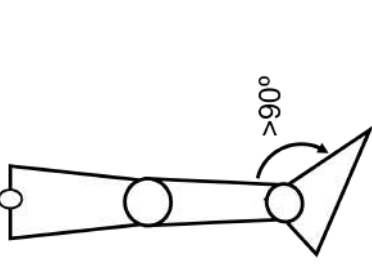
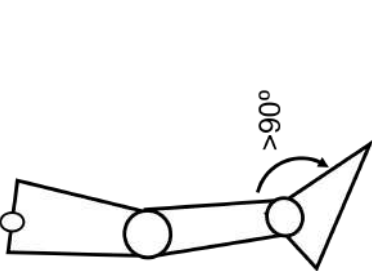
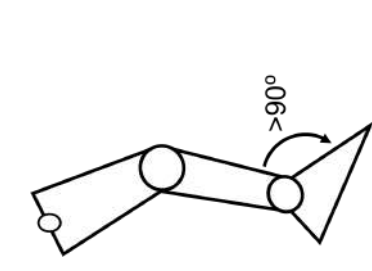
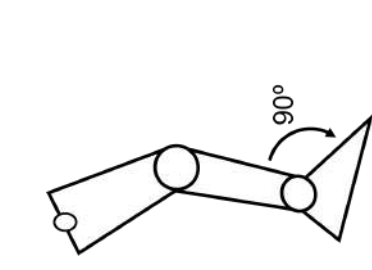
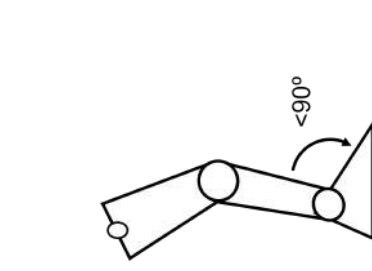
Firstly, atypical joint and segment biomechanics are developed across the lower limb. These individual impairments are classified into gait patterns based on topography, muscular involvement and deviations in joint biomechanics[6]–[9]. However, due to the heterogeneity of CP, few individuals fall discretely into one pattern, instead presenting with a continuum of deviations. Nonetheless, a systematic review reached a consensus on the atypical patterns most commonly referenced in literature[41]. These were the genu recurvatum pattern, defined by Simon et al.[42], Winters' drop foot pattern[6], and Roddas's true equinus, apparent equinus, jump gait and crouch gait patterns[9] (Table 1.1). In this study, genu recurvatum and drop foot were considered patterns, as the original definitions included disturbances across multiple joints.

Drop foot, true equinus and genu recurvatum all have distal muscular involvement and are more prevalent in unilateral CP. Drop foot is the least severe, where a weak or underactive tibialis anterior, results in plantar flexion during swing and toe contact, with no restriction on dorsiflexion. This is accompanied by increased knee flexion from terminal

swing to loading response, hip hyper-flexion in swing and increased lordosis throughout the gait cycle[6]. True equinus and genu recurvatum often co-present due to their shared aetiology. Spasticity and/or contracture of the gastroc-soleus complex causes the ankle to remain plantar flexed throughout gait. Consequently, the plantar flexor-knee extension couple is excessively engaged, referring to control of tibial advancement and knee extension during mid-stance, via eccentric plantar flexor action. This results in the knee being forced into extension or recurvatum, depending on the severity of the gastroc-soleus impairment or integrity of the soft tissues in the knee. Furthermore, trunk advancement is limited, and the hip remains in extension, reducing forward momentum and gait efficiency[8], [42].

Alternatively jump gait, apparent equinus and crouch gait have a more proximal muscular involvement and are more common in bilateral CP. They have similar aetiology, primarily caused by contractures and/or spasticity of the hamstrings, iliopsoas and gastroc-soleus complex, and illustrate how the severity of impairments can increase with age. Jump gait is seen in younger children characterised by increased knee flexion during early stance which corrects in the latter stages, whilst the foot remains in an equinus position throughout. This is often accompanied by increased lumbar lordosis, anterior pelvic tilt and hip flexion, which does not reach full extension[8], [43]. However, as the child grows and becomes heavier, the plantar flexion-knee extension couple is exceeded, resulting in increased knee and hip flexion. Now the ankle is in a typical dorsiflexion range however toe walking prevails, resulting in an apparent equinus pattern[9]. Finally, in older children crouch gait develops, highlighted by excessive hip and knee flexion and ankle dorsiflexion throughout gait. Here there is a continuous external knee flexion moment, placing excessive eccentric demands on the quadriceps and gastroc-soleus muscles to prevent a collapse into flexion[8], [43]. As a result, it is a highly inefficient gait pattern, reducing the individual's ability and capacity to ambulate independently.

Table 1.1: The six most common atypical gait patterns associated with CP[41]. DF = Dorsiflexion, PF = Plantar flexion.

Structure	Drop Foot[6]	True Equinus[9]	Genu Recurvatum[42]	Jump Knee[9]	Apparent Equinus[9]	Crouch Gait[9]
Trunk & Pelvis	Increased lordosis	Anterior tilt	Normal kinematics in stance	Anterior tilt	Anterior tilt	Anterior/posterior tilt
Hip	Hyper-flexion in swing	Full extension	Normal kinematics in stance	Hyper-flexion in early stance, extension in late stance	Hyper-flexion in stance	Hyper-flexion in stance
Knee	Increased flexion in terminal swing to loading response	Full extension	Hyperextension in stance	Hyper-flexion in early stance, extension in late stance	Hyper-flexion in stance	Hyper-flexion in stance
Ankle	Excessive PF in swing	Excessive PF in stance	Excessive PF in stance	Excessive PF in stance	Normal kinematics	Excessive DF in stance
Muscle	Anterior Tibialis	Gastrocnemius	Gastrocnemius	Gastrocnemius Hamstrings Rectus Femoris	Gastrocnemius Hamstrings Rectus Femoris Psoas	Gastrocnemius Hamstrings Rectus Femoris Psoas
						

Meanwhile, these atypical gait patterns are reflected in the spatiotemporal characteristics of gait. In typically developing children, the development of a more stable, heel-toe gait pattern by the ages of 3.5-4 years, coincides with increases in velocity, step length and single-support time, alongside decreases in cadence and stance time[43]. Conversely, the opposite has been shown for children with CP[44]. In bilateral cases, a reduction in velocity of between 60-75%[45], [46], cadence 77%[47], stride length 73%[45], [46] and single-limb support 82-83%[46] when compared to typically developing peers has been shown, whilst step width and double limb support increased to 160% and 179-188% respectively[46]. Furthermore, a similar pattern has been highlighted in unilateral cases, with double-support time between 15-20% higher than for normative controls[48], whilst the difference in velocity increased with severity[49]. Furthermore, children with CP display higher gait variability and asymmetry[50], [51]

In addition, atypical kinematics, a decrease in stride length and single-support time and an increase in step width imply individuals with CP have reduced dynamic stability, considered one of the key characteristics of gait as it facilitates the other four[44]. Despite this, comparisons between the dynamic stability during steady-state walking in individuals with CP and their typically developing counterparts is equivocal[52]–[56]. Furthermore, paradoxically, individuals with CP show tendencies towards maintaining higher mediolateral stability during dual task and fast walking[52]–[56], considered an important indicator for the risk of falling[52]. However, these findings may be explained by the fact that children with CP widen their base of support to compensate for their instability[57]. Furthermore, larger differences between the two populations may be found if the severity of motor function was considered.

The severity of motor function impairment in individuals with CP is classified using the gross motor function classification system, based on the individual's ability to perform motor tasks such as sitting, walking, running and jumping[58]–[60]. The loss of motor function is dictated by the severity of the primary, secondary, and tertiary impairments associated with CP. Furthermore, it is correlated with increased rates of fatigue in adolescents with CP[61]–[63] and reduced energy efficiency of gait[64]. As a result, a loss of gait function is linked to limitations in activity and participation levels in individuals

with CP[10]–[13].

1.2 The management of gait impairments associated with CP using Ankle-Foot Orthoses (AFOs)

Once the treatment objectives have been set, decisions on the most appropriate interventions can be made. Given the complexity of the condition and variety of potential goals, no two cases of CP follow the same management pathway. Several interventions are available, targeting specific impairments, however, in practice, they are often used in combination to achieve functional outcomes (Figure 1.3).

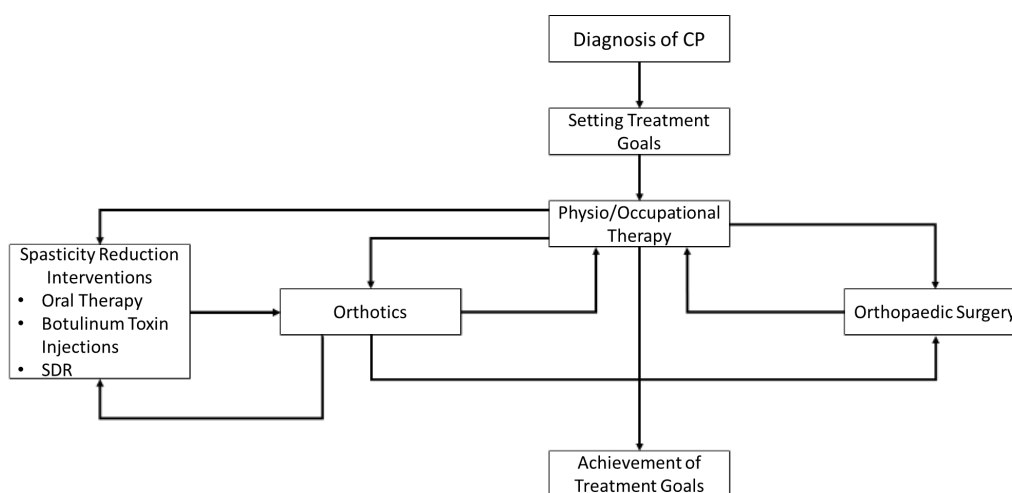


Figure 1.3: The management paradigm for treating gait impairments in children with CP. (CP = Cerebral Palsy and SDR = Selective Dorsal Rhizotomy.)

At the centre of this, sits physiotherapy, recommended for all children with CP suffering with mobility deficits and spasticity. Tailored programs are designed to maintain or improve range of motion, reduce pain and increase strength[65], [66], with the aim of “*enhancing skill development, function, and ability to participate in everyday activities*”[33]. However, the severity of spasticity and other musculoskeletal impairments mean additional treatments are often required to facilitate goal attainment

The most common supplementary intervention is orthotics, which reinforce and realign the musculoskeletal system during weight-bearing activities. Although several types are available, foot orthoses have limited application in treating gait impairments, as they can only align and protect the foot. Meanwhile, knee-ankle-foot orthoses can be used

to treat knee instability, muscle weakness, knee hyperextension and valgus during gait, whilst hip-knee-ankle-foot orthoses may be required to manage hip abductor impairments[67]. However, these orthoses are rarely seen in children with CP, due to their size and weight, which means they are not well tolerated and increase the energy cost of walking[68]–[70]. Instead, *'appropriate use of surgery, rehabilitation and below-knee bracing [can be used to manage] the problems that adversely affect walking function[69].*

Therefore, Ankle-foot Orthoses (AFOs) are the most commonly prescribed orthotic device, typically used to improve walking ability, stability, and range of motion[14]. A cross-sectional population study of six countries in Northern Europe, Sweden, Norway, Finland, Iceland, Scotland and Denmark, found AFO use amongst children with CP aged 0–18 years, ranged from 35% (74 children) in Iceland to 57% (1955 children) in Scotland, although in Sweden, prevalence peaked at age 5 (67%), before dropping to 19% aged 19[14]. Furthermore, AFOs were most widely used to treat spasticity and were more common in bilateral cases, whilst their use increased with the severity of motor impairment[71].

In cases where spasticity is particularly high, spasticity reduction interventions may also be utilised. The most common is botulinum toxin injections, a neurotoxin which provides rapid, targeted partially reversible denervation of muscles[72]. Consequently, it is preferred to oral baclofen, which causes globalised weakness[73], and selective dorsal rhizotomy, a neurosurgical procedure involving the lesion of sensory spinal nerves, which has the potential for serious adverse effects. However, there are uncertainties around the long-term effects of botulinum toxin[74], [75] and its potentially detrimental effects on muscle strength[76]. Therefore, National Institution for Health and Care Excellence guidelines advise caution when prescribing botulinum toxin injections and do not recommend its use unless the individuals are likely to engage with a post-treatment physiotherapy program and the use of AFOs to enhance stretching and practice functional skills[33].

Finally, orthopaedic surgery, including tendon lengthening and transfer, rotational osteotomies and joint stabilisation procedures, is available to treat fixed contractures, hip dysplasia and bony deformities[77]. Consequently, they play an important role

in the treatment of transverse impairments, typically resulting from tibial torsion and femoral anteversion[8]. Whilst necessary, intensive rehabilitation programs involving physiotherapy and AFOs are required to maintain musculoskeletal benefits[33]. Furthermore, the results in younger individuals, with immature musculoskeletal systems, are unpredictable[77]. Therefore, it should be used as a last resort, with non-operative interventions, such as physiotherapy and AFOs, prioritised.

As a result, AFOs play a pivotal role in the management of gait impairments in children with CP. They are used alongside physiotherapy to facilitate weight-bearing activities and apply extended passive stretching, whilst enhancing the effects of spasticity reduction procedures and orthopaedic surgery. Furthermore, early implementation may even reduce the need for orthopaedic surgery by facilitating earlier weight-bearing activities and therefore typical maturation of the musculoskeletal system. Therefore, they may be used to target impairments across the ICF domains, including encouraging typical skeletal development and enhancing joint range of motion, maintaining muscle length, strength, and extensibility, optimising biomechanics during standing, stepping, and walking, providing opportunities for motor learning and decreasing pain [68], [78].

An AFO is defined as *“an externally applied device used to compensate for impairments of the structure and function of the neuromuscular and skeletal systems that encompasses the ankle joint and the whole or part of the foot”*[79]. Within the NHS, paediatric AFOs are typically manufactured from thermoplastics via vacuum-forming. Thermoplastics are preferred over metals or carbon fibre as they provide acceptable material properties at relatively low costs and weight, and are easy to manufacture[80]. According to Eddison et al., there are six types of bespoke, thermoplastic AFOs[81] (Figure 1.4). These include, supra-malleolar, flexible, articulated, rigid, rigid with an incorporated anterior shell and rigid with a separate anterior shell. However, despite the considerable variations between these designs, there are currently no NHS guidelines for the use of thermoplastic AFOs in CP. Instead, the most detailed recommendations were outlined by Owen and Bjornson[82], which align with NHS guidelines for stroke populations[2] and indications for use provided by NICE[33]. Together, these concur that rigid AFOs are required for individuals with high tone, spasticity, or contracture

in the gastroc-soleus complex, mediolateral instability of the foot, and knee and hip impairments. As a result, they are the most widely used type of AFO in CP, particularly when treating more severe gait patterns such as jump gait, apparent equinus and crouch gait[83], [84], and will therefore form the focus of the remainder of this thesis.

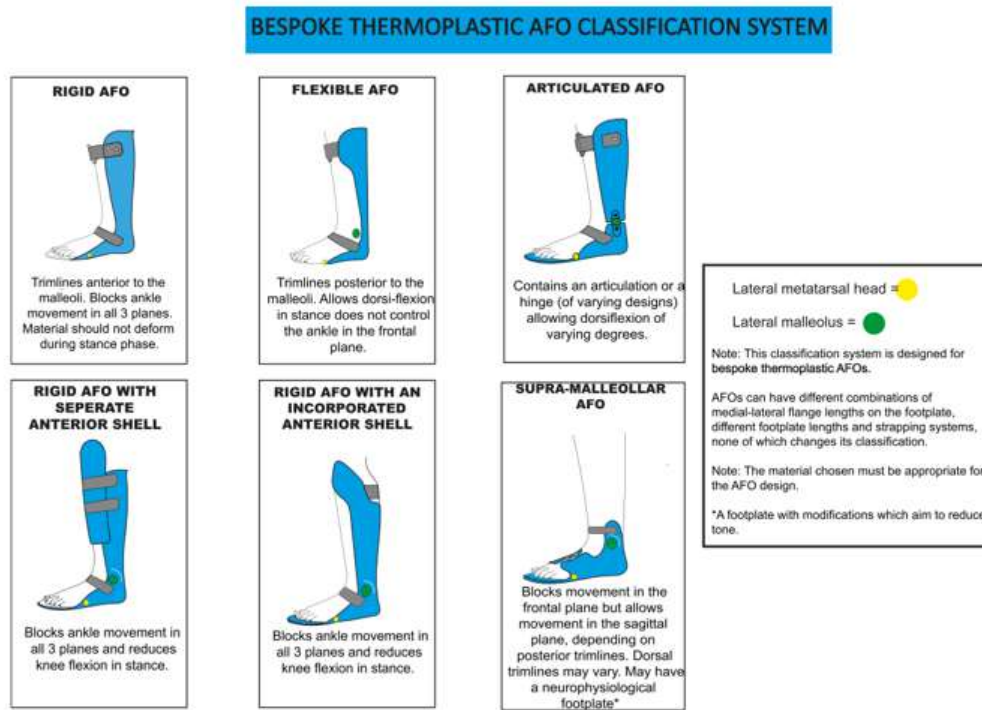


Figure 1.4: Classification of bespoke thermoplastic AFOs designs. Reproduced from Eddison et al.[81]

1.3 The biomechanical principles of AFO intervention

1.3.1 Direct biomechanical control

Rigid AFOs work by immobilising the ankle in all three planes, therefore reinforcing the musculoskeletal system and modifying the system of external forces and moments acting across lower limbs[15]. As a result, they exert both direct biomechanical control over the foot, ankle, and shank and indirect biomechanical control over the proximal joints and segments. Direct biomechanical control is achieved by applying a 3-point force system about the ankle joint (Figure 1.5). Firstly, two forces are applied proximal (F_p) and distal (F_d) to the joint, which generate moments opposing the direction of rotation. Then, to maintain both rotational and translational equilibrium, a third antagonistic force (F_c) is exerted as close to the joint centre as possible [15], [85].

For complete direct control, 3-point force systems should be applied in all three planes of motion. However, due to short lever arms, AFOs have little effect on transverse shank kinematics and therefore have little impact on impairments in this plane. Excessive internal rotation reduces clearance and therefore increases the risk of falls, whilst external rotation can affect the plantar flexion/knee extension couple through lever arm dysfunction. However, transverse plane impairments are typically caused by long bone deformities or atypical rotation of the hip and pelvis and are, therefore, typically treated with surgery[86].

Additionally, AFOs are typically worn with footwear, meaning the moments applied to the ankle are a summation of the moments generated by both the AFO and footwear[85]. However, although footwear contributes to these systems, the AFO is responsible for the majority of the applied force given its longer lever arms and superior material stiffness.

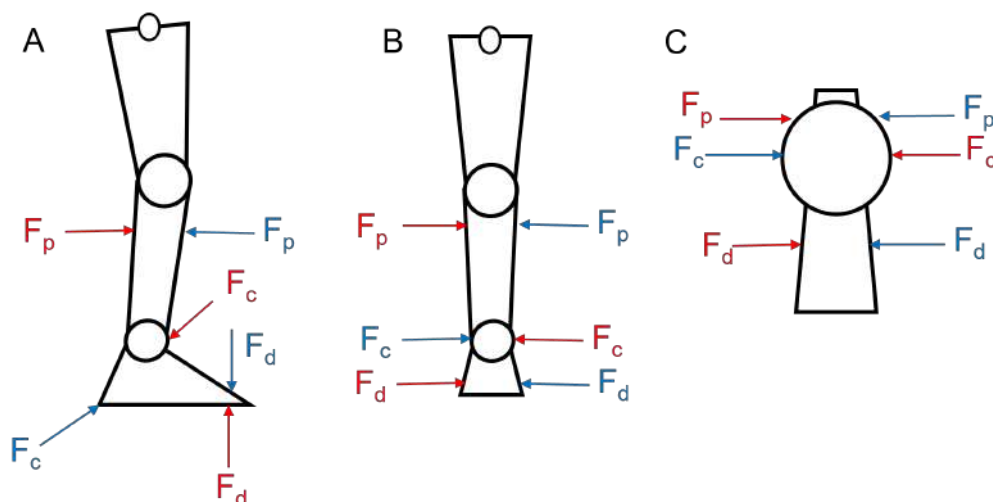


Figure 1.5: Three-point force systems required to control ankle motion in all three planes. A) Sagittal control, red = plantar flexion, blue = dorsiflexion. B) Coronal control, red = pronation, blue = supination. C) Transverse control, red = external rotation, blue = internal rotation

1.3.2 Indirect biomechanical control via shank alignment

Additionally, rigid AFOs also influence the biomechanics of the joints and segments proximal to the device. During stance, the ground exerts a force on the body, which is equal in magnitude and opposite in direction to body weight, known as the Ground Reaction Force (GRF). It induces a system of external moments on the joints and

segments of the lower limb, the magnitude, and direction, of which are determined by the alignment of the GRF with them. As a result, the net moment acting on a joint or segment is equal to the sum of the internal moments, generated by the muscles and connective tissue, and the external moments generated by the GRF (Figure 1.6).

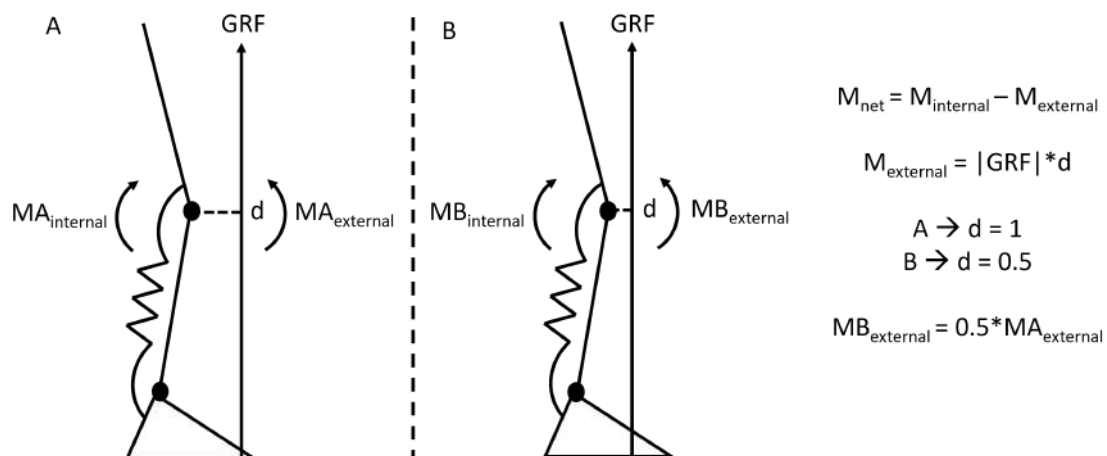


Figure 1.6: Diagram showing the net sagittal moment acting on the knee in stance and the relationship between the external moment and ground reaction force (GRF) alignment. The spring represents the knee flexor muscles.

As a result, in typical gait, the alignment of the GRF is regulated to minimise external moments and generate stabilising external knee and hip extension moments during single-limb support (Figure 1.7). In turn, this reduces the need for active control of joint movement, creating a more energy-efficient, stable gait pattern. The GRF alignment is regulated via selective motor control, which coordinates the sequence of muscle activity required to control the movement of the segments of the lower limbs, and the four rockers of gait, the heel, ankle, forefoot and toe, which act as centres of rotation, allowing the proximal segments of the lower leg to transition smoothly over the non-advancing foot[87]–[89].

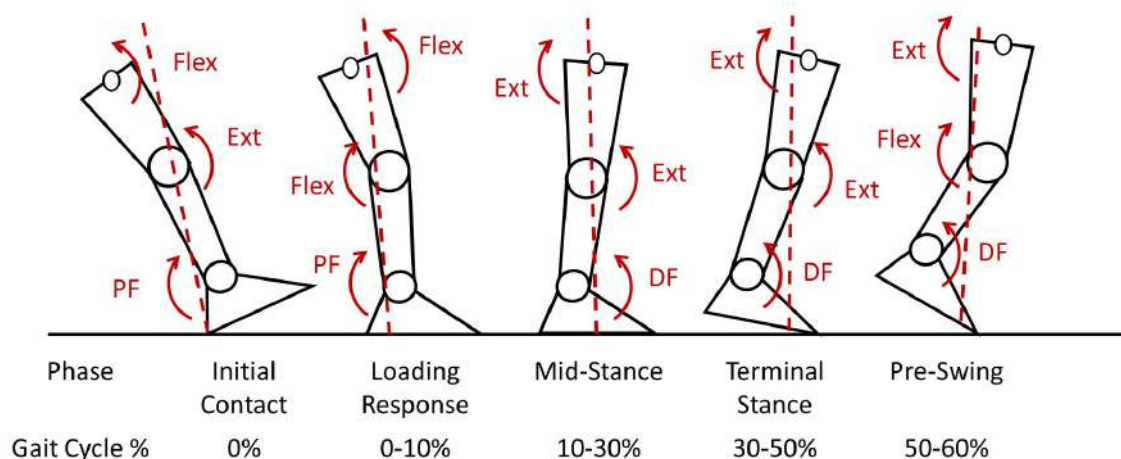


Figure 1.7: Typical GRF alignment with the joints of the lower limb throughout stance. Dashed line = The GRF. PF = Plantar Flexion. DF = Dorsiflexion.

However, in children with CP, control of the GRF can be lost if either of these mechanisms is inhibited by the neurological and musculoskeletal impairments associated with the condition. In turn, this leads to atypical knee and hip kinematics and unstable, inefficient gait patterns, such as those outlined in Section 1.1.4[90]. In their absence, rigid AFOs can control the GRF alignment. This is according to work by Cooks and Cozzen[19] and Butler and Nene[18], [91], who established that the position of the shank dictates the alignment of the GRF with the knee and hip. Therefore, by immobilising the ankle using a rigid AFO, shank kinematics during mid and terminal stance can be manipulated using heel wedging to normalise the GRF alignment (Figure 1.8). Consequently, rigid AFOs can indirectly influence the external moments acting at the knee and hip, restoring typical kinematics and gait stability and energy efficiency.

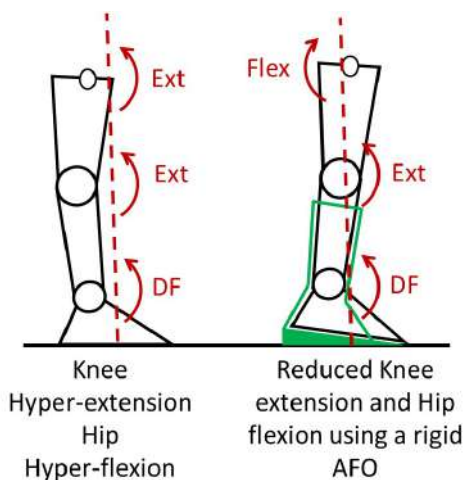


Figure 1.8: Representation of how a rigid AFO can normalise ground reaction force alignment. Dashed line = The GRF. DF = Dorsiflexion.

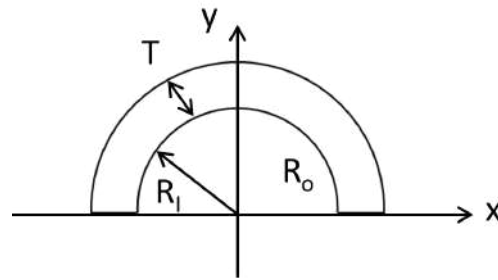
This theory of adjusting shank kinematics through wedging is thought to be critical to the performance of rigid AFOs. As a result, it forms the basis of The Optimal Segment Kinematic Alignment Approach to Rehabilitation (OSKAR) using rigid AFOs, which provides algorithms on how to conduct this process and biomechanically optimise rigid AFOs. However, it relies on the AFO resisting deformation and restricting ankle motion during gait. Consequently, the stiffness of a rigid AFO is fundamental to both the direct and indirect biomechanical control it exerts and the clinical outcomes achieved.

1.3.3 The factors that influence rigid AFO stiffness

Stiffness is defined as *"the moment around the ankle joint exerted by the AFO per degree of ankle joint rotation"*[92] and is measured as the linear region of a moment versus deflection curve in $\text{Nm}/^\circ$. Essentially, it refers to the AFOs resistance to deformation. During stance, the direction of loading is phase-dependent whilst the magnitude is related to the individual's mass, height, tone, and activity level. For individuals aged 4–21 years, external plantar flexion and internal dorsiflexion moments reach a maximum of $\approx 0.01\text{--}0.2\text{Nm/kg}$ during loading response[93]–[99], whilst external dorsiflexion and internal plantar flexion moments reach a maximum of $\approx 0.8\text{--}1.5\text{Nm/Kg}$ [93]–[100] during terminal stance. Therefore, the load on an AFO is around ten times greater in the dorsiflexion direction, meanwhile, its half-cylindrical geometry means AFOs are inherently more resistant to plantar flexion loads. As a result, AFOs are more susceptible to failure under dorsiflexion, which results in buckling at the ankle and a loss of control over shank alignment[101].

AFO stiffness is determined by several design factors including thermoplastic type and thickness, the mediolateral trim lines at the ankle, and additional reinforcements. Polypropylene is the standard thermoplastic used within clinical practice, of which there are two types. Homopolymer Polypropylene (PPH) consists of one polymer, packed into a highly organised, crystalline structure, whilst Copolymer Polypropylene (PPC) is produced via the polymerisation of polypropylene with an additional polymer, usually polyethylene, creating a more amorphous structure. As a result, PPH is considered the stiffer of the two materials however, it is also more brittle and has a sharp melting point, which may make it more difficult to form[102], [103].

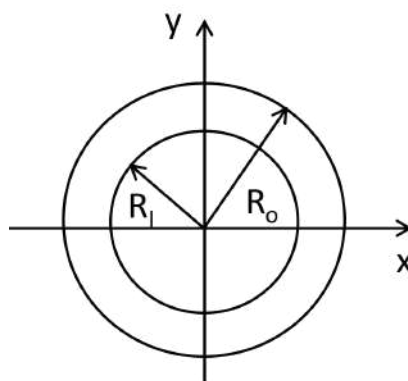
The influence of thermoplastic thickness and mediolateral trim line design on stiffness can be explained theoretically. During mid-stance, where the peak external dorsiflexion moment occurs, an AFO acts analogously to a cantilever beam, where it is fixed at the sole under body weight and a load is applied through the proximal strap. Therefore, assuming an AFO has a semicircular annulus cross-section, the second moment of inertia about an axis passing through its radial centre is given as



$$I_{xx_{semicircle}} = \left(\frac{\pi}{8}\right)(R_o^4 - R_i^2) \quad (1.1)$$

where R_o = the outer radius and R_i = the inner radius

Therefore, increasing polypropylene thickness will decrease R_i , resulting in an increased moment of inertia. Likewise, the second moment of inertia of a circular annulus is twice that of a semicircular annulus.



$$I_{xx_{circle}} = \left(\frac{\pi}{4}\right)(R_o^4 - R_i^2) = 2 \cdot I_{xx_{semicircle}} \quad (1.2)$$

Therefore, increasing the outer circumference of the AFO, by increasing the depth of the trim lines at the ankle also results in a greater moment of inertia. Both types of

polypropylene are available in sheets ranging from 2-6mm in thickness, whilst medio-lateral ankle trim lines vary depending on the type of AFO. Flexible AFOs are characterised by posterior to the malleoli trim lines, whilst rigid devices typically have through or anterior to the malleoli trim lines, which provide greater rigidity[81]. However, when determining the thickness and trim line design of the AFO, user requirements such as ease of donning, compatibility with footwear and comfort must be considered.

Finally, greater stiffness at the ankle can be achieved by incorporating several reinforcements into the AFO structure during the vacuum-forming process. Reinforcements have the benefit of providing localised stiffness without increasing the global thickness of the device, however, they also increase manufacturing complexity and may inhibit post-draping modifications.

1.4 The Optimal segment kinematics and alignment approach to rehabilitation (OSKAR)

1.4.1 Overview

OSKAR was developed by Elaine Owen[16], [17], founded on the work by Cook and Cozzens[19] and Butler and Nene[18], outlined in Section 1.3.2. It emphasises the importance of normalising segment, rather than joint, kinematics when managing gait impairments using AFOs, arguing that normalised shank kinematics contribute to non-active dynamic stability and allows the ballistic movement of the proximal segments, which in turn facilitates typical kinematics and GRF alignment. As a result, it may also have a secondary effect on gait efficiency[104]. Furthermore, it recognises that an AFO and footwear work together as one system, known as the Ankle Foot Orthosis Footwear Combination (AFOFC). Therefore, to achieve optimal shank kinematics, the design of each must be considered.

To aid the clinical implementation of OSKAR, Owen has published clinical algorithms which detail the process of biomechanically optimising an AFOFC[16], [17], [105], [106], defined as *“the process of designing, aligning and tuning an AFOFC to optimise its per-*

formance”[17] (Figure 1.9). It is the most complete set of AFO prescription guidelines for CP, whilst its principles have been adopted into the NHS best practice guidelines for individuals with stroke[2]. Although OSKAR can be applied when prescribing all AFO types, it is deemed essential when using rigid AFOs which can inhibit both the second (ankle) and third (forefoot) rockers of gait. Furthermore, it is recommended for all children with CP. However, it is acknowledged that impairments including excessive musculotendinous stiffness, tone, and shortening, which prevent full passive hip and knee extension, and excessive foot progression angle, which results from transverse impairments and reduces sagittal lever arms, can limit its effects[107].

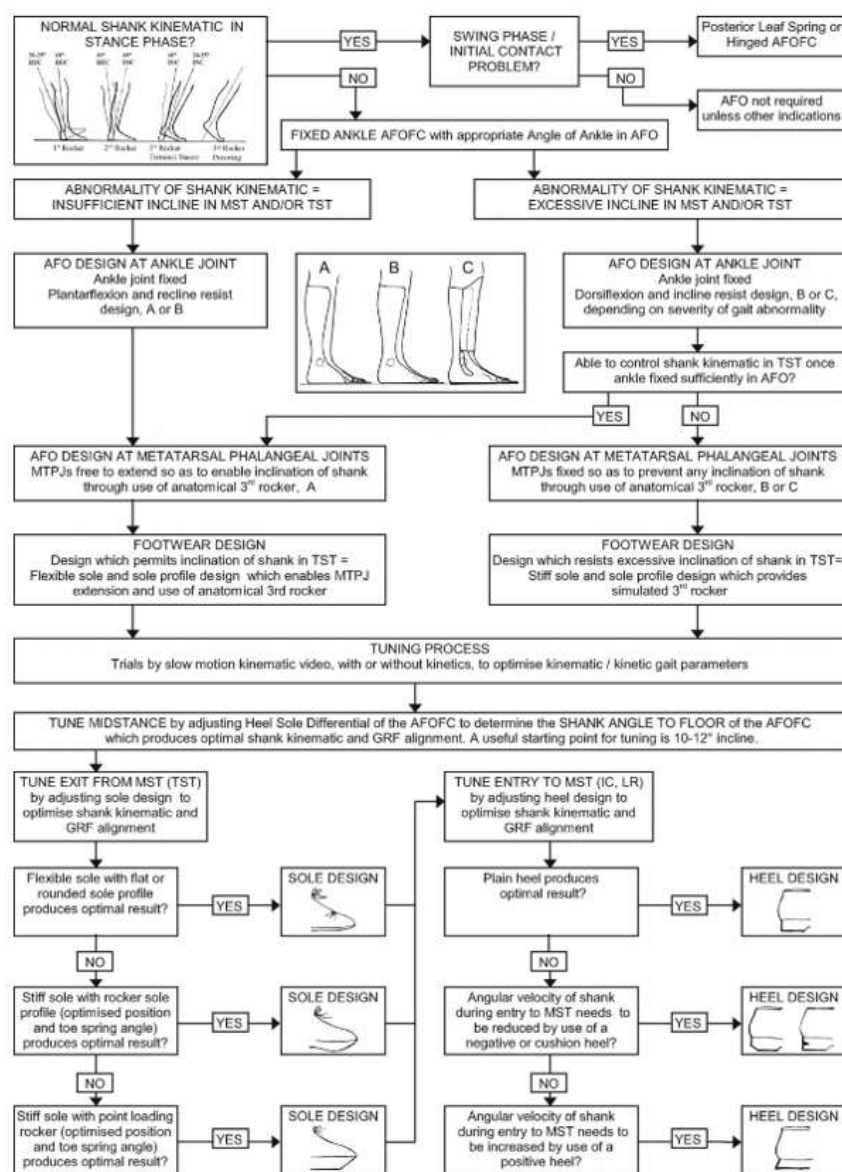


Figure 1.9: The optimal segment kinematics and alignment approach to rehabilitation (OSKAR) algorithm for the biomechanical optimisation of rigid ankle-foot orthoses for children with cerebral palsy. Image reproduced from Owen, 2014[16].

1.4.2 Determining the design of the ankle-foot orthosis-footwear combination (AFOFC) through classification of gait impairments

OSKAR begins with assessing the individual's gait to identify the phases where atypical shank kinematics are seen. This information is then used to determine the most appropriate AFO and footwear design. The first consideration is whether atypical kinematics occur during stance or swing, with impairments in swing alone indicating the need for a flexible or articulated AFO. However, if stance impairments are present, they are then classified using a system defined by Owen, to determine which type of rigid AFO is required and which joints should be controlled[16]. This system was based on clinical observations and, unlike previous classifications[6]–[9], [42], focuses on shank kinematics during mid and terminal stance, categorising them into two groups (Figure 1.10). Group one refers to when the shank is insufficiently inclined and is subdivided based on whether there is retrograde shank movement. As these patterns are characterised by knee extension, a rigid AFOFC that facilitates extension of the metatarsophalangeal joint is desirable, to allow roll-over. Alternatively, group two refers to excessive shank inclination, which is sub-categorised based on whether there is toe or full foot contact. These impairments may require a rigid AFO with an anterior shell, depending on the severity of the impairment. Furthermore, immobilisation of the metatarsophalangeal joint and footwear adaptations may be required to control atypical shank kinematics in terminal stance.

Despite focusing on shank impairments, there are analogies between Owen's gait classifications and the common atypical gait patterns outlined in section 1.1.4). For example, group one shank kinematics are commonly observed alongside true equinus and knee recurvatum, meanwhile, group two kinematics are seen with jump gait, apparent equinus and crouch gait. As a result, they can be applied in combination to gain a complete description of an individual's gait. However, unlike other classification systems, its reliability has not been verified[41], and so its validity as an independent classification system can be questioned.

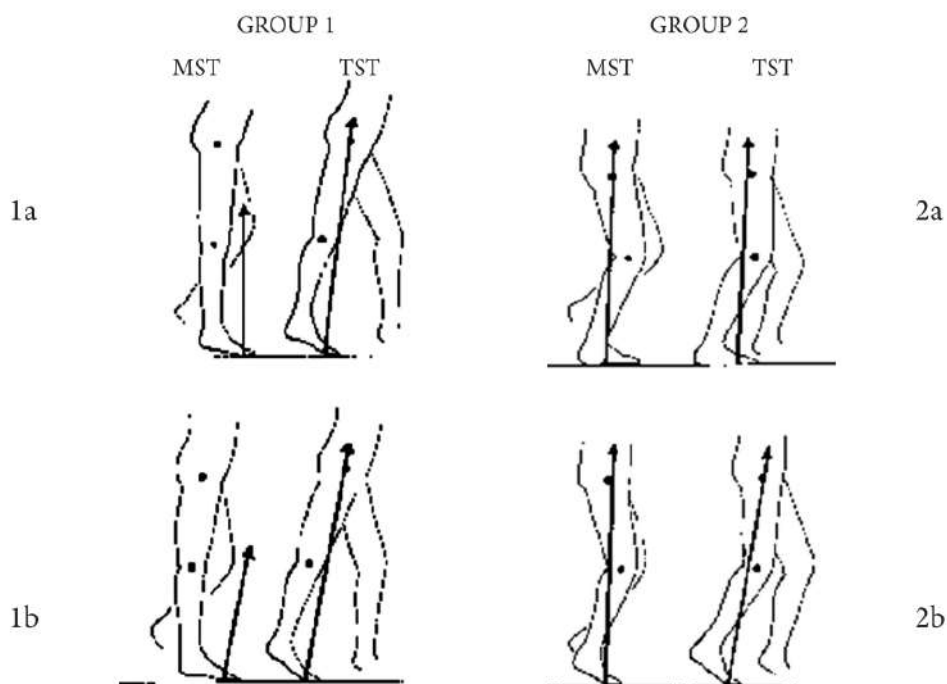


Figure 1.10: Owen's system for classifying the gait of children with spastic cerebral palsy, based on shank kinematics. Image reproduced from Owen, 2014[16]

1.4.3 Determining the ankle angle of the AFO

The next stage in the algorithm is to determine the ankle angle, at which it is cast, defined as *“the angle between the line of the shank relative to the line of the foot”* where *“the line of the foot is defined as the line between the base of the heel and the most inferior point of the foot under the fifth metatarsal head”*[17]. Historically, AFOs were set at 90° , based on the belief that the shank and thigh are vertical during static standing[108]. However, analysis of segment kinematics during gait contradicts this[109]. Furthermore, spasticity and contracture of the gastrocnemius, prevalent in CP, may limit an individual's ability to achieve full knee extension. Therefore, prescribing an AFO cast at 90° may lead to compensatory strategies including reduced step length, early heel rise, increased hip flexion and knee hyperextension, or, more worryingly, over-stretching of the gastrocnemius and mid-foot ligaments which may accelerate the development of fixed contractures and crouch gait[110], [111].

Consequently, OSKAR proposes that the ankle angle should be individualised based on the lowest passive ankle range when measured via clinical examination with the knees extended and foot pronated, neutral and supinated[106] (Figure 1.11). The viability

of using individualised ankle angles in AFOs, is supported by the fact that typically developing individuals adapted foot kinematics to maintain typical shank alignment, in response to increased heel height[112], [113]. Therefore, the foot can remain plantar flexed throughout gait, with the sole of the footwear acting as the 'effective' foot, without altering shank kinematics and GRF alignment.

However, there is limited evidence for the beneficial effects of individualised ankle angles. Owen et al. demonstrated that plantar flexed ankle angles increased calf length in six children over 2 years[114]. This demonstrates that individualised ankle angles facilitate stretching during gait by not exceeding the muscles' functional lengths, discrediting counterarguments that casting at a plantar-flexed angle may lead to plantar flexor shortening. However, sampling bias may be present, as little detail was provided on the recruitment process. Meanwhile, Kane et al. demonstrated that 5/10 children experienced net positive improvements in the gait variable score with ankle parameters removed[115]. Despite the lack of robust evidence, individualised AFO ankle angles have been adopted by multiple studies in both CP[116]–[119] and stroke populations[120], [121] and have been recommended for orthotic management by both the International Society for Prosthetics and Orthotics[1] and NHS[2]. Therefore, they should be adopted during AFO prescription in CP.

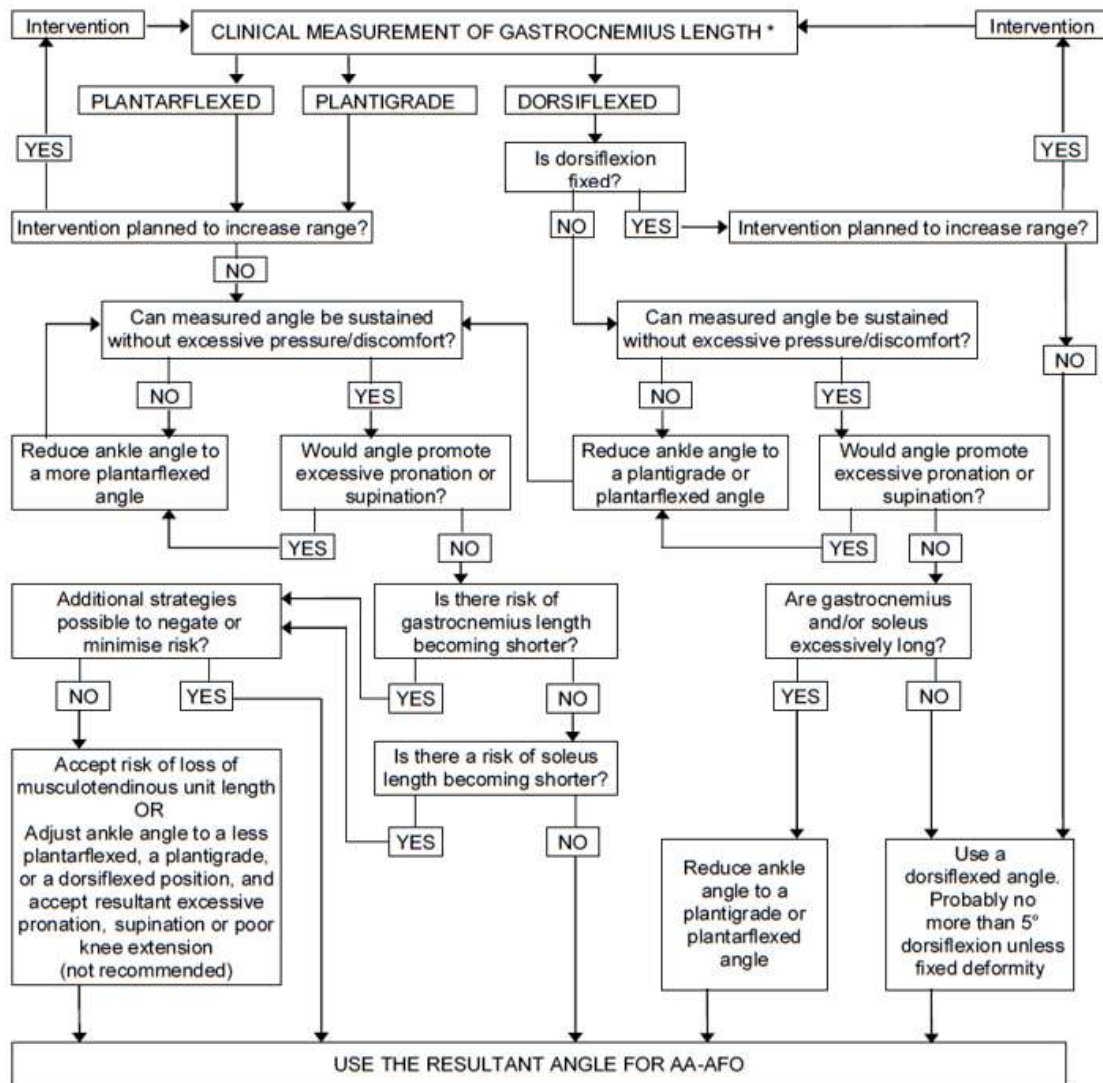


Figure 1.11: Owen's clinical algorithm for determining the ankle angle of the AFO[106]

1.4.4 Tuning shank alignment

The remaining stages of OSKAR are concerned with tuning the design and alignment of the AFOFC during the fitting to achieve optimal shank alignment throughout the gait cycle. Alignment is measured via the Shank to Vertical Angle (SVA), defined as “the angle of the line of the shank relative to the vertical when standing in the AFOFC with weight equally distributed between the heel and forefoot”[17]. It is determined by both the ankle angle of the AFO and the heel-to-sole differential, defined as “the difference between the height of the heel (at mid-heel) and the sole at the metatarsal heads”[113]. Consequently, it can be manipulated heel wedges applied to either the AFO or footwear. The aim is to manipulate the shank alignment until optimal GRF alignment with the

knee and hip is achieved during mid and terminal stance.[107].

Firstly, shank kinematics are tuned at Temporal Mid-Stance (TMST), defined as 30% of the gait cycle[122] or as *“the moment the head, trunk and pelvis are aligned directly over the base of support, the foot”*[16]. It is recommended that initially the static SVA, measured during standing, is set at 10-12° inclined[16]. Then, the dynamic alignment, measured at 30% of the gait cycle, is manipulated until optimal alignment is achieved. Generally, this is considered to be when the GRF passes through the knee and just behind the hip, with the final static SVA likely to be in the range of 7-15°[123]. These ranges are based on the static SVA from 112 tuned AFOFCs[123] and supported by the mean SVA at mid-stance in 11 healthy children[124].

Following tuning at TMST, footwear may need adaptations to control shank kinematics during the entry to and exit from mid-stance. Negative and positive heels decrease and increase shank angular velocity during loading response. Alternatively, rocker soles]mimic the natural roll-over shape of the third rocker during terminal stance and pre-swing, when the metatarsal-phalangeal joint has been immobilised[16]. Additionally, point-loaded rockers may be required to control the timing of heel rise and inhibit roll-over, when there is excessive knee flexion in late stance. This facilitates the forward progression of the GRF along the foot and alignment anterior to the knee, creating an external extending moment. The main considerations for these soles are apex position, apex angle and rocker radius[125].

1.4.5 Normalisation of lever arm lengths

Finally, the algorithms highlight the importance of normalising lever arm lengths. This involves equalising leg lengths through shoe raises and normalising the foot length-to-height ratio by extending the AFO footplate length. Leg length discrepancy has been shown to negatively impact gait[126]–[128] and recent work has recommended that the clinically significant threshold should be lowered from 2cm to 1cm[126], [129]. However, the benefit of normalising the foot length-to-height ratio for paediatric populations is challenged. Firstly, the algorithms do not state the threshold of clinical significance in foot segment shortening. Secondly, evidence comparing full and 3/4 length footplates in

adult stroke populations found no significant effect on knee hyperextension[130], [131] or forward excursion of the centre of pressure[130]. Considering that children exhibit smaller foot segments and lower moments, this would suggest that foot segment length does not significantly influence paediatric gait.

1.4.6 Challenges with implementing OSKAR in clinical practice.

Despite the publication of the algorithms in the early 2000s and recommendations for its use[1], [2], a survey by Eddison et al. found that clinical uptake of OSKAR has been limited[116]. Of the 41 orthotists that responded to the survey, only 50% reported they performed tuning as standard during AFO prescription. The main barriers identified were the accessibility of 3-Dimensional Motion Capture (MOCAP) (30%) and a lack of time (27%). However, whilst only 7% of respondents identified a lack of understanding of OSKAR as a barrier, the author found that the responses imply this is a larger issue. Firstly, OSKAR is performed using 2-dimensional video vector analysis, meaning accessibility to MOCAP should not limit its application. Furthermore, approximately half (49%) of respondents said they did not consider the design of the AFO when applying OSKAR, whilst 94% failed to identify all the physical barriers which may limit the success of the process[116]. This confusion could result from either limited training opportunities or the complexity of the algorithms. Combine this with the issue of time, and it would suggest there is a need to streamline the process to aid clinical implementation. Furthermore, a valid criticism of this survey is its scope, as it was restricted to private orthotists only and the number of responses equated to 9% of the total UK orthotist workforce. However, extending the survey to NHS-based orthotists, where time constraints are generally higher and accessibility to technology more limited, it is likely even more alarming results would be seen.

However, whilst there is a need to improve the efficiency of OSKAR, paradoxically, the addition of another algorithm is of greater importance. As discussed in Section 1.3.2 and 1.3.3, the success of OSKAR is dependent on prescribing a rigid AFO with sufficient stiffness to immobilise the ankle and control shank kinematics. However, although rigid AFO stiffness is determined by its design, OSKAR does not explain how to tailor the design to account for the mass, height and activity levels of the individual, which will

dictate the magnitude of the external moments generated during gait. As a result, even if OSKAR is implemented, its effectiveness could be undermined by the flexibility of the prescribed AFO. This may have detrimental effects on the patient, allowing the severity of musculoskeletal impairments to progress, as alignment facilitating stretching is lost, and increasing the risks of falls, through insufficient musculoskeletal support. Meanwhile, the replacement of the faulty device will incur additional costs and appointments, and delay the start of the intervention. Therefore, developing an additional algorithm that directs the design process is arguably a more pressing issue. Consequently, the remainder of the thesis will focus on understanding the relationship between rigid AFO design factors, the mechanical properties of the device and their clinical performance, beginning with an extensive review of the literature.

Chapter 2

Review of literature surrounding the clinical performance and mechanical properties of rigid AFOs.

Chapter Overview

The following chapter presents three consecutive reviews (Figure 2.1). The first is a scoping review that aimed to map the literature on the effects of rigid AFOs on gait outcome measures in children with CP and identify gaps for future research. It concluded that the inappropriate rigid AFO design may limit the effects on gait outcomes. As a result, the second review explored the evidence for the relationship between AFO design factors and the mechanical properties of the devices. This highlighted a lack of research in paediatric, rigid AFOs and a need to investigate the interactions between all four design factors to inform clinical practice. Finally, the third narrative review, aimed to determine the most appropriate method for quantifying AFO mechanical properties, building on previous reviews in the area.

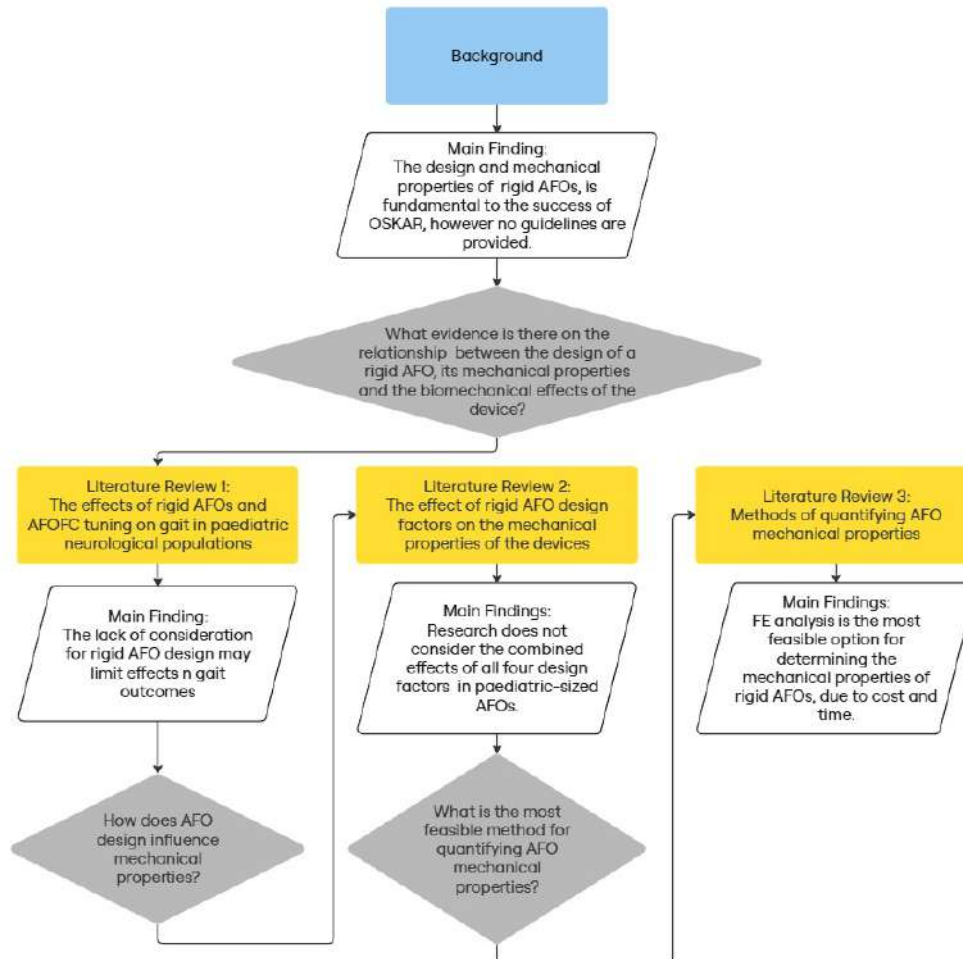


Figure 2.1: Flowchart for the link between the three literature reviews.

2.1 The effects of rigid AFOs and AFOFC tuning on gait in paediatric neurological populations

2.1.1 Introduction

Rigid AFOs play a key role in managing gait impairments in CP. However, there is a growing belief that to optimise their performance, both the design and alignment of the devices must be considered during prescription, through a process known as OSKAR. However, despite recommendations for the use of OSKAR[1], [2] and published algorithms to guide its implementation[16], [17], results of a survey suggest clinical uptake of OSKAR has been limited, with only 50% of the 41 respondents performing tuning as standard[116]. As a result, the following review aims to evaluate the effects of rigid AFOs on gait impairments in children with central nervous system disorders and highlight any differences in performance when the principles of OSKAR have been applied. Therefore, it will identify the benefits of the approach and any limitations on rigid AFO performance.

Previously, several reviews have critiqued the literature surrounding the efficacy of AFOs on gait outcome measures in CP[1], [132]–[141], although only one focused on the benefits of tuning AFOs[108]. Moreover, they often have limited scope, with papers excluded based on study design[133], [135], [136], [138], [140]–[142], patient characteristics[142] and the outcome measures assessed[135]. Furthermore, existing reviews tend to present the global effects of AFOs[1], [133], [137], [141], [143], neglecting the functionality of the various subtypes, whilst those that isolate each subtype are now outdated[134], [136]. Meanwhile, only two previous reviews have considered additional paediatric central nervous system disorders, such as spina bifida[144], [145], which may provide additional information considering the similarities between the conditions. Finally, systematic reviews have been favoured, which requires homogeneity between papers to conduct meta-analysis[146]. However, heterogeneity between papers investigating interventions in CP has been highlighted due to variation in the impairments between participants and poor reporting standards[1], [147]. As a result, critical flaws have been found in most systematic reviews in this area[148], indicating that a systematic, scoping review methodology is more appropriate.

2.1.2 Identification of research questions

Methodologies outlined by Arksey and O'Malley[149], PRISMA guidelines[150] and additional available literature[151] were followed when conducting this scoping review. This methodology begins with identifying research questions, which are as follows.

1. What are the effects of rigid AFOs on the outcome measures of gait in children with central nervous system disorders?
2. What effect has the biomechanical optimisation of rigid AFOs, through OSKAR, had on the performance of the devices?
3. What are the limitations on the performance of rigid AFOs in managing gait impairments in children with central nervous disorders, and how could they be improved?

2.1.3 Identification of relevant studies

PubMed, APA PsycInfo, Cochrane, CINHALL, Embase and Google Scholar databases were searched using the strategy outlined in Table 2.1 for papers published before 2021.

Table 2.1: Search strategy used to identify relevant articles.

Search terms	Boolean operator	Search fields by database
"AFO" OR "ankle foot orthos*" OR (ankle AND (brace OR bracing OR splint* OR strap*))	-	Title, Abstract & Keyword
neuro* OR "cerebral palsy" OR CP OR "spina bifida" OR "multiple sclerosis" OR diplegia OR hemiplegia OR quadriplegia OR dyskin* OR myelomeningocele OR nervous OR "brain injury" OR "neuromuscular"	AND	Title, Abstract & Keyword
gait OR walk* OR move* OR flex* OR exten* OR stability OR balance OR standing OR metabolic OR energy OR muscle OR kinetic* OR kinematic* OR force OR joint angles OR motion OR reaction OR biomechanical OR activity OR exercise	AND	Title, Abstract & Keyword
botulinum OR surg* OR FES OR stimulation OR upper OR robotic OR hand OR elbow OR wrist OR finger OR shoulder OR arm OR "brain machine interface"	NOT	Title

2.1.4 Study Selection

The results of these searches were screened against the criteria presented in Table 2.2. Title and abstracts were initially screened, before screening the full texts of the remaining sources. The first 50 papers were screened by two assessors (SD and JR) to ensure selection bias was mitigated. Any disagreements between the two assessors were resolved through discussion with a third (RJ). Figure 2.2 presents the results of this process.

Table 2.2: Inclusion and Exclusion criteria for the scoping review. AFO = Ankle-foot orthosis. CP = cerebral palsy. GMFCS = Gross motor function classification system. SEML = Single-event multi-level surgery.

Inclusion Criteria	Exclusion Criteria
Studied the isolated effects of a solid/rigid/fixed AFO	Studies that included multiple interventions Cohorts which included individuals who had undergone isolated surgery within 12 months of the study, SEML surgery within 24 months, botox injections within 6 months
Studied the effects of the AFO on children (0-18yrs) with a central nervous system disorder	Primary CP diagnosis other than spasticity
GMFCS level 2 or ambulatory without the additional walking aids	GMFCS level 3 and above or the use of additional walking aids during testing
Quantitative evaluation of the AFO in walking trials	Studies that did not use dynamic walking trials or a baseline comparator Solely qualitative or simulation studies
Peer-reviewed journal articles	Conference proceedings, commentaries, and reviews

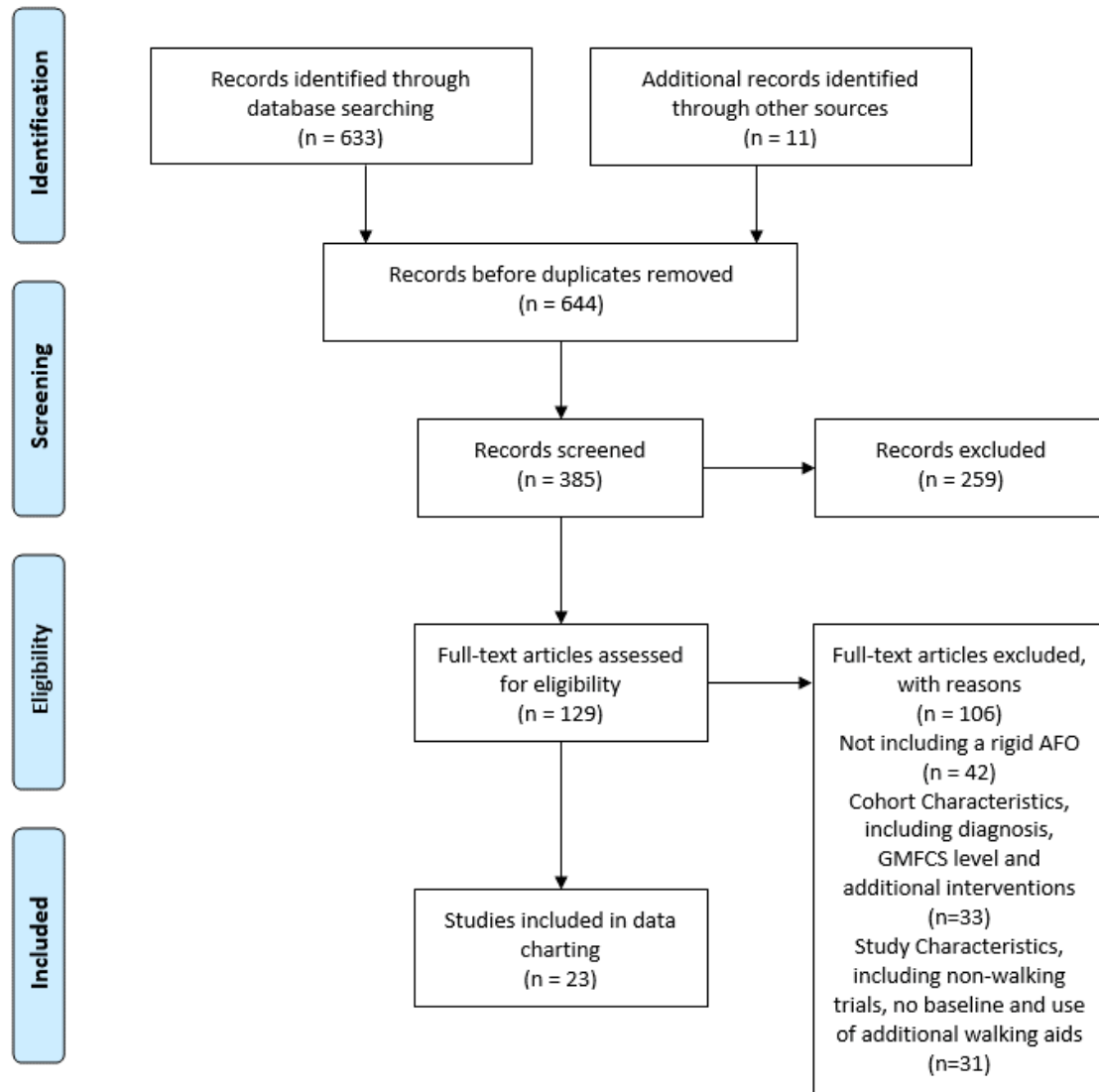


Figure 2.2: PRISMA flowchart of the screening process for the scoping review

2.1.5 Charting Data

Several charting forms were designed and piloted to include all the relevant information to answer the research questions. The first five papers were charted by two assessors (SD and JR) to mitigate charting bias. The study characteristics were analysed based on best reporting guidelines for AFO interventions in CP[117], [147] and the outcome measure tested were charted to identify how the effects of AFOFC tuning had been assessed.

2.1.6 Summary of results

Table 2.3: Characteristics of papers related to rigid AFO outcomes on gait in paediatric neurological populations. AS = Anterior Shell, BF = Barefoot, BI, Brain Injury, CF = Carbon Fibre CP = Cerebral Palsy, HypExt = Knee Hyperextension, NT = Non-tuned, P = Pathological, PP = Polypropylene, PPC = Copolymer Polypropylene, PPH = Homopolymer Polypropylene, SB = Spina Bifida, SMO = Supramalleolar Orthosis, TD = Typically Developing. ^a = AFO type dependent. ^b = GMFCS I & II combined.

Article	Study Design		Participant Characteristics					AFO Design Properties				
	Sample Size (P / TD)	Controls	Age / yrs	Diagnosis	Topography (Uni/Bi/Quad)	GMFCS (L1/L2/L3)	Gait Impairment	AFO Type	Material Type	Thickness / mm	Trim line (Ankle/MTPJ)	Ankle Stiffness / Nm/°
Eddison et al., 2020b[118]	4/0	BF NT TD	7-11	CP	1/4	0/4/0	Winter's II + IV	Rigid	PPH	4.5, 5	Anterior / Distal	-
Eddison et al., 2020a[152]	4/0	BF NT	7-11	CP	1/4	0/4/0	Winter's II + IV	Rigid	PPH	4.5, 5	Anterior / Distal	-
Meyns et al., 2020[153]	15/0	S	10(2)	CP	1/14	2/11/2	-	AS-Rigid	CF	-	-	0.7-3.8
Ries & Schwartz, 2019[154]	147	-	11.5±3.8 or 14.1±6.5 ^b	CP	0/174	5/36/51	Crouch	Rigid AS-Rigid	-	-	-	-

Jagadamma et al., 2015[119]	8/11	BF TD NT	P = 5.6-12.5 TD = 5-15	CP	5/3	-	Crouch Jump Equinus	Rigid	PP	3, 4.5, 6	Anterior / -	-
Kerkum et al., 2015[155]	15/0	S	10(2)	CP	1/14	2/11/2	-	AS-Rigid	CF	-	-	0.7-3.8
Dalvand et al., 2013[156]	30/0	BF	4-8	CP	0/30	10/1/3	-	Rigid Articulated	PP	-	Anterior / Distal	-
Kane & Barden, 2010[157]	1/0	BF TD	14	SB	0/1	-	crouch	AS-Rigid Articulated	PP	5 or 6 ^a	Anterior / Proximal	-
Jagadamma et al., 2009[158]	5/0	NT	5.6-12.6	CP	3/2	-	Genu recurvatum	Rigid	-	-	-	-
Brehm, Harlaar & Schwartz, 2008[159]	181/0	BF	4.6-18.4	CP	23/103/55	-	-	Rigid Flexible	-	-	-	-
Hayek et al., 2007[160]	56/0	BF	4-17	CP	18/38	15/23	-	Rigid Articulated	-	-	-	-
Buckon et al., 2004[161]	16/0	BF S TD	4.33-11.5	CP	0/16	4/12/0	-	Rigid Articulated Flexible	PP	4, 4.8	Anterior / Distal	-

White et al., 2002[162]	115/25	BF TD	P= 5-15 TD = 4-12 or 18-21	CP	18/97	62 ^b /53	-	Rigid Articulated	PP	3.2, 4.8	Anterior / Distal	-
Buckon et al. 2001[163]	30/0	BF S TD	5.25-15.25	CP	30/0	-	-	Rigid Articulated Flexible	PP	4, 4,8	Anterior / Distal	-
Duffy, Gra- ham & Cosgrove, 2000[164]	12/10	BF	6-16	SB	0/12	-	-	Rigid	PP	-	Anterior / Distal	-
Galli et al., 2000[165]	10/20	BF TD	6-14	SB	-	-	-	Rigid	-	-	-	-
Freeman, Orendurff & Moor, 1999[166]	1/0	BF TD	15	SB	0/1	-	-	AS-Rigid	PPC	4.8	- / Distal	-
Rethlefsen et al., 1999[167]	21/0	TD	5.3-13.5	CP	0/21	-	-	Rigid Articulated	-	-	-	-
Thomson et al., 1999[168]	28/0	BF TD	2-9	SB	2/26	-	-	Rigid	PP	-	-	-
Abel et al., 1998[169]	35/0	BF	2.5-19	CP	0/35	-	Equinus	Rigid	PP	-	Anterior / -	-

Brunner, Meier & Ruepp, 1998[170]	13/0	BF	6.46 - 20.08	CP BI	13/0	-	-	Rigid Flexible	PP	-	Anterior / Distal	-
Radtka et al., 1997[171]	10/0	BF	3.5-8.5	CP	4/6	-	Equinus	Rigid SMO	PP	4.8	Anterior / Distal	-
Middleton, Hurley & McIlwain, 1988[172]	1/0	S	4.5	CP	0/1	-	Genu recurvatum	Rigid Articulated	PP	-	-	-

Study Characteristics

In total, 23 papers were included in this review, however the papers by Meyns and Kerkum et al.[153], [155] and the two papers by Eddison et al.[118], [152] both represented multiple analysis of one data set. The characteristics of these articles are broken down in Table 2.3. The papers included participants aged 2-19yrs and mainly focused on CP populations, except for five which looked at spina bifida[157], [164]–[166], [168] and one brain injury[170]. Eleven investigated a rigid AFO in isolation[118], [119], [152], [153], [155], [158], [164]–[166], [168], [169], whilst the remaining 12 drew comparisons between at least one other type of AFO. The majority used barefoot controls, however shod was used in five[153], [155], [161], [163], [172] and 10 studies included normative data[118], [119], [157], [161]–[163], [165]–[168]. Reporting of patient characteristics was varied with all the papers detailing the topography of the disorder, however only nine classified the participants' gait patterns[118], [119], [152], [154], [157], [158], [169], [171], [172], although others provided information on specific gait impairments[153], [155], [163], [164], [166], [167], and only nine of the 21 papers published after its creation in 1997, provided gross motor classification system levels[118], [152]–[156], [160]–[162]. A similar pattern was seen when looking at AFO characteristics. Fifteen studies specified polypropylene as the material[118], [119], [152], [156], [157], [161]–[164], [166], [168]–[172]. However, only three differentiated between the types of polypropylene[118], [152], [166] and only nine reported the thickness, which ranged from 3-6mm[118], [119], [152], [157], [161]–[163], [166], [171]. Meanwhile, two studies tested prepeg carbon devices[153], [155] and six did not state the material of the AFO[154], [158]–[160], [165], [167]. Twelve papers tested AFOs with anterior to the malleoli trim lines[118], [152], [156]–[158], [161]–[164], [169]–[171], whilst 11 reported the trim lines at the the metatarsal-phalangeal joint[118], [152], [156], [157], [161]–[164], [166], [170], [171]. In addition, only two papers reported the stiffness of the device used, ranging from 0.7–3.8 Nm/°[153], [155], however they represented multiple analysis of the same data set.

Finally, the principals of OSKAR were applied in seven papers[118], [119], [152], [153], [155], [158], [172] representing five distinct data collections, however, one paper was published before the development of OSKAR and so only referred to individualising the ankle angle of the AFO[172]. All the remaining six papers optimised shank kinematics

at TMST, whilst Eddison et al.[118], [152] and Jagadamma et al.[119] used adapted footwear to tune shank kinematics during the entry and exit from TMST. In the other studies, no footwear adaptations were made, which seems appropriate given there were no indications for this[153], [155], [158]. When considering the design of the rigid AFO, all referred to the device being stiff enough to resist deformation during stance, however only Kerkum et al.[155] and Meyns et al.[153] reported the stiffness of the AFO. Furthermore, only Eddison et al.[118], [152] and Jagadamma et al.[119] individualised ankle angles based on passive ankle range, whilst only Jagadamma et al.[158] referenced normalisation of lever arms. Four compared the effects of tuned to untuned AFOs[118], [119], [152], [158].

Table 2.4: Breakdown of outcome measures assessed by article. Grey shading = Articles which compared tuned v untuned AFOFCs. * = Additional outcome measures were tested, but the effects of rigid AFOs could not be isolated.

Article	Kinematics	Kinetics	Muscle structure & function	Spatiotemporal	Gait Quality	Gait stability	Gait Efficiency	Functional Scores
Eddison et al., 2020b	✓			✓				
Eddison et al., 2020a				✓			✓	
Meyns et al., 2020	✓	✓		✓		✓	✓	
Ries & Schwartz, 2019	✓							✓
Jagadamma et al, 2015	✓	✓		✓				
Kerkum et al, 2015	✓	✓		✓			✓	
Dalvand et al, 2013								✓
Kane & Barden, 2010	✓			✓				
Jagadamma et al, 2009	✓	✓		✓				
Brehm, Harlaar & Schwartz, 2008*				✓	✓		✓	
Hayek et al, 2007*	✓			✓	✓			
Buckon et al, 2004	✓	✓		✓			✓	✓
White et al, 2002				✓				
Buckon et al 2001	✓	✓		✓			✓	✓
Duffy, Graham & Cosgrove, 2000	✓	✓		✓			✓	
Galli et al, 2000		✓					✓	
Freeman, Orendurff & Moor, 1999	✓	✓	✓	✓				
Rethlefsen et al, 1999	✓	✓	✓	✓				
Thomson et al, 1999	✓	✓		✓				
Abel et al, 1998*		✓						
Brunner, Meier & Ruepp, 1998	✓		✓					
Radtka et al, 1997	✓		✓	✓				
Middleton, Hurley & McIlwain, 1988	✓	✓			✓			

Ankle Kinematics and kinetics

Compared to barefoot controls, rigid AFOs restricted ankle range of motion[157], [161], [163], [168], [170], resulting in greater dorsiflexion during early stance[161], [163], [168], [170], [171] and swing[161], [168], coupled with limited dorsiflexion in terminal stance[166], [168]. Furthermore, one study found they can normalise foot progression angle[168]. However, their effect on the timing of peak angles is equivocal[161], [168]. Similarly, compared to shod controls, the range of motion was reduced[155] whilst dorsiflexion at initial contact was increased[155], [167]. However, no significant difference was found in dorsiflexion at mid-stance[155] or terminal stance[167].

Comparing the behaviour of rigid AFOs to articulated AFOs, dorsiflexion at terminal stance was reduced[167], alongside the magnitude and timing of maximum dorsiflexion in stance[157], [161], [163]. However, there was no difference in dorsiflexion at initial contact[155], [160], [161], [163], [167], mid-stance[155] or swing[161], whilst conflicting evidence for the effects on range of motion[155], [157], [161], [163] was reported.

Meanwhile, compared to flexible AFOs, Brunner et al. found maximum dorsiflexion and plantar flexion were significantly increased and decreased respectively[170]. However, Buckon et al. found that dorsiflexion at initial contact and range of motion was only significantly affected in unilateral CP, whilst maximum dorsiflexion in stance or swing was not significantly different in either uni- or bilateral[161], [163]. In addition, Radtka et al. found no significant difference in dorsiflexion at initial contact or mid-stance when comparing rigid AFOs to supra-malleolar orthoses[171]. Finally, ankle kinematics were not used as an outcome measure in any of the four studies comparing tuned to non-tuned AFOFCs[118], [119], [152], [158].

In terms of kinetics, rigid AFOs increased internal and external dorsiflexion and plantar flexion moments across the gait cycle towards typical levels when compared to barefoot[119], [161], [164], [166], [168], [169] and shod controls[155], [167]. However, these results were not replicated against other AFO types[155], [161], [167], whilst an adverse reduction in ankle power generation was reported against all control types[153], [155], [161], [163], [167]–[169], whereas, power absorption[161] and timing of peak power[155],

[161] were not affected. Finally, AFOFC tuning significantly increased external plantar flexion moments beyond normative controls in one study, whilst external dorsiflexion moments were unaffected[119].

Knee kinematics and kinetics

Rigid AFOs were found to both increase and decrease knee flexion across the gait cycle and knee range of motion versus barefoot controls[119], [163], [166], [168], [170], whilst decreasing peak extension and flexion in stance versus shod controls[153], [155]. Furthermore, one study found knee transverse range of motion increased[168]. However, generally, rigid AFOs were found to have little impact on knee kinematics when compared to barefoot[119], [157], [161]–[164], [170], [171], shod[155], [167] or additional AFO baselines[153]–[155], [157], [161], [167], [170]. A similar pattern was found when looking at knee kinetics. Four studies reported either a significant decrease in internal knee extension moment[153], [155], [166], [168] or an increase in external knee flexion moment[119] versus barefoot and shod, however the majority of studies reported no change in kinetics compared to additional AFO types[119], [153], [155], [158], [161], [166], [167], [169], [172].

Three papers compared the effects of tuned and untuned rigid AFOs on the knee. Eddison found that knee extension and range improved in 2/5 children, whilst 3/5 experienced an improvement in knee flexion, where an improvement meant closer to typically developing controls[118]. Meanwhile, Jagadamma reported that tuned AFOFCs significantly reduced knee range of motion and peak knee extension in stance, in all participants. This was coupled with non-significant increases in knee flexion at initial contact and peak knee flexion during stance[119]. These changes were reflected in kinetics, where peak external knee flexion moments were non-significantly increased and peak external extension moments reduced. At a group level, all these changes were away from typical controls, however, when looking at specific gait patterns, knee extension was reduced towards normative controls for extended and jump gait patterns. Furthermore, similar increases in knee flexion were reported in five children with knee hyperextension, however, there were no significant differences in knee moments[158].

Hip kinematics and kinetics

Unlike the ankle and knee, the hip was observed in all three planes of motion, however, there were only isolated significant results reported. Duffy et al. found a significant increase in mean flexion at initial contact[164]. Meanwhile, significant changes in the sagittal and coronal range of motion were reported[119], [165], [170] alongside a significant increase in external flexion/extension moments[119] against barefoot controls. However, generally, AFOs had limited impact on hip kinematics and kinetics when compared to barefoot and shod controls[119], [155], [157], [161], [164], [170], [171]. In addition, two studies looked at the effect of AFOFC tuning on the hip. Eddison et al. reported that all five children in their case series experienced improvements in hip flexion following the use of a tuned AFOFC, whilst 4/5 saw improvements in hip range of motion and extension[118]. Alternatively, Jagadamma et al. found that AFOFC tuning had no significant impact on hip or pelvis kinematics or external moments in 8 children[119].

Pelvis kinematics and kinetics

No change in sagittal pelvic kinematics versus barefoot or shod controls was reported[119], [161], [165], [170], [171], however, the range and peak obliquity and transverse motion decreased in rigid AFOs versus barefoot in two studies[165], [170]. Furthermore, whilst Jagadamma et al. found no significant effect on pelvis tilt following AFOFC tuning[119], Eddison et al. reported that for 4/5 children, the range of pelvic tilt improved following tuning, defined as moving closer to the typical developing control[118].

Trunk kinematics and kinetics

Finally, only Meyns[153] and Radtka et al.[171] reported on trunk kinematics, with the only significant results being an increase in lateral flexion and rotation range of motion when comparing rigid AFOs to shod controls[153]. The effects of AFOFC tuning on the trunk were not explored.

Muscles Structure and Function

Three studies have investigated the effects of rigid AFOs on muscle activation[166], [167], [171], however, only Freeman et al. reported any significant difference, finding

anterior shell rigid AFOs reduced mean vastus lateralis and rectus femoris activity in late stance to near normal levels.

Spatiotemporal Parameters

When comparing walking in rigid AFOs to barefoot walking, the literature is equivocal to the effects on walking speed and cadence compared to barefoot. Seven studies found an increase in gait velocity whilst wearing a rigid AFO compared to barefoot walking[119], [157], [159], [162], [164], [168], [170], whilst five studies found no difference[118], [161], [163], [166], [171]. Similarly, four studies found a significant decrease in cadence[161], [163], [170], [171] whilst four found no difference or that cadence increased[119], [162], [164], [168]. Alternatively, there was an increase in step or stride length when walking[119], [161]–[164], [166], [168], [170], [171], alongside an increase in single[162], [170] and double support time[164], [167], [170], when compared to barefoot conditions. However, study cohorts tended to walk slower and take shorter strides than typically developing controls[119], [161], [163], [166]. Alternatively, out of the nine studies which compared rigid AFOs to shod or additional AFO conditions[153], [155], [157], [159], [161], [163], [167], [170], [171] only two studies reported a difference in spatiotemporal outcomes. Brunner et al. found significant differences between rigid and flexible AFOs for velocity, stride length and single support time[170], whilst Rethlefsen et al. found double support to be significantly longer than when wearing articulated AFOs[167]. Finally, two studies found cadence, velocity, and stride length were not significantly affected by AFOFC tuning[119], [158], whilst, Eddison et al. reported that 4/5 children covered the most distance and walked the quickest in tuned conditions[118].

Overall Gait Quality

Brehm et al. assessed overall gait function using the Gillette gait index but found no difference between rigid and flexible AFO or barefoot conditions[159]. In addition, Middleton et al. assessed gait symmetry between limbs, finding it improved when rigid AFOs were worn versus barefoot walking[172]. Finally, the effects of AFOFC tuning on gait quality were not investigated.

Gait Stability

Two papers, representing one data set, reported on gait stability, which did not consider AFOFC tuning. This demonstrated that anterior shell, rigid AFOs reduced the medio-lateral margin of stability compared to shod and articulated AFO conditions. However, no difference was found in the anteroposterior direction[153], [155].

Gait Efficiency

Walking in rigid AFOs was found to significantly reduce the energy cost of walking ($\text{mlO}_2/\text{kg}/\text{m}$) compared to shod conditions[153], [155], [161]. However, Buckon et al. only saw these results in cohorts with bilateral topography[163]. Alternatively, Brehm et al. found no difference in non-dimensional energy cost when comparing rigid AFO walking to barefoot[159]. In terms of oxygen consumption ($\text{mlO}_2/\text{kg}/\text{min}$), Buckon et al. again found this was significantly reduced in bilateral cohorts only when comparing rigid AFOs to shod conditions[161], [163], however three studies found no difference when comparing to barefoot[152], [164], [165]. Finally, no difference was seen in any measure when comparing walking in different AFO types[153], [155], [159], [161], [163], although Eddison et al. did show improvements in oxygen consumption and the energy demand to complete a task following rigid AFO tuning in 3/4 children[152].

Functional Ability

When comparing rigid AFO walking to barefoot, Buckon found significant improvements in subsections of gross motor function and performance, motor proficiency and the paediatric evaluation of disability inventory. However, these were topography-specific, and these results were not replicated when compared to additional AFOs[161], [163]. However, improvements in gross motor function were supported by results from Dalvand et al.[156] compared to barefoot walking. Finally, the effects of AFOFC tuning on functional ability were not investigated.

2.1.7 Discussion

The effects of rigid AFOs were most prominent at the ankle, reinforcing the relationship between increased AFO stiffness and reduced range of motion and power genera-

tion[132]–[134], [136], [138], [173]. Although, this did not translate into a decrease in the efficiency of gait, increasing AFO stiffness has been shown to increase the energy cost of walking by restricting push-off[174]–[176]. This highlights that biomechanical control exerted by rigid AFOs can inhibit some gait functions. Additionally, rigid AFOs are intended to increase stability, one of the key attributes of gait. Increases in stability during static standing and functional tasks have been demonstrated in both CP[177], [178] and stroke populations[179], [180]. However, although this review highlighted increases in step and stride length[119], [161]–[164], [166], [168], [170], [171], [181] and single-limb support[162], [170] when wearing a rigid AFO, only Meyns et al. directly assessed dynamic stability, finding rigid AFOs reduced mediolateral stability[153]. This may be because immobilising the ankle limits the individual's ability to react to gait perturbations, as shown in young typically developing adults wearing semi-rigid AFOs[182], however, there is insufficient evidence to conclude from.

On the other hand, evidence supporting the effects of rigid AFOs on the more proximal joints and segments is scarce. The lack of consensus is partly due to how the studies were structured, with the majority adopting a cross-sectional, cohort design. Previously, it has been highlighted that the heterogeneity within CP study cohorts may confound group mean response to interventions, masking beneficial effects for the individual[136], [138], [183]. This review echoes these findings, as studies frequently grouped children with varying Gross Motor Function Classification System (GMFCS) levels and failed to provide sufficient detail on musculoskeletal and gait impairments. Furthermore, these effects were illustrated by Jagadamma et al, who highlighted the beneficial effects of tuning rigid AFOs for specific gait patterns, which were not evident across the cohort[119]. Therefore, future work should adopt single-subject or case series designs, as utilised by Eddison et al[118], [152], or apply best practice reporting guidelines[147].

Alternatively, the limited effects at the proximal joints may be due to a lack of consideration for shank alignment[108], [134]. When shank alignment was optimised, there was a tendency towards increased knee flexion and external flexion moments during stance[118], [119], [158]. This echoes previous observations that individuals exhibiting equinus or genu recurvatum patterns see the most improvement in knee kinematics from

shank tuning[120], [184], [185]. Meanwhile, the introduction of excessive knee flexion at initial contact[118], [119], [158] also suggests that weak quadriceps and hip extensors may be a contraindication to tuning[118]. On the other hand, improvements in pelvis, hip, and knee kinematics in individuals with excessive knee flexion were seen[118], [155], contradicting conclusions drawn by Butler[184] and Jagadamma et al.[119]. However, these were based on knee kinematics in isolation, demonstrating the benefit of a holistic approach when observing the effects of AFOFC tuning on gait outcomes.

The limited use of OSKAR within existing research reflects the trends in clinical practice highlighted by Eddison et al.[116], where a need to streamline the process was highlighted. In this review, differences were seen in the methodologies used to tune the shank kinematics. Several definitions for TMST were adopted, whilst the line representing the shank, used to measure the SVA differed with the measurement tool used. These methodological variations result in small differences in the measured SVA[122], [186], the clinical significance of which is unknown. Furthermore, the "optimal" alignment used in these studies was reported as the static SVA, without a clear definition for this position[118], [152], [158]. Although the static SVAs agreed with previously reported ranges[16], [120], [185], [187], the equivocal evidence on the agreement between the static and dynamic SVA[188], [189], challenges the validity of using the static SVA as an assessment measure. Meanwhile, the lack of an objective definition for the optimally tuned position could lead to variations across practice. As a result, OSKAR would benefit from a standard methodology for tuning shank kinematics.

Finally, the limited indirect effects of rigid AFOs may be due to deficiencies in AFO design[134]. Some studies reported ankle range of motion of greater than 5° when wearing a rigid AFO[86], [155], [157], [161], [163], [166], [168]–[170], and in two, ankle range was no different to additional AFO types designed to allow ankle motion[161], [169]. This would imply, that rigid AFOs tested, were insufficiently stiff to immobilise the ankle during gait, which may be the reason for the limited effects at the knee and hip seen in these articles[155], [157], [161], [163], [168], [170]. Meanwhile, reporting of AFO design was inadequate in the majority of studies, whilst only two papers reported the stiffness of the AFO tested[153], [155]. This is in line with existing work[1], [173],

[190], particularly the review by Eddison et al. which found the reporting of thermo-plastic type, thickness, trim line design and reinforcements ranged from 18.2% (10/55) to 43.6% (25/55), whilst stiffness was only quantified in 3.6% (2/55) of papers investigating the effects of rigid AFOs on gait in CP[190]. Consequently, it is difficult to draw inferences on rigid AFO design from current literature, as it is unclear whether the design of the AFO is suitable for its intended purpose. Together, these findings suggest issues surrounding AFO design within research, which likely impacts clinical practice as there is limited evidence to support decision-making during prescription. As a result, this reinforces the need to update OSKAR with an additional algorithm for rigid AFO design, supported by evidence for the relationship between rigid AFO properties and device stiffness.

2.1.8 Conclusions

In conclusion, rigid AFOs have been shown to exert direct biomechanical control over the ankle, however, their effects on the proximal joints are limited. One explanation for this may be the lack of use of OSKAR, reflecting the clinical findings by Eddison et al.[116]. This strengthens the need to streamline the process, which could be helped by the development of a standard tuning methodology. However, more pressingly, OSKAR lacks guidance on how to design rigid AFOs with adequate stiffness, which is fundamental to the shank tuning process and the performance of the devices. This review highlighted evidence which suggests that the indirect biomechanical effects of rigid AFOs may be hampered by the use of inappropriately designed devices. As a result, the remainder of this thesis will focus on the relationship between rigid AFO design and the mechanical properties of the device, with the long-term aim of developing an algorithm to guide AFO prescription.

2.2 The effects of rigid AFO design factors on the mechanical properties of the devices

2.2.1 Introduction

As highlighted in Section 1.3.3, AFO stiffness determines the biomechanical control exerted by the device over the ankle joint and is therefore fundamental to the clinical outcomes of OSKAR. Despite this, the previous review (Section 2.1) highlighted examples where rigid AFOs with insufficient stiffness to immobilise the ankle joint were tested[86], [155], [157], [161], [163], [166], [168]–[170], suggesting issues with the design of these devices. During gait, AFOs are susceptible to buckling during mid-stance when rotation is centred at the ankle. As a result, to maintain optimal shank alignment, the AFO must be stiff enough to resist deformation under the external dorsiflexion moments, which can reach $\approx 1\text{Nm/kg}$ [93]–[95], [97]–[99], [191].

The ankle stiffness of AFOs is determined by several design factors including thermoplastic type and thickness, trim line design and reinforcements[80]. During the prescription process, the clinician tailors the AFO to the individual's needs, including customisation of the design. However, in the absence of clinical guidelines, the prescription is reliant on expertise, which may result in an inefficient trial and error process to achieve the desired mechanical properties, or worse, the provision of a rigid AFO with insufficient stiffness. As a result, clinical practice would benefit from a more thorough understanding of how AFO design properties influence the stiffness of the device.

Previously, Nagaya found that the depth of the trim line at the ankle and the thickness of the material were the key predictors for flexible AFO stiffness[192], however, this research has not been replicated in rigid devices. Therefore, the following review collates and critiques the literature surrounding the influence of AFO design factors on the mechanical properties of the devices. To the best of the author's knowledge, it is the first to do so, and will therefore identify areas which require further investigation.

2.2.2 Identification of research questions

1. How do thermoplastic rigidity and thickness, trim line design, and reinforcements influence the mechanical properties of thermoplastic AFOs?
2. How has the relationship between AFO design factors and mechanical properties been studied?
3. What are the gaps in the literature surrounding the relationship between AFO design factors and mechanical properties?

2.2.3 Search Strategy

The search strategy outlined in Table 2.5 was applied in MEDLINE, CINHALL and the Child and Adolescent Studies database, via EBSCO, ProQuest, and Web of Science to identify relevant articles published before 2024.

Table 2.5: Search strategy used to identify relevant articles. WoS = Web of Science, NOFT = Any field except full text

Search terms	Boolean operator	Search fields by database		
		EBSCO	ProQuest	WoS
AFO OR (Ankle AND orthos*)	-	Title	Title	Title
mechanical OR character* OR design OR manufacture OR fabrication OR construction OR stiff* OR rigid* OR resistance	AND	Title	Title	Title
material OR plastic OR thermoplastic OR polypropylene OR thickness OR trim OR shape OR geometry OR reinforce*	AND	Abstract	NOFT	Abstract
"knee-ankle" OR "hip-knee-ankle"	NOT	Title	Title	Title

After removing duplicates, papers were screened based on the criteria highlighted in Table 2.6. This was a two-step process, first papers were screened based on the title and abstract and then the full paper. Figure 2.3 presents the results of this process, which yielded 18 papers which were included in this review.

Table 2.6: Inclusion and Exclusion criteria for the review. AFO = Ankle-foot orthosis, CAM = Computer-aided manufacture.

Inclusion Criteria	Exclusion Criteria
A non-articulated, passive AFO made from a solid material.	No AFO or An AFO which is articulated, non-solid, modular or active e.g. fabric braces/ powered orthotics.
Quantifies the mechanical properties of the AFO.	Papers which fail to quantify mechanical properties
Compares at least one AFO design condition to a baseline AFO.	Papers which do not compare the design condition to a baseline.
Any age group or condition.	Papers investigating the feasibility of CAM or comparing AFOs made from different manufacturing techniques.
Full papers published in English in a peer-reviewed journal.	Abstracts/short communications, conference proceedings, commentaries/opinions pieces, qualitative studies, reviews.

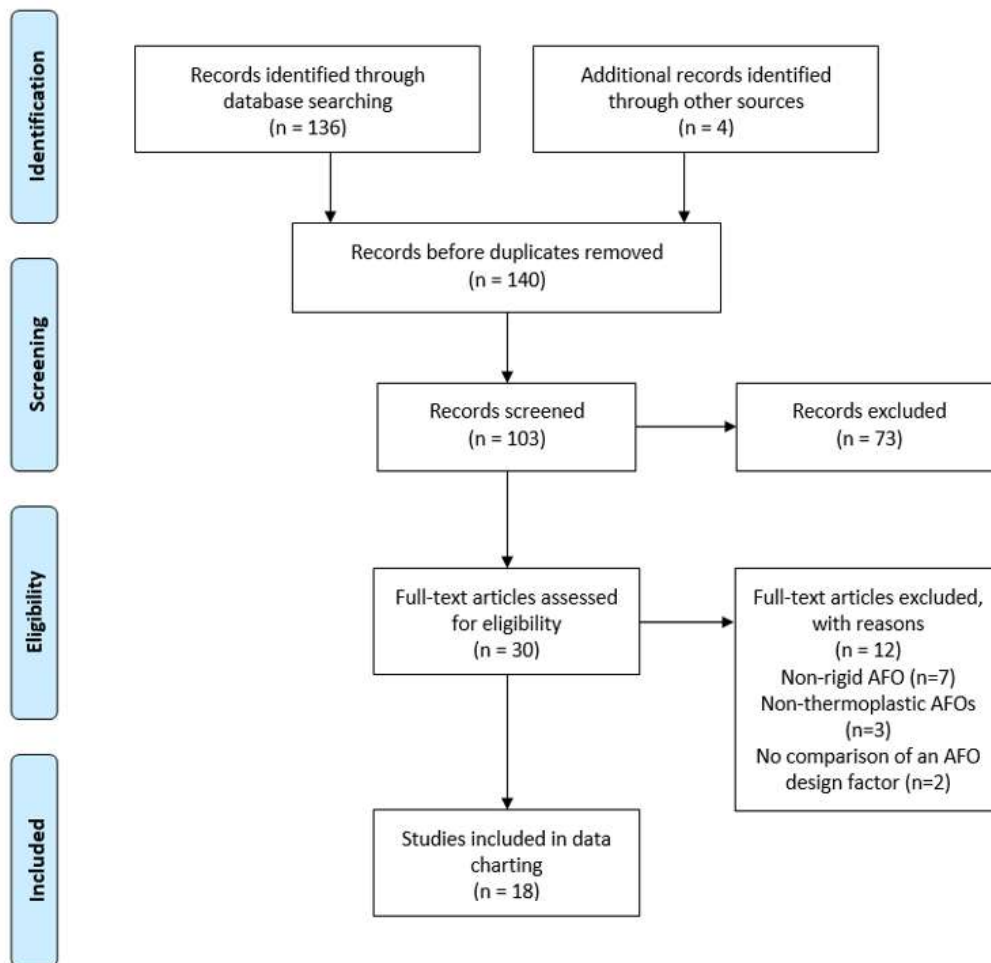


Figure 2.3: PRISMA flowchart of the screening process for the scoping review

2.2.4 Results

Table 2.7: Characteristics of articles investigating the effects of AFO design factors on the mechanical properties of the devices. FE = Finite Element Analysis

Articles	Design factors				AFO type	AFO size	Mechanical properties	Measurement technique
	Material type	AFO thickness	Trim line design	Reinforcements				
Chazistergos et al., 2023[193]		✓		✓	Rigid	Adult	Stiffness (Nm/°)	FE
Fatone et al., 2022[194]		✓		✓	Rigid	Child	Stiffness (Nm/°)	Test rig
Go et al., 2022[195]		✓	✓		Rigid Flexible	Adult	Torque at applied deflection (Nm/°)	Test rig
Sumihira et al., 2022[196]			✓		Flexible	Adult	Torque at applied deflection (Nm/°) In- and out-plane energy (J)	FE
Surmen & Arslan, 2021[197]			✓		Flexible	Child	Peak Von Mises stress (MPa)	FE
Kubasad et al., 2020[198]	✓	✓	✓		Rigid Flexible	Adult	Peak Stress (MPa) Deformation (mm) Factor of safety	FE
Surmen et al., 2018[199]			✓		Flexible	Child	Peak Von Mises Stress (MPa)	FE
Gao & Bedard, 2013[200]	✓			✓	Rigid	-	Deflection at applied torque (Nm/°)	Test Rig
Ramsey, 2011[201]		✓	✓		Flexible	Adult	Stiffness (Nm/°) Factor of safety	FE
Bielby et al., 2010[202]			✓		Rigid Flexible	Child	Stiffness (Nm/°)	Test rig
Novacheck et al., 2007[203]	✓	✓		✓	Flexible	Adult Child	Stiffness (Nm/°)	Test rig
Polliack et al., 2001[204]		✓			Rigid	Adult	Stiffness (lbs/°)	Test Rig

Convery, Ross & Socklingam, 2004[205]	✓				Rigid	Child	Stiffness (mm/Nm)	Test rig
Major, Hewart & MacDonald, 2004[206]				✓	Rigid	-	Torque at applied deflection (Nm/°)	Test rig
DeToro, 2001[207]	✓		✓		Rigid Flexible	Adult	Resistance to applied deflection (lbs/°)	Test rig
Singerman, Hoy & Mansour, 1999[208]			✓		Rigid Flexible	Adult	Stiffness (Nm/°)	Test rig
Sumiya, Suzuki & Kasahara, 1996[209]			✓		Flexible	Adult	Torque at applied deflection (Nm/°)	Test rig
Yamamoto et al., 1993[210]			✓		Flexible	Adult	Stiffness (Nm/°) Hysteresis	Test rig

Study characteristics

A total of 18 articles were identified that investigated at least one of the four design factors linked to AFO stiffness (Table 2.7). However, De Torro[207] and Fatone et al.[194] did not adequately control design variables so the effects of the individual factors cannot be isolated. Eight studies investigated multiple design factors[193]–[195], [198], [200], [201], [203], [207], however none studied all four. Whilst rigid AFOs were assessed in 11 studies, only three researched paediatric rigid devices [194], [202], [205]. Finally, six papers, all published since 2011, used Finite Element (FE) analysis to assess mechanical properties [193], [196]–[199], [201], whilst the rest used a test rig.

Type of thermoplastic

Four studies compared PPH and PPC AFOs[200], [203], [205], [207], although data cannot be extracted from one[207]. Devices made from PPH were found to have greater dorsiflexion and plantar flexion stiffness than PPC AFOs[200], [203] except for one study which found no difference across rigid AFOs manufactured across three centres[205]. However, this may have been due to variability in AFO thickness between the two ma-

terials. Furthermore when comparisons are made within each centre, PPH AFOs were 2-12.9% stiffer under dorsiflexion, which is comparable to the 5% increase reported by Gao et al.[200].

Meanwhile, two papers compared polypropylene and carbon fibre or carbon fibre-reinforced thermoplastic[200], [203]. Gao & Bedard found polypropylene rigid AFOs were less stiff in both dorsiflexion and plantar flexion and deformed more[200], whereas flexible AFOs tended to have greater dorsiflexion stiffness when made from PPH[203].

Additionally, one study compared rigid AFOs made from polypropylene and high-density polyethylene, finding no difference in maximum stress during dorsiflexion loading. However, polypropylene devices deformed less and had a marginally higher factor of safety[198]. Out of these five studies, only two provided the properties of the materials tested[198], [205].

Thickness of thermoplastic

Seven papers referenced the AFO thickness of both rigid and flexible AFOs[193]–[195], [198], [201], [203], [204]. However, data could not be extracted for two papers[194], [203], whilst Polliack et al. investigated loading in terminal stance, where bending occurs at the forefoot[204], and Ramsey et al. only measured plantarflexion stiffness[201].

The thicknesses tested ranged from 2.45 to 6.35mm, however, Chatzistergos et al. found their FE model did not converge for <2.62mm AFOs[193]. Go et al.[195] and Kubasad et al.[198] found increasing polypropylene thickness from 3mm to 4mm resulted in a $\approx 45\%$ increase in dorsiflexion stiffness and a $\approx 45\%$ decrease in deformation, respectively. Chatzistergos et al. found the relationship between thickness and AFO stiffness was non-linear, associated with buckling of the device[193]. In addition, increasing thickness was found to reduce maximum stress and therefore increase the factor of safety[198].

Trim line design

In total, 11 articles investigated the effect of trim line design on AFO mechanical properties. Four investigated mediolateral trim lines of flexible AFOs in isolation[196], [201],

[209], [210], however, one only looked at plantar flexion stiffness[201]. Meanwhile, five compared mediolateral trim lines in flexible and rigid devices[195], [198], [202], [207], [208], however the data could not be extracted from one[207]. Alternatively, two papers looked at a new concept which introduced flexibility by removing material from the posterior ankle[197], [199].

AFO dorsiflexion stiffness was reduced by posterior placement of the mediolateral trim lines[195], [198], [202], [208]–[210]. Meanwhile, Bielby et al found that trim lines impacted AFO stiffness in all three planes, having the largest impact in the sagittal plane and least in the transverse plane[202].

The majority of studies defined the mediolateral trim line as anterior or posterior to the malleoli, however trim lines that passed through the malleoli were seen in two studies[195], [202]. Furthermore, only five studies provided dimensions or an anatomical definition which could be used to replicate the results[195], [201], [202], [209], [210].

Reinforcements

Five articles referenced trim lines, although their effects could only be isolated in four[193], [200], [203], [206]. These reinforcements included ribbing[193], [200], [206], polypropylene cylindrical beams which followed the contours of the trim line[193], carbon fibre or carbon fibre-reinforced polypropylene L-shaped inserts[200], [206] and polypropylene Y-shaped or chevron reinforcements that sit on the posterior ankle and wrap under the malleoli[194], [203].

Novacheck et al. found the effect of the posterior chevron reinforcements on flexible AFO dorsiflexion stiffness varied with AFO size[203]. Meanwhile, Gao & Bedard, reported that posterior to the malleoli ribbing reduced polypropylene dorsiflexion stiffness by 4-10%, whilst carbon fibre-reinforced polypropylene reinforcements did not affect PPH AFO stiffness[211]. Conversely, Major, Hewart and MacDonald found ribbing increased PPC AFO stiffness by 37.5% and carbon fibre reinforcements by 55%[206]. However, they only tested one AFO of each design and AFO thickness was not monitored.

The difference in the effect of ribbing may be due to placement. Generally, the position of mediolateral reinforcements was described in relation to the malleoli[200], [206], whilst the dimensions, excluding thickness, were not reported[203], [206], [211]. Alternatively, Chatzistergos et al. investigated optimal placement and dimensions of mediolateral reinforcements through FE modelling of idealised polypropylene cylindrical beams. They found mediolateral reinforcements should be placed as anteriorly as possible and extend from around half the AFO height proximal of the ankle joint to the plantar surface of the foot[193]. Following this, they experimentally validated these findings by demonstrating that optimally designed ribbing increased rigid AFO stiffness by 83% versus clinically placed ribbing, however, AFO thickness also rose by 0.5mm.

2.2.5 Discussion

The limited evidence available supports the hypotheses that AFO stiffness increases with thermoplastic rigidity and thickness, anterior placement of the mediolateral trim lines and the use of reinforcements. However, although significant differences between conditions were reported, variations in methodologies between studies were apparent. Both bench testing and FE modelling were used and neither the reliability nor the measurement error of the technique were reported frequently. Furthermore, there were differences in how stiffness was calculated from the data. Some measured stiffness in $\text{Nm}/^\circ$ via linear regression of a moment versus deflection curve[193], [194], [201]–[203], [208], [210], as advised by Bregman et al.[92], whilst others reported stiffness in mm/Nm [205] or Nm/lbs [204], or calculated instantaneous stiffness at specific moments or deflections[195], [196], [200], [206], [207], [209]. As a result, comparing these studies is difficult and therefore the evidence is not unequivocal.

In addition, the majority of research has been conducted in adult-sized AFOs. However, the age of the model will influence both the moment of inertia of the device and the loading conditions it will experience during use. Therefore, it is difficult to generalise the behaviour of adult AFOs to paediatric populations. The same rationale can be applied to research which generalises the behaviour of one paediatric AFO across ages. Given growth rates during adolescence, it is plausible that the optimal AFO design for a 5-year-old and 15-year-old are not the same. This was highlighted by Novacheck et

al. who found AFO size was a significant factor in the stiffness of flexible devices[203]. Consequently, future investigations should assess a range of AFO sizes, aimed at different paediatric age groups, to develop a more thorough understanding of design.

Categorising the articles based on the design factors, highlighted trends within current literature. For example, the difference in AFO stiffness between posterior and anterior to the malleoli trim lines has been established. However, this is of little value when prescribing rigid AFOs, where the clinician must find a trade-off between device stiffness and the ease of donning. Instead, greater insight would come from investigating the response of AFO stiffness to incremental changes in the anteroposterior placement of trim lines. This has been carried out for flexible devices but is yet to be reciprocated in rigid AFOs[195], [201], [209], [210]. To achieve this an anatomical definition for rigid AFO trim lines is required to ensure internal validity and repeatability, however again this has only been presented for flexible AFOs[195], [201], [209], [210].

Furthermore, it highlighted that reinforcements were investigated in the joint fewest studies. The debate surrounding reinforcements is complex. Whilst they offer localised stiffness, they also influence cost, fabrication complexity and post-manufacture adjustability. The issue is further complicated by the fact there are several designs of reinforcement available. Only Major, Hewart and MacDonald[206] and Gao & Bedard[200] compared the performance of different reinforcements, producing contrasting effects of ribbing and carbon-fibre-based reinforcements. Furthermore, they only covered a section of the designs seen. Additionally, Chatzistergos et al. demonstrated that reinforcement geometry and positioning can influence stiffness[193], highlighting further considerations for their use.

Finally, grouping papers highlighted that the majority of studies only considered a single AFO design factor[196], [197], [199], [202], [204]–[206], [208]–[210]. Whilst this has provided important evidence, in practice, a clinician must consider all four factors when prescribing a rigid AFO. Moving forward, a holistic approach is required to determine the interactions between each of the four design factors. Only this will provide the evidence required to optimise the design of a rigid AFO which meets both the functional and user

requirements.

However, any future research involving vacuum formed AFOs must consider the manufacturing conditions. Firstly, the rectification of the positive moulds should be controlled, as the build-up around the malleoli can significantly reduce stiffness by pre-buckling the device and creating behaviour similar to an articulation[101]. In the articles within this review, the rectification was typically controlled using the same mould during manufacture. However, computer-aided design and manufacture offer a more efficient method of standardising the replication of positive AFO moulds. Secondly, the heating and vacuum conditions used during the draping process can influence the thickness of the device, particularly at the malleoli region where stiffness is desirable[212]. In this region, AFO thickness may be reduced by 18-29%, when compared to the pre-draped sheet thickness[101], [193], [205], [213]. Whilst it is difficult to determine whether this would result in a clinically significant change in stiffness, Convery et al. found that altering vacuuming forming conditions statistically changed AFO dorsiflexion stiffness. However, they also reported non-significant variation between AFOs manufactured by the same technician, suggesting this can act as a proxy control measure[205]. Unfortunately, many of the studies in this review were vague on how the manufacturing conditions were controlled, therefore it would be beneficial to investigate the influence of manufacturing conditions on AFO thickness further.

2.2.6 Conclusion

In conclusion, previous literature is limited, however, lends support to general hypotheses that thermoplastic rigidity and thickness, anterior trim lines, and reinforcements increase the stiffness of thermoplastic AFOs. However, it is difficult to assess the clinical significance of their effects, whilst methodological differences limit comparisons between studies. Furthermore, there were noticeable gaps surrounding the nuances of rigid AFO design, including the placement and geometry of trim lines and reinforcements, whilst a holistic approach is needed to gain an insight into the relationships between all the AFO design factors across a range of paediatric ages. However, the feasibility of achieving this using bench testing is questionable, therefore additional techniques should be explored.

2.3 Methods of quantifying AFO mechanical properties

2.3.1 Introduction

The previous reviews within this chapter have highlighted that issues surrounding rigid AFO design may be limiting their clinical performance. As a result, they argue further investigation into the relationship between design factors and the mechanical properties of the device is required to help inform AFO prescription. However, to build on existing literature, it is necessary to take a holistic approach to future work which considers the synergistic effects of several AFO design factors. To achieve this, a method of quantifying the mechanical behaviour of multiple rigid AFO design iterations is required.

Therefore, the following narrative review aims to explore the existing body of research regarding the quantification of mechanical properties of AFOs. Previous reviews into this area of literature, conducted in 2011[214] and 2019[215], identified three strategies for measuring AFO mechanical properties, including functional testing, bench testing and computational analysis. As a result, the review looks to build on these articles, incorporating relevant proceeding work to examine the merit and feasibility of each. Ultimately, the findings will provide the rationale for determining the measurement technique used to quantify AFO mechanical properties in subsequent studies conducted as part of this thesis.

2.3.2 Functional Analysis

Functional analysis involves measuring AFO stiffness in situ. Previously, the stress distribution within different polypropylene AFO designs[216] and the contribution of the AFO to ankle moments[217] have been measured using strain gauges. Meanwhile, torque sensors have been used to characterise spasticity during gait to help inform design[218], and the use of an experimental AFO facilitated the development of an AFO with adjustable plantar flexion resistance to enable heel strike within adult, post-stroke populations[210], [219]–[222].

The appeal of functional analysis is that mechanical properties are assessed within real-world conditions, meanwhile, the effects on gait outcomes can be measured simultaneously. However, the test environment is patient-specific, making comparisons across studies difficult. Furthermore, its repeatability is influenced by the consistency of gait. Therefore, issues may arise when studying individuals with CP who typically exhibit heterogeneous gait patterns, characterised by above typical stride-to-stride variability[51], [223], [224] and fatigue. Furthermore, performing functional analysis in CP populations introduces recruitment demands which are difficult to fulfil[225], [226].

2.3.3 Bench Testing

The most widely adopted technique for measuring AFO mechanical properties is bench testing, where bespoke rigs are designed to replicate the in situ loading conditions of gait, providing *"more accurate control of conditions [which] theoretically improves reliability"*[214]. Currently, there is no standard bench testing system, with designs reflecting the study aims and the environment in which it is used[173]. Most examples are purpose-built, whilst others adapted axial-torsion[193], [227] and material testing machines[206], [228]. Despite the variety of designs, all the previous solutions primarily assessed stiffness at the ankle in the sagittal plane during the second rocker of gait. However, stiffness in additional planes[202], [208], [229], [230] and at the metatarsal-phalangeal joint,[92], the neutral angle[92], [231], hysteresis[92], [203], [211], [231], [232] and diametric strain or buckling[101] were also assessed. Furthermore, when looking at existing rigs, several key design considerations are universal across all designs including the fixation of the AFO, the ankle model adopted, the loading conditions and the measurement tools used.

The majority have tended to assess the flat-foot phase of gait, clamping the entire length of the foot section of the AFO using a range of destructive[205], [206], [208], [228], [229] and non-destructive[92], [101], [102], [194], [195], [202], [203], [206], [211], [227], [230]–[236] clamping systems. There is flexibility in the design of the foot clamping system, as long as heel lift is prevented, although destructive clamping should be avoided as it may introduce atypical stress concentrations, which could influence behaviour. Meanwhile, the proximal shank is typically strapped around a bespoke last, modelled on the internal surface of the AFO[101], [102], [194], [195], [202], [207]–[209], [211], [229], [230], [232],

[233], [235], or idealised cylindrical blocks[92], [173], [203], [227], [228]. Practically, the use of idealised blocks offer greater flexibility to AFO size, which is advantageous when looking at paediatric populations. Alternatively, non-patient-specific blocks may deform the AFO before loading, pre-tensioning the material and altering its cross-section and therefore second moment of inertia. However, the significance of these effects on the behaviour of the AFO has not been studied. Alternatively, the use of a cadaver[237] or user's limb[238] was seen. This has the advantage of incorporating physiological material properties into the rig, but significantly limits scalability and introduces undesirable ethical considerations.

Regardless of the AFO clamping system, alignment of the rig rotational axis to the anatomical ankle axis is key, given a misalignment of 10mm was shown to influence both plantar flexion resistance and hysteresis by Gao et al.[239]. Anatomically, the structure of the talocrural and subtalar joints means there is debate over the location and plane of the ankle axis[240], [241]. However, the majority of rigs utilised an uniaxial hinge to represent the ankle[101], [102], [195], [203], [207], [211], [227], [231]–[233], [236], valid when investigating mechanical properties in a single plane. Multi-axis joints were seen when the behaviour in all three planes was tested[202], [208], [229], whilst some negated an ankle joint entirely[192], [203], [205], [206], [208], [229], [234], [242], however this is undesirable as AFO deformation is unconstrained. Typically, the axes were aligned visually based on both anatomical and non-anatomical definitions, which is susceptible to assessor error and potentially time-consuming when testing several AFO designs. Alternatively, Bregman et al. used a series of dummy feet, designed using paediatric normative anthropometric data, to approximate the position of the rig rotational axis[92]. Although this potentially compromises accuracy, it offers a more repeatable, user-friendly method of aligning the two axes. Moreover, Totah et al. used a coordinate transformation algorithm, based on the user's anthropometric data, to match the locations of the rig and ankle axes[231]. This negated the need for alignment altogether but increased the data processing demands. In any case, the effects of misalignment below 10mm have not been studied.

The next consideration is the measurement tools used to quantify deflection and force/torque.

An array of different tools have been used, varying in accuracy, resolution, and cost. These include goniometers[101], [209], [213], dial gauges[205], [229], [242], potentiometers[92], [202], [233], [238], encoders[194], [211], [230]–[232] and MOCAP[203], [208], [234], [237] for measuring deflection and hanging weights[205], [237], [242], force gauges[192], [207], [213], load/torque cells[194], [195], [202], [208], [231]–[233], [238], [239], [243] and force plates[92], [203], [234] for measuring force/torque. Systems using a combination of goniometry and hanging weights or manual force gauges are the most cost-effective, however produce discrete data and introduce sources of assessor error which can impact repeatability. Therefore, they are less ideal, despite Sumiya et al. developing a rig with high within-session repeatability[209]. Instead, potentiometers/optical encoders and load/torque cells facilitate continuous measurement, however, these components can vary considerably in cost and require more complex calibration. Alternatively, rigs have utilised MOCAP[203], [208], [234], [237] alongside force plates[203], [234], with Novacheck et al. demonstrating a between-session error in stiffness of 8%, considered less than the manufacturing precision of AFOs[203]. These designs may be more accessible as the technology is available across research facilities and some clinical settings, which specialise in gait analysis. Furthermore, MOCAP offers the possibility of studying AFO shell displacement, providing greater insight into how an AFO buckles during loading, building on previous work by Golay et al.[101]. However, none of the existing studies using MOCAP systems have observed this.

Finally, how rigs load the AFOs differed. Most moved the AFO through a prescribed range of motion, ranging from 50-25° plantar-dorsiflexion[92], [101], [102], [195], [202], [203], [206], [207], [211], [227], [231]–[234], [236], [238], 40-40° abduction-adduction[202], [230], [235] and 40-40°[202], [230], [235] internal-external rotation. Alternatively, torques were applied to AFOs ranging from 29-140Nm plantar-dorsiflexion[192]–[194], [205], [228], [229], [237], [242], however only Fatone et al.[194] and Klassons et al.[229] used moments relevant to gait of the user. Although both methods are acceptable, analysis of mechanical properties under the peak moments seen in gait provides information that is directly translatable to clinical practice. However, the applied torques must be relevant to the study population. For example, Chatzistergos et al.[193], applied a 30Nm dorsiflexion torque to an AFO of an adult with a mass of 64-88kg, which is less than the

peak dorsiflexion moment seen in gait, given as $\approx 1\text{Nm/Kg}$.

Additionally, loading speed varied from $0.5\text{-}100^\circ/\text{s}$ across designs[194], [206], [211], [227], [231], [232], [235], [236], [238]. Given polypropylene exhibits viscoelastic properties, it is argued speed should reflect the ankle angular velocity during the phase of gait being investigated, which in the most part, was the second rocker, where the ankle rotates at $\approx 44\text{-}\approx 93^\circ/\text{s}$ in typically developing adults, depending on walking speed[244]. However, evidence suggests that these viscoelastic effects are only significant during cyclic loading or when assessing hysteresis. Neither Yamamoto et al.[245] nor Novacheck et al.[203] found speed affected stiffness over a single load cycle, although Yamamoto failed to present evidence supporting this claim. Meanwhile, Totah et al. reported that the stiffness, hysteresis, and neutral angle of three AFOs significantly changed when increasing speed from $5\text{-}100^\circ/\text{s}$ over 10 loading cycles[246]. However, only a $0.02\text{Nm}/^\circ$ increase in stiffness was seen for the polypropylene AFO. Furthermore, comparisons between Bregman et al.'s manually operated rig and Totah et al.'s automated rig over a single cycle found they performed similarly in terms of stiffness but differed in the hysteresis loops recorded[231], [247]. This demonstrates that both manual and automated loading is acceptable, depending on the primary outcome measure being assessed.

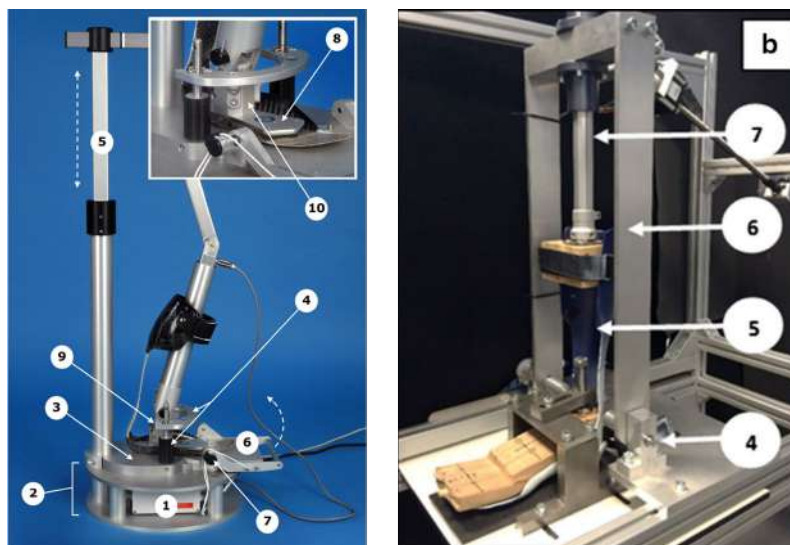


Figure 2.4: Examples of existing test rigs. Bregman et al.[92], and Ielapi et al.[248] (Left to right)

2.3.4 Finite Element (FE) Analysis

The final technique used to determine the mechanical properties of AFOs is FE analysis. This involves simulating complex physical problems as idealised mathematical models. These models consist of partial differential equations derived from the fundamental laws of physics. Complex geometry is divided into small, discrete parts known as finite elements, across which the partial differential equations are solved, allowing complex physical behaviour to be predicted[249]. Whilst FE analysis has been readily used in both structural engineering and biomechanics, until recently it has been utilised less than bench testing to investigate AFO mechanical properties, most likely due to the accessibility of technology[214], [215]. When developing a FE model there are three main considerations, discretisation, material properties and the loading and boundary conditions, all of which are critical to the accuracy of the predicted behaviour.

Previously, FE analysis has been used to determine AFO sagittal ankle stiffness and stress distribution. The simulations assess AFO models, generated through 3D or CT scanning of manufactured devices[193], [197], [232], [250]–[254], or computer-aided design based on a scan or anthropometric measurements of a leg[196], [198], [201], [255]–[260]. However, models created through computer-aided design, have an idealised shape which does not incorporate alterations made to the AFO positive moulds during rectification, such as the build-up applied to the malleoli, which have been found to affect the stiffness of the AFO[101]. Therefore, 3D scanning a manufactured AFO is preferable. Furthermore, AFOs have been modelled as both 3-dimensional, solid meshes, which replicate all three dimensions of the AFO[197], [198], [201], [250]–[255], [258], [260], and 2-dimensional, shell meshes[193], [196], [232], [256], [257], which only replicate a surface of the AFO and apply a user inputted thickness, during calculations (Figure 2.5). Shell meshes are beneficial as they simplify the models, reducing computation time. Additionally, they allow the thickness of the model to be altered manually, which could reduce the number of models required to test multiple AFO designs. However, shell meshes are prone to transverse shear locking, a phenomenon that occurs when the ratio of element size to thickness becomes too small, artificially increasing the stiffness of the mesh[249], [261]. Furthermore, shell meshes are not appropriate for surfaces with a small thickness to radius of curvature ratio as elements in the mesh can become inverted[249], [261], which

may explain why AFOs are more typically modelled using solid meshes.

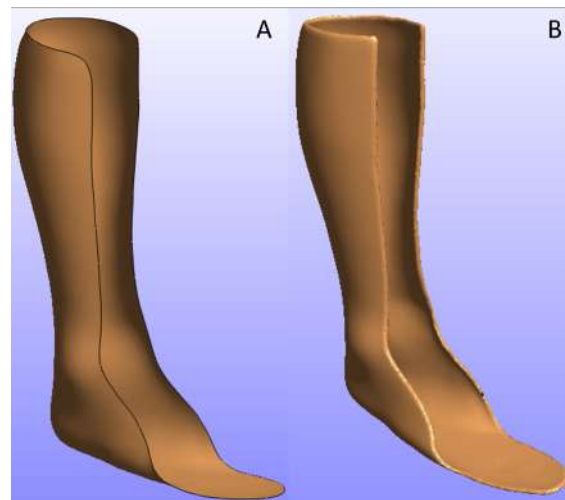


Figure 2.5: Types of FE models. A) 2-dimensional, shell model. B) 3-dimensional, solid model.

The type of mesh also influences the type of element used when discretising or meshing the AFO. Both the shape and order of the elements affect the accuracy and computational time of the model (Figure 2.6). Therefore, the decision on which type to use is a trade-off between these two factors. However, generally, quadratic elements are preferable to linear as they have additional mid-edge nodes, which allow more realistic mesh deformation[249]. For example, previous solid models have tended to use 3-dimensional, quadratic tetrahedral elements[197], [252], [253], [260], despite 3-dimensional, quadratic hexagonal elements being considered more accurate. This is because quadratic hexagonal elements have 20 nodes, compared to 10 nodes on a quadratic tetrahedral element, greatly increasing the computation time. Alternatively, 2-dimensional, linear tetrahedral[196], linear quadrilateral[232] and quadratic quadrilateral elements[193], [256], [257] have all been used when working with shell meshes. Despite this, 2-dimensional linear tetrahedral elements should be avoided, as their triangular shape creates an inherently stiff mesh. Meanwhile, 2-dimensional quadratic, quadrilateral elements would be the preferred choice as they are suitable for double-curved surfaces, such as AFOs, and less prone to transverse shear locking[261]. Regardless of the mesh and element type used, it is important to perform a mesh convergence analysis to demonstrate that the predicted behaviour is independent of the properties of the mesh. Previously stress distribution[232], [256], [257], displacement[256], [257] and stiffness[196], [232] have been used, although several articles did not perform one.

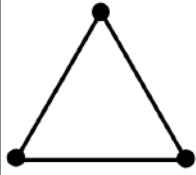
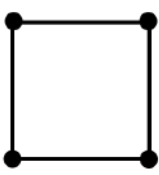
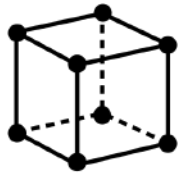
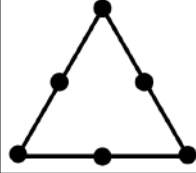
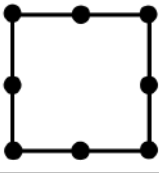
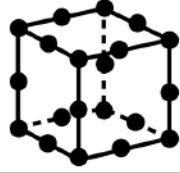
	Shell Elements (2-Dimensional)		Solid Elements (3-Dimensional)	
Linear				
Quadratic				

Figure 2.6: Examples of mesh elements used in FE analysis. Black dots = nodes.

The next consideration is how the materials are modelled. Most previous FE analyses simulate loading over one cycle and so polypropylene can be assumed to act as an isotropic, elastic[193], [196], [199], [201], [251], [252]. This is analogous to the debate surrounding the loading speed of test rigs, where it is argued the viscoelastic properties of polypropylene are only significant during cyclic loading. Furthermore, modelling viscoelastic materials adds complexity to the simulation, both computationally and in terms of defining the material properties through experimental testing[232]. Isotropic elastics are defined based on their tensile material properties, including the elastic modulus, yield stress and Poisson's ratio. Previously, papers sourced these properties from material databases, manufacturer specifications or previous literature[196], [198], [201], [212], [251], [256], [257]. However, determining properties through material testing according to ISO standards is considered best practice[193], as there may be variation between suppliers, particularly for PPC where different suppliers may use different proportions of polymers. Interestingly, even when material testing was performed, Poisson's ratio for polypropylene was taken to be within 0.35-0.45 based on typical values for plastics[256], [257]. This is likely because determining Poisson's ratio requires both the longitudinal and transverse elastic modulus, adding complexity and cost to the material testing protocol. Furthermore, Syngellakis et al. reported that the behaviour of their FE simulation was insensitive to the Poisson's ratio within this range, although data for this was not presented[256].

The thickness of the material is also inputted into the model when using either a shell mesh or a solid mesh with a uniform thickness. This was often assumed to be the

thickness of the pre-draped polypropylene sheet[196], [198], [201], [255], [257]–[260], however thermoplastic AFOs typically have non-uniform thickness due to the vacuum-forming process. Previously, two methods have been presented for taking measurements from the manufactured AFO. Firstly, Syngellakis et al. found the ratio of AFO thickness in several key locations to maximum AFO thickness and applied these values to different areas of the AFO shell mesh, creating non-uniform thickness[256], [257]. This resulted in a model which predicted ankle moments under 5° of rotation to within $\pm 10\%$ of experimental data. Alternatively, Chatzistergos et al. adopted a simpler method, assuming the shell mesh had a uniform thickness equal to the mean thickness of the AFO, measured along the trim lines in the malleoli region[193]. They argued that this was appropriate as measurements were taken in areas where high stresses concentrate during loading[212]. Using this technique, they demonstrated that the error in maximum deflection of the FE model, compared to experimental data, was 0.1°. However, neither of the papers adequately assessed the validity of the FE models against experimental data. Furthermore, in both cases, the location where thickness can be measured will be restricted by the use of traditional measurement devices such as digital callipers, which could affect the validity of the assumption.

Finally, the majority of previous work did not include a foot model within the simulation. Instead, they replicated the constraints placed on the AFO by fixing the elements of the foot section and applying a load, proximally, in the area where the strap would be[193], [197], [198], [201], [232], [250]–[260]. Loads were applied as forces, ranging from 34N to 275N[198], [199], [250], [252], [253], [255], [258]–[260], moments (30Nm[193]) and as prescribed rotations, ranging from 8-20° plantar-dorsiflexion[196], [201], [232], [256], [257]. These boundary and loading conditions aligned with the typical design of the bench testing rigs, however it was apparent a number of FE models did not simulate the ankle joint, such as Ielapi et al.[232] and Syngellakis et al.[256], [257]. As a result, a rotational axis was not imposed and deformation may have been under-constrained. Furthermore, Syngellakis et al. constrained the foot section by applying pressure to it, noting that fixing the displacement of elements may cause artificial stress concentrations. Alternatively, Chu et al.[212] and Uning et al.[251] constrained the AFO using a leg model. Here, contacts were made between the AFO and the shank of the model

where the straps would be, before fixing the proximal end of the shank and articulating the foot. These models incorporated bone, muscle and connective tissues, however, modelled each of these as isotropic elastic materials. Therefore, although in theory, a leg model would provide a more realistic prediction of in situ AFO deformation, this is only true when the properties of the soft tissues and the contact forces between the leg and AFO are accurately modelled, which adds significant complexity.

2.3.5 Summary of findings

From the papers discussed in this narrative review, it is evident that functional assessment techniques are unsuitable for this thesis, as they would limit the number of designs which could be tested. However, it could be considered in the event of a proof-of-concept study on a particular design. Furthermore, whilst bench testing offers a viable solution to these problems, using this technique alone would require each AFO design iteration to be manufactured, which is expensive, labour-intensive and introduces environmental impacts. Therefore, this review supports recommendations made by Ielapi et al. that a FE model, validated against experimental data, is *"the appropriate methodology for the quantification of the AFOs behaviour"*[215]. However, previously the experimental data used to validate FE models has been collected via bench testing, therefore a test rig will also be developed to provide this data.

When designing the test rig, outlining clear specifications, relevant to its application, will be crucial. For example, given the novelty of the research area, subsequent studies will pilot rigid AFO designs. Therefore, at these initial stages, fatigue across the lifetime of the designs is not relevant. As a result, a fully automated rig may not be necessary. Instead, a simpler design may be suitable, similar to that developed by Bregmann et al.[92]. This performed similarly when determining stiffness, as more complex designs[247], and exhibited comparable within-session and between-assessor Intra-class Correlation Coefficient (ICC)s to automated counterparts[231], [248]. Furthermore, given there is no standardised bench testing system, it may be useful to explore a design which is more translatable across institutions. As a result, a system that utilises MOCAP and force plates, is appealing. In any case, the repeatability of the rig must be demonstrated, which was a major issue with a number of the designs previously developed[214], [232].

The FE model should then be developed to simulate the behaviour of the rig. When developing the FE model, discretisation is a key issue. Ideally, shell meshes will be utilised as they would reduce the amount of modelling required in future studies. However, they may be unsuitable depending on the designs modelled. The accuracy of the simulation is also influenced by the material model used. As material testing facilities are available at the University, material properties will be tested experimentally, unlike several previous studies. Furthermore, an alternative approach to measuring the thickness of the AFOs should be explored which negates the limitations of using traditional measurement devices. Finally, when validating the FE model against the experimental data, this should include comparisons of the primary outcome measures and the moment versus deflection curves as presented by Ielapi et al.[232]. Often, previous FE models were either unvalidated[196]–[198], [212], [251], [254], [255], [259] or inadequately validated[193], [250], leaving question marks over their validity.

Chapter 3

Understanding the stakeholder requirements related to rigid AFO design

Chapter Overview

The previous chapter extensively reviewed the literature, concluding that the remainder of this thesis should focus on the relationship between AFO design and mechanical properties, to optimise the performance of the devices. However, when optimising AFO design, it is necessary to consider the needs of all the stakeholder related to their use. Therefore, the following chapter presents a literature review into the barriers and facilitators to AFO use according to the user, parent/carer and clinician, followed by a report of patient and public involvement and engagement within research (PPIE) sessions held with a clinical advisory group of orthotists, to understand current AFO prescription.

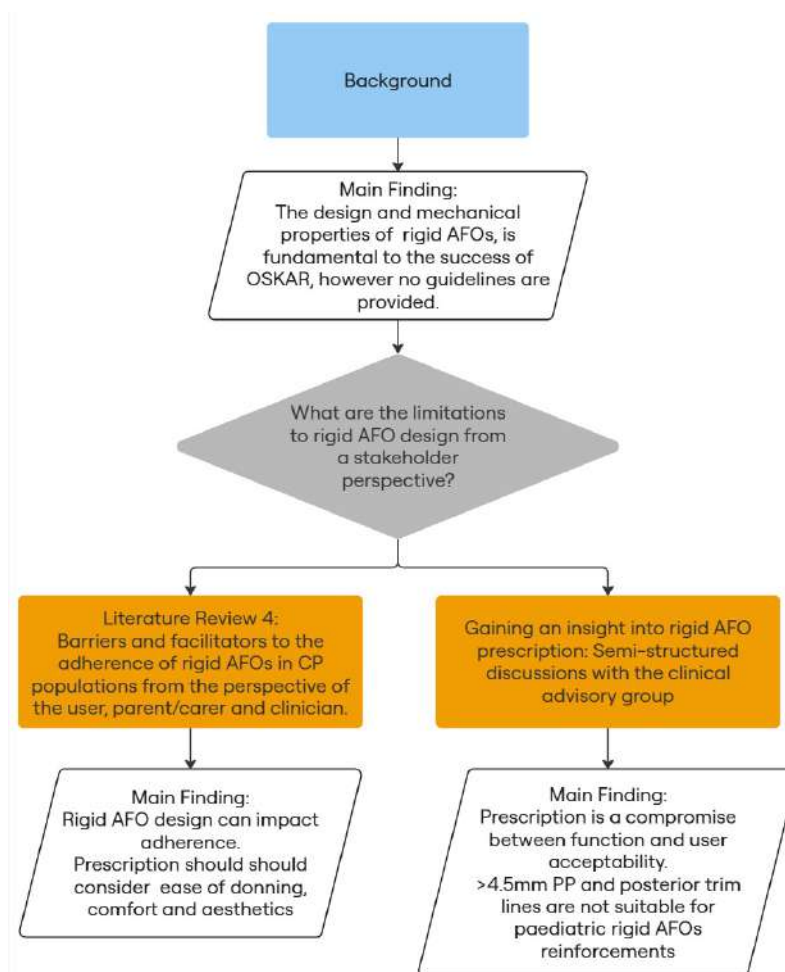


Figure 3.1: Flowchart for the rationale of the stakeholder analysis.

3.1 Barriers and facilitators to the adherence of rigid AFOs in CP populations from the perspective of the user, parent/carer and clinician.

3.1.1 Introduction

The success of any medical intervention is reliant on adherence to dosage recommendations, defined by the World Health Organisation as *“the extent to which a person’s behaviour – taking medication, following a diet, and/ or executing lifestyle changes – corresponds with agreed recommendations from a health care provider”*. Previously, issues with adherence to orthotic devices within CP populations have been highlighted, with AFO use in Sweden decreasing from 67% of children with CP aged 5, to 19% by the age of 19[14]. This is supported by evidence from reviews into both paediatric[262] and adult pathological populations[263] and studies into AFO usage in CP[264] and stroke[265], which found discrepancies between AFO usage and dosage recommendations. However, psychosocial pressures and user expectations of wearing an AFO may differ significantly between adult and paediatric populations. Meanwhile, a child’s lack of independence means the family/care unit also plays a key role in administering the intervention. As a result, OSKAR advises a family-centred care approach[68], where collaboration between the care team, user, and family throughout the intervention process aims to mitigate for any adherence barriers[266]. Therefore, to ensure these principles are reflected within research, the needs and requirements of these stakeholders must be understood. To this end, a literature review has been proposed to understand the clinical, user and family requirements regarding AFO design and provision in paediatric CP populations. Consequently, the findings will help to define the design limitations on rigid AFOs, to ensure they are applicable within the real world.

3.1.2 Aims

To determine the facilitators and barriers to adherence to rigid AFOs in CP populations, from the perspective of the user, parent/carer and clinician.

3.1.3 Search Strategy

The search strategy outlined in Table 2.5 was applied in MEDLINE, CINHALL and the Child and Adolescent studies databases, via EBSCO, ProQuest, and Web of Science to identify relevant articles published before 2024.

Table 3.1: Search strategy used to identify relevant articles. WoS = Web of Science, NOFT = Any field except full text

Search terms	Boolean operator	Search fields by database		
		EBSCO	ProQuest	WoS
AFO OR (Ankle AND orthos*)	-	Title	Title	Title
Compliance OR "needs" OR satisfaction OR adherence OR perception* OR perspectives OR opinion	AND	Title	Title	Title
Patient OR care* OR child* OR user OR clinician OR orthotist OR therapist OR cerebral palsy	AND	Title	Title	Title
"knee-ankle" OR "hip-knee-ankle" OR stroke OR "peripheral artery disease" OR charcot	NOT	Title	Title	Title

After removing duplicates, papers were screened based on the criteria highlighted in Table 3.2. This was a two-step process, first papers were screened based on the title and abstract and then the full paper. Figure 3.2 presents the results of this process.

Table 3.2: Inclusion and Exclusion criteria for the review. AFO = Ankle-foot Orthosis, CP = Cerebral Palsy

Inclusion Criteria	Exclusion Criteria
Studies investigating AFO use.	Studies investigating additional assistive technologies, where findings regarding AFOs cannot be isolated.
Studies which investigate user, parent/carer or clinical perspectives of AFO design and functionality.	Studies quantifying the effect of AFOs on an outcome measure or presenting perspectives relating to AFO provision, service performance or clinical decision-making
Studies which present perspectives associated with AFO use in CP	Studies investigating other conditions, or those studying multiple conditions where the views relating to CP cannot be isolated.
Original, peer-reviewed research studies	Reviews, abstracts, supplementary papers, conference proceedings or grey literature.

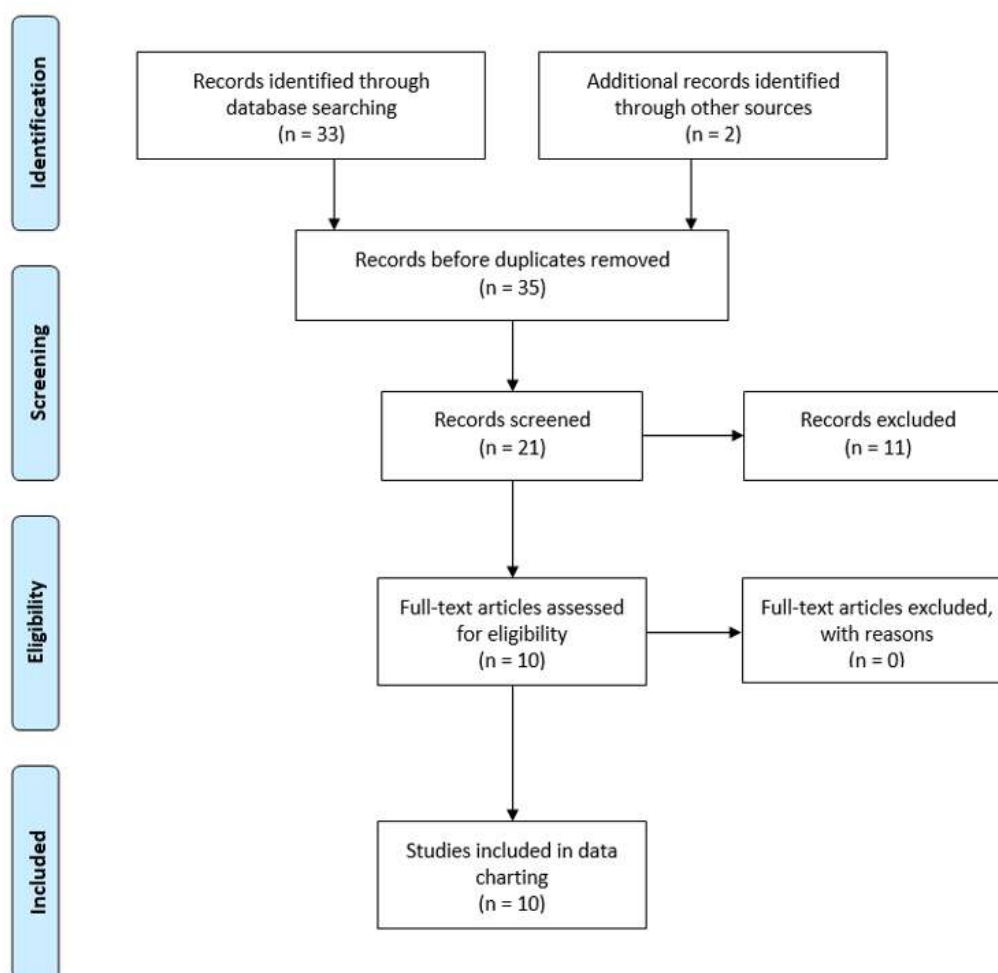


Figure 3.2: PRISMA flowchart of the screening process for the scoping review

3.1.4 Results

Study Characteristics

A total of 10 papers satisfied the inclusion criteria for this review. Six papers reported user perspectives[190], [267]–[271], five parent/carer[267], [269], [271]–[273] and five clinician[268], [271], [274], [275], however in the studies by Bayón et al.[271] and Zaino et al.[267], users and parents/carers were grouped together. Various study designs were used including questionnaires/surveys[190], [270], [271], [274], [275], focus groups[267], [268], interviews[272] and content analysis of secondary data[269]. Finally, two studies included users with additional conditions including stroke, multiple sclerosis and traumatic brain injury.

Facilitators of the use of AFOs

The facilitators and barriers identified in the included articles were grouped into three themes, the functional benefits of the device, the design of the device and the user experience with the device. Table 3.3 outlines the facilitators to AFO adherence, with the majority falling under the theme of functional benefits of the device. From a user and parent/carer perspective, improvements in walking and independence were the most widely reported facilitators, however stability and participation were equally cited by parents/carers. Independence was also an important facilitator from a clinical perspective, alongside metrics such as speed, balance and endurance.

Additionally, Bayón reported users and parents/carers rated the ease of donning/doffing, comfort and adaptability to walking speeds as the most important consideration (>90% of respondents)[271]. They also prioritised improvements in gait pattern, speed, and task performance. Meanwhile, Bayón et al.[271] and Heinemann et al.[274] found clinicians rated ease of donning/doffing, comfort and adaptability to terrains as the most important design features (>90% of respondents)[271], [274].

Table 3.3: Facilitators of the adherence to AFO use in CP populations

Theme	Facilitator	Stakeholder Perspectives		
		User	Parent/Carer	Clinician
Functional Benefits	Walking	[190], [267]	[267], [272], [273]	
	Falls	[190]		
	Standing/ Balance	[190]	[273]	[274]
	Independence	[267], [268]	[267], [272]	[274]
	Quality of Life	[268]		[274]
	Speed			[274]
	Gait Pattern			[274]
	Endurance			[274]
	Range of Motion			[274]
	Stability	[267]	[267], [272], [273]	
	Participation	[267]	[267], [272]	
	Posture	[272]		

	Muscle flexibility	[272]		
	Cycling	[272]		
	Transfer activities	[272]		
	Sitting	[272]		
	Upper limb function	[272]		
	Motor learning	[272]		
	Prevention of surgery		[272]	
	Prevention of future deformities		[273]	
AFO Design	Aesthetics	[269]	[269]	[269]
User Experience	Reduce the need for stretching		[272]	

Barriers to the use of AFOs

Alternatively, the barriers to AFO adherence tended to relate to the design of and user experience with the device (Table 3.4). Here, aesthetics, ease of use, pain, comfort, and compatibility with footwear were identified most frequently across all three stakeholders.

Table 3.4: Barriers to the adherence to AFO use in CP populations

Theme	Barrier	Stakeholder Perspectives		
		User	Parent/Carer	Clinician
Functional Benefits	Falls	[267]	[267]	
	Activities of daily living	[271]	[271]	[271]
AFO Design	Aesthetics	[190], [267]–[269]	[267], [269], [273]	[268]
	Materials	[269]	[269]	[274]
	Durability	[268], [270], [271]	[271]	[271]
	Adjustability	[268], [270]		
	Modifiability			[274]
	Weight	[268], [270], [271]	[271]	[271]

	Dimensions	[270], [271]	[271]	[271]
	Adaptability	[271]	[271]	[271]
User Experience	Ease of use	[267], [270], [271]	[267], [271]–[273]	[271], [274]
	Pain	[267], [269]–[271]	[267], [269], [271]–[273]	[271], [274], [275]
	Thermal discomfort	[267], [269], [270]	[269], [272], [273]	[274], [275]
	Compatibility of footwear	[190], [267], [269], [271]	[267], [269], [271]–[273]	[271]
	Cost	[271]	[271]	[271]

3.1.5 Discussion

The findings in this review support earlier research into adherence to AFO use. Firstly, Holtkamp et al. found dissatisfaction rates towards AFO use were highest amongst users under the age of 18[270], reflecting the findings by Wingstrand et al.[14]. Meanwhile, there were similarities between the barriers to adherence identified in both paediatric and adult pathological populations[262], [263], [265]. Comfort, associated with both pain and thermal discomfort in hot and cold temperatures, and ease of use, referring to donning and doffing, were identified as barriers by all three stakeholders, across multiple papers[190], [267], [269], [271], [273]. Furthermore, Holtkamp et al. reported the highest dissatisfaction rates for this criteria[270] and Bayón et al. found > 90% users and clinicians rated them as important[271]. Consequently, these features should be prioritised during rigid AFO design. However, whilst pain is alleviated through accurate casting and rectification, padding and post-draping modifications, thermal discomfort and ease of use are more difficult to address. This is because thicker AFOs with anterior trim lines will have a detrimental effect on both criteria, meaning achieving desirable AFO stiffness could likely impact adherence.

In addition, aesthetics of both the AFO and modified footwear were repeatedly cited as key barriers to adherence amongst all three stakeholders[190], [267]–[269], [273], [274]. Observations made regarding the stigma attached to wearing AFOs and orthopaedic

footwear, concur with historical links between negative self-image and clothing associated with disabilities[276] and orthopaedic footwear[277], [278]. However, negative perceptions of aesthetics may be age-related, as Lahoud et al. identified the ability to customise the AFO as a facilitator to adherence in younger age groups[269]. This may explain the age-related decrease in adherence reported by Wingstrand et al.[14], however further investigation is required to demonstrate the causality of this relationship. Furthermore, the need for adapted clothing and footwear introduces additional issues relating to the cost and time required to find compatible, desirable solutions[190], [267], [269], [273]. Whilst this appears to be a wider issue with all lower limb orthotics[279], it is particularly pertinent when discussing biomechanical optimisation of AFOs using OSKAR. Considerable shoe modifications are recommended to control shank alignment during entry and exit from stance, for certain individuals. As a result, these are likely to be aesthetically undesirable and cost-prohibitive, causing direct conflict with OSKAR.

However, despite these barriers, several studies found that the functional benefits provided by the AFOs, were a sufficient motivation for continued use[190], [267], [269], [273]. This is supported by the fact that aesthetics was identified as the third-least important design feature amongst users, however, this could also be influenced by parents/carers providing proxy responses in some cases[271]. Interestingly, some functional benefits of AFOs, such as walking and stability or balance, identified by all three stakeholders, may be contradicted by the findings of the review into the effects of rigid AFOs on gait (Section 2.1). Here, rigid AFOs were found to reduce the mediolateral margin of stability[153], [155], although increases in step length[119], [161]–[164], [166], [168], [170], [171], [181] and single-support time[162], [170] were seen, whilst gait quality was unaffected[159] and improvements in specific motor activities were topography specific[156], [161], [163]. Therefore, this may lend weight to the argument that the use of grouped statical analysis in previous research may have masked some beneficial effects of rigid AFOs, within individual cases[183], however, it could also reflect the fact that the stakeholder perspectives are not specific to rigid AFOs. In any case, given some issues surrounding AFO design are difficult to address with thermoplastic devices, it suggests that the best method of ensuring adherence to biomechanically optimised AFOs is growing the body of evidence supporting their functional benefits.

3.1.6 Conclusions

It is clear from this review that ease of use, comfort, and aesthetics are key issues regarding the adherence to AFOs and therefore need to be considered during the design process. Consequently, limitations are placed on the thickness and depth of the mediolateral trim lines that will be tolerated by the user, without compromising ease of donning/doffing and comfort. Furthermore, although it is difficult to address issues regarding the aesthetics of thermoplastic AFOs, AFO design should prioritise compatibility with typical footwear, providing the user and parents with a greater variety of options.

3.2 Gaining an insight into rigid AFO prescription: Semi-structured discussions with the clinical advisory group

3.2.1 Rationale for forming clinical advisory group

Understanding clinical practice is important when conducting research, to ensure that it is relevant and findings are translatable. However, it is particularly crucial when investigating AFOs in CP as the decisions made by clinicians during prescription directly impact the performance of the devices. Whilst the previous review highlighted the potential barriers and facilitators to rigid AFO adherence, it does not investigate the specifics of the prescription process (Section 3.1). Furthermore, current literature on clinical practice tends to focus on the use of outcome measures and evidence-based practice[280]–[283], whilst only one study has focused on the specifics of AFO prescription. Eddison et al. found consensus on a baseline design of a rigid AFO for a hypothetical adult male amongst 14% of UK-based practising orthotists[284] (Table 3.5). However, given patient characteristics such as mass and height influence AFO design, it cannot be assumed that the consensus for a paediatric AFO would be the same. As a result, there is very little evidence to inform investigations into the design of rigid AFOs in paediatric populations.

Table 3.5: Baseline rigid AFO prescription determined by Eddison et al. based on the views of UK-based orthotists[284].



Rigid AFO Description
4.5mm PPC
No additional reinforcements
Full-length footplate with mediolateral trim lines behind the metatarsal heads
3-point-correction with parallel sides
Padded VELCRO® straps with D-rings at the calf and heel
No forefoot or additional strapping
3mm PORON® padding at the malleoli
AFO height that finishes 2cm below the fibular head

An alternative approach to obtaining this information is patient and public involvement

and engagement within research. This is a strategy, endorsed by the National Institute of Health and Care Research, to ensure projects are conducted *''with' members of the public, rather than 'for' them''*[285]. Through this framework, researchers can gain opinions and insights from various stakeholders, informing a range of processes within the research cycle, including study design. Considering this, a clinical advisory group, consisting of UK-based orthotists with varying clinical experience and backgrounds, was established. The aim was to gain an insight into typical clinical practice regarding rigid AFO prescription for managing gait impairments in paediatric populations. This will provide the rationale for the design and scope of primary research studies conducted within this thesis, ensuring their clinical value.

3.2.2 The demographics and role of the clinical advisory group

The clinical advisory group were selected via convenience sampling, to ensure a range of experiences and expertise were included. Eight orthotists, two females, from across the UK, agreed to become members of the clinical advisory group. Their experience as a qualified professional varied from 1 to 30 years, across both public and private sectors, however, all had prescribed rigid AFOs to manage gait impairments in children with CP. Six members were currently practising, whilst the other two were involved in orthotic practice through undergraduate teaching and at an organisational level in a governing body. All members of the clinical advisory group were expected to complete one discussion with the author, however, those willing to provide advice on further matters could indicate they were happy to be contacted via email when necessary.

3.2.3 Structure of the PPIE Session

Each member was invited to complete one discussion session with the author of this thesis, hosted on Teams (version 24335.208.3315.1951, Microsoft, USA), which lasted approximately 1 hour. These discussions were semi-structured interviews, prompted by questions regarding the design of rigid AFOs for children with CP. It was ensured that each question was answered, however, discussions were organic, allowing the clinician to discuss their own experiences. The full list of questions can be found in Appendix A. Furthermore, one-to-one discussions were chosen to ensure every member's opinion was heard and because they were more feasible to organise.

The discussions were recorded using an audio recording device before being transcribed using Word (version 2410, Microsoft, USA). The transcribed files were then checked for accuracy against the original recordings. Discussions were analysed by grouping responses relating to the four AFO design factors and then any additional comments. This was performed for each member determining the occurrence of each response as a proxy measure of agreement. Finally, a summary of the discussions was produced, before discussing their impact on future research.

3.2.4 Summary of discussions with clinical advisory group

During the one-to-one discussions, all members of the advisory group identified material type, thickness, trim line design and reinforcements as the key properties of rigid AFOs which influence the stiffness of the device. Furthermore, all identified the height and mass of the child as the main considerations when determining the stiffness of an AFO, alongside activity levels (2/8), the severity of neurological impairment (3/8), fixed contractures (1/8) and control of the knee (1/8). Interestingly some accepted that rigid AFOs would permit a small amount of deflection (3/8) and hinted that this could be beneficial in terms of comfort.

Exploring each of these properties in more depth also highlighted some interesting trends. Firstly it was clear that paediatric AFOs were typically thermoplastic, as only two individuals spoke of carbon-fibre being available. However, the group were split between which type of polypropylene they preferred, with four members using PPC as standard, three PPH and one indicating the choice is case specific. The benefits of using PPC were it was more ductile and therefore less prone to fracture (4/8), easier to drape and perform post-drape modifications (4/8) and was more "forgiving" and so improved comfort (2/8). Alternatively, PPH was more rigid and achieved the desired stiffness with a thinner device, which benefitted donning footwear (3/8). Finally, one member indicated that technician preference was also a factor.

Alternatively, there was greater consensus surrounding thermoplastic thickness. Six members opted for 3-4.5mm polypropylene for paediatric populations, whilst 2mm was

highlighted as an option by three individuals. Only one member used >4.5mm plastic, however, four acknowledged it was an option, but was rarely used. All the clinicians referred to the thickness of the AFO causing issues with the donning of footwear, whilst the weight of the AFO (1/8) and the definition of bony landmarks during vacuum-forming (1/8) were also mentioned. Additionally, two members highlighted potential discrepancies between the pre and post-draped AFO thickness.

When discussing trim line design, the majority (6/8) utilised anterior to the malleoli trim lines as standard, whilst through the malleoli trim lines were preferred by one member and used on occasion by three others. Furthermore, although only three identified posterior to the malleoli trim lines as a contradiction to achieving adequate AFO stiffness, the others did not refer to posterior trim lines for rigid AFOs. All indicated that AFO stiffness increased with trim line depth at the ankle, whilst three members spoke of the need for the trim lines to be in the same position on both sides to reduce torsion during gait. Meanwhile, 7/8 members highlighted the position of the trim line is a compromise between stiffness and ease of donning the device, so trim lines could not extend further than the apex of the medial malleolus. Finally, three members noted occasional differences between the position of the prescribed and manufactured trim lines due to the technician's interpretation. Despite this, no industry-wide trim line standards were identified, although manufacturer-specific standards were mentioned (3/8).

The most variation in responses regarded reinforcements. A range of reinforcements was highlighted including ribbing (6/8), carbon fibre (6/8) or EVA (2/8) half-moon inserts, polypropylene Y-shaped structures (1/8) and double layering at the ankle (1/8). Ribbed reinforcements were the most cost-effective choice, whilst two members spoke of anecdotal evidence that they performed similarly to carbon fibre inserts. However, two individuals also indicated that ribbing could cause issues with footwear due to widening the AFO. Therefore, one member preferred the Y-shaped reinforcements as they allowed post-drape modifications and did not widen the AFO. The benefit of using reinforcements was localised stiffness, which was accumulative if multiple were used. Meanwhile, worse aesthetics, impacting post-drape modifications, and increased manufacturing complexity were considered drawbacks. As a result, there was variability in reinforcement use, with

three members indicating they would reinforce an AFO before increasing thickness, two doing the opposite, and two believing they were unnecessary if appropriate trim lines and thickness were used.

3.2.5 Interpretation of these discussions

Research must be aligned to clinical practice, to ensure findings are translatable. Therefore, in the absence of qualitative evidence into AFO prescription, the insight provided by the clinical advisory group should be incorporated into the design of this thesis to ensure its relevance. When considering the discussions regarding the design of the rigid AFO, there was agreement that >4.5mm polypropylene is rarely prescribed to paediatric populations. This seems logical given Eddison et al. found that a 4.5mm thick rigid AFO would be the standard for an adult male[284]. Furthermore, whilst this isn't necessarily reflective of the findings of the first review (Table 2.3), where four studies used ≥ 5 mm thermoplastic rigid AFOs in paediatric populations[118], [119], [152], [157], the majority did not report the thickness.

Additionally, the responses indicated a trend towards anterior trim lines for pediatric rigid AFOs, which agreed with Eddison's standard adult prescription[284] and the findings of the first literature review (Table 2.3). Furthermore, it was evident that a posterior to the malleoli trim lines was inappropriate for rigid AFOs, so the value of investigating these in future studies is questionable. However, four individuals also indicated the use of the through-the-malleoli trim lines, analogous to those tested by Go et al.[195] and Bielby et al.[202]. Given that the difference in mechanical properties through and anterior trim lines has not been established, this warrants further investigation.

Alternatively, there was a lack of consensus on the preferred polypropylene, which is logical given the current literature. Firstly, there is equivocal evidence of the increased stiffness of PPH AFOs[200], [205], whilst the majority of previous research into AFOs in gait either did not differentiate between the type of polypropylene used or failed to report the material entirely (Table 2.3). Therefore, the clinical perspectives support the need for further assessment of the effect of polypropylene type on AFO mechanical properties.

Furthermore, there was also a lack of consensus around reinforcements. Again, this aligned with Eddison's study, which found that only 50% of respondents used reinforcements as standard[284]. Additionally, whilst the reinforcements highlighted during discussions aligned with the designs seen in the literature (Table 2.7), the previous review found that ribbing and carbon fibre inserts have been evaluated[193], [200], [206]. As a result, there is limited evidence to support the clinical use of reinforcements.

Finally, the responses highlighted a compromise between optimal performance and user and clinical requirements. For example, the ease of donning the AFO and compatibility with footwear influenced decisions made regarding all four design factors, whilst the use of reinforcements was influenced by the need to make post-drape modifications. This reflects the findings of the review into stakeholder perspectives (Section 3.1) which found a number of the barriers to AFO adherence would cause conflict with the principles of OSKAR. As a result, it emphasises the need to consider the functional, clinical and user requirements when developing the design of rigid AFOs in future studies.

3.3 Impact of the clinical advisory group discussion on future studies

Firstly, discussions with the clinical advisory group identified the clinical relevance of rigid AFO design features. For example, >4.5mm thickness is rarely used in paediatric populations, whilst posterior to the malleoli trim lines are unsuitable for rigid devices. Therefore, there is little value in investigating these conditions in future studies. Alternatively, there was variability in reinforcements use and polypropylene type, suggesting further research is merited. Furthermore, this variability can be linked to the lack of robust evidence to support clinical decision-making and highlights how rigid AFOs with inadequate stiffness were used in research previously[155], [157], [161], [163], [168], [170]. Finally, it demonstrated that consideration is given to balancing rigid AFO functionality and user acceptability, during prescription, confirming the findings of the review into adherence (Section 3.1). Therefore, future research should incorporate user and clinical requirements into the design process.

Chapter 4

Aims and objectives of the thesis

Chapter overview

The next chapter presents the aims and objectives of the thesis. It also summarises the key findings from the literature reviews and the analysis of stakeholder requirements and demonstrates how these have influenced the aims and objectives of the thesis. Finally, it outlines the plan to achieve these objectives.

4.1 Aims and Objectives

Following the extensive review of the literature, it was determined that the aims of the thesis were

Aim 1: To investigate the relationships between rigid AFO design factors and the stiffness of the device

Aim 2: To move towards an optimised design for paediatric rigid AFOs.

To achieve these aims, the following objectives were outlined

1. Design a repeatable test rig to measure rigid AFO stiffness.
2. Develop a FE model which simulates the AFO loading during gait and validate this against experimental data from the test rig.
3. Test the effects of AFO design features on the sagittal ankle stiffness, using clinically relevant conditions.
4. Test the influence of AFO size on ankle stiffness by testing rigid AFOs designed for a range of paediatric ages.
5. Develop an optimised design for paediatric rigid AFOs that achieves desired stiffness and accommodates user requirements surrounding ease of donning, aesthetics and comfort.

4.2 Rational for the aims and objectives

The Key findings of the previous literature reviews and stakeholder analysis are presented in Table 4.1. The first literature review (Section 2.1), demonstrated the link between the design of rigid AFOs and their clinical performance. Highlighting, that a lack of consideration for rigid AFO design in research may limit effects on several gait outcomes. Meanwhile, the second literature review (Section 2.1) found that evidence for

the influence of AFO design factors on mechanical properties, is limited and equivocal. Together, these show a clinical need for additional research into these relationships to support decision-making. However, the stakeholder analysis (Chapter 3) stressed the importance of considering the user and clinical requirements during the prescription, to ensure adherence. Therefore, future research should be taken one step further, by investigating how AFO design can be optimised to achieve desired performance with acceptable stakeholder properties. As a result, the aims of the thesis, outlined in Section 4.1, were developed to meet these clinical needs.

In addition, the findings of the reviews and stakeholder analysis informed the design of the planned research and therefore the thesis objectives. For example, the second review highlighted how the current knowledge base could be improved, including investigating the combined effects of all four design factors in multiple paediatric-sized AFOs. Meanwhile, the third review (Section 2.3) determined that FE analysis was the most feasible method for quantifying AFO mechanical properties, and the steps needed to develop a validated model. Finally, the second review and stakeholder analysis provided the scientific and clinical rationale for the conditions tested and the design criteria adopted in the planned research.

Table 4.1: Impact of the literature reviews and stakeholder analysis on the thesis.

Thesis Section	Key Findings	Impact on Thesis
Literature Review 1	<p>The effects of rigid AFOs on gait outcomes may have been influenced by inappropriate design.</p> <p>This was inferred from reports of $>5^\circ$ ankle range of motion in rigid AFOs and poor reporting of key design properties.</p>	<p>Demonstrates the clinical need for research into the mechanical properties of rigid AFOs by highlighting the link between rigid AFO design and the performance of the devices.</p>
Literature Review 2	<p>Research into the design for rigid AFOs is generally limited (<3 papers) and equivocal. Trim lines were the most investigated factor however this was mostly in flexible devices or comparing posterior to anterior placement.</p> <p>Research into the mechanical properties of rigid AFOs has tended to be in adult-sized devices, which does not account for the difference in size and loading conditions in paediatric AFOs.</p> <p>Differences in methodologies used and poor reporting of the conditions tested limit between-paper comparisons which means the interaction of all four design factors is poorly understood.</p>	<p>Demonstrates the need for more evidence to support clinical decision-making.</p> <p>Highlights how future research should be designed to improve the current knowledge base, for example</p> <ul style="list-style-type: none"> ▪ Consider several paediatric AFO sizes ▪ Investigate all four AFO design factors ▪ Test conditions which are relevant to rigid AFO design ▪ Ensure methodologies are validated ▪ Adequately describe the conditions tested <p>Provided the rationale for design criteria used in the primary research studies</p>

		<ul style="list-style-type: none"> ▪ The anatomical definition for rigid AFO trim lines ▪ The mean reduction in AFO thickness due to manufacturing ▪ The threshold for clinically significant deflection
Literature Review 3	<p>FE analysis is the most feasible method of assessing the mechanical properties of AFOs as it is the most efficient and cost-effective.</p> <p>FE models must be validated against experimental data. Bench testing offers the most repeatable method for experimentally quantifying mechanical properties.</p>	<p>Provided the rationale for using FE analysis to quantify AFO mechanical properties and the need to validate the simulations with experimental, bench-testing data.</p> <p>Highlighted the design considerations for both the rig and FE model and how previous examples have addressed these.</p>
Stakeholder Analysis	<p>An 'optimal' AFO design must achieve desired performance and consider user and clinician requirements.</p> <p>>4.5mm thermoplastic is rarely used for paediatric rigid AFOs and posterior-to-malleoli trim lines are inappropriate for rigid AFOs.</p>	<p>Highlighted the need to include user and clinician requirements during the AFO design process, to move towards an optimal design.</p> <p>Provided clinical rationale for determining the design conditions tested in the primary research studies.</p>

4.3 Plan to deliver the aims of the thesis

The following plan was made to achieve the aims of the thesis (Figure 4.1). First, an FE model, which simulated the loading of AFOs during the second rocker, was developed to evaluate the mechanical properties of rigid AFOs design for a 5-, 10-, and 15-year-old. This also involved the design of a test rig to produce experimental AFO stiffness data, which was used to validate the FE model.

The FE models were then used to evaluate the mechanical properties of several AFO designs reflecting current clinical practice. The rationale for these designs came from the second literature review and stakeholder analysis. As a result, it achieved the aim of investigating the relationship between the four AFO design properties and the mechanical properties of the devices. Furthermore, it provided an insight into current clinical practice, identifying aspects of rigid AFO design which could be improved.

These findings then directed the optimisation of rigid AFO design. Here, several prototype reinforcements were evaluated, based on design criteria incorporating the functional, user and clinical requirements, using the 5-year-old FE model. The optimal design was then scaled to the larger AFOs to determine its effects on AFO mechanical properties across a range of paediatric sizes. Consequently, the second aim of moving towards an optimal design for paediatric rigid AFOs was met.

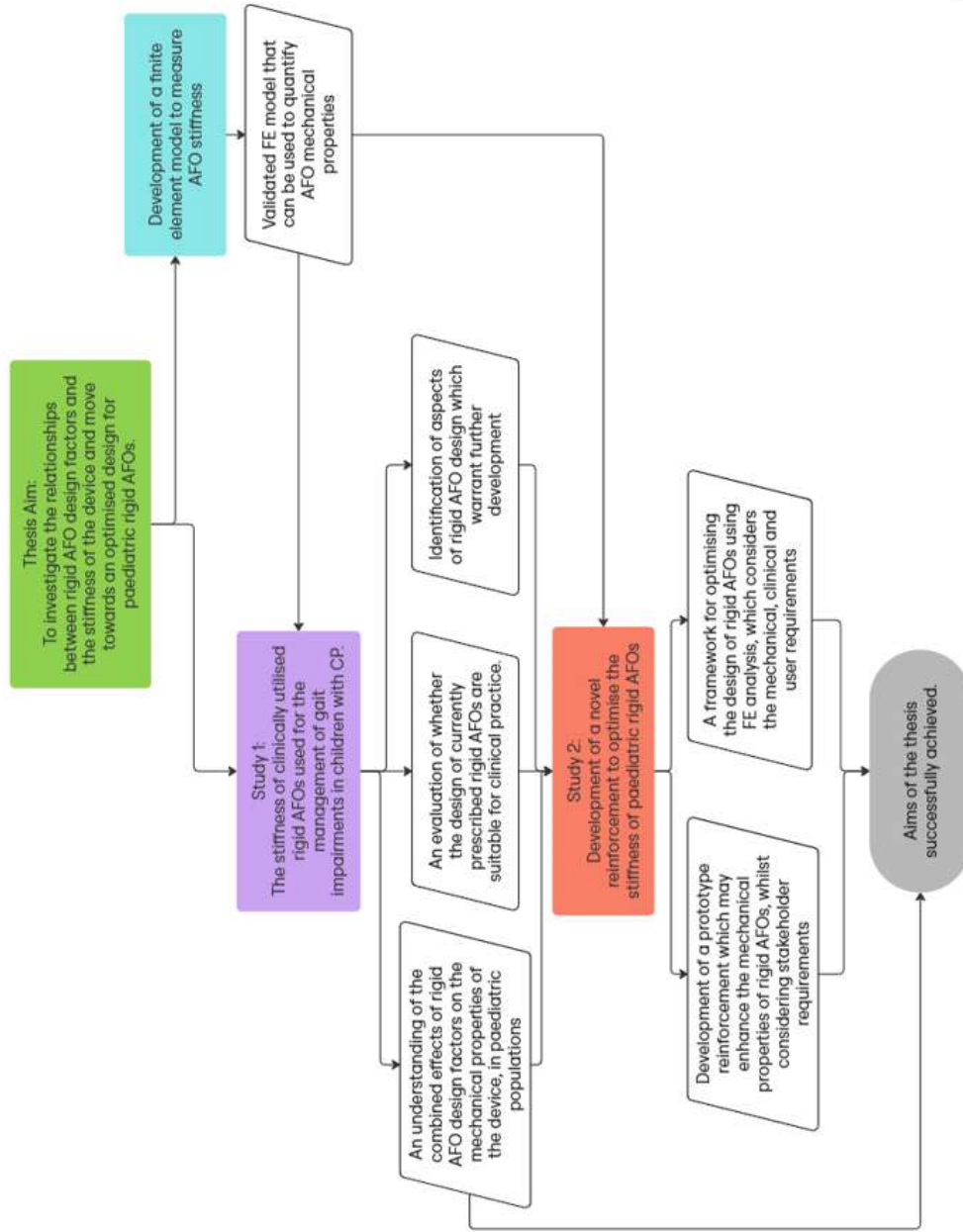


Figure 4.1: Plan to achieve the aims of the thesis. Green = Chapter 4. Turquoise = Chapter 5. Purple = Chapter 6. Red = Chapter 7

Chapter 5

Development of a FE model to measure AFO stiffness

Chapter Overview

The following chapter details the process of developing and validating the FE models to quantify the mechanical properties of rigid AFOs, highlighted in figure 5.1. This includes the AFO manufacturing process, the design and repeatability of the test rig and finally the development and validation of the FE simulation. The FE model also required accurate material properties, which were determined through tensile material testing, full details of this procedure can be found in appendix F.

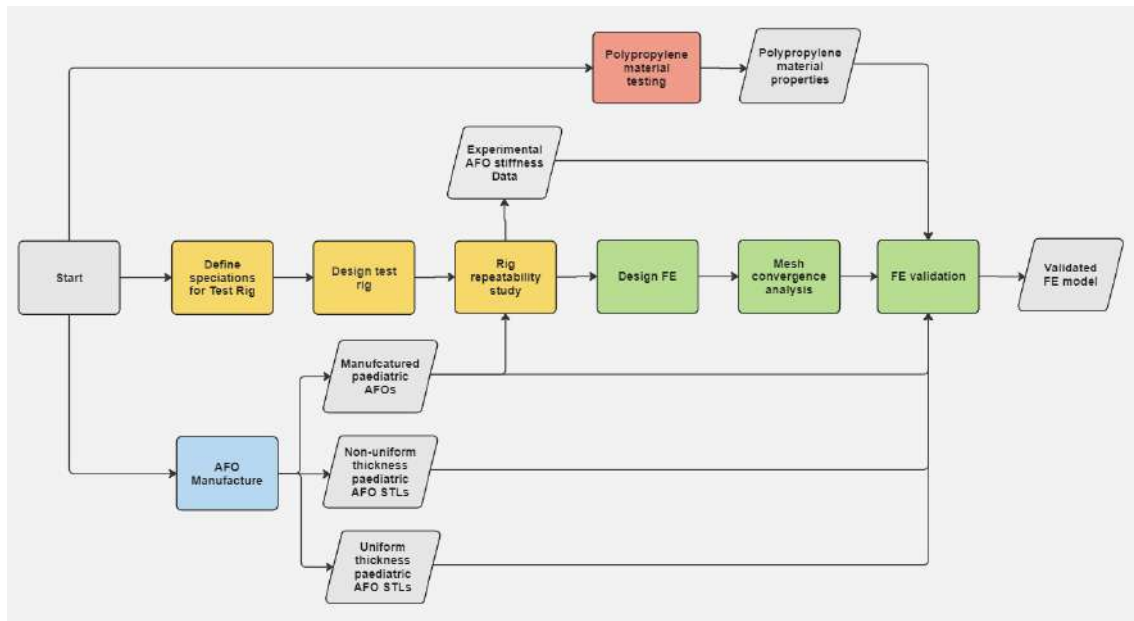


Figure 5.1: Process of developing and validating a FE model for quantifying AFO mechanical properties.

5.1 AFO Manufacturing and Modelling Process

One of the gaps in previous research into AFO design, was that there had only been limited focus on paediatric populations, whilst none had considered the effects of AFO size, found to be significant between adult and paediatric AFOs by Novacheck et al.[203] (Section 2.2). Consequently, this thesis aimed to explore these effects using AFOs designed for a 5-, 10- and 15-year-old. These ages were chosen as they span the typical age range of children with CP who are treated at paediatric care facilities. However, when creating AFO models for use in FE analysis, the preferred option is to digitise a manufactured AFO, using 3-dimensional scanning technology, to ensure the model incorporates build-up applied during the rectification process which can influence stiffness[101] (Section 2.3). Therefore, to create models of the paediatric AFOs, the decision was taken to scale a model of an adult AFO using anthropometric data. The rationale for this was that it would include the build-ups made during the rectification process whilst removing the variability in shape between rectifications and avoiding the need to recruit children from each age group. Figure 5.2 details this process.

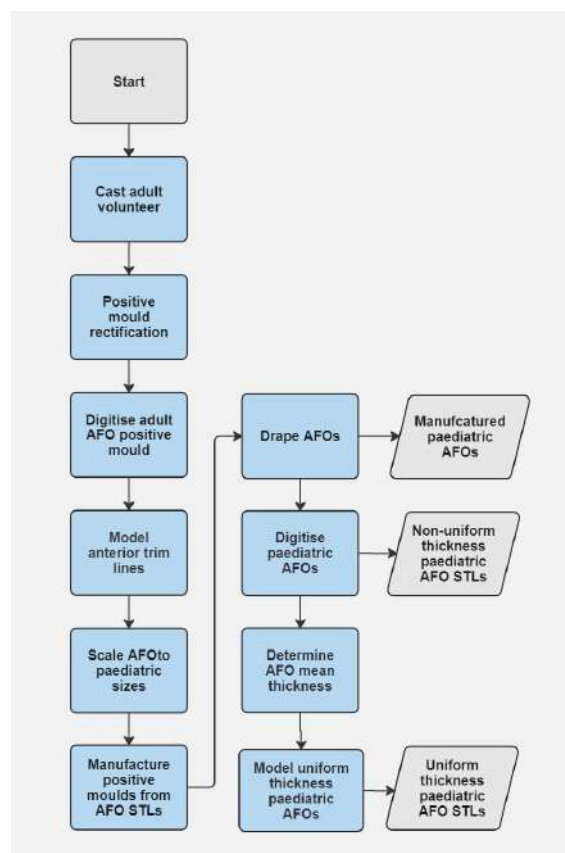


Figure 5.2: Flow chart of the AFO manufacturing and modelling process.

First, a negative cast of the right leg of an adult male, 31yrs, was taken using plaster of Paris bandages. From this cast, a positive plaster mould was created, which was then rectified according to a standard protocol. Afterwards, the rectified mould was digitised using a 3D scanner (FreeScan UE Pro, Shinning 3D, China), creating an STL of the adult, positive mould. Using this STL, the shape of the adult AFO was modelled using Fusion (v2.0.20470, Autodesk, USA) and exported in STL format. The dimensions for the trim lines were defined anatomically, based on anthropometric measurements taken from the AFO model, representing the first attempt to standardise rigid AFO trim lines (Figure 5.3). The definition took inspiration from the previous work into flexible AFOs[195], [209] and considered practical limitations highlighted by the clinical advisory group (Section 3.2), such as the need for a sufficient entry point.

The trim lines were defined in the sagittal plane and replicated on both the medial and lateral sides of the AFO to ensure uniaxial bending in the sagittal plane during testing. The proximal half of the calf section covered $\frac{3}{5}$ of the maximum calf depth, after which the anterior border tapered until it became tangential to an arc of radius $\frac{1}{2}$ medial malleolus width, placed half the malleoli width anterior to the mid-point of the malleoli. The mid-point between the malleoli apices was used to achieve adequate coverage of the medial malleoli, whilst allowing sufficient room to don the device. Below the malleoli, the trim lines taper down to $\frac{3}{5}$ of the foot height, at half-foot length, before finishing proximal to the 5th metatarsal head. Before use, the trim line definition was discussed with members of the clinical advisory group, who deemed it suitable.

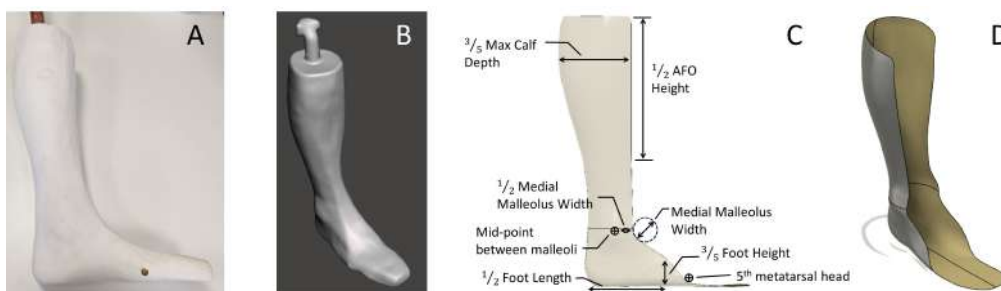
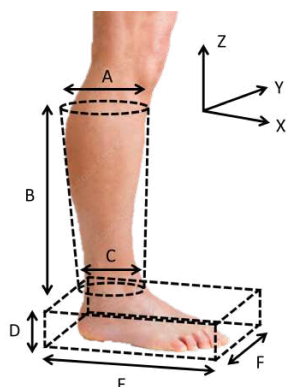


Figure 5.3: Process of modelling the adult AFO. A) Adult rectified positive mould. B) STL of the positive mould. C) Trim line definition. D) Adult AFO STL

The adult AFO STL was then exported to MATLAB (v2024a, MathWorks, USA), where a transformation matrix was applied to X-Y-Z coordinates of the vertices of the STL to scale the AFO to the three paediatric sizes. Then, the resultant vertices were re-

triangulated using the connectivity list from the adult AFO STL, to form STLs of the three paediatric AFOs. To define the transformation matrix, scaling factors were calculated from the ratio between anthropometric measurements taken from the adult male, who the AFO was manufactured for, and data from the 50th percentile of paediatric populations presented by Snyder et al.[286], [287] (Appendix C). This was necessary as segment growth is not linear, therefore scaling based on a single factor, such as height, would lead to distorted morphologies. When scaling, the foot section of the AFO was assumed to be rectangular, whilst, the shank was assumed as a truncated cone (Table 5.1). As a result, the height of the AFOs (z-coordinate) was scaled by sphyrion height, distal to the mid-point of the malleoli, and knee height proximal to the malleoli. Meanwhile, the length (x-coordinate) and width (y-coordinate) were scaled by the maximum calf circumference and minimum ankle circumference proximal to the midpoint of the malleoli and foot length and width, respectively, distal to the malleoli.

Table 5.1: AFO Scaling Method



Anthropometric Measure		Scaling Factor		
		5yr	10yr	15yr
A	Max calf Circumference	0.58	0.80	0.97
B	Knee Height	0.53	0.73	0.86
C	Min Ankle Circumference	0.68	0.82	0.94
D	Sphyrion Height	0.65	0.80	0.95
E	Foot Length	0.65	0.83	0.95
F	Foot Width	0.64	0.78	0.89

After scaling, the shell meshes were reverse-engineered into solid components, using Fusion (v2.0.20470, Autodesk, USA), which were used to carve foam, positive moulds of the paediatric AFOs. As a result, the modelled trim lines were visible on the AFO foam mould, meaning they could be more accurately transferred onto manufactured AFOs. Six AFOs were then manufactured using these moulds according to the details in Table 5.2. To reduce the manufacturing variability, the AFOs were manufactured at the University of Salford by the same, experienced technician according to a standard protocol. Polypropylene sheets were heated at 200°C for 3 min/mm, as specified by the manufacturer. After draping, they were allowed to cool with the vacuum applied for 25 minutes before the vacuum was turned off, and they were left to cool on the moulds overnight. Following this, the AFOs were cut from the moulds according to the

anterior trim lines defined previously and finished, resulting in six manufactured AFOs which could be assessed experimentally using the test rig (Section 5.2).

The final stage was to digitise the AFOs to create STLs for analysis in the FE validity study (Section 5.3). Two STLs of each AFO were required. The first was an exact replication of the manufactured AFO, with non-uniform thickness. This was created using 3D scanning, as before. The second was an AFO with a uniform thickness equal to the average thickness of the manufactured AFO. The thickness of the AFO was measured using a novel approach which found the distance between vertices on the internal and external surface of the AFO STL (Appendix D). To create these STLs, an STL of the inner surface of the AFO was taken using the same 3D scanner as before. This was then imported into Fusion (v2.0.20470, Autodesk, USA), where it was converted into a surface component and thickened by the average thickness (Table G). Finally, it was converted back to STL format.

Table 5.2: Mean thickness of the AFOs tested in the rig repeatability study. Pre-draped material thickness was assumed to be the value stated by the manufacturer.

Age / yrs	Material	Material Thickness / mm	Mean AFO thickness / mm	$\Delta\%$ in thickness
5	PPC	3	2.483	-17.22
	PPH	3	2.683	-10.55
10	PPC	4.5	3.317	-26.31
	PPH	5	4.143	-17.13
15	PPC	4.5	3.577	-21.92
	PPH	5	4.095	-18.09

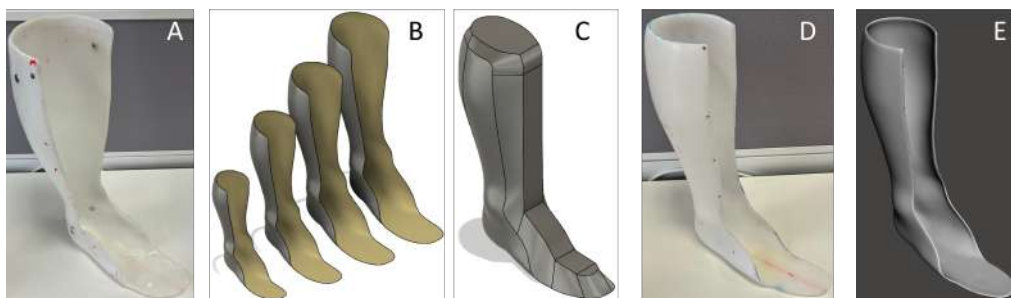


Figure 5.4: AFO manufacturing and modelling process. A) Adult AFO. B) Scaled AFO STLs. C) AFO mould. D) 10-year-old AFO. E) 10-year-old AFO STL.

5.2 The repeatability of a test rig to measure the stiffness of rigid AFOs

5.2.1 Specifications for the test rig

Following a narrative review (Section 2.3), a FE model validated against experimental data from a test rig was determined to be the most appropriate method of quantifying AFO mechanical properties to achieve the aims of this thesis. However, this review also highlighted the variety of rigs previously developed, demonstrating the need to outline clear specifications for the test rig.

The first step in this process is to outline the scope of subsequent studies, as the validity of both the rig and FE model depends on how accurately the in situ loading conditions are replicated. As explained in Section 1.3.3, the main failure mode for rigid AFOs is under dorsiflexion moments experienced during the second rocker of gait. During this phase, the foot is flat, with pressures concentrated at the heel and metatarsal heads. As a result, the external dorsiflexing moment is applied about the ankle joint and reaches a maximum of $\approx 1\text{Nm}/^\circ$ [93]–[95], [97]–[99], [191], [194]. As a result, the primary outcome measure will be sagittal dorsiflexion stiffness during the second rocker of gait.

Additionally, the target population for this line of research is children with CP. Therefore, the rig must accommodate AFOs for ages ranging from 5 to 15 years old, the age range of children typically managed within paediatric care facilities in the UK. Paediatric anthropometric data presented by Snyder et al. will be used to inform the dimensions of the rig [286], [287]. Furthermore, looking beyond the aims of this thesis, one potential barrier to the lack of research in this area is the lack of a standard method for quantifying AFO mechanical properties. Therefore, focusing on accessibility during design could have a wider impact on the scientific and clinical community. As a result, the following specifications for the test rig were outlined.

Table 5.3: Specifications for the test rig for quantifying the mechanical properties of rigid AFOs.

Criteria	Specifications
Boundary Conditions	The system must clamp the foot section of the AFO maintaining flat foot contact throughout loading.
	Secure the shank of the AFO in a way that replicates strapping around the user's limb and does not excessively deform the shape of the AFO
	Utilise an uniaxial hinge to constrain the deformation to the sagittal plane only. The bending axis of the hinge should align with the anatomical ankle joint to within 10mm[239]
Loading Conditions	Apply a sagittal dorsiflexing moment to AFO equalling 1.0Nm/kg[93], [193], [194]
	Loading speed should be consistent but does not need to reflect ankle angular velocity during the second rocker
Outcome measures	The rig must continuously measure force/torque and deflection data to allow stiffness to be derived during analysis.
Size and Weight	The rig should be able to accommodate AFOs ranging from 17-24.7cm in length, 26.2-42.7cm in height and 6.2-10.5cm in width[286], [287]
	The rig should be portable and easily stored.
User and Environment	The rig should be designed to integrate into different research institutions and, potentially, clinical environments.
	The rig should not require additional specialist training or software to operate, that is not already accessible within these environments
	The rig should be user-friendly to operate
Parts and Materials	Materials should be durable and readily available
	The rig design should be easy to replicate using facilities common to research institutions
Reliability	The repeatability of the rig should be comparable to existing solutions

5.2.2 Test rig design

A test rig was designed to meet the specifications outlined above. The design evolved across an iterative process (Figure 5.5), with an earlier prototype version being presented at the ISPO World Congress 2024 (Appendix B). The final solution utilised MOCAP and force plate technology so that it was applicable across research institutions and in specialised clinical practice, which was shown to be viable by Novacheck et al.[203]. However, it developed this prototype design by improving the foot and shank surrogates

and rotational axis alignment by incorporating aspects of the rigs presented by Ielapi et al.[248] and Bregman et al.[92]. As a result, the rig was adjustable to a range of AFO sizes. Finally, to fix the rig to the force plates, it is designed around the existing connections for instrumented stairs (AMTI, USA) [288].

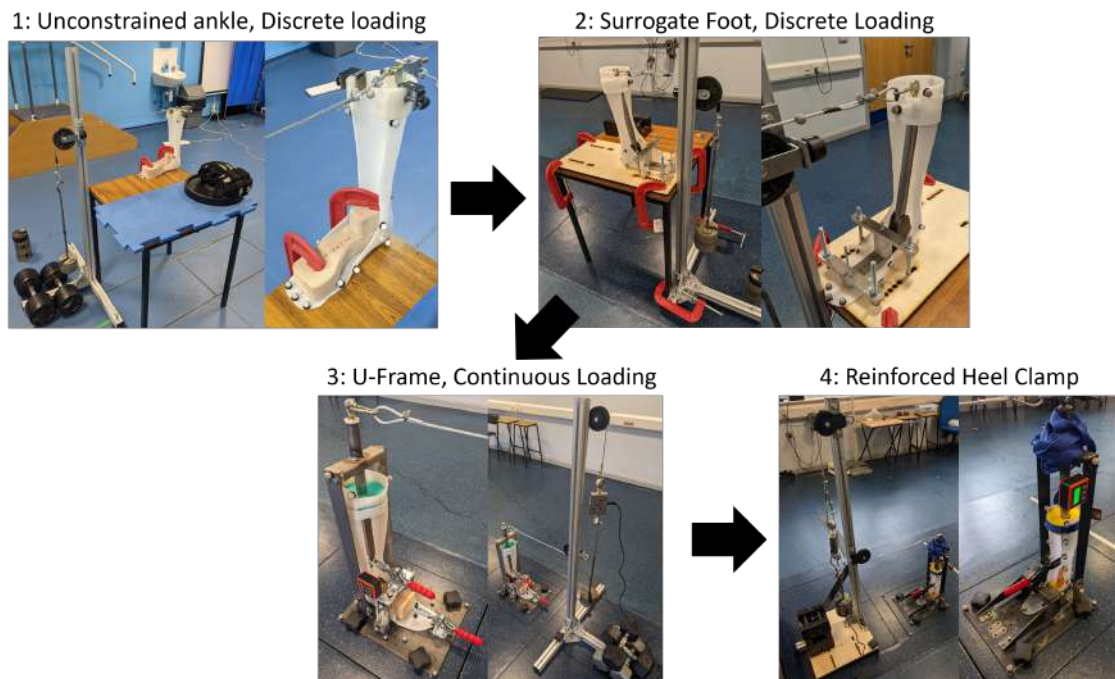


Figure 5.5: Evolution of the test rig design.

The system consists of two components, the mounting rig, within which the AFO is fixed, and the weight rack, which is used to apply the dorsiflexing load (Figure 5.6). The two components of the rig are secured to opposing force plates. The mounting rig consists of a U-frame, with a central steel tube, which pivots around two L-brackets connected to the baseplate. Furthermore, a toggle clamp is mounted onto the baseplate, along the centre line, which is used to secure the foot section of the AFO. Finally, the centre line of the baseplate is marked and there is a backplate welded at 90° to its rear end to assist positioning of the AFO within the rig. The weight rack consists of a T-shaped base and a vertical upright. It houses a pulley system which converts a vertical force, generated by hanging weights, to a horizontal force, which is applied to the top of the mounting rig via a steel cable. The weight rack is counterbalanced, as only two connections were available on this force plate.

The U-frame, L-brackets and toggle clamp mount are made from 3mm mild steel sheet-

ing, bent into C-shaped cross-sections to increase bending stiffness. Furthermore, the toggle clamp mount is reinforced with triangular supports on either side. Meanwhile, the baseplate is made from two 4.5mm mild steel sheets welded together, to provide stiffness and house the bolt heads which connect the brackets and mounts. The weight rack is manufactured from a 45mm square aluminium strut, chosen for its high strength-to-weight ratio and to allow the height of the pulleys to be adjusted. Furthermore, there is a 4.5mm mild steel cross-beam from the upright to the long tail of the T-frame to prevent the upright from bending.

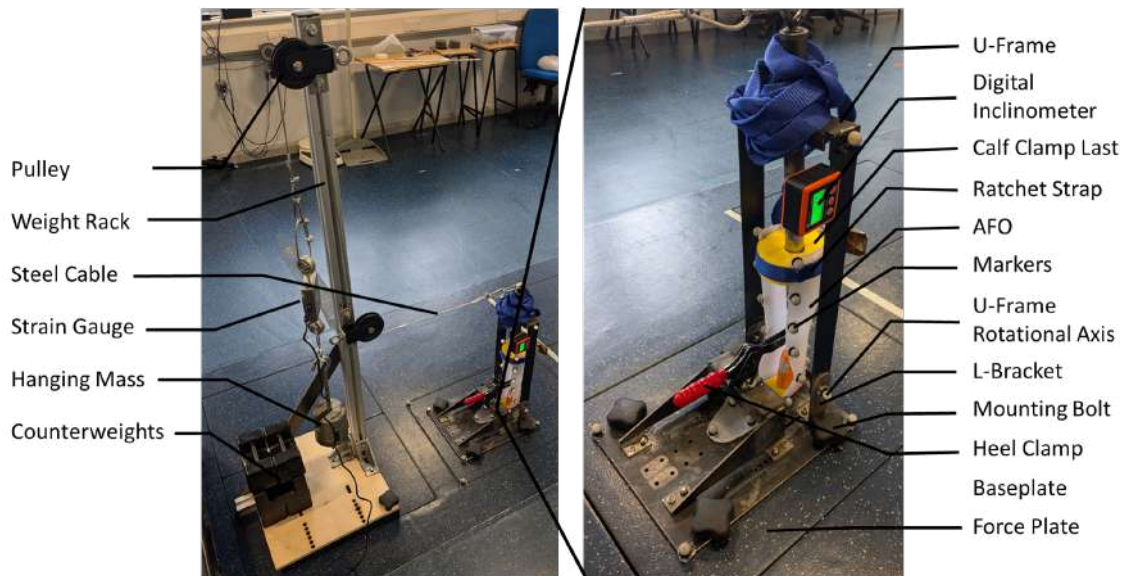


Figure 5.6: Final Test Rig Design

The system has been designed to accommodate a range of AFO sizes. Firstly, two sets of L-brackets allow the pivot point of the rig to be moved vertically from 45 to 85mm, whilst the horizontal position ranged from 40-90mm from the backplate, both in 5mm intervals. These ranges were used to cover the range of paediatric (<18-year-old) sphyrion height, presented by Snyder et al.[286], [287] and the ankle locations used by Bregman et al., calculated through foot regression equations based on data from 5000 children[92]. The position of the pivot is determined before testing, taken as the closet setting to the mid-point of the malleoli apexes, measured anatomically from the AFO wearer. Furthermore, the toggle clamp can be raised using 10mm aluminium spacers, whilst the height of the lower pulley can be adjusted to ensure the direction of the force is horizontal when loading begins, verified using a spirit level.

To secure the AFO into the mounting rig, the mid-line of the foot is marked onto the AFO, assumed as the line which runs through the apex of the heel and the mid-point of the footplate in the metatarsal region. This line was used to improve repeatability, as accurately marking the line passing through the second toe is not possible without anatomical landmarks. The AFO is positioned with the heel pressed against the back-plate and the mid-line of the foot in line with the centre line of the rig. It is then secured using the toggle clamp, which applies pressure to the heel area via a bespoke foot last to ensure full contact. Meanwhile, the calf section of the AFO is fastened around a bespoke last of the proximal fifth of the AFO, mounted onto the central steel tube of the U-frame, using a ratchet strap. The calf last is moulded so that it does not pretension the AFO during fixation. The two lasts are manufactured from nylon via selective laser sintering (Fuse 1, FormLabs, USA), based on plaster moulds from the AFO. When finished, nylon is self-lubricating, creating a frictionless contact between the central steel tube and the calf last.

5.2.3 Experimental procedure

A MOCAP system consisting of 15 optoelectric cameras (OQUS, 100Hz, Qualisys, Sweden), three video cameras (2x OQUS, 100Hz, Qualisys, Sweden, 1x Miquis, 100Hz, Qualisys, Sweden) and two force plates (1000Hz, AMTI, USA), was used to measure AFO deflection and the applied force. A 29-marker array was used to model the AFO, mounting rig, and steel cable (Figure 5.7). A full description of the model can be found in Appendix E. However, in short, the AFO was modelled as separate shank and foot segments, defined by markers on the proximal, mediolateral shell trim lines, the malleoli apexes, the heel, and the toe, whilst the rig U-frame was modelled by a marker on the eye bolt and rotational axes and finally the steel cable by markers at either end. The system was calibrated before securing the rig and weight rack to the force plates. In addition to MOCAP, a magnetic digital inclinometer (NTK061, $\pm 0.2^\circ$, Neoteck, China) was attached to the arm of the U-frame and a strain gauge (S Beam Load Cell 50kN, 4800Hz, Richmond Industries Lt, UK and USD fast strain converter, FSU-SSBD-A, Mantracourt UK) was connected, in series, to the end of the steel cable (Figure 5.6). These components have been used in previous rigs and provided a gold standard measure of deflection and applied force to determine the reliability of MOCAP and force plates.

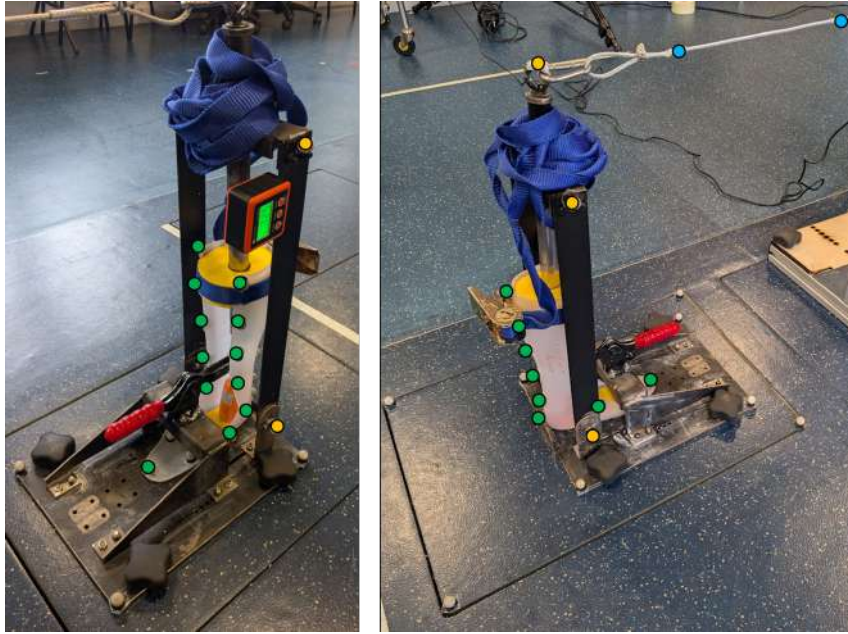


Figure 5.7: Marker array used to model the test rig. Green = AFO. Yellow = Test Rig. Blue = Steel Cable.

The six rigid, polypropylene AFOs manufactured in Section 5.1, were tested using the rig. They were mounted onto the rig as described in Section 5.2.2 before a static trial was taken. For each AFO size, the position of the rotational axis of the U-frame was adjusted to correspond to the mid-point of the malleoli apices, which was measured from the AFO positive moulds. Following this, a dorsiflexion moment, equalling 1Nm/kg [93], [193], [194], was applied to the AFOs. The moment was based on the mass of the 50th percentile of each age group which was taken as 17.9kg, 31.9kg and 54.2kg, for a 5-, 10- and 15-year-old child respectively[286], [287]. The moment was generated by applying a known mass to the steel cable, which applied force to the rig at a lever arm of $\approx 0.5\text{m}$. Therefore, the mass required to apply a moment equivalent to the peak dorsiflexion moment in stance equalled

$$Mass_{total} = (2 \cdot Moment_{PeakGC})/9.81 \quad (5.1)$$

where

$$Mass_{total} = Mass_{strain\ gauge} + Mass_{hanging\ mass} \quad (5.2)$$

When the mass of the strain gauge was measured as 2.139kg.

Table 5.4 outlines the applied loads and rotational centres used during testing. Hanging masses were available in 0.5kg, therefore applied loads were overestimated for some conditions. Alternatively, for the 5-year-old sized PPC AFO and the 15-year-old sized, 4.5mm PPC AFO, the applied load was reduced due to buckling of the AFO.

Table 5.4: Rig Settings used in the repeatability study. GC = Gait Cycle. Hor = horizontal. Vert = Vertical

AFO	Ankle axis / mm		Rig axis / mm		GC moment / Nm	Load for GC Moment / N	Applied Load / N
	Hor	Vert	Hor	Vert			
5yr PPC 3mm	37.5	56.5	40	55	17.9	35.8	30.79
5yr PPH 3mm	37.5	56.5	40	55	17.9	35.8	35.70
10yr PPC 4.5mm	46	71	45	70	31.9	63.8	79.84
10yr PPH 5mm	46	71	45	70	31.9	63.8	79.84
15yr PPC 4.5mm	52.5	83.5	55	85	54.2	108.4	79.84
15yr PPH 5mm	52.5	83.5	55	85	54.2	108.4	119.08

Each AFO was tested three times, with a break between each test to allow the AFO to return to its preloaded state, as indicated by the digital inclinometer returning to $0^\circ \pm 0.1^\circ$. Force plate and strain gauge data were synchronised using an external trigger to start and stop data collection. Before each test, the force plates, strain gauge and digital inclinometer were zeroed. This procedure was then repeated on a second occasion, one day later, by the same assessor. During the second session, only three AFOs were tested, one from each age group, selected at random.

5.2.4 Data Analysis

Marker trajectories for each trial were labelled within Qualisys track manager (2021.2, Qualisys, Sweden), then exported to Visual3D (2023.10, HAS-motion, Canada) as a .c3d file. Here, the marker model was applied (Figure 5.7, Appendix E) and trials were filtered using a low-pass Butterworth filter (cut off-frequency 6Hz[289], [290]) and interpolated (maximum gap of 10). Following this, the sagittal angle of the rig U-frame with respect to the lab coordinate system, and the positional data for the markers on the AFO were exported as .txt and .mat files, respectively. Meanwhile, force plate data was exported

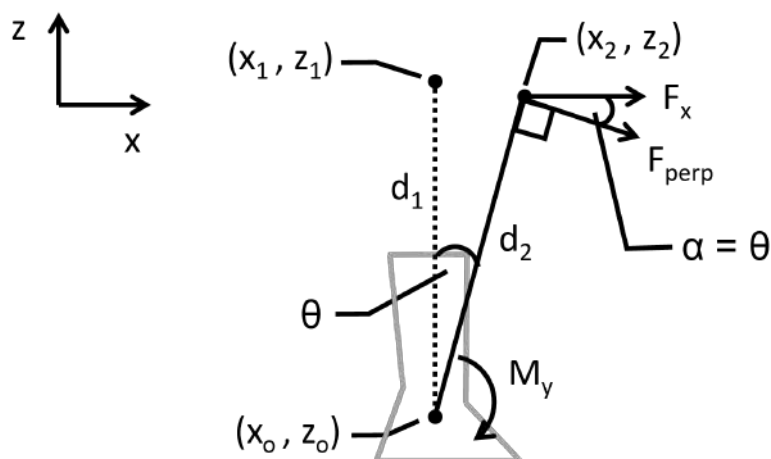
directly from Qualisys track manager as a .mat file and strain gauge data was saved as .csv file, before both were filtered using the same Butterworth filter as before, and the strain gauge data (4800Hz) was downsampled to the same frequency as the force plate data (1000Hz) using linear interpolation, within MATLAB (v2024a, MathWork, USA). Finally, the value on the digital inclinometer at the end of each trial was determined from the video recordings and stored within a .xlsx file.

Data was then analysed using MATLAB (v2024a, MathWork, USA). First comparisons between the measurement systems were made, to check the suitability of using MOCAP and force plates to determine AFO stiffness. For these comparisons, data from the six AFOs recorded in the first session was used. The first comparison was made between the maximum deflection measured using MOCAP and the digital inclinometer. For MOCAP, this was determined as the difference between the mean of the first and last 50 points of the rig U-frame sagittal angle data. Meanwhile, for the digital inclinometer, this was taken as the value from the video recordings, as the inclinometer was zeroed before each trial. The mean difference and standard deviation across the three repeats were calculated, before using a two-tailed, T-test to determine the significance of this difference. The second comparison was between the maximum applied force measured by the force plate and strain gauge. This value was determined as the difference between the first and last 50 points for the force plate and strain gauge data. After this, the same analysis, used to compare maximum deflection, was applied.

Afterwards, AFO stiffness was determined for the three AFOs repeated across both sessions. First, the force plate data (1000Hz) was down-sampled to the same frequency as the MOCAP data (100Hz) using linear interpolation. Then, both the force and angle data were cut between the instance at which the applied force increased above the 95% confidence interval of the starting force for the final time (mean of the first 50 data points) and remained within the 95% confidence intervals of the final force (mean of last 50 frames).

Following this, the deflection of the rig was calculated by subtracting the starting value of the remainder of the data set, before the applied moment was calculated using the

following equation



$$M_y = F_x \cdot d_2 \cdot \cos(\theta) \quad (5.3)$$

$F_x = \text{applied force}$

$$d_2 = \text{lever arm} = \sqrt{(x_2 - x_0)^2 + (z_2 - z_0)^2}$$

$\theta = \text{deflection}$

After which the change in moment was calculated by subtracting the starting value of the remainder of the data set.

Finally, stiffness was calculated via linear regression, as the gradient of the linear portion of the applied moment versus deflection curve. The mean stiffness and standard deviation were calculated for each AFO and for both sessions and two-tailed, paired T-tests were used to determine the significance between sessions. Furthermore, the within- and between-session ICCs were calculated using a two-way mixed model (type=mean of K, definition= agreement)[291], before calculating the Standard Error of Measurement (SEM) and Smallest Detectable Difference (SDD), using the same method as Totah et al.[231].

$$SEM = \sqrt{\frac{\sum (Std_{AFOi}^2)}{n}} \quad (5.4)$$

within session = $n = 3$ (trials)

between session = $n = 2$ (sessions)

$$SDD = SEM * 1.96 * \sqrt{2} \quad (5.5)$$

ICCs were interpreted as poor if less than 0.5, moderate between 0.5 and 0.75, good between 0.75 and 0.9 and excellent above 0.9[291].

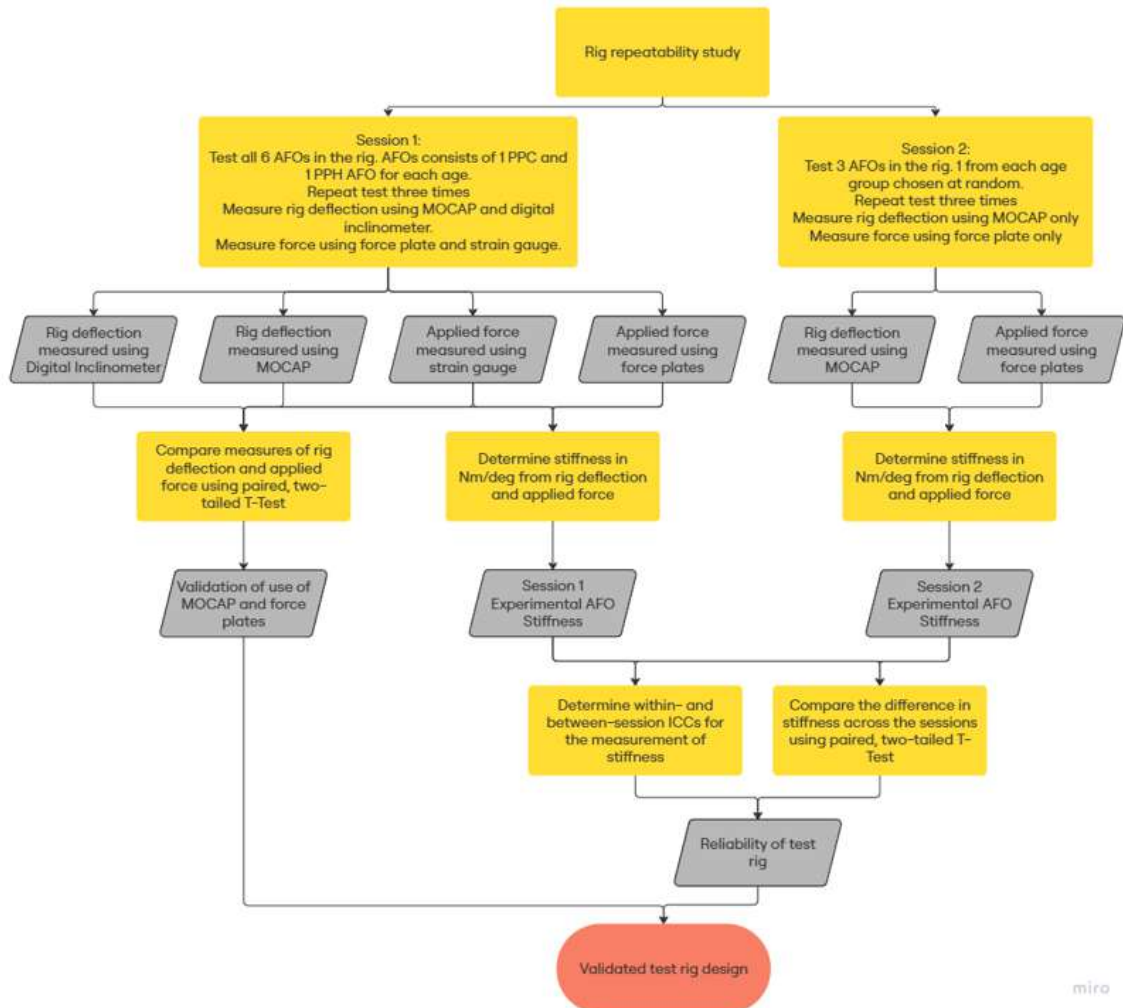


Figure 5.8: Structure of the rig repeatability study

5.2.5 Results

Comparison between MOCAP and the digital inclinometer

When comparing the deflection measured using MOCAP and the digital inclinometer, the average difference between the two measurement techniques varied from 0.04–0.09° across the six AFOs (Table 5.5). Furthermore, the only significant difference between tools was for the 5-year-old-sized, 3mm PPC AFO, however for this AFO the standard

deviation for the MOCAP and digital inclinometer were 0.01° and 0.02° , respectively.

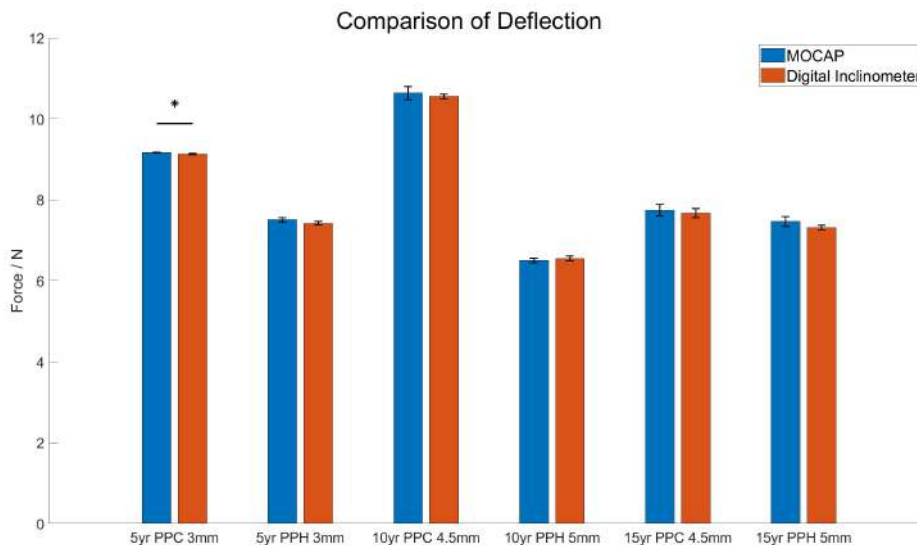


Figure 5.9: Comparison of deflection measured using 3D MOCAP and a digital inclinometer. Columns represent the mean of 3 repeats. Error bars represent \pm stdev. The star represents significance at $p < 0.05$.

Table 5.5: Comparison of deflection measures. MOCAP = 3-Dimensional Motion Capture, PPC = Copolymer Polypropylene, PPH = Homopolymer polypropylene.

AFO	Deflection / $^\circ$ (Mean \pm std)		P-value
	MOCAP	Digital Inclinometer	
5yr PPC 3mm	9.17 \pm 0.01	9.13 \pm 0.02	0.042
5yr PPH 3mm	7.51 \pm 0.05	7.42 \pm 0.04	0.981
10yr PPC 4.5mm	10.64 \pm 0.17	10.55 \pm 0.06	0.973
10yr PPH 5mm	6.50 \pm 0.06	6.55 \pm 0.06	0.989
15yr PPC 4.5mm	7.75 \pm 0.14	7.67 \pm 0.11	0.985
15yr PPH 5mm	7.46 \pm 0.12	7.31 \pm 0.06	0.967

Comparison between the force plate and strain gauge

Alternatively, when comparing the force measured using the force plate and strain gauge, issues calibrating the strain gauge meant data for the 5-year-old-sized 3mm PPC and 10-year-old-sized 4.5mm PPC AFOs was unavailable and two repeats were used for the 15-year-old-sized AFO. The average difference between the strain gauge and the force plate data ranged from 3.057-6.22N, however, this was only significant for two of the four AFOs (Table 5.6).

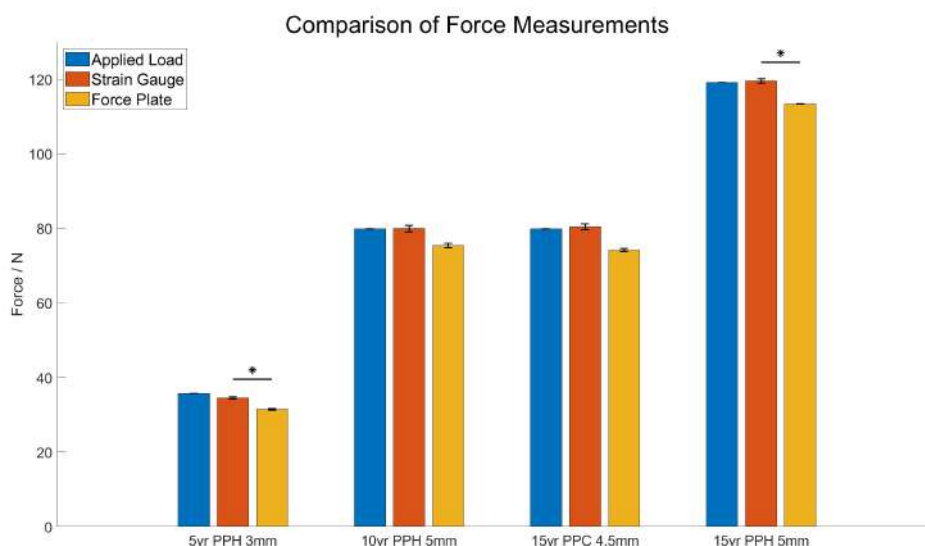


Figure 5.10: Comparison of force measured using force plates and the strain gauge. Columns represent the mean of 3 repeats. Error bars represent \pm std. The star represents significance at $p < 0.05$.

Table 5.6: Comparison of force measures. P-value = result of a T-test between the strain gauge and force plate data.

AFO	Applied load / N	Strain Gauge / N (Mean \pm std)	Force Plate / N (Mean \pm std)	P-value
5yr PPC 3mm	30.79	-	28.130 \pm 0.178	-
5yr PPH 3mm	35.70	34.524 \pm 0.271	31.467 \pm 0.204	0.000
10yr PPC 4.5mm	79.84	-	74.205 \pm 0.413	-
10yr PPH 5mm	79.84	79.911 \pm 0.871	75.442 \pm 0.610	0.907
15yr PPC 4.5mm	79.84	80.420 \pm 0.735	74.200 \pm 0.412	0.870
15yr PPH 5mm	119.08	119.505 \pm 0.578	113.334 \pm 0.059	0.009

Rig repeatability

Finally, for the 5- and 15-year-old AFO, there was no significant difference between the stiffness measured across the two sessions, however the difference in the 10-year-old AFO was significant (Table 5.7). Meanwhile, the rig demonstrated excellent ($ICC > 0.9$) within-session and between-session repeatability. Furthermore, the SEM was $\approx 0.1\text{Nm}/^\circ$ for both metrics.

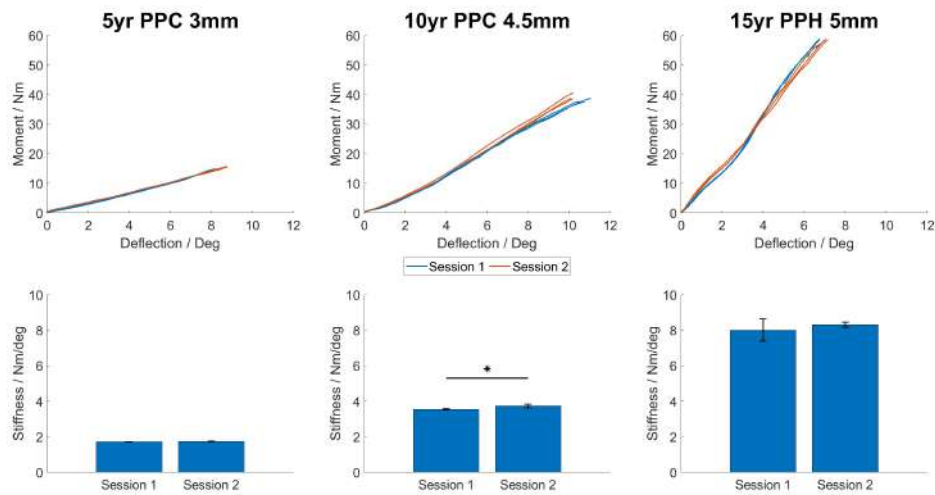


Figure 5.11: Moment versus deflection curves and corresponding stiffness from both sessions. Columns represent the mean of 3 repeats. Error bars represent \pm stdev. The star represents significance at $p < 0.05$.

Table 5.7: AFO stiffness used in the repeatability calculations

AFO	Stiffness / Nm $^{\circ}$ (Mean \pm std)		P-value
	Session 1	Session 2	
5yr PPC 3mm	1.709 \pm 0.016	1.732 \pm 0.015	0.129
10yr PPC 4.5mm	3.536 \pm 0.035	3.737 \pm 0.098	0.028
15yr PPH 5mm	8.000 \pm 0.626	8.306 \pm 0.144	0.455

Table 5.8: Within- and between-session (within-assessor) rig repeatability. CI = Confidence Interval, ICC = Intra-class correlation, SDD = Smallest Detectable Difference and SEM = Standard Error of Measure.

	ICC (95% CI)	SEM / Nm/ $^{\circ}$	SDD / Nm/ $^{\circ}$
Within-session	0.997 (0.987-1.000)	0.105	0.290
Between-session	0.999 (0.953-1.000)	0.128	0.355

5.2.6 Discussion

The test rig was designed to quantify AFO stiffness at the ankle in the sagittal plane during the second rocker of gait. The rig demonstrated excellent test-retest and intra-assessor repeatability, and low SEM, which were in line with existing manual[92], semi-automated[232] and automated rigs[231]. Meanwhile, it produced a lower test-retest percentage error than a previous rig which utilised MOCAP[203]. Furthermore, whilst

there was a significant, 0.201Nm/° (5.68%) increase in stiffness for the 10-year-old AFO between the two sessions, it is less than the SDD for the rig and the variation in AFO stiffness that could be caused by the manufacturing process[203]. Therefore, it is not thought to be clinically significant.

MOCAP has been used infrequently in test rigs, therefore comparisons were made with measurement tools used within previous rigs, to determine the validity of using this technology. Comparisons between deflection measured using MOCAP and a digital inclinometer demonstrated close agreement, with the average difference $< 0.1^\circ$ across all AFOs. This is likely due to a combination of noise within the MOCAP system, where the mean residual error across all 15 cameras was 0.505 ± 0.101 mm, and the accuracy of the digital inclinometer, which was $\pm 0.2^\circ$.

Alternatively, larger differences were seen when comparing the horizontal component of the force plate data and the force measured using the strain gauge. Here, the force plate data was, on average, 3.057-6.22N lower than the strain gauge across the four AFOs, whilst the strain gauge data was within ± 1.176 N of the applied load. A small part of this can be attributed to the assumption that the force remained horizontal throughout loading. In reality, there was a change in the angle between the direction of force and the horizontal, equivalent to the rig deflection. Therefore, the force exerted on the rig will equal

$$Force_{rig} = Force_{applied} \cdot \cos(\theta) \quad (5.6)$$

where $\theta = rig\ deflection$

However, based on the maximum deflection for the four AFOs measured using MOCAP, the change in force would be 0.297N, 0.511N, 0.727N and 1.016N (0.90%), equating to less than 1% of the force measured using the force plate.

Instead, this is likely an error in the force plate readings, which on average, equated to $7.46 \pm 2.3\%$ the applied force. However, the force plate readings were consistent between trials and always lower than the applied load. Therefore, although this error may

lead to a significant underestimation in AFO stiffness, from a clinical perspective, it would be more concerning if the rig overestimated AFO stiffness as this could lead to the provision of AFOs with inadequate mechanical properties. Instead, this error could be considered a factor of safety, ensuring future AFO designs have sufficient stiffness.

Furthermore, as the research being conducted within this thesis is the start of the process towards an optimised rigid AFO design, investigating hysteresis or fatigue was deemed beyond the scope of the work at this stage. As these properties are loading speed-dependent, reliably measuring these properties with a manually operated rig is challenging, as demonstrated previously by Bregman et al.[92] and Novacheck et al.[77]. However, this current design could be automated to meet these requirements as this line of research progresses. Additionally, it only measured dorsiflexion stiffness during the second rocker in the sagittal plane, as this is the main failure mode of AFOs during gait. Previously only three rigs have observed stiffness in additional planes[202], [208], [229] and the clinical value of this can be debated as transverse and coronal biomechanical control exerted by rigid AFOs is limited compared to the sagittal. Meanwhile, Bregman et al. observed stiffness at the metatarsal-phalangeal joint, during the third rocker[92], however it may be difficult to achieve with this design as it is fixed to the force plate.

Continuing to look beyond the scope of this research, making the rig accessible across research institutions and some clinical facilities was considered during the design process. The current design is compact, easily transported and utilises technology available in these settings. Therefore, it has the potential to be used in both research and scientific environments, however, to improve accessibility further developments could be made. For example, trialling non-patient-specific lasts, as used by Bregman et al.[92] and Totah et al.[232], and developing a system that allows the position of the rotational axis to be changed whilst mounted to the force plate would improve the efficiency of testing multiple AFOs. Furthermore, the mounting to the force plates is designed around existing fixings for instrumented stairs (AMTI, USA) [288]. Therefore, a new method which did not require these fixings would be more universal.

5.2.7 Conclusions

The excellent test-retest and intra-assessor repeatability achieved using the rig demonstrates it is suitable for providing the experimental data required to validate the FE model. Looking beyond the scope of the thesis, it has the potential to be used across research and specialist clinical environments, however further development of the design is required before this could happen.

5.3 The validation of a FE model for measuring AFO stiffness

5.3.1 FE model Design

The FE model was designed within FEBio Studio (2.2.0, University of Utah, USA), to replicate the test rig developed during the previous section (Figure 5.12). The model adopted the same coordinate system as the MOCAP system, with the X-axis denoting the sagittal axis, the y-axis coronal and the z-axis transverse. The boundary conditions applied to the foot section mimic the clamping of the AFO to the baseplate of the rig. Firstly, a circle of elements in the heel were prescribed zero displacement in the X-Y-Z directions, whilst a rigid wall constraint was applied to the outer surface of the mesh, preventing it from penetrating the X-Y plane. Meanwhile, three rigid bodies were used to replicate the fixation of the shank section of the AFO to the rotating U-frame of the rig. The first rigid body represented the U-frame centre of rotation and was located at the X-Z coordinates of the rig pivot point and fixed in all six degrees of freedom. This was connected to a second rigid body, located 500mm proximal, which acted as the connection between the rig eye bolt and the pulling cable. These were connected via a 'revolute joint', which constrained the movement of the second body to rotation about the first body in the X-Z plane alone. Next, a third rigid body representing the shank last was located along the axis between the first and second bodies at the height of the shank last. This body was connected to the second rigid body via a 'prismatic joint', allowing it to translate along this axis, as the second rigid body rotated. The elements of the AFO mesh in the area where the strap was applied were connected to the third rigid body, constraining these elements to the movement of this body. Finally, to generate the dorsiflexion moment about the centre of rotation, a horizontal force in the x-direction was applied to the second rigid body.

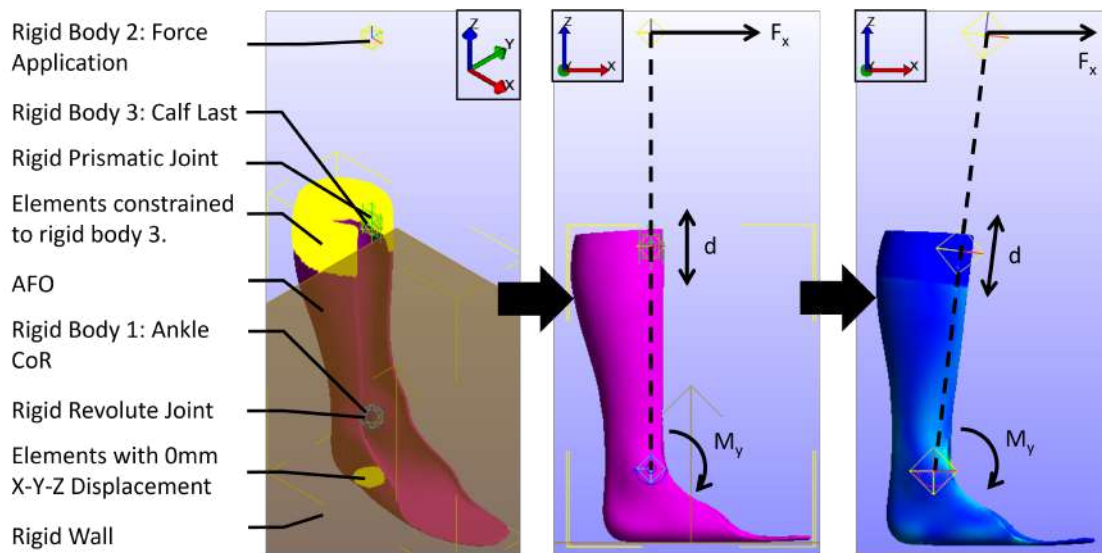


Figure 5.12: Diagram of the Finite Element Model. F_x = Force in the x-direction, M_y = Moment about the Y-axis. d = Displacement along the axis symbolised by the dotted line.

5.3.2 Experimental procedure

To validate the FE model for future primary research, comparisons were made between computational stiffness, from the FE model, and experimental data from the test rig. FE models were created for all 12 AFO STLs modelled in Section 5.1, to ensure the material properties of both PPC and PPH had been validated for all three age groups, 5-, 10- and 15-year-old. This equalled two FE models of each of the six manufactured AFOs. The first was a solid mesh capturing the real, non-uniform thickness of the AFO, which results from the vacuum-forming process. This was used to demonstrate the validity of the model material properties and boundary and loading conditions. The second was a solid mesh of the AFO with uniform thickness, modelled from the inside surface of the AFO with an assumed thickness equal to the average thickness of the device, measured using a novel technique (Appendix D). Validation of this mesh was necessary to demonstrate that assuming the AFO had a uniform thickness equal to the average thickness was valid, allowing the effects of polypropylene thickness to be observed in future studies.

After creating the digital AFO geometries, they were imported into the FE model and aligned so that the foot axis and X-axis were congruent, and the posterior heel aligned

with the z-axis. Then they were meshed using 10-node, quadratic tetrahedral elements, with a target maximum edge length of $\approx 3.5\text{-}4\text{mm}$. Both PPC and PPH were modelled as isotropic elastic materials with the properties highlighted in Table 5.9. The elastic modulus and yield stress were determined through material testing (Appendix F), whilst the Poisson's ratio was quoted from literature[193] and the density taken from the manufacturer's specifications.

Table 5.9: Polypropylene material properties used in the FE models.

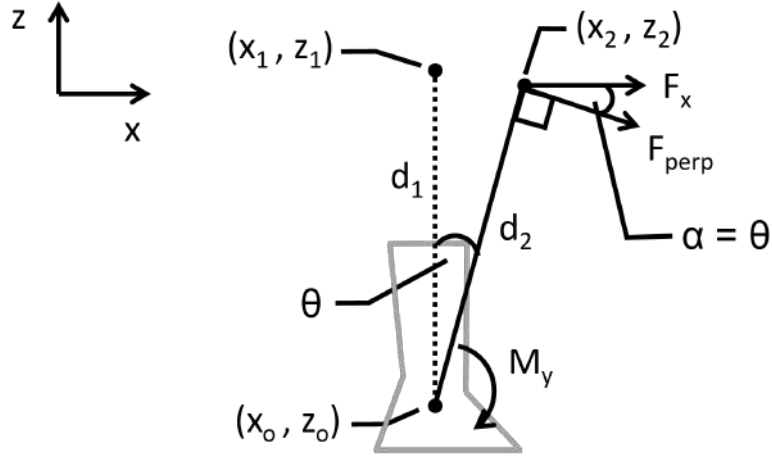
Type	Density / kg/m ³	Elastic Modulus / MPa	Yield Stress / MPa	Poisson's Ratio
PPC	910	796.96	28.33	0.43
PPH	900	979.46	39.40	0.43

Finally, AFOs were tested according to the peak dorsiflexion moments seen in gait, which are $\approx 1\text{Nm}/^\circ$ [93], [193], [194]. During experimental testing, the 10-year-old-sized AFOs and the 15-year-old-sized PPH AFO, were loaded to full capacity. Therefore, the forces applied in the FE analysis equalled the force required to generate the peak dorsiflexion moment in gait, calculated as 63.8N and 108.4N, respectively (Table 5.4). However, for the 5-year-old-sized AFOs and the 15-year-old-sized PPC AFO, the force applied during experimental testing was reduced to avoid buckling. Therefore, the force applied during FE analysis equalled the maximum force measured by the force plates for these AFOs, which equalled 30N and 80N, respectively (Table 5.6).

Meanwhile, a mesh convergence analysis was performed using the 5-year-old-sized 3mm PPC, 10-year-old-sized 4.5mm PPC and 15-year-old-sized 5mm PPH, non-uniform AFO models, the same AFOs used to measure the rig repeatability, which were chosen at random. The STL mesh density was decreased incrementally, resulting in three maximum edge lengths that could be approximately grouped as $\approx 2.5\text{mm}$, $\approx 3.5\text{-}4\text{mm}$ and $\approx 5.5\text{-}6\text{mm}$. Furthermore, the sensitivity of computational stiffness to the Poisson's ratio was tested by applying a range of values from 0.35-0.45, seen in literature[193], [197], [250], [256], to the non-uniform, 5-year-old models in both PPC and PPH.

5.3.3 Data Analysis

The position and force applied to the second rigid body were exported from the FE as a .txt file and exported to Matlab (v2024a, MathWorks, USA) for processing and analysis. First, the deflection was calculated as the angle between two vectors using the following equations.



$$\theta = \cos^{-1}\left(\frac{d_1 \cdot d_2}{|d_1| |d_2|}\right) \quad (5.7)$$

$$\theta = \cos^{-1}\left(\frac{dx_1 \cdot dx_2 + dz_1 \cdot dz_2}{|d_1| \cdot |d_2|}\right) \quad (5.8)$$

$$dx_1 = (x_1 - x_o)$$

$$dx_2 = (x_2 - x_o)$$

$$dz_1 = (z_1 - z_o)$$

$$dz_2 = (z_2 - z_o)$$

$$|d_1| = \sqrt{dx_1^2 + dz_1^2} \quad (5.10)$$

$$|d_2| = \sqrt{dx_2^2 + dz_2^2}$$

Then the applied moment was calculated as

$$Moment = F \cdot d \cdot \cos(\theta) \quad (5.11)$$

F = applied force, d = lever arm and θ = deflection

Then a first or second-order polynomial was fitted to the raw moment versus deflection data, with its appropriateness determined using the adjusted R^2 value calculated using the following equations.

$$R_{adj}^2 = 1 - \frac{n-1}{n-p} \cdot \frac{SSE}{SST} \quad (5.12)$$

Where

$$SSE = \text{Squared sum residuals} = \sum (y_i - \hat{y}_i)^2 \quad (5.13)$$

y = actual y value

\hat{y} = predicted y value

$$SST = \text{Squared sum total} = \sum (y_i - \bar{y})^2 \quad (5.14)$$

Using the line of best of fit, linear regression was performed on the linear portion of the curve to determine the stiffness of the AFO. To determine the validity of the FE models, the stiffness, and moment versus deflection curves were compared to the test rig data.

Meanwhile, for the mesh convergence study, the change in stiffness with model computation time and edge length, and the change in thickness with edge length were compared for each model and the three element sizes.

Finally, the effect of Poisson's ratio on stiffness for the 5-year-old PPC and PPH models with non-uniform thickness, was compared, with stiffness calculated as outlined previously.

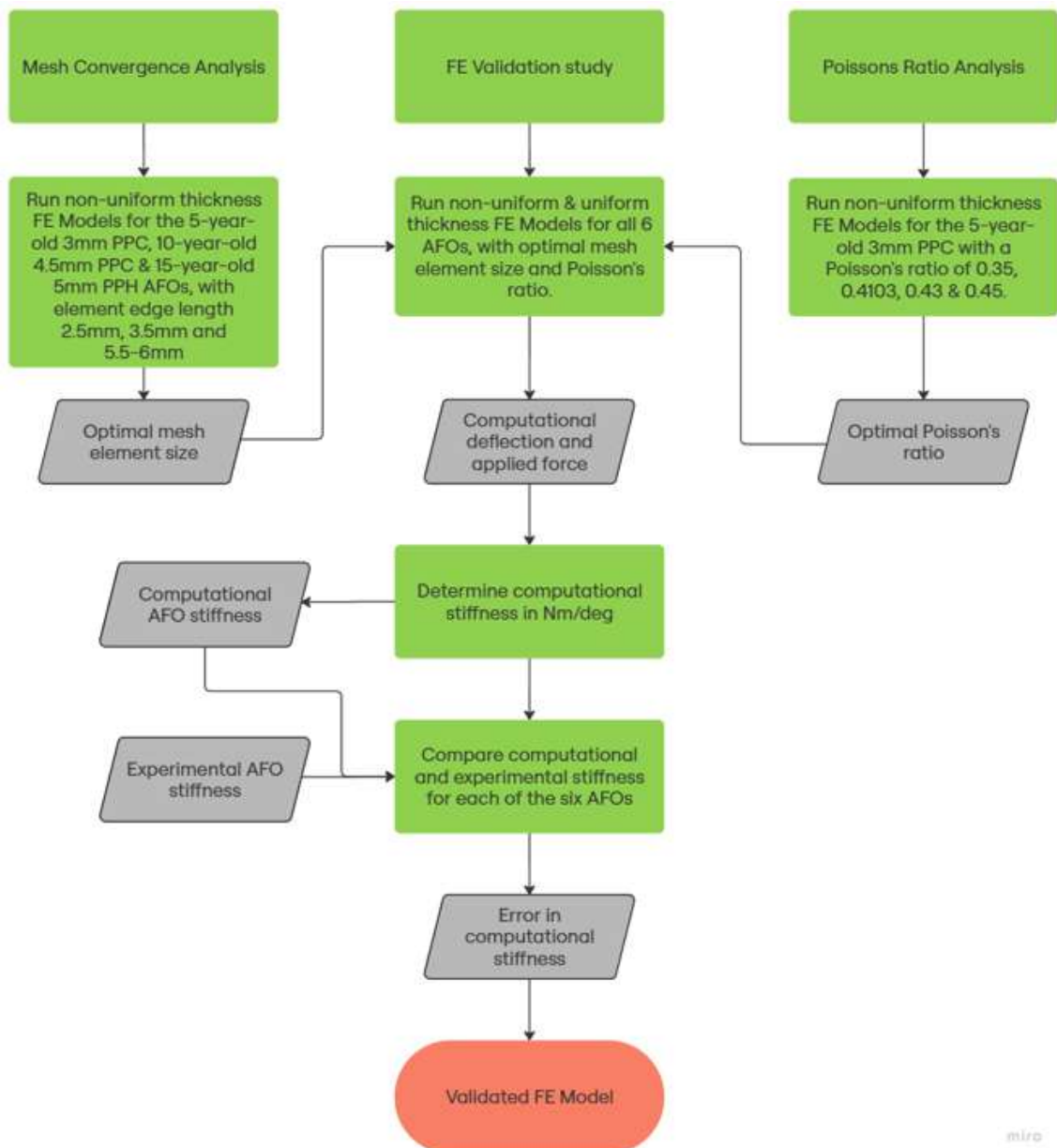


Figure 5.13: Structure of the FE validation study

5.3.4 Results

Mesh Convergence Analysis

The results of the mesh convergence analysis are presented in Figures 5.14 and Table 5.10. They indicate that for each of the three models, increasing the edge length of the FE mesh resulted in a thicker, stiffer model which took a shorter time to run. For the 5-year-old model, increasing the edge length from 2.491mm to 3.834mm increased AFO stiffness by $0.067\text{Nm}/^\circ$, whilst the computational time decreased by 1375s. Meanwhile, increasing the edge length from 2.491mm to 5.809mm saw the stiffness increase

by $0.14\text{Nm}/^\circ$ and the computational time reduced by 1561s.

Similar differences were seen for the 10-year-old model (Table 5.10). Here, an increase in edge length from 2.424mm to 3.581mm resulted in the AFO stiffness increasing by $0.068\text{Nm}/^\circ$ and the computational time decreasing by 339s. Alternatively, comparing the 2.424mm and 5.581mm demonstrated an increase in stiffness of $0.144\text{Nm}/^\circ$ and a decrease in computation time of 835s.

Finally, for the 15-year-old model (Table 5.10) there were larger differences in computational stiffness. The difference between the 2.676mm edge length and the 4.120mm and 6.231mm edge length was $+0.084\text{Nm}/^\circ$ and $+0.199\text{Nm}/^\circ$, respectively. Meanwhile, the difference in computation time was -876s and -1450s.

Table 5.10: Results of the Mesh Convergence Analysis

FE Model	Max Edge Length / mm	Stiffness / $\text{Nm}/^\circ$	Computation Time / s	Thickness / mm
5-year-old	2.491	1.805	1935	2.619
	3.834	1.872	560	2.776
	5.809	1.945	374	3.116
10-year-old	2.424	3.370	1014	3.394
	3.581	3.438	675	3.509
	5.551	3.514	179	3.760
15-year-old	2.676	8.307	1627	4.192
	4.120	8.394	751	4.316
	6.231	8.506	177	4.568

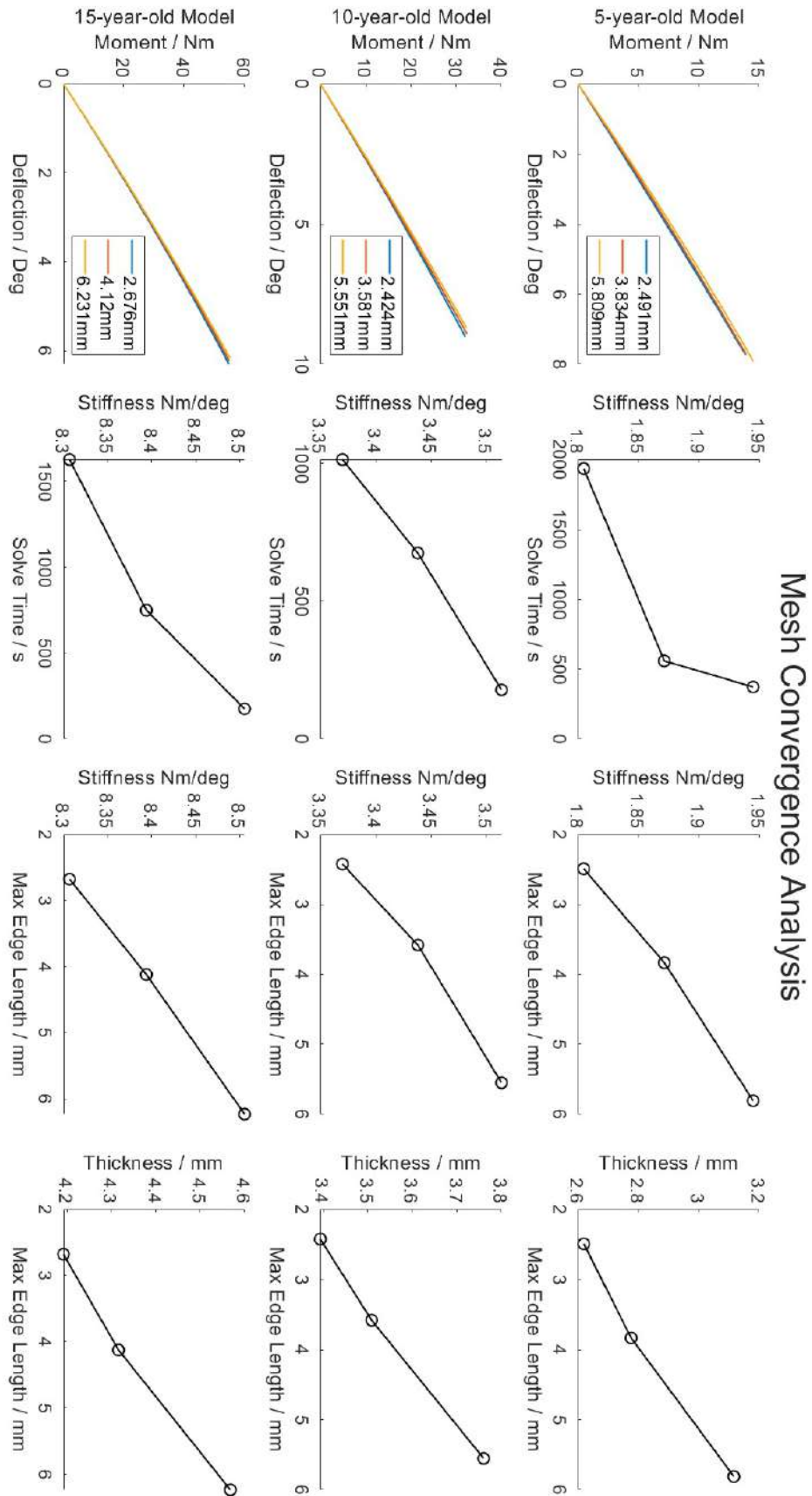


Figure 5.14: Mesh Convergence Analysis for the 5, 10 and 15-year-old FE models.

Poisson's Ratio dependency

Poisson's ratio of 0.35, 0.4103, 0.43 and 0.45 resulted in AFO stiffness of 1.864 Nm/°, 1.887Nm/°, 1.866Nm/° and 1.852Nm/°, respectively, for PPC and 2.258Nm/°, 2.284Nm/°, 2.296Nm/° and 2.309Nm/° for PPH (Figure 5.15). The maximum difference in stiffness between Poisson's ratio values was 0.035Nm/° for the PPC model and 0.051Nm/° for PPH.

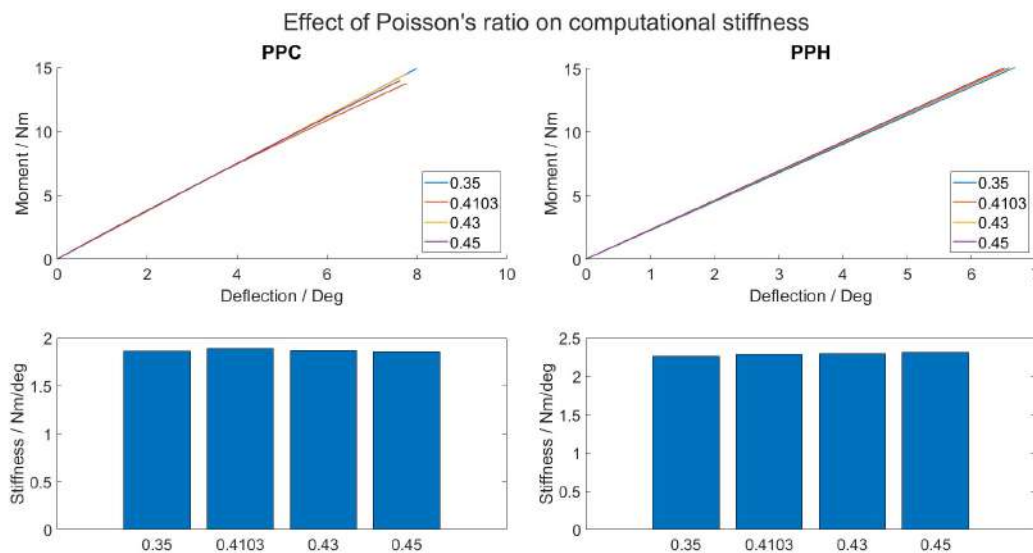


Figure 5.15: Effect of Poisson's ratio on computational stiffness

Computational versus Experimental Stiffness

For all the AFOs, except the 15-year-old, 4.5mm PPC AFO, the behaviour predicted by both FE models and measured experimentally using the rig were similar. However, for the 15-year-old 4.5mm, PPC AFO there was a considerable discrepancy in the behaviour (Figure 5.16). Excluding the 15-year-old 4.5mm, PPC AFO, the difference between the rig and non-uniform FE models, ranged from $-2.247\text{Nm}/^\circ$ to $0.211\text{Nm}/^\circ$, translating to a percentage difference of -2.78% to 2.54% , whilst the difference between the uniform thickness model ranged from $-0.069\text{Nm}/^\circ$ to $-0.127\text{Nm}/^\circ$ or -0.060% to 5.92% . However, for the 15-year-old PPC, 4.5mm AFO, the differences were $-2.247\text{Nm}/^\circ$ (-33.86%) and $-2.341\text{Nm}/^\circ$ (-35.26%) respectively (Table 5.12).

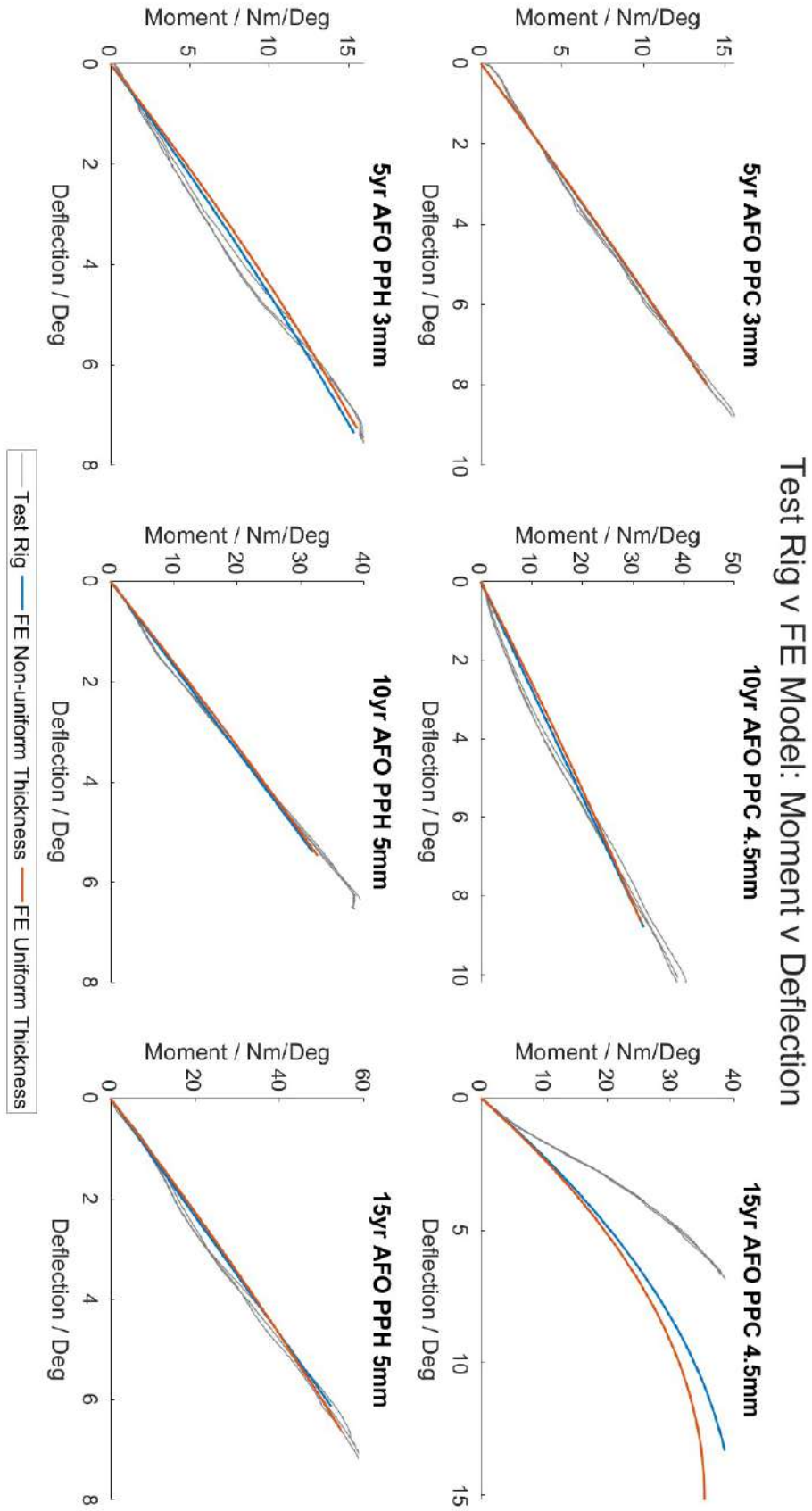


Figure 5.16: Computational versus Experimental Deflection-Curves

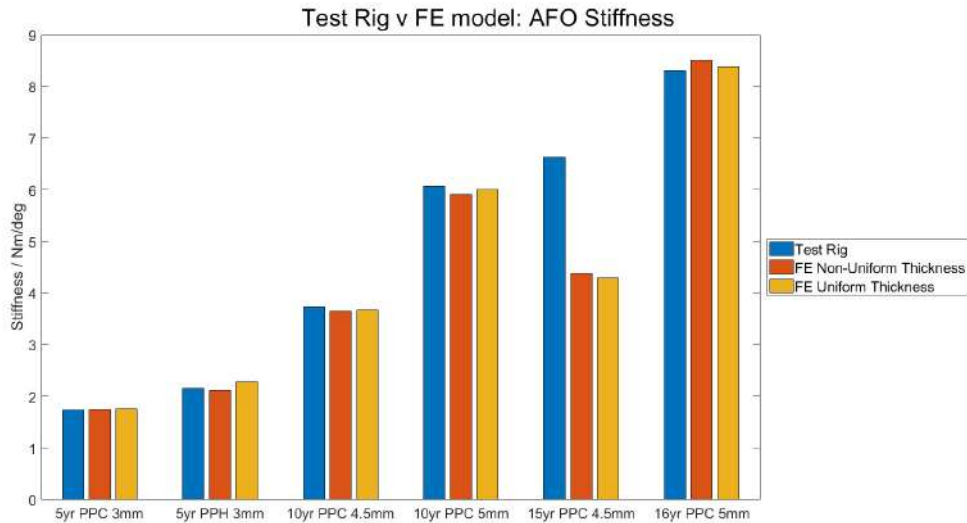


Figure 5.17: Computational versus Experimental AFO Stiffness

Table 5.11: Computational and Experimental AFO Stiffness. FE = Finite Element Analysis, PPC = Copolymer Polypropylene and PPH = Homopolymer Polypropylene.

AFO	Stiffness / Nm/° (Mean ± Std)		
	Test Rig	Non-Uniform thickness FE	Uniform Thickness FE
5yr PPC 3mm	1.732 ± 0.015	1.746	1.754
5yr PPH 3mm	2.151 ± 0.007	2.117	2.278
10yr PPC 4.5mm	3.737 ± 0.098	3.651	3.677
10yr PPH 5mm	6.075 ± 0.065	5.906	6.005
15yr PPC 4.5mm	6.637 ± 0.605	4.390	4.297
15yr PPH 5mm	8.306 ± 0.144	8.517	8.391

Table 5.12: Error in Computational Stiffness. Abs. = Absolute error. % = Percentage error. FE = Finite Element Analysis, PPC = Copolymer Polypropylene and PPH = Homopolymer Polypropylene.

AFO	Non-Uniform FE v Rig		Uniform FE v Rig		Non-Uniform v Uniform FE	
	Abs./ Nm/°	%	Abs./ Nm/°	%	Abs./ Nm/°	%
5yr PPC 3mm	0.014	0.81	0.022	1.28	0.008	0.46
5yr PPH 3mm	-0.033	-1.54	0.127	5.92	0.160	7.58
10yr PPC 4.5mm	-0.086	-2.31	-0.060	-1.62	0.026	0.71
10yr PPH 5mm	-0.169	-2.78	-0.069	-1.14	0.099	1.68
15yr PPC 4.5mm	-2.247	-33.86	-2.341	-35.26	-0.093	-2.13
15yr PPH 5mm	0.211	2.54	0.085	1.03	-0.126	-1.48

5.3.5 Discussion

Firstly, the mesh convergence analysis demonstrated a linear increase in computational stiffness with element size (Figure 5.14). This is caused by the artificial thickening of the mesh as the larger triangular elements approximate the curvature of the AFO geometry. Meanwhile, increasing the element size, decreases the number of nodes in the model, at which the model behaviour is calculated. Therefore, the computational time of the models decreases. Consequently, the optimal mesh size is a compromise between the accuracy of the predicted stiffness and efficiency. The increase in stiffness for the largest element size tested exceeded the SEM of the test rig ($0.105\text{Nm}/^\circ$) for all three models. Therefore, the optimal edge length for the FE models was between 3.5-4.2mm as this reduced the computational time by a minimum of a third, whilst the increase in stiffness was within the SEM of the rig.

Furthermore, when excluding the 15-year-old-sized, 4.5mm, PPC AFO, the error between the test rig and the non-uniform FE model was within the within-session SEM of test rig ($\pm 0.105\text{Nm}/^\circ$), for both the 5-year-old-sized AFOs and the 10-year-old-sized 4.5mm PPC AFO, whilst the error in the remaining two AFOs equated to $<3\%$ of the experimental stiffness. Meanwhile, the difference between the rig and uniform thickness FE model was within $\pm 0.105\text{Nm}/^\circ$ for all the AFOs, except the 5-year-old-sized 3mm PPH AFO, where there was a percentage error of 5.92%. Previously, the percentage error in computational stiffness has been reported as $<10\%$ [201] and 2.11-10%[232] for polypropylene AFOs and 3%[258] for PLA devices. As a result, for five of the six AFOs tested, both FE models were found to predict the mechanical properties of rigid AFOs with confidence.

However, for the 15-year-old-sized, 4.5mm PPC AFO the percentage error between the rig and FE models was considerably higher. Here the FE model predicted a lower AFO stiffness that buckled during loading, illustrated by the plateau in the curve. When considering the source of the error, it is unlikely to be in the rig data as the experimental stiffness of this AFO aligned with the other devices tested. However, to rule out procedural errors, testing was repeated producing results consistent with the first data collection (Figure 5.18). However, this highlighted that the calf clamp was constricting

the proximal shell of the AFO, potentially altering the second moment of inertia of the device. Therefore, this was simulated using the FE model and was shown to have minimal impact on stiffness (Figure 5.18). Therefore, the only potential sources of error in the experimental data could be an impurity in the PPC sheet or an issue during vacuum-forming, which are not accounted for in the FE material model. However, there was no visible issue with the AFO shell so this is improbable.

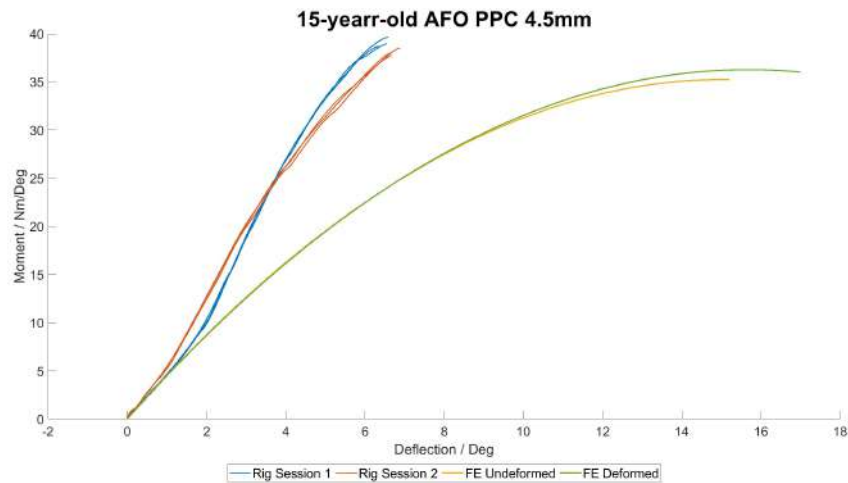


Figure 5.18: Experimental and computational behaviour of the 15-year-old, PPC, 4.5mm AFO.

Alternatively, from a FE perspective, the model set-up and material properties were analogous to other validated models. Therefore, the only differences were in the shape and thickness of the AFO STL. However, there were no clear differences between the thickness distribution of this AFO and the others (Appendix G). Furthermore, the AFO was rescanned, which demonstrated comparable thickness distribution to the original (Appendix H). Furthermore, the behaviour of the non-uniform and uniform thickness model for this AFO are similar (-2.13% percentage error) demonstrating the average thickness was measured accurately. Consequently, this would imply the error is related to the shape of the AFO and the interaction between the geometry and the rigid wall constraint. The rigid wall constraint applies a penalty force to the mesh to prevent it from penetrating the plane which defines the constraint. Therefore if the footplate of the AFO is not flat, it may break this constraint, leading to an excessive penalty force being applied to the mesh, causing excessive bending. In any case, the error is likely attributable to this specific AFO geometry. Therefore, as the FE model set-up and in-

puts are validated by the other five AFOs, the simulation can be used with confidence in future studies.

Additionally, the 5-year-old models were only validated up to 15Nm, due to AFOs buckling in the rig over this load. Physiologically, the peak dorsiflexion moment for a 5-year-old would be $\approx 17.9\text{Nm}$, limiting the inferences on clinical performance which can be made during future studies. However, for the remaining age groups, at least one of the models was validated to the full physiological loading conditions.

Meanwhile, small differences in the behaviour of the two FE models were seen. For five out of the six AFOs the percentage error in stiffness was within $\pm 3\%$ and can therefore be accredited to measurement error caused by slight variations in the set of elements in the heel of the AFO that were constrained to zero displacement in all directions. However, for the 5-year-old PPH AFO, the stiffness of the uniform FE model was 7.58% higher. Therefore, this is more likely due to the fluctuations in AFO thickness caused by the vacuum-forming process. For this AFO, there appeared less thinning in the shank and toe sections, when compared to the other devices (Appendix G). Therefore, the average thickness is likely skewed by the thickness in these areas, which typically do not affect the stiffness of the device [212], [232], [250].

One of the key assumptions of this simulation is that PPC and PPH behave like isotropic, elastic materials during one loading cycle. This in-line with previous examples [193], [196], [197], [201], [212], [251], [252] and reduced the complexity of the model without compromising on accuracy. However, like the rig, as this line of research develops and the assessment of fatigue is required, a more complex material model which incorporates the viscoelastic behaviour of the materials, such as the parallel rheological framework model used by Ielpai et al. [232]. Furthermore, the material properties inputted into these models were determined through material testing, except for Poisson's ratio which was taken from literature [193]. The elastic modulus for PPC agreed with the modulus measured by Chatzistergos et al. [193], however, was $\approx 200\text{MPa}$ less than the values often quoted in literature [196], [201], [212], [251], [256], [257]. This highlights the importance of determining material properties through material testing and may suggest some existing

models have over-estimated stiffness, particularly those which used an elastic modulus of 2400MPa[198], [252]. Alternatively, the validation process found the model was insensitive to the Poisson's ratio within the typical range for plastic, supporting earlier findings by Syngellakis et al.[256].

Finally, the current model imposed the rotational axis of the ankle through a series of rigid bodies, presenting a solution to constraining deformation without a complex foot model. This is a development on many previous simulations which did not include this[193], [196]–[198], [201], [255]. Furthermore, instead of using a fixed boundary condition along the whole plantar aspect of the AFO, only a small set of elements in the heel were fixed, whilst a rigid wall constrained the remaining plantar surface of the mesh. Fixing elements can result in artificial areas of high stress, which were seen in this model, and may restrict the normal deformation of the shell. As a result, the boundary conditions in this model may be more realistic than those often used previously, however, these could be developed by applying a force or pressure distribution along the inner surface of the foot, as used by Syngellakis et al.[256], should be explored.

5.3.6 Conclusions

Comparisons with experimental data from the test rig demonstrated that the FE model accurately predicts the dorsiflexion stiffness of rigid AFOs and can therefore be used in future studies to assess the mechanical performance of AFO designs and direct the optimisation process.

Chapter 6

The stiffness of clinically utilised rigid AFOs used for the management of gait impairments in children with CP.

Chapter Overview

In the next chapter of the thesis, the FE models were used to evaluate the stiffness of clinically relevant rigid AFO designs. The designs were determined based on discussion with the clinical advisory group and additional literature (Section 3.2). The purpose was to determine whether current clinical practice resulted in AFOs with sufficient stiffness to achieve their clinical goals. In doing so it highlighted areas where AFO design could be improved, which was taken forward into the second study, where the optimisation of rigid AFO design was explored.

6.1 Introduction

Rigid AFOs are widely prescribed to children with CP to manage gait impairments. Fundamentally, they are used to immobilise the ankle joint and alter lower limb biomechanics during gait[240]. Their ability to achieve this depends on their stiffness, which is influenced by design factors including the type and thickness of thermoplastic, trim line design and use of additional reinforcements, all of which must be determined by the clinician during prescription[80]. Despite this, there are currently no clinical guidelines on how to design rigid AFOs for paediatric populations, one of the main flaws in the OSKAR algorithms[16], [17]. As a result, AFO prescription is non-standardised, potentially leading to AFOs with inadequate stiffness being provided, which could lead to more severe gait impairments or increase the risk of falls. The lack of consideration of rigid AFO design is also evident in existing studies through the poor reporting of AFO properties[117], or the fact that rigid AFOs permitted more than 5° ankle motion[155], [157], [161], [163], [168], [170], which in some cases was not significantly different to flexible or articulated devices[161], [163]. As a result, this may explain why existing evidence on the indirect effects of AFOs on the kinematics and kinetics of the joints and segments proximal to the ankle is limited (Section 2.1).

Consequently, there is a need to investigate rigid AFO design, with the long-term aim of developing clinical recommendations. This process should begin by evaluating clinical practice, to determine the appropriateness of rigid AFOs being prescribed. Previously, the effects of all four design factors on stiffness have been assessed, generally concluding that stiffness increases with material rigidity, thickness, and trim line depth (Section 2.2). However, the majority have focused on adult and/or flexible devices[193], [195]–[199], [201], [204], [207]–[209], [245]. Whilst this provides an insight into the effect of AFO design, differences in AFO size, loading conditions and intended function make it difficult to generalise results from these studies directly to paediatric rigid AFOs. This may also be true for studies which have only considered one paediatric AFO size, given the significant difference in size and mass between a 5- and 15-year-old[194], [197], [199], [202]. Additionally, studies have tended to look at the design considerations in isolation[196], [197], [199], [202], [204]–[206], [208], [209], [245]. Instead, studying the combined effects of these factors and the interactions between them would be more

valuable from a clinical perspective.

As a result, the following study looks to investigate the stiffness of AFO designs, used clinically to manage gait impairments in paediatric CP populations, using FE analysis. The aim is to determine if the designs deflect less than 5° and are therefore suitable for clinical practice. The 5° threshold is based on work by McGinley et al. into the clinical significance of kinematic changes[292] and was adopted by Hovroka et al. as a criterion for adequate AFO mechanical properties of AFOs[237]. Multiple design iterations will be tested, demonstrating the combined effects of the four design factors. Furthermore, the influence of AFO size will be considered by testing AFOs for a 5-, 10- and 15-year-old child.

6.2 Aims

To determine if clinically utilised AFOs, designed for a 5-, 10-, and 15-year-old, deflect <5° under physiological loading conditions, and therefore have adequate stiffness for clinical application.

To investigate whether the design of the AFO needs to be adapted depending on the size of the AFO or the user's age.

6.3 Methodology

6.3.1 Experimental procedure

Table 6.1 outlines the AFO designs tested within this study, which were chosen based on discussion with the clinical advisory group (Section 3.2) and wider literature[284]. The material thicknesses are taken as the value stated by the manufacturer, assuming there is minimal discrepancy between the manufacturer's specifications and the thickness of the sheet supplied. To test the stiffness of each of these designs and the influence of AFO size, the 5-year-old-sized PPC, 10-year-old-sized PPC and 15-year-old-sized PPH FE models with uniform thickness, validated in Section 5.3, were used.

Table 6.1: Design of AFOs tested. All designs were replicated for the three ages.

Trim Lines	Reinforcement	Material	Thickness / mm
Anterior	No ribbing	PPC	3
			4.5
		PPH	3
			4
Through	No ribbing	PPC	3
			4.5
		PPH	3
			4
Anterior	Ribbing	PPC	3
			4.5
		PPH	3
			4

STLs for the anterior trim line designs were modelled as described in Section 5.1, however, the inside surface mesh was thickened by an idealised thickness of either 3mm, 4mm or 4.5mm, instead of the average AFO thickness, measured from the manufactured AFO. These thicknesses corresponded to the thickness of PPC and PPH sheets which were available from UK suppliers (Algeos, LimbTex and North Sea Plastics) and <4.5mm, which was considered the clinical threshold for paediatric AFOs based on the discussion with the clinical advisory group and Eddison et al.'s survey into the prescription of AFOs[284].

From these STLs, the additional designs were then modelled. Firstly, the through the malleoli trim lines were defined in the sagittal plane by two lines extending from the anterior trim line at 1/2 of the AFO height to the midpoint between the medial and lateral malleoli apexes, then to the anterior trim line at 1/2 foot length. The vertex of these two lines was then filleted with a radius equal to half the malleoli width, measured from the foam mould manufactured in Section 5.1 (Figure 6.1). As with the anterior trim lines, the through trim lines were replicated on both the medial and lateral sides to avoid torsional deformation during loading. The through trim lines were tested as they

were used by some orthotists in the clinical advisory group (Section 3.2), to allow easier donning of the AFO.

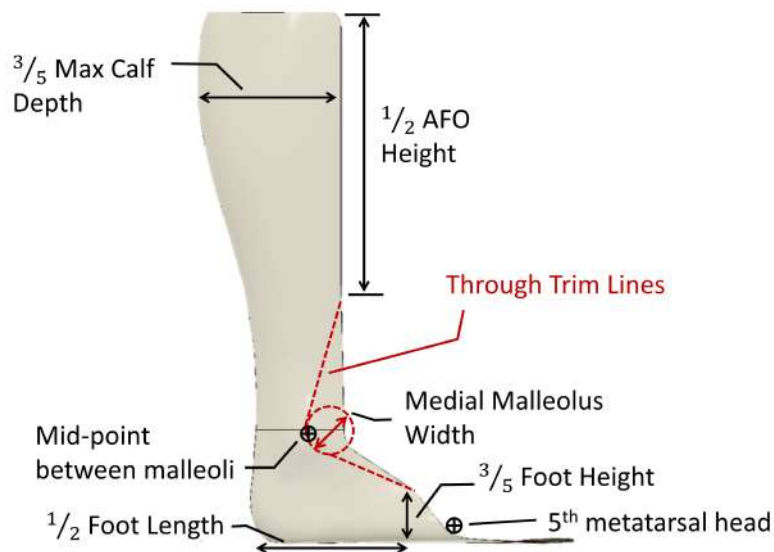


Figure 6.1: Through the malleoli trim line definition

Following this, the ribbed design was created. The ribs were L-shaped with a 10mm circular cross-section. Based on clinical guidance, they were placed posterior to the lateral malleolus to allow post-drape modifications[200], [293]. The proximal arm of the rib extended vertically to $2/3$ the AFO height, whilst the distal arm extended to a point which was 15mm normal, from the trim line, at half the foot length. Again, the vertex of these two lines was filleted with a radius equal to half the malleoli width. The proximal height of the rib was based on work by Chatzistergos et al. on the optimal dimensions for a mediolateral reinforcement[193]. However, on clinical advice, the distal length was only extended to half the foot length as it was thought that extending the ribbing beyond this point would impact footwear fit. Before testing, two members of the clinical advisory group approved the designs (Figure 6.2).

Once all the AFO designs had been modelled, they were imported into their age-matched FE models and meshed with 10-node, quadratic tetrahedral elements with an average maximum edge length between 3.5-4.1mm. A full description of how the model was set up can be found in Section 5.3. The 5-, 10-, and 15-year-old-sized AFOs were tested up to an applied force of 30N, 63.8N and 108.4N, respectively. These were the forces calculated to generate a moment of 1Nm/kg based on the average mass of a 5-, 10- and 15-year-old according to anthropometric data[286], [287], except for the 5-year-old

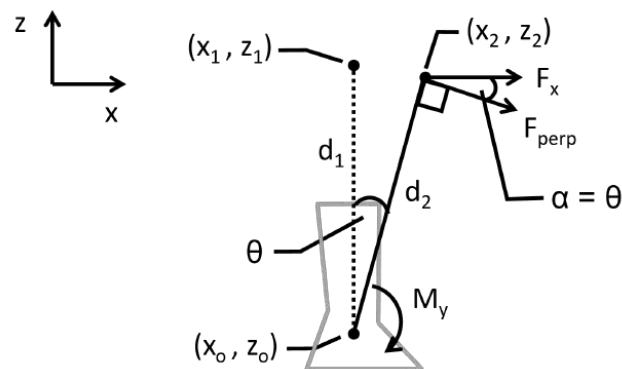
model, as this was only validated up to 30Nm as the AFO buckled before reaching full loading capacity during experimental stiffness testing (Section 5.2).



Figure 6.2: Clinical AFO designs for the 5-year-old AFO.

6.3.2 Data Analysis

The position and force applied to the second rigid body were exported from the FE as a .txt file and exported to Matlab (v2024a, MathWorks, USA) for processing and analysis. First, the deflection was calculated as the angle between two vectors.



$$\theta = \cos^{-1}\left(\frac{d_1 \cdot d_2}{|d_1| |d_2|}\right) \quad (6.1)$$

$$\theta = \cos^{-1}\left(\frac{(dx_1 \cdot dx_2) + (dz_1 \cdot dz_2)}{|d_1| \cdot |d_2|}\right) \quad (6.2)$$

Then the applied moment was calculated as

$$Moment = F \cdot d \cdot \cos(\theta) \quad (6.3)$$

F = applied force, d = lever arm, and θ = deflection

Then a first or second-order polynomial was fitted to the raw moment versus deflection curve, with its appropriateness determined using the adjusted R^2 value calculated using the following equations.

$$R_{adj}^2 = 1 - \frac{n-1}{n-p} \cdot \frac{SSE}{SST} \quad (6.4)$$

Where

$$SSE = \text{Squared sum residuals} = \sum (y_i - \hat{y}_i)^2 \quad (6.5)$$

y = actual y – value

\hat{y} = predicted y – value

$$SST = \text{Squared sum total} = \sum (y_i - \bar{y})^2 \quad (6.6)$$

Using the line of best of fit, linear regression was performed on the linear portion of the curve to determine the stiffness of the AFO. A design was deemed to have appropriate mechanical properties if it had a maximum deflection of $> 5^\circ$ [292]. However, a revised value of 4.19° was used for the 5-year-old model, as the FE model was only validated up to $\approx 15\text{Nm}$, $\approx 2.9\text{Nm}$ less than the mean peak external dorsiflexion moment in stance for this age group[286], [287]. This revised figure was determined by calculating the stiffness required to limit deflection to 5° under a 17.9Nm moment, assuming linear bending behaviour, and then deriving the corresponding deflection at 15Nm , based on this gradient.

Finally, the Von Mises stress (MPa) distribution and coronal plane deformation were analysed using colour maps exported from FEBio Studio (2.2.0, University of Utah, USA). Von Mises stress (σ_y) is a value of effective shear stress and is calculated from the principal stresses.

$$\sigma_y = \sqrt{\frac{1}{2}[(\sigma_1 - \sigma_2)^2 + (\sigma_2 - \sigma_3)^2 + (\sigma_3 - \sigma_1)^2]} \quad (6.7)$$

It is based on the maximum distortion energy failure theory and typically adopted in FE analysis for ductile materials such as polypropylene[197], [198], [232], [255], [260]. This theory recognises that yielding in a ductile material is caused by the shear stress and is independent of the hydrostatic stresses which cause a volume change. Principal stress theory is unsuitable for ductile materials as it assumes that yield occurs when the maximum principal stress exceeds the yield or ultimate stress of the material and therefore does not account for plastic deformation.

6.4 Results

5-year-old-sized AFO designs

For the 5-year-old-sized AFO, the 4.5mm PPC and 4mm PPH AFOs with anterior trim lines, both with and without ribbing, produced sufficiently stiff devices which restricted deflection to below 4.19°. However, devices made from 3mm thick polypropylene or with through trim lines did not restrict deflection to <4.19° (Figure 6.4). Compared to the 3mm PPC AFOs, 3mm PPH AFOs were 22.69-25.03% stiffer, 4.5mm PPC AFOs were 87.80-105.08% and 4mm PPH AFOs were 87.02-101.50% (Table 6.2). Meanwhile, reducing the trim lines from the anterior to through position reduced stiffness by 35.05-38.11%, whilst introducing mediolateral ribbing reduced stiffness between 3.40-8.90%.

Table 6.2: Comparison of 5-year-old-sized AFO clinical designs

Design	Material	Thickness / mm	Stiffness / Nm/°	Max Deflection / °	Δ% in designs	Δ% in material
Anterior	PPC	3	2.64	5.63	-	-
		4.5	5.10	2.74	-	93.64
	PPH	3	3.24	4.55	-	22.86
		4	5.03	2.81	-	90.80
Through	PPC	3	1.68	13.10	-36.18	-
		4.5	3.16	4.70	-38.11	87.80
	PPH	3	2.10	9.81	-35.05	25.03
		4	3.15	4.77	-37.45	87.02
Ribbed	PPC	3	2.40	6,22	-8.79	-
		4.5	4.93	2.89	-3.40	105.08
	PPH	3	2.95	5.01	-8.90	22.69
		4	4.84	2.95	-3.67	101.50

10-year-old-sized AFO designs

The same pattern was seen for the 10-year-old-sized AFO, the 4.5mm PPC and 4mm PPH AFOs with anterior trim lines and ribbing produced sufficiently stiff AFOs which restricted deflection to below 5° (Figure 6.4). Meanwhile, the 3mm and through trim line devices did not achieve the desired stiffness, with the 3mm through models failing to converge fully. When comparing the different materials, 3mm PPH was 15.67-25.60% stiffer than 3mm PPC, 4.5mm PPC was 108.04-115.01% stiffer and 4mm PPH 104.11-120.21% stiffer (Table 6.3). Finally, reducing the trim lines from the anterior to through position reduced stiffness by 40.77-46.35%, whilst introducing mediolateral ribbing reduced stiffness between 0.13-10.49%

Table 6.3: Comparison of 10-year-old-sized AFO clinical designs. DNC = Did Not Converge, meaning the FE model did not run to completion

Design	Material	Thickness / mm	Stiffness / Nm/°	Max Deflection / °	Δ% in designs	Δ% in material
Anterior	PPC	3	3.11	10.40	-	-
		4.5	6.47	4.78	-	108.04
	PPH	3	3.73	8.87	-	19.85
		4	6.86	4.58	-	120.21
Through	PPC	3	1.76	DNC	-43.48	-
		4.5	3.68	10.56	-43.19	108.99
	PPH	3	2.21	DNC	-40.77	25.60
		4	3.68	11.30	-46.35	109.03
Ribbed	PPC	3	3.01	12.54	-3.43	-
		4.5	6.46	4.79	-0.13	115.01
	PPH	3	3.48	9.54	-6.80	15.67
		4	6.14	5.07	-10.49	104.11

15-year-old-sized AFO designs

For the 15-year-old-sized AFO, the 3mm PPH, 4.5mm PPC, and 4mm PPH AFOs were 21.88-24.31%, 100.26-131.99% and 112.83-128.74% stiffer than the PPC 3mm AFOs respectively (Table 6.4). However, none of the 3mm models ran to completion, whilst neither the 4mm PPH nor 4.5mm PPC designs were stiff enough to limit deflection to <5° (Figure 6.4). Finally, reducing the trim lines from the anterior to through position reduced stiffness by 42.54-50.11%, however, unlike the previous ages, introducing mediolateral ribbing increased stiffness by 4.68-7.86%.

Table 6.4: Comparison of 15-year-old-sized AFO clinical designs. DNC = Did Not Converge, meaning the FE model did not run to completion.

Design	Material	Thickness / mm	Stiffness / Nm/°	Max Deflection / °	Δ% in designs	Δ% in material
Anterior	PPC	3	3.84	DNC	-	-
		4.5	7.74	7.06	-	101.43
	PPH	3	4.68	DNC	-	21.88
		4	8.18	6.79	-	112.83
Through	PPC	3	1.92	DNC	-50.11	-
		4.5	4.45	19.58	-42.54	131.99
	PPH	3	2.38	DNC	-49.21	24.08
		4	4.38	21.02	-46.38	128.74
Ribbed	PPC	3	4.05	DNC	5.30	-
		4.5	8.10	6.73	4.68	100.26
	PPH	3	4.99	DNC	6.61	24.31
		4	8.82	5.887	7.86	118.02

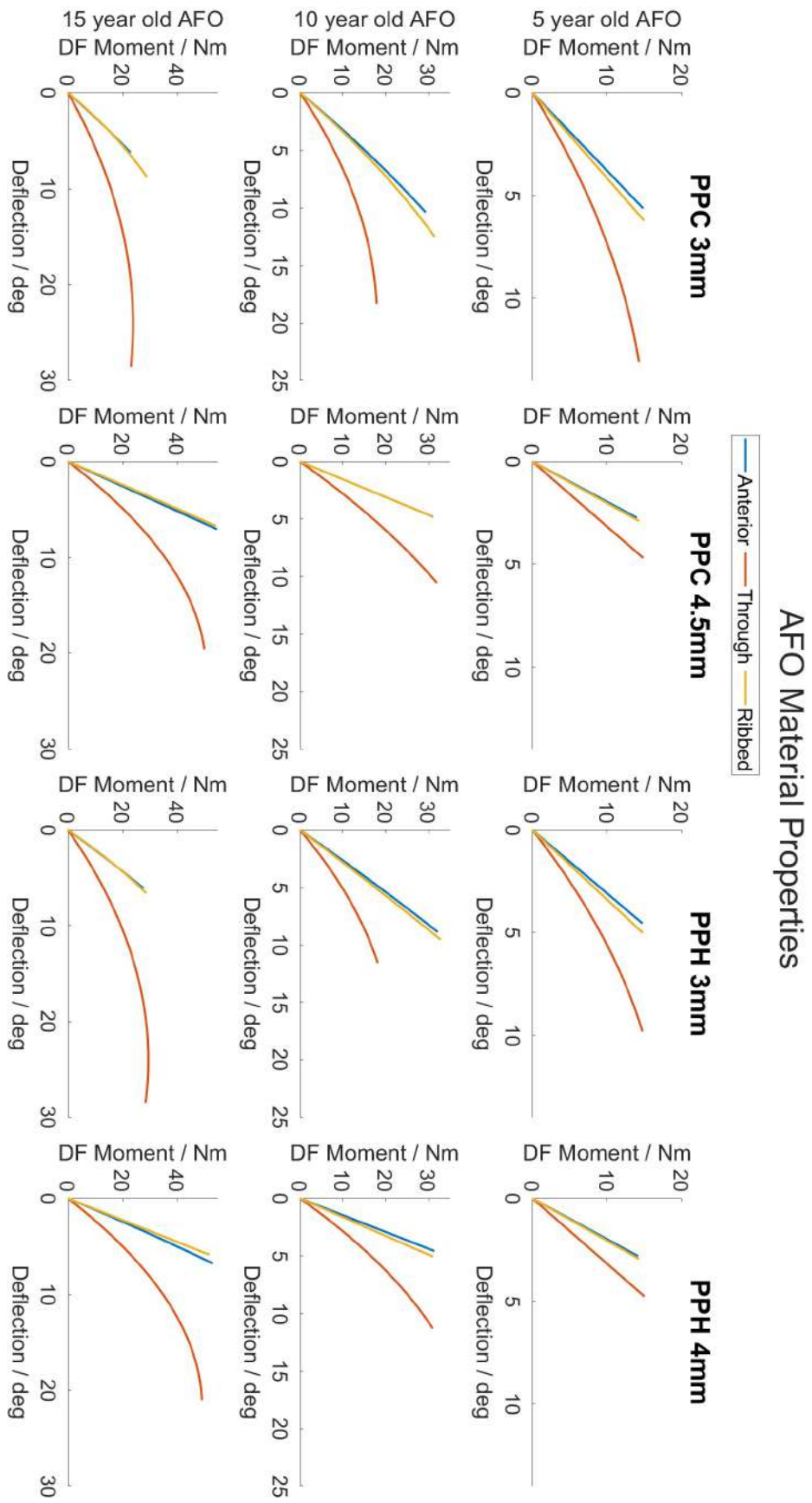


Figure 6.3: Computational bending behaviour of the clinically utilised AFO designs for the three age groups.

AFO Mechanical Properties Comparison

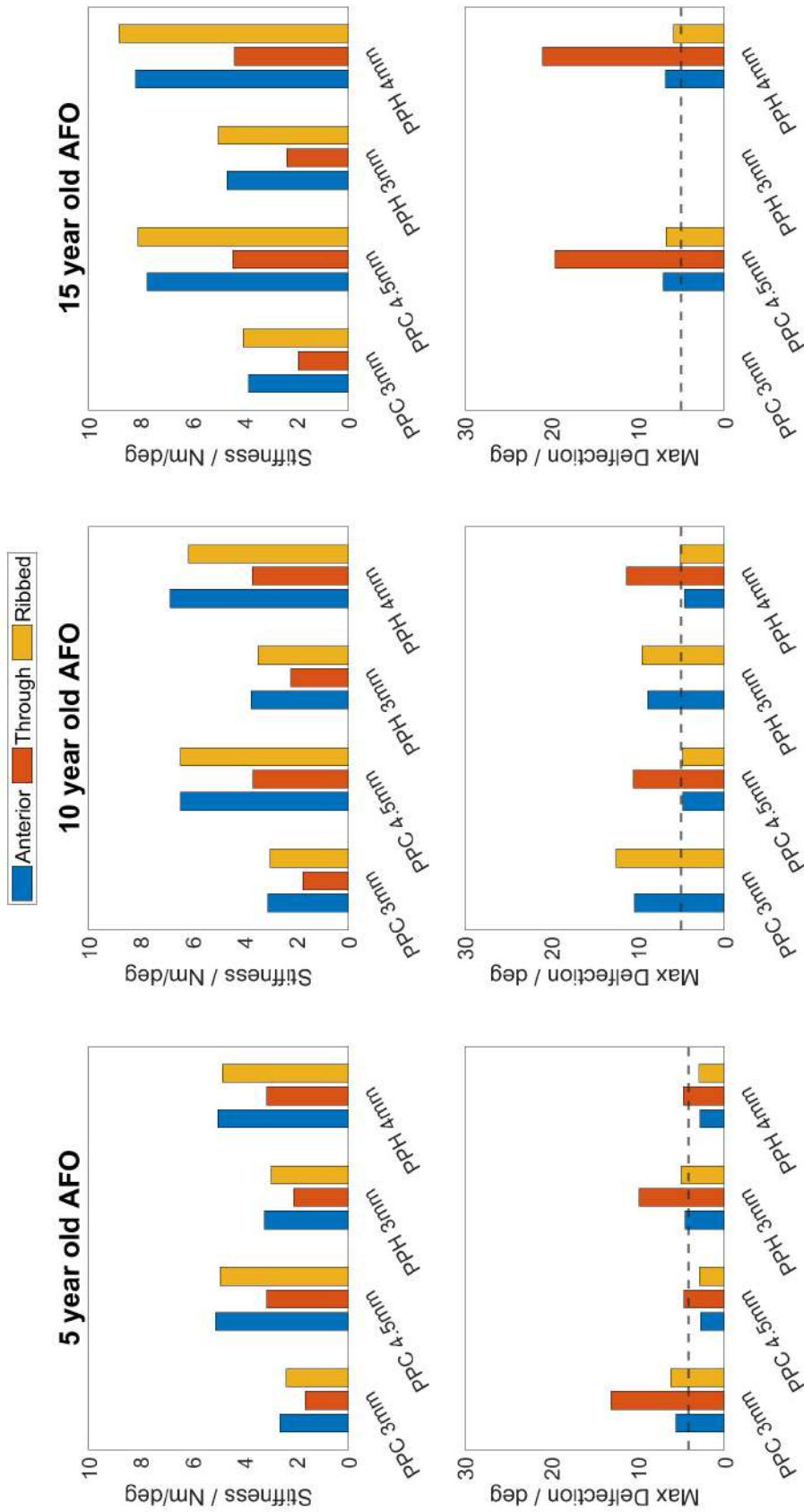


Figure 6.4: Computational mechanical properties of the clinically utilised AFO designs for the three age groups. Dashed line = Clinically significant deflection.

Analysis of Von Mises Stress and coronal plane deformation

When analysing the Von Mises stress, artificial peak stress concentrations were located in the heel, owing to the set-up of the FE model, where elements in the heel were constrained to zero displacement to mimic the rig clamp (Figure 6.5, 6.6, 6.7). Therefore, observing changes in the peak stress values is unreliable, as these stress concentrations would not occur during gait. Instead, observations were made on how the stress distributions changed with the AFO design properties. Furthermore, for succinctness, trends are primarily presented using data from the 5-year-old-sized AFO model, as it is representative of the patterns seen across the AFO sizes.

When looking at the anterior trim line AFO design, the highest stress concentrations were seen at the trim lines in the malleoli region. However, additional concentrations were seen on the trim lines at the metatarsal heads, along the anterior border of the AFO, proximal to the malleoli on both the medial and lateral sides and on the posterior aspect of the AFO, just proximal to the malleoli (Figure 6.5). These observations were consistent across all AFO sizes (Figures 6.6 and 6.7).

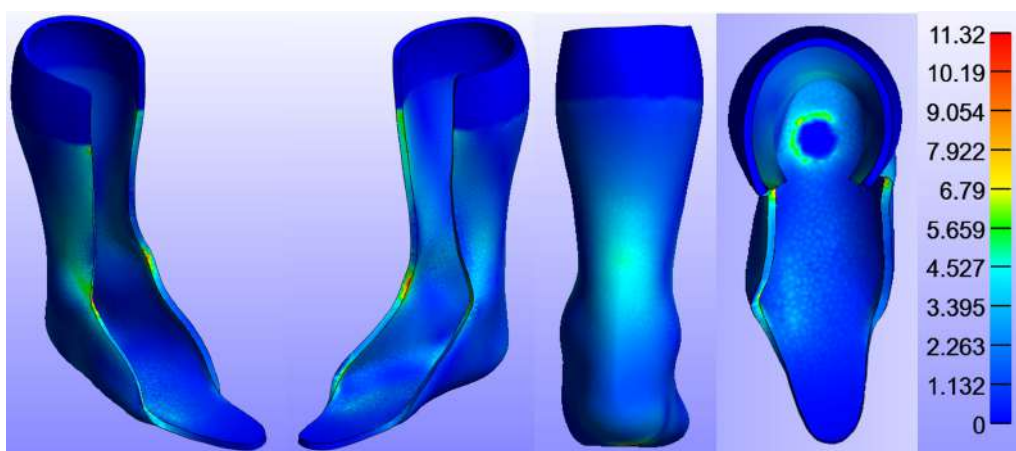


Figure 6.5: Von Mises stress distribution in the 5-year-old-sized 4mm PPH AFO with anterior trim lines. Von Mises stress measured in MPa.

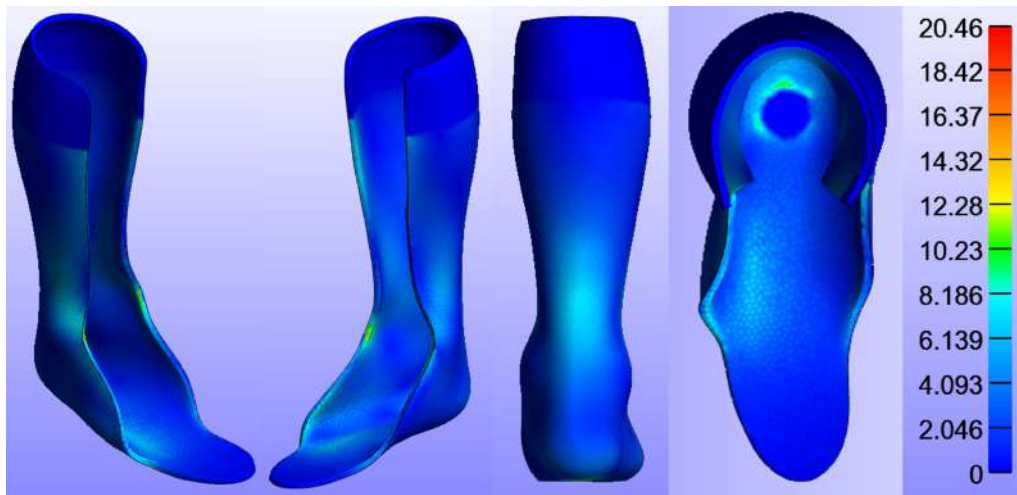


Figure 6.6: Von Mises stress distribution in the 10-year-old-sized 4mm PPH AFO with anterior trim lines. Von Mises stress measured in MPa.

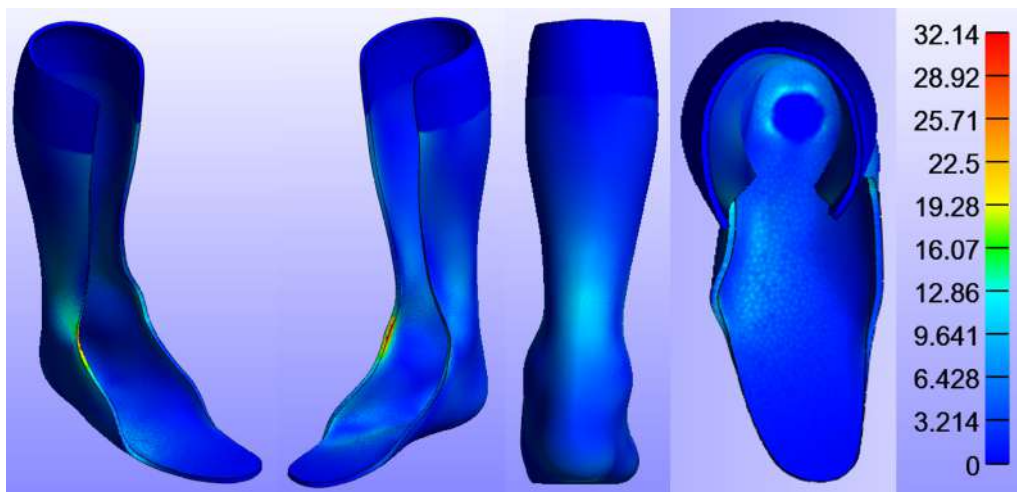


Figure 6.7: Von Mises stress distribution in the 15-year-old-sized 4mm PPH AFO with anterior trim lines. Von Mises stress measured in MPa.

These areas of high stress were reflected in coronal plane deformation, where two distinct regions were identified. The first was distal to the malleoli along the anterior border of the mediolateral walls. Here the AFO shell was found to deform laterally on both sides. Meanwhile, proximal to the malleoli, the distal portion of the AFO shell was found to deform medially, along the anterior border. These observations were consistent across all AFO sizes (Figure 6.8).

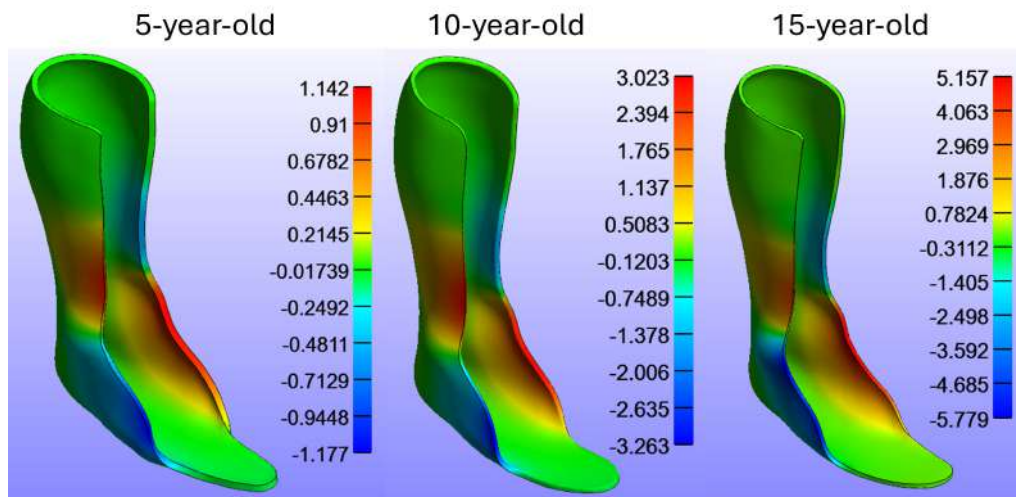


Figure 6.8: Coronal deformation in the 5-, 10- and 15-year-old-sized, 4mm PPH AFO with anterior trim lines. Deformation measured in mm.

When observing the difference in stress distribution and coronal plane deformation with polypropylene type and thickness, the 3mm PPH AFO with anterior trim lines were compared to both the 3mm PPC and 4mm PPH AFO with the same trim lines. Generally, Von Mises stress was slightly higher in the more flexible, PPC AFO, whilst it reduced as thickness increased (Figure 6.9). This pattern resulted in the peak coronal plane deformations increasing and decreasing with polypropylene rigidity and thickness, respectively (Figure 6.10).

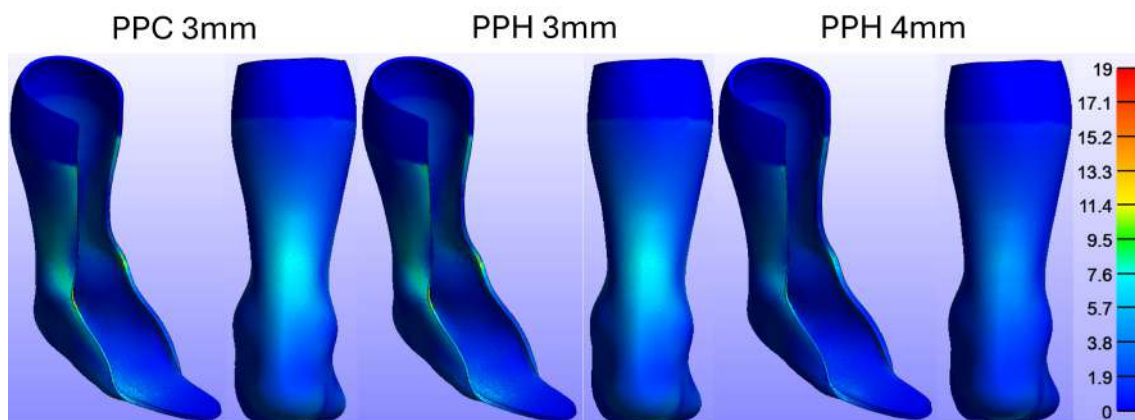


Figure 6.9: Change in Von Mises stress distribution with polypropylene type and thickness for the 5-year-old-sized AFO with anterior trim lines. Von Mises stress measured in MPa. The range of the colour bar has been manually adjusted.

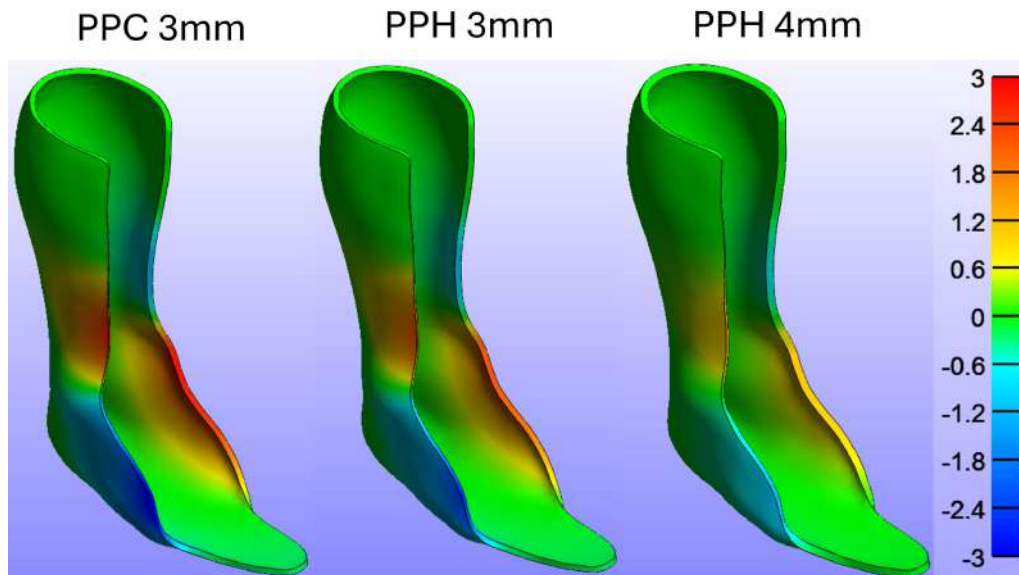


Figure 6.10: Change in coronal deformation with polypropylene type and thickness for the 5-year-old-sized AFO with anterior trim lines. Deformation measured in mm. The range of the colour bar has been manually adjusted.

Finally, the change in stress distribution between the trim line and reinforcement design was compared, with the results from the 5-year-old-sized 4mm PPH AFO presented. Altering the trim lines so they passed through the mid-point of the malleoli, resulted in considerably higher stress concentrations at the malleoli trim lines, which in some cases exceeded the yield stress of the material. This resulted in increased coronal plane deformation, which mostly occurred distal to the malleoli and was larger on the lateral side. Alternatively, ribbing had little effect on the stress distribution (Figure 6.11). However, there was a tendency towards less symmetric coronal deformation, with higher deformation seen in the medial wall distal to the malleoli and the lateral wall proximal to the malleoli.

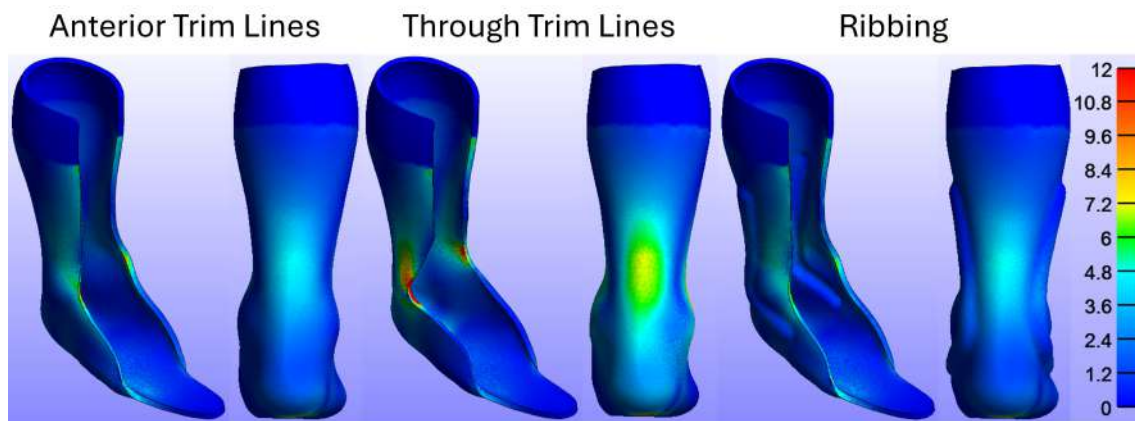


Figure 6.11: Change in Von Mises stress distribution with AFO design for the 5-year-old-sized 4mm PPH AFO. Von Mises stress measured in MPa. The range of the colour bar has been manually adjusted.

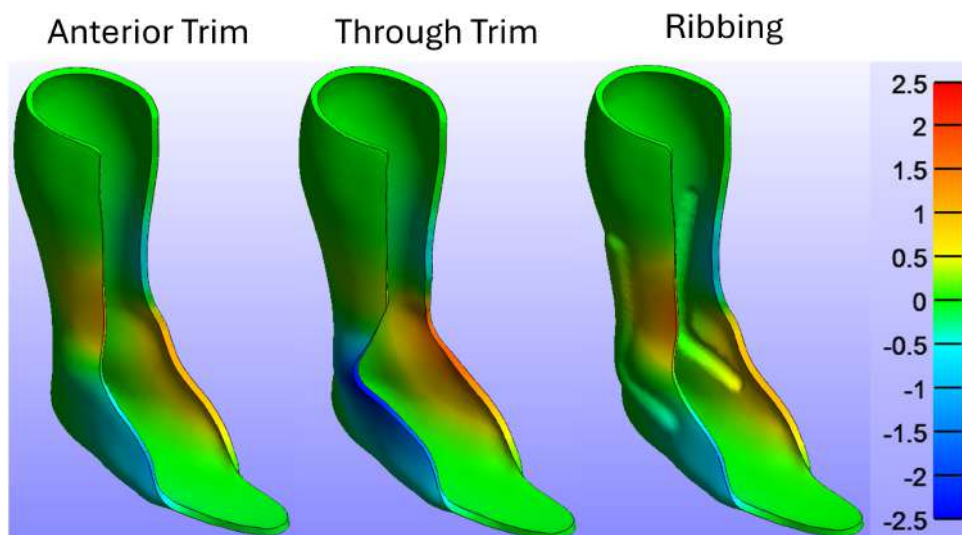


Figure 6.12: Change in coronal deformation with AFO design for the 5-year-old-sized 4mm PPH AFO. Deformation measured in mm. The range of the colour bar has been manually adjusted.

6.5 Discussion

To the author's knowledge, this is the first study to investigate the combined effects of thermoplastic rigidity and thickness, trim line design and ribbing on the stiffness of rigid, polypropylene, paediatric AFOs. It found that the stiffness of the devices ranged from $1.68\text{Nm}/^\circ$ to $8.18\text{Nm}/^\circ$ depending on the size of the AFO, the design and the material used. Previously, Bielby et al. found the dorsiflexion stiffness of 4.7mm, polypropylene rigid AFOs for a 15-year-old was $\approx 10\text{Nm}/^\circ$ [202], whilst Fatone et al. reported stiffnesses between $8.08\text{-}18.30\text{Nm}/^\circ$ for AFOs of varying thicknesses and reinforcement

designs[194], which were similar in height to the 10-year-old AFO tested here. The stiffness reported for these ages in this study was not dissimilar, installing confidence in the FE model behaviour.

Additionally, it was the first to investigate the influence of AFO size within paediatric populations, building on work by Novacheck et al., who found a significant difference in stiffness between adult and paediatric flexible AFOs[203]. However, the most flexible design tested in this study, the through the malleoli trim line, demonstrated similar stiffness across each age group (5-year-old = 1.68-3.16Nm/°, 10-year-old = 1.76-3.68Nm/°, 15-year-old = 1.92-4.45Nm/°), suggesting size may be of less significance. Alternatively, for thicker, anterior trim line designs, the stiffness increased by around 1.5Nm/° with size, implying size may become a factor when the AFO can resist buckling.

The results of this study also confirmed trends in experimental studies regarding the influence of polypropylene type on AFO stiffness. Firstly, 3mm PPH AFOs were \approx 15-25% stiffer than 3mm PPC devices, whilst 4mm PPH and 4.5mm PPC AFOs performed similarly, across designs within each age group. This percentage increase is higher than seen in experimental testing[205], [239], which is due to the FE model assuming an idealised, uniform AFO thickness. In any case, it demonstrates that PPH offers a higher stiffness-to-thickness ratio. Despite this, the survey by Eddison et al. into adult AFO prescription suggests PPC is favoured clinically[284]. This may be due to concerns relating to the manufacturing behaviour and failure mode of PPH[102], which were raised by the clinical advisory group. However, in paediatric populations, AFOs are typically worn for less than a year due to rapid growth during adolescence. As a result, further investigation into the fatigue of PPH AFOs across their life-cycle is required to determine if concerns over their failure behaviour are relevant.

Discussions with the clinical advisory group also highlighted that some clinicians may opt for through malleoli trim lines, to facilitate easier donning of the device. However, this study suggests that AFOs with through trim lines and polypropylene thickness <4.5mm do not provide sufficient rigidity for individuals above 10 years old. Furthermore, the through malleoli trim lines were between \approx 35% and \approx 50% more flexible than anterior

to the malleoli trim lines, representing a larger effect on stiffness than thermoplastic rigidity, which increased with AFO size. This aligns with the trends seen in adult flexible devices[195], [198], [202], [209], and implies anterior to the malleoli trim lines are more appropriate for rigid devices. However, these effects may also be related to the shape of the through malleoli trim line, which was designed to remove minimal material and maintain the anterior position of the trim lines along the shank. However, this created an acute angle at the mid-point of the malleoli, resulting in considerably higher stress concentrations (Figure 6.11). Therefore, these stress concentrations and the buckling behaviour of the AFO may change if the shank trim line was moved posteriorly to align with the mid-point of the malleoli, removing this acute bending point.

Furthermore, the results indicate the thickness of the AFO has the biggest impact on stiffness, agreeing with the findings by Nagaya et al.[192]. Increasing the thickness of PPC by 1.5mm resulted in an 87.80% to 131.99% rise in stiffness, whilst increasing PPH by 1mm saw a 49.58-84.34% difference. This was more modest than the 230% rise in computational stiffness achieved by Chatzistergos et al., when thickening a rigid PPC AFO from 3.11 to 4.09mm[193], which may reflect the differences in the boundary conditions of the FE models as the elastic modulus of PPC was similar. However, it aligns with the differences presented by Go et al.[195] and Kubasad et al.[198]. Furthermore, given that 3mm devices were not stiff enough to restrict deformation to below 5° for any age group, previous studies testing 3mm polypropylene rigid AFOs may have been flawed[119], [156], [162]. Furthermore, the desired stiffness was not achieved with 4mm PPH or 4.5mmPPC, for the 15-year-old-sized AFO, whilst only borderline acceptable stiffness was seen for the 10-year-old models. Given, the thickness of vacuum-formed AFOs can vary up to ≈30% compared to the pre-draped sheet[101], [193], [205], [213], these results suggest thicker materials would be required for older children. However, discussions with the clinical advisory group and Eddison's survey[284] suggest AFO thickness is limited by the need to fit the orthosis into footwear. Therefore, an alternative solution is reinforcing areas of high-stress concentrations.

With this in mind, mediolateral ribbing was tested, chosen as it was the most frequently identified type of reinforcement in both discussions with the clinical advisory group and

in Eddison's survey[284]. However, the ribbing used in this study only had a small effect ($\pm \approx 10\%$) on computational AFO stiffness across all ages, in line with the effects reported by Gao et al.[200], who also used a posterior to the malleoli placement, according to the design by Clark and Lunsford[293]. Alternatively, Major et al. increased stiffness by 37% using ribbing placed "*around the malleoli*"[206]. Given the lack of clarity in this definition, this may suggest that the difference in stiffness between these studies may result from the placement of the ribbing. As a result, a through the malleoli placement was piloted in the 4mm PPH AFOs, which increased stiffness by 22.82%, 6.60% and 12.57% for the 5, 10 and 15-year-old-sized AFOs respectively, when compared to the anterior trim line designs (Appendix I). These values are closer to Major's findings, suggesting mediolateral reinforcements should have a more anterior placement, whilst the differences seen across the models may be due to variations in the proximity of the ribbing to the trim line. This is supported by Chatzistergos et al.[193], [232], who found the optimal placement for ribbing was anterior to the malleoli[193].

However, ribbing widens the AFO, making it more difficult to fit in footwear, and limiting post-drape modifications to improve comfort and fit. Therefore, alternative designs would be more appropriate. Analysis of the Von Mises stress distribution supported previous conclusions that peak stresses are seen near the trim lines in the malleoli region[212], [232], [250]. However, it also identified secondary locations such as along the trim lines in the metatarsal heads, in the posterior ankle and along the mediolateral, anterior borders proximal to the ankle (Figure 6.5, 6.6, 6.7). Consequently, designs like the Y-shaped or chevron reinforcements used by Fatone et al.[194] and Novacheck et al.[203], may provide the desired reinforcement whilst considering user and clinician requirements.

6.6 Conclusions

This study is the first to investigate the combined effects of the four AFO design factors on AFO stiffness in paediatric populations. It is also the first to test a range of paediatric AFO sizes and provides the first example of an anatomical definition for AFO trim lines. From a clinical perspective, the study highlighted that polypropylene thickness had the

largest effect on AFO stiffness and that 3mm thick polypropylene provided insufficient stiffness for all ages. Furthermore, the results challenged the appropriateness of through malleoli trim lines for rigid devices.

Additionally, thickness had the biggest influence on stiffness, however, it is limited by the need to fit the AFO in footwear. Instead, reinforcements can provide localised stiffness, without increasing the global size of the AFO. However, the ribbed reinforcements used in this study were largely ineffective, whilst other mediolateral reinforcements presented in the literature cause conflict with both user and clinician needs. As a result, new reinforcement designs will be developed using the Von Mises stress analysis, to optimise the design and stiffness of rigid AFOs.

Chapter 7

Development of a novel reinforcement to optimise the design of paediatric rigid AFOs

Chapter Overview

The following chapter details a two-step process to design a novel reinforcement and then scale it to multiple-sized AFOs. The reinforcement was developed to provide additional stiffness to rigid AFOs, whilst aligning with the needs of the clinician and user, in response to the issues discussed with ribbing. Therefore it moves towards a more optimal rigid AFO design.

7.1 Introduction

The findings of the previous study (Chapter 6) suggest that a 3mm AFO provided insufficient stiffness to adequately control ankle motion in a 5-, 10-, and 15-year-old child, whilst for a 15-year-old, an AFO thicker than 4.5mm may be necessary. This challenges current clinical and research practice, where paediatric thermoplastic rigid AFOs are typically manufactured from 3-4.5mm thick polypropylene sheets (Section 3.2 and 2.1). Furthermore, it may imply that some individuals are prescribed substandard rigid AFOs, which are less effective at managing gait impairments, particularly when considering the predicted behaviour did not account for the thinning of AFOs in areas of high stress, that occurs during the vacuum forming process[193], [205], [213]. One solution to improve the stiffness of rigid AFOs is to increase thickness, identified as a significant contributor to the mechanical properties of the device[192], [193], [195]. However, this causes conflict with user requirements such as the ease of donning, the AFO's compatibility with non-adapted footwear, the AFO's mass and comfort[190], [267]–[269], [271], [274].

Alternatively, reinforcements can be used to target areas of high stress, providing localised stiffness, without increasing the global thickness of the device. Previous examples tend to target the malleoli region of the AFO, identified as a key site where buckling occurs[212], [232], [250]. These include ribbing, which had mixed effects on stiffness[200], [206], although when optimised were found to increase stiffness by $\approx 83\%$ [193] and carbon fibre L-shaped[206] reinforcements, which were shown to increase stiffness by $\approx 55\%$. However, mediolateral reinforcements in the malleoli region may pose issues with device comfort, as they limit the clinician's ability to complete post-drape modifications, and impact footwear fit, as they widen the AFO ankle region.

As a result, designs such as the polypropylene chevron and Y-shaped reinforcements, used by Novacheck et al.[203] and Fatone et al.[194], which reinforced the posterior aspect of the AFO may be more suitable. Unfortunately, the effects of the Y-shaped reinforcement cannot be isolated from the results presented, whilst the impact of the chevron reinforcement on flexible AFOs varied depending on size. Consequently, the following study focuses on developing a novel reinforcement which avoids the malleoli region of the AFO. In doing so, the aim is to optimise the design of rigid AFOs for 5-, 10-

and 15-year-olds, creating a device with adequate mechanical properties to control ankle, foot, and shank biomechanics, and that considers the requirements of the stakeholders involved in the provision of paediatric AFOs. When designing the novel reinforcement, a two-step process was used. First, an iterative design process was undertaken using the 5-year-old-sized AFO model, as it was the fastest to run. Then, once the final design had been created, it was scaled to the larger AFO sizes. This structure was chosen as it allowed several designs to be prototyped efficiently and meant the most minimal reinforcement, which met all the design specifications, was created.

7.2 Aims

To optimise the design of a rigid AFO for a 5-, 10- and 15-year-old, by developing a novel reinforcement that provides sufficient stiffness to restrict maximum deflection to below clinically significant levels and accounts for clinician and user requirements.

7.3 Specifications for the design of an 'optimal' rigid AFO reinforcement

The review of stakeholder requirements surrounding the provision of AFOs highlighted several factors that affect the adherence to rigid AFOs (Section 3.1). Therefore, when designing a novel reinforcement for rigid AFOs, the stakeholder requirements must be considered alongside the mechanical performance of the device, to ensure it has the potential to be translated into clinical practice. Therefore, the following specifications were outlined, which directed the reinforcement design process (Table 7.1).

The primary objective was to design a reinforcement that could restrict AFO maximum deformation to less than 5°. This was based on the threshold for a clinically significant change in kinematics, established by McGinley et al.[292], and has been used previously by Hovorka et al.[237]. However, for the 5-year-old-sized AFO, a revised threshold of 4.19° was used. The reason for this was outlined in the previous study (Chapter 6).

However, vacuum forming thins the AFO, impacting the device's mechanical proper-

ties. Therefore, to compensate for this, the mechanical performance of the design was evaluated using an AFO of 80% of the pre-draped sheet thickness. This was based on the average reduction in thickness across multiple locations on an AFO, according to the data presented by Convery et al.[205] and Lunsford et al.[213]. Furthermore, it aligned to the mean reduction in AFO thickness in the six AFOs draped for this thesis, which ranged from 10.55% to 26.31% (Figure 5.2). A full description of how this figure was calculated can be found in Appendix J.

Additionally, there were secondary considerations when developing the reinforcement. Firstly, from a user's perspective, the overall thickness of the AFO distal to the malleoli should be minimised, to facilitate the donning of non-adapted footwear. The use of adapted footwear is considered a key barrier to the adherence of AFOs due to the associated cost and negative perception of aesthetics[190], [267], [269], [271], [272]. Moreover, the overall mass of the AFO should be minimised. This has been highlighted as an issue by stakeholders[268], [270], [271], [274], linked to increasing fatigue in children with CP, although these effects have not been investigated. Finally, placement of the reinforcements across the malleoli prominences may increase pressure on bony landmarks depending on their design. Alternatively, from a clinician's perspective, placing reinforcements across or anterior to the malleoli prominences may also limit the modifications which can be made to the AFO to improve the fit and comfort.

Finally, the manufacturing process should also be aligned with the UK public health system. Therefore, the cost should be minimal, whilst it should be made from materials typically used during the prescription of paediatric rigid AFOs. In addition, the method in which it is manufactured should not require any specialist technician training.

Table 7.1: Specifications for the novel rigid AFO reinforcement.

Criteria	Specifications
Mechanical	The final design should achieve a maximum deflection below the threshold for a clinically significant change in kinematics[292] at an AFO thickness of 80% of the pre-draped PPH thickness. Clinical threshold for the 10- and 15-year-old model = 5° Clinical threshold for the 5-year-old model = 4.19°
Design	The reinforcement should not be placed across or anterior to the malleoli prominences.
	The design should be scalable to different AFO sizes.
	The reinforcement should not restrict the ability of the clinician to make post-drape modifications to the AFO.
Size and weight	The global thickness of the final AFO distal to the malleoli should be minimised.
	The mass of the final AFO should be minimised.
Materials & Manufacturing	The reinforcement should be easily manufactured without specialist expertise.
	The reinforcement should be manufactured from materials used in paediatric rigid AFOs within the public health system in the UK.
Cost	The cost of the reinforcement should be minimal.

7.4 Development of a novel reinforcement for the 5-year-old-sized AFO

7.4.1 The design process

The reinforcement was developed over an iterative, four-stage process. Each iteration aimed to reinforce a secondary stress concentration identified in the Von Mises stress analysis of the clinical AFO designs in the previous study (Figure 6.5,6.6,6.7). The first targetted the concentrations in the posterior aspect of the AFO, the second the concentrations distal to the malleoli and the third and fourth, the concentrations along the anterior border proximal to the malleoli.

The reinforcements were designed to be manufactured from PPH and laminated onto the AFO shell during vacuum-forming. As a result, they would be cost-effective and easily manufactured using current techniques. Furthermore, both the AFO and the reinforcement were made from PPH, due to its superior rigidity (Chapter 6).

At each stage, the mechanical properties of the designs were analysed using the FE model for the 5-year-old-sized AFO, developed in FEBio Studio (2.2.0, University of Utah, USA) and validated in Chapter 5. Every iteration was modelled as a solid part within Fusion (v2.0.20470, Autodesk, USA) before they were imported into FE model as STLs and meshed with quadrilateral, tetrahedral elements with a maximum edge length of 3.5-4.2mm. The models were then set up and run as before (Section 5.3).

Initially, the reinforcement designs were tested on AFOs with a uniform thickness equal to the polypropylene sheet thickness quoted by the supplier (Algeos, UK). It was assumed the discrepancy between the manufacturer's specification and the supplied sheets would be minimal. If the maximum deflection for this model was below 5°, the reinforcement was re-evaluated after reducing the AFO thickness by 20%, to account for thinning during the vacuum-forming process.

At each stage, the merits of each design were evaluated, considering the specification outlined in Section 7.3, before, the most appropriate was taken forward to the next

iteration of the process. The primary objective was to achieve the desired mechanical properties of deflecting less than the revised clinically significant threshold of 4.19° , with an AFO thickness equal to 80% of the pre-draped thickness. However, when this criteria was either not met, or met by multiple designs, the secondary user, clinical and manufacturing specifications were considered. Figure 7.1 the decision matrix for this process. Once the process was complete, the mechanical properties, stress distributions and coronal plane deformation of the reinforcement design after each iteration were compared to illustrate the reinforcement's evolution (Table 7.7, Figure 7.11, Figure 7.12).

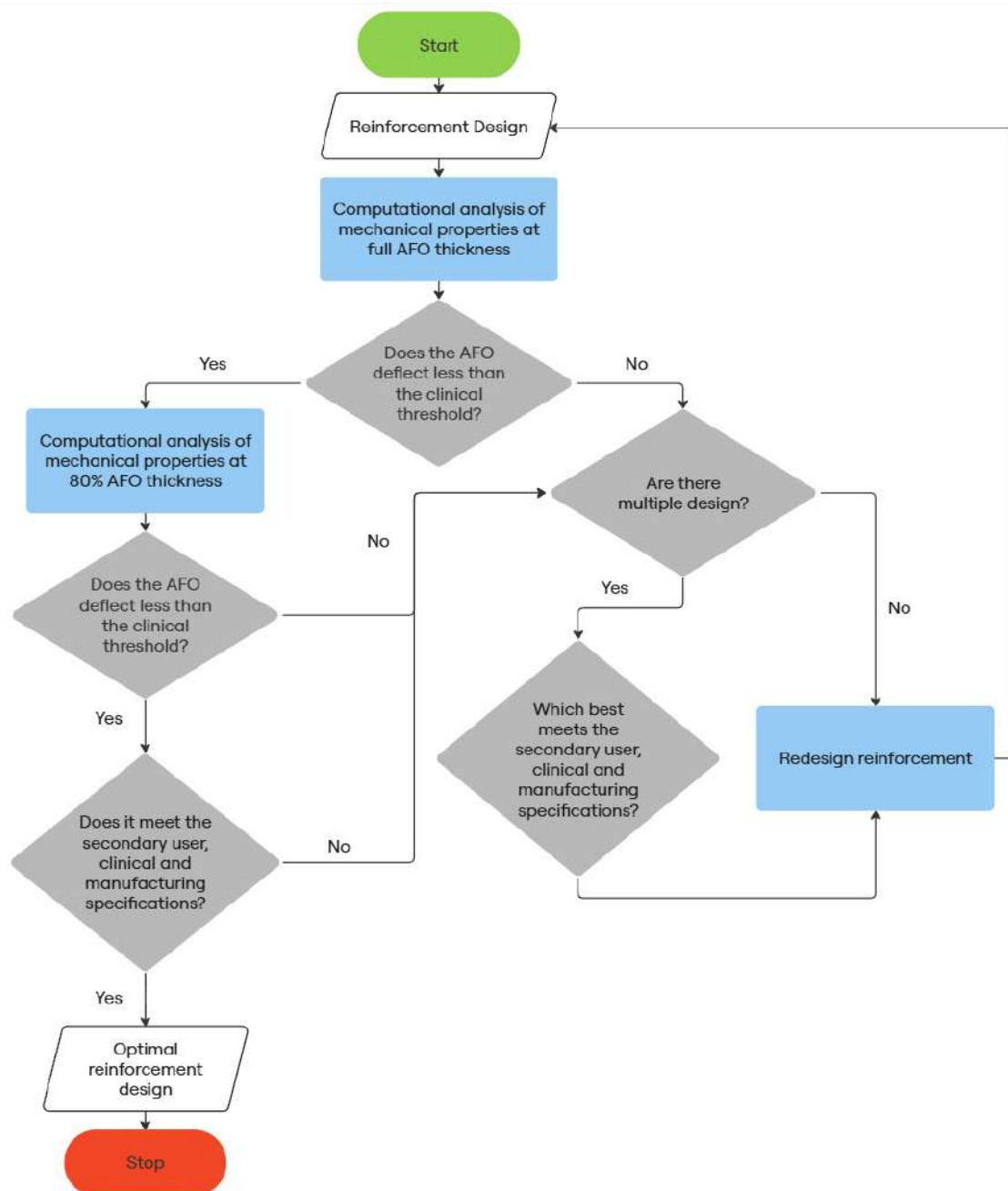
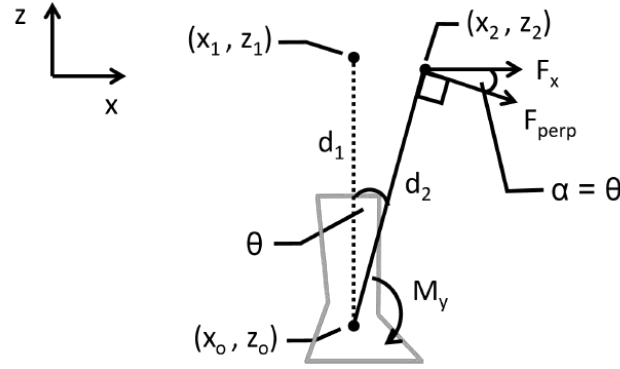


Figure 7.1: Decision matrix used during the development of the reinforcement

7.4.2 Data Analysis

The same data analysis was used in the previous study. The position and force applied to the second rigid body were exported from the FE as a .txt file and exported to Matlab (v2024a, MathWorks, USA) for processing and analysis. First, the deflection was calculated as the angle between two vectors using the following equations.



$$\theta = \cos^{-1}\left(\frac{d_1 \cdot d_2}{|d_1| |d_2|}\right) \quad (7.1)$$

$$\theta = \cos^{-1}\left(\frac{(dx_1 \cdot dx_2) + (dz_1 \cdot dz_2)}{|d_1| \cdot |d_2|}\right) \quad (7.2)$$

Then the applied moment was calculated as

$$Moment = F \cdot d \cdot \cos(\theta) \quad (7.3)$$

F = applied force, d = lever arm and θ = deflection

Then a first or second-order polynomial was fitted to the raw moment versus deflection data, with its appropriateness determined using the adjusted R^2 value calculated using the following equations.

$$R_{adj}^2 = 1 - \frac{n-1}{n-p} \cdot \frac{SSE}{SST} \quad (7.4)$$

Where

$$SSE = \text{Squared sum residuals} = \sum (y_i - \hat{y}_i)^2 \quad (7.5)$$

y = actual y - value

\hat{y} = predicted y - value

$$SST = \text{Squared sum total} = \sum (y_i - \bar{y})^2 \quad (7.6)$$

After each iteration, the loading behaviour, the stiffness and the maximum deflection were compared using line and bar charts. Furthermore, the difference in mechanical properties at the full and 80% AFO thickness, were plotted as stacked columns, with the dark blue bar the full sheet thickness and the light blue bar the 80% sheet thickness.

Finally, the Von Mises stress distribution and coronal plane deformation were analysed as colour maps exported from FEBio studio (2.2.0, University of Utah, USA) for selected designs. The rationale for the Von Mises stress was outlined in Section 6.3.2.

7.4.3 Stage 1: Rear Reinforcement

Reinforcement Design

The first reinforcement design targeted the area of high stress and strain seen on the posterior shell of the AFO (Figure 6.5). An additional PPH beam was applied along the posterior shell, centred around the mid-line of the AFO in the coronal plane. The rationale was that during the second rocker, the AFO behaves analogously to a cantilever beam, with the plantar surface fixed to the floor by body weight and a dorsiflexion moment applied at the proximal shank, where the strap is located. Therefore, the additional beam will stiffen the device by increasing the thickness and moment of inertia of the AFO where bending occurs.

A 3mm thickness was chosen to minimise the overall thickness of the device, however the optimal length and width of the beam required investigation. Therefore, the reinforcement extended the full length of the AFO whilst the widths were increased from 10 to 35mm in 5mm increments. The width did not exceed 35mm as this would have overlapped with the malleoli prominences. Once the optimal width had been determined, the length was reduced from the full height of the AFO to the height of the malleoli in fifths. Given the centre of rotation is at the ankle, it was theorised that a reinforcement shorter than the malleoli height would have little effect on stiffness.



Figure 7.2: Rear Reinforcement Design

The effect of rear reinforcement width

Results

Increasing the width of the rear reinforcement from 10mm to 35mm, in 5mm increments, saw a rise in stiffness from 3.45Nm/° to 4.16Nm/°, which equated to a percentage increase in stiffness of 6.57% to 28.46% when compared to a 3mm PPH AFO with no reinforcement (Table 7.2). Furthermore, a near-linear relationship between the two variables was demonstrated with stiffness increasing by an average of 0.142 ± 0.038 Nm/° for every 5mm added in width (Figure 7.3). All the reinforcements were stiff enough to restrict deflection to less than the clinical threshold of 4.19°, when the thickness of the AFO was equal to the pre-draped sheet thickness, although the 10mm width was borderline. However, none achieved the stiffness of a non-reinforced, 4mm PPH AFO.

Table 7.2: Effect of mechanical properties rear reinforcement

Reinforcement Width / mm	Stiffness / Nm/°	Max Deflection / °	Mass / g	Δ% in stiffness vs non-reinforced
None	3.24	4.55	109.26	-
10	3.45	4.17	115.11	6.57
15	3.57	4.04	118.08	10.19
20	3.76	3.85	121.32	16.04
25	3.94	3.70	124.38	21.55
30	4.07	3.58	127.89	25.80
35	4.16	3.49	131.67	28.46

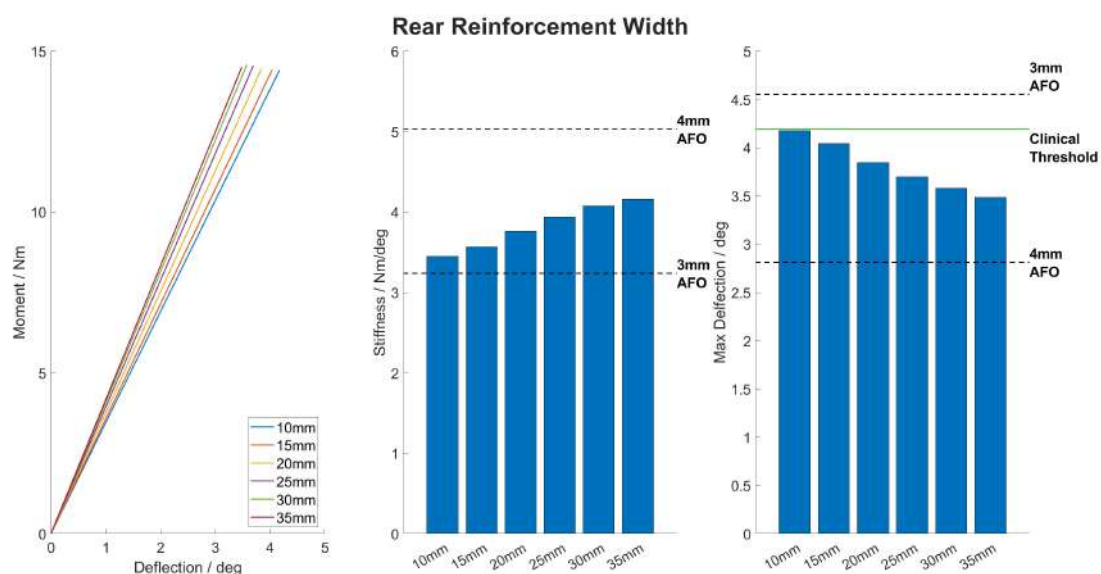


Figure 7.3: Effect of rear reinforcement width on AFO mechanical properties. Error bars denote the mechanical properties when the AFO thickness is reduced by 20%.

Rationale for design taken forward

The near linear relationship between the rear reinforcement width and AFO stiffness would indicate that maximising the width of the reinforcement is best from a functional perspective. However, from a clinical point of view, the device must be compatible with footwear to aid adherence. Therefore, the width of the rear reinforcement is likely limited by the heel tab of the shoe, rather than the position of the malleoli prominences. Unfortunately, the width of the heel tab is difficult to estimate, as manufacturers do not detail these dimensions in open-source materials. Therefore, 20mm was taken forward as this was estimated to be the width of the heel counter based on measurements taken from a UK size 10 kids orthopaedic shoe last.

Effect of Rear Reinforcement Height

Results

Increasing the length of the reinforcement from the height of the malleoli to the full length of the AFO saw a fairly linear increase in stiffness of $0.185 \pm 0.037 \text{ Nm/}^\circ$ for every 20% (32mm) increase in length, up to 3/5 (151mm) length, after which the increase to full length was only 0.02 Nm/° (Table 7.3). Here, only reinforcements $>119 \text{ mm}$ (40% length) were stiff enough to restrict deflection below the clinical threshold. Finally, the

55mm beam was marginally less stiff than the 3mm, non-reinforced AFO, whilst none were as stiff as the 4mm thick AFO (Figure 7.4).

Table 7.3: Effect on mechanical properties of rear reinforcement height

Reinforcement Length / mm	Stiffness / Nm/°	Max Deflection / °	Mass / g	Δ% in stiffness vs non-reinforced
None	3.24	4.55	109.26	-
55	3.18	4.56	112.32	-1.70
87	3.35	4.34	114.12	3.54
119	3.50	4.11	115.92	8.16
151	3.74	3.88	117.81	15.46
183	3.76	3.85	119.61	16.22
215	3.76	3.85	121.32	16.04

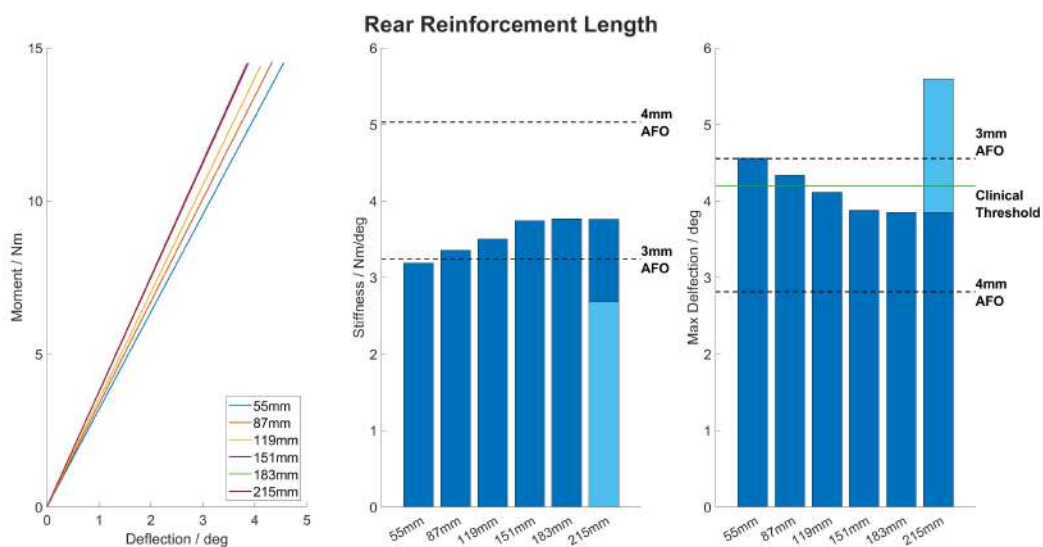


Figure 7.4: Effect of rear reinforcement height on AFO mechanical properties. Dark blue bars = mechanical properties at 100% thickness. Light blue bars = mechanical properties at 80% thickness.

Rationale for design taken forward

The 55mm rear reinforcement results support the hypothesis that reinforcing the AFO shell distal to the ankle centre of rotation, along the posterior aspect alone, has little impact. Furthermore, although the 55mm long rear reinforcement was 0.06Nm/° (1.70%) less stiff than the non-reinforced, 3mm AFO, given this difference was minimal it is likely due to measurement error caused by a discrepancy in the number or location of the

elements in the heel which were prescribed zero displacement in X-Y-Z directions, in the FE model.

Meanwhile, a fairly linear relationship between the reinforcement length and stiffness was demonstrated up to 3/5 of the distance between the malleoli and AFO height, after which the stiffness plateaued. This may indicate an optimal length of the rear reinforcement or reflect the set-up of the FE model, which constrains elements in the proximal fifth of the AFO shell to a rigid body, restricting the movement of these elements. In any case, adding length proximal to the malleoli does not conflict with clinical requirements, whilst a full-length reinforcement requires less accurate placement during manufacturing and is arguably more aesthetically acceptable. Furthermore, given there was a 3.51g in mass between the 3/5 (151mm) and full-length design, a full-length rear reinforcement was taken forward. However, further development was required as the full-length, 20mm wide reinforcement did not achieve a maximum deflection below the clinical threshold when the thickness of the AFO was reduced by 20% (Figure 7.4).

7.4.4 Stage 2: Distal to the malleoli reinforcements

Reinforcement Design

Although the previous stage indicated that reinforcing the posterior aspect of the shell below the ankle centre of rotation was ineffective, during loading, areas of high stress were seen along the trim lines at the metatarsal-phalangeal joint the metatarsal-phalangeal joint (Figure 6.5), and high lateral deformation occurred in the mediolateral walls (Figure 6.10). Therefore, it was theorised that reinforcing the mediolateral areas of AFO below the malleoli may be beneficial. Furthermore, it was noted that introducing, the rear reinforcement may create a void between the mediolateral heel of AFO and the heel counter within the shoe. As a result, it may impact the stability of the rear foot within the shoe and how securely it can be fastened. This led to two designs of distal to the malleoli reinforcements being trialled.

The first was referred to as the T-Bar design, which had the addition of two, 20mm wide arms extending from the heel to the metatarsal-phalangeal joint along the distal, mediolateral border of the AFO (Figure 7.5). This aimed to reduce the stress at the

metatarsal-phalangeal joint and reinforce the mediolateral walls of the AFO to limit buckling. However, it was perceivable that it may impact footwear fit by increasing the width of the AFO at the metatarsal heads.

The second design consisted of adding a heel cup to the rear reinforcement, which ran diagonally from the height of the mid-point of the malleoli on the posterior surface, to its horizontal position on the plantar surface (Figure 7.5). The rationale behind this design was to fill the void in the footwear created by the rear reinforcement applied in stage 1, whilst applying bracing to the cantilever reinforcement. Furthermore, it had the added benefit of adding additional material to the heel where thinning of the AFO is seen (Section 5.2). The heel cup was designed to fit within the heel counter to avoid widening the shoe. However, without heel counter dimensions from shoe manufacturers, the dimensions were based on the mid-point of the malleoli to make the design scaleable to different AFO sizes.



Figure 7.5: Distal Reinforcement Design

Results

The T-Bar design was stiffer than the heel cup design ($4.11\text{Nm}/^\circ$ versus $3.93\text{Nm}/^\circ$) (Table 7.4). This resulted in the T-Bar reducing maximum deflection by 1.07° compared to the non-reinforced 3mm baseline, whilst the heel cup only achieved a reduction of 0.59° . Compared to the rear reinforcement design, the T-Bar increased stiffness by 9.28% and the heel cup 4.48%. However, neither of the distal reinforcements achieved a maximum deflection lower than the clinical threshold when AFO thickness was reduced

by 20% (Figure 7.6).

Table 7.4: Mechanical properties of Distal Reinforcements

Reinforcement Design	Stiffness / Nm/°	Max Deflection / °	Mass / g	Δ% in stiffness vs non-reinforced
None	3.24	4.55	109.26	-
Rear	3.76	3.85	121.32	16.04
T-Bar	4.11	3.48	134.01	26.82
Heel Cup	3.93	3.69	127.80	21.24

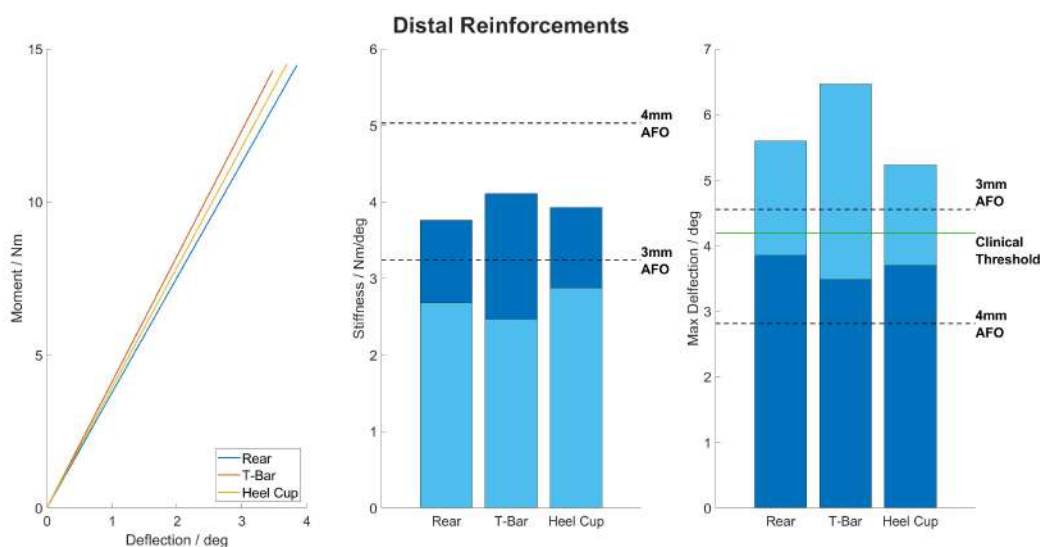


Figure 7.6: Comparison of distal to the malleoli reinforcements. Dark blue bars = mechanical properties at 100% thickness. Light blue bars = mechanical properties at 80% thickness.

Rationale for design taken forward

When comparing the two distal to the malleoli reinforcement designs, it was clear that the T-Bar design was more effective. However, the increase in stiffness achieved with this design was still relatively small (<10%). This may be improved by widening the arms of the T-Bar, however, from a clinical perspective, concerns were raised about the design's effect on footwear fit and adding pressure to the foot arches. As a result, it was not deemed suitable.

Meanwhile, the heel cup only produced a modest increase in stiffness (<5%) compared to the rear reinforcement alone, indicating that it had a limited bracing effect on the

cantilever rear reinforcement. To increase this, the height and length of the heel cup would need to be extended, however, doing so would encroach on the malleoli prominences and impact footwear fit. Furthermore, incorporating the heel cup may increase manufacturing complexity, as it would require precise positioning of the reinforcement to ensure it fits within the shoe heel counter.

Alternatively, it may have benefits beyond the mechanical properties of the AFO, for example aiding footwear fit in the heel region and how securely the shoe can be fastened. As a result, the decision was taken to include the heel cup in future designs, whilst recognising that further investigation into its impact on manufacturing and footwear fit is required.

7.4.5 Stage 3: Proximal to the malleoli reinforcements

Reinforcement Design

Next adaptations were made to reinforce the areas of high stress and deformation in the mediolateral sides of the AFO proximal to the malleoli (Figure 6.5, 6.10). The first, termed the X-Bar, included arms that wrapped around the mediolateral shell proximal to the malleoli, forming a cross shape in the coronal plane. The lower border of the arm was positioned 25mm proximal to the mid-point of the malleoli, which was equal to the malleoli diameter, to ensure the arm did not interfere with the malleoli prominences. Meanwhile, the arms were 16mm wide, equal to a fifth of the distance between the minimum position and 60mm distal the AFO height, which is the position where the proximal strap would finish (Figure 7.7).

The second was the Y-Bar design which had 20mm wide arms that wrapped diagonally around the mediolateral sides of the AFO, from the height of the mid-point of the malleoli on the posterior shell to the proximal, anterior corner of the shell (Figure 7.7).



Figure 7.7: Proximal Reinforcement Design

Results

When compared to the rear reinforcement with a heel cup, the X-bar and Y-bar reinforcements produced an increase in stiffness of $0.15\text{Nm}/^\circ$ and $0.2\text{Nm}/^\circ$, which translated into a decrease in maximum deflection of 0.15° and 0.2° , respectively (Table 7.8). However, neither achieved a maximum deflection lower than the clinical threshold when the AFO thickness was reduced by 20% (Figure 7.8).

Table 7.5: Mechanical properties of Proximal Reinforcements

Reinforcement Design	Stiffness / $\text{Nm}/^\circ$	Max Deflection / $^\circ$	Mass / g	$\Delta\%$ in stiffness vs non-reinforced
None	3.24	4.55	109.26	-
Heel cup	3.93	3.69	127.80	21.24
X-Bar	4.08	3.54	132.57	25.92
Y-Bar	4.13	3.49	144.45	27.66

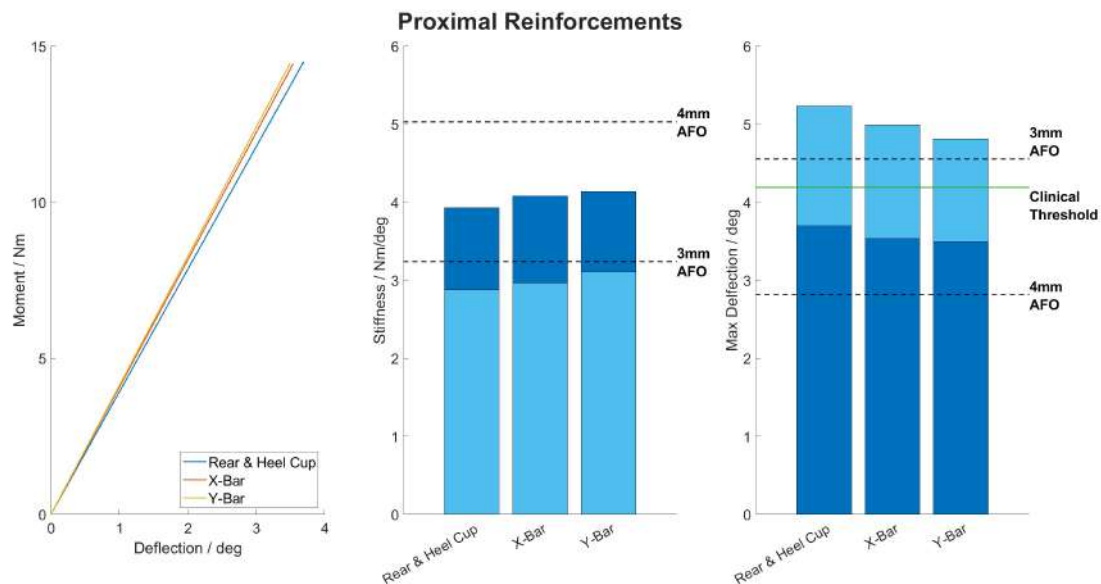


Figure 7.8: Comparison of proximal to the malleoli reinforcements. Dark blue bars = mechanical properties at 100% thickness. Light blue bars = mechanical properties at 80% thickness.

Rationale for design taken forward

Whilst the Y-Bar design achieved marginally higher stiffness, the effects of both reinforcements were minimal. This may indicate that further refinement of the designs is required, following a similar strategy as used in stage 1. However, when deciding which design to take forward, the X-Bar is favourable for two reasons. Firstly, the Y-Bar has a larger surface area, meaning the X-Bar has a slightly more favourable stiffness-to-mass ratio of $0.0309\text{Nm}/^\circ$ compared to $0.0286\text{Nm}/^\circ$. Furthermore, when considering the practicalities of manufacturing the reinforced AFO, the Y-Bar would be more difficult to replicate accurately, as the technician would have to calculate the angle at which the arms extend and be more precise with the placement. Therefore, the X-Bar offers a more feasible solution.

7.4.6 Stage 4: X-Bar Optimisation

Reinforcement Design

The final stage of the reinforcement development was to optimise the design of the X-Bar by determining the effects of arm width on mechanical properties. From a practical perspective, the width of the arms must consider the proximal AFO strap, which is around $\approx 60\text{mm}$ wide (Algeos, UK). As a result, the arms of the X-bar must either

run to the proximal edge of the AFO or finish 60mm distal to this to allow the straps to be fastened securely. Theoretically, arms which extend to the top of the AFO would provide the greatest increase in stiffness, however, from a clinical perspective, this would also add the most mass to the AFO and restrict the ease at which the AFO can be donned.

As a result, the arms of the X-Bar were extended incrementally, to determine the optimal position which achieved adequate stiffness whilst minimising AFO mass. The arms started at 25mm proximal to the mid-point of the malleoli, equal to the diameter of the malleoli, and were increased in width to 60mm distal to the AFO height (80mm length), in fifths (16mm), before extending the arms to the full height of the AFO (140mm length). The optimal design was interpreted as the one with the narrowest arms that achieved a maximum deflection below the clinical threshold at an AFO thickness of 20% less than the pre-draped sheet.



Figure 7.9: X-Bar Reinforcement Design

Results

Increasing the width of the X-Bar from 16mm to 80mm produce a near linear relationship between width and stiffness (Figure 7.10), with stiffness increasing by $0.282 \pm 0.012 \text{ Nm}/^\circ$ for every 16mm (1/5) increase. However, increasing the width from the strap height (80mm) to the full length (140mm) only produced a $0.29 \text{ Nm}/^\circ$ increase in stiffness (Table 7.6).

At an idealised AFO thickness of 3mm, the 80mm (strap height) and 140mm (full length) reinforcements produced an AFO that was stiffer than a 4mm AFO without

reinforcements, however, the mass was 157.14g and 183.60g respectively compared to 147.69g for the 4mm AFO. At the 20% reduced AFO thickness, the 64mm (3/5s) arm width was the first reinforcement to achieve deflect less than the clinical threshold.

The optimal X-Bar design (64mm arm width), achieved a stiffness of 4.92Nm/° and a maximum deflection of 2.96° at the idealised AFO thickness. This was 1.68Nm/° (52.02%) stiffer than the non-reinforced baseline, 1.16Nm/° (30.85%) stiffer than the rear design from stage 1 and 0.99Nm/° (25.19%) stiffer than the heel cup design in stage 2 (Table 7.7).

Table 7.6: Comparison of mechanical properties across the X-Bar arm widths

Arm Width / mm	Stiffness / Nm/°	Max Deflection / °	Mass / g	Δ% in stiffness vs non-reinforced
None	3.24	4.55	109.26	-
16	4.08	3.54	132.57	25.92
32	4.35	3.31	137.70	34.17
48	4.62	3.11	143.37	42.76
64	4.92	2.96	149.40	52.02
80	5.20	2.78	157.14	60.71
140	5.49	2.68	183.60	69.54

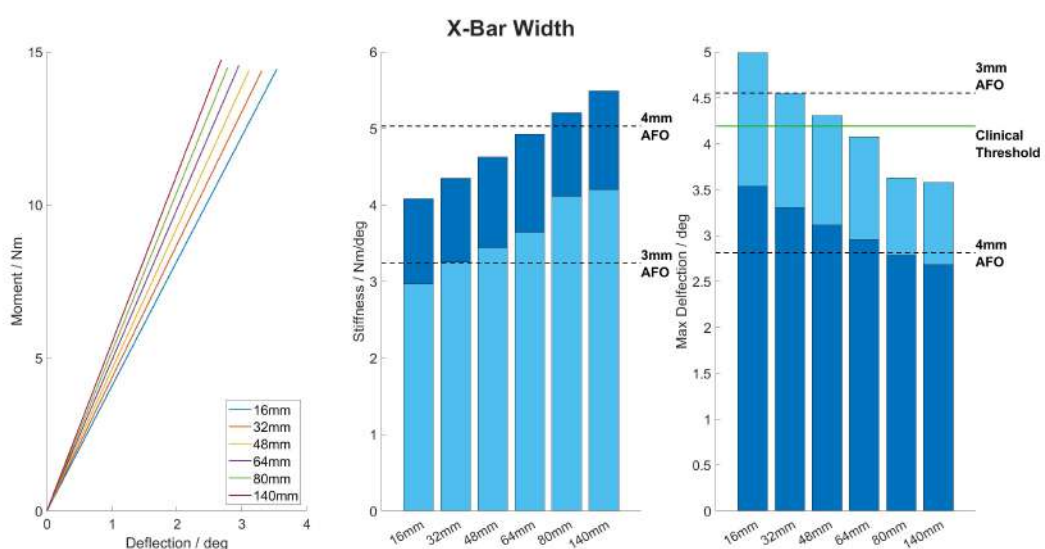


Figure 7.10: Comparison of X-Bar Width. Dark blue bars = mechanical properties at 100% thickness. Light blue bars = mechanical properties at 80% thickness.

Table 7.7: Mechanical properties of each reinforcement design iteration

Design	Stiffness / Nm/°	Max Deflection / °	Mass / g	Δ% in stiffness vs non-reinforced
No Reinforcement	3.24	4.55	109.26	-
Rear	3.76	3.85	121.32	16.04
Heel Cup	3.93	3.69	127.80	21.24
Optimised X-Bar	4.92	2.96	149.40	52.02

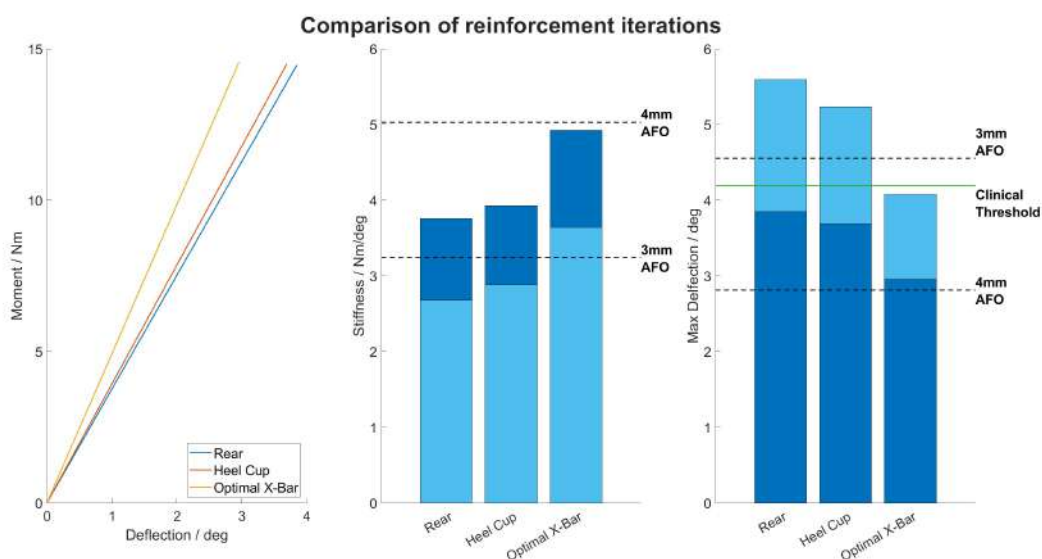


Figure 7.11: Comparison of each reinforcement design iteration. Dark blue bars = mechanical properties at 100% thickness. Light blue bars = mechanical properties at 80% thickness.

Finally, the effect of the reinforcement designs on Von Mises stress distribution and coronal plane deformation was analysed. Throughout the iterative design process, the stress was reduced in the areas which were reinforced. This was most notable for the optimal X-bar design, which reduced the stress in both the malleoli and posterior region of the AFO (Figure 7.12). Furthermore, the stress reduction was accompanied by a decrease in coronal plane deformation (Figure 7.12).

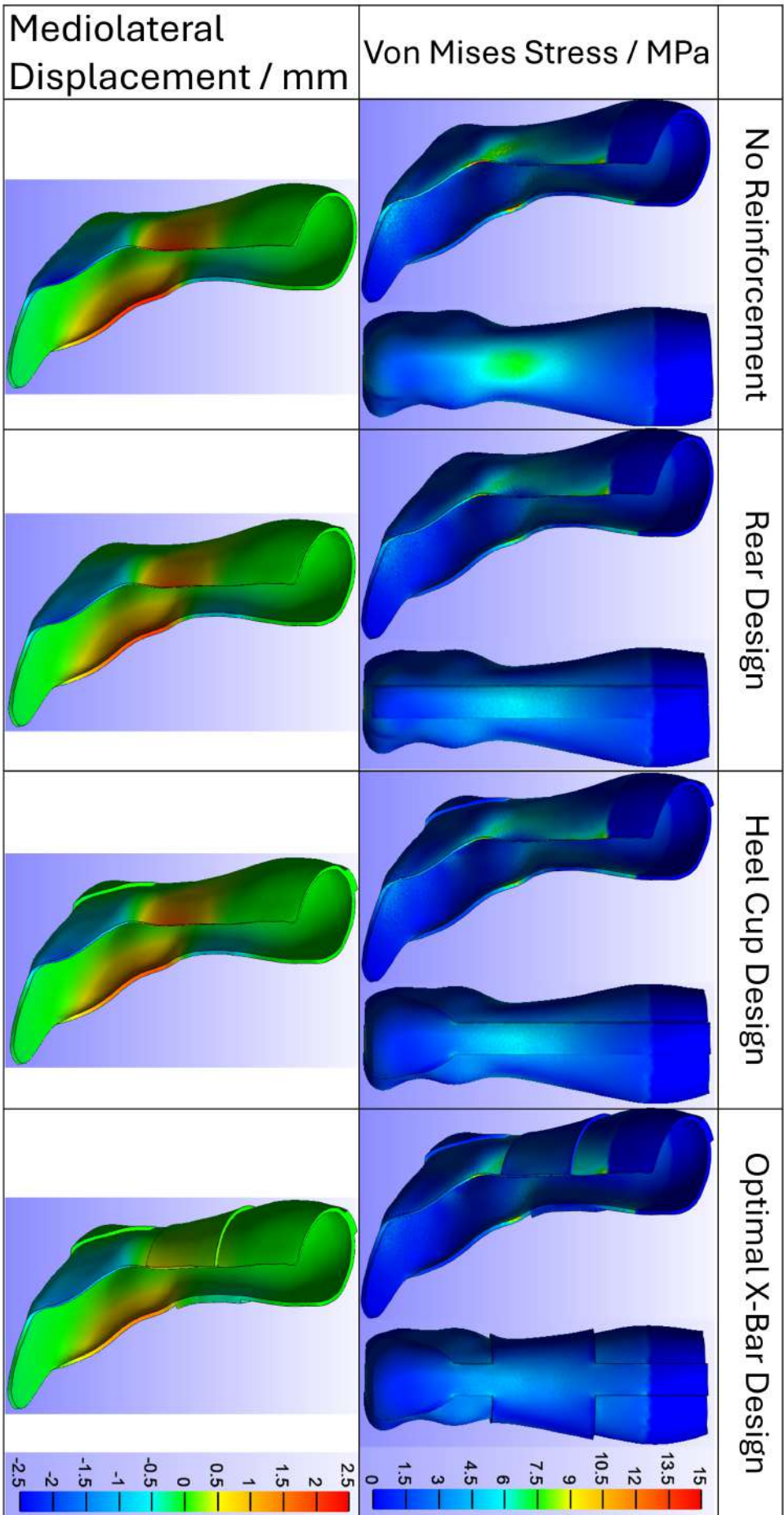


Figure 7.12: Comparison of the Von Mises stress distribution and coronal deformation for the reinforcement design iterations. The range of the colour bars has been manually adjusted.

Discussion

Increasing the width of the X-bar arms demonstrated a similar pattern to increasing the rear reinforcement height in stage 1, where the relationship was linear until a plateau around 60mm distal the top of the AFO. This was thought to be due to the set-up of the model, however, may reflect the fact that the stress concentrations on the mediolateral sides become smaller and more concentrated on the anterior boundary towards the proximal end of the AFO, and so reinforcing these areas was less effective (Figure 7.12).

The X-bar reinforcement with 64mm arms (4/5 strap height) was the first design that achieved the desired mechanical properties, at the reduced AFO thickness. This resulted in an AFO that was $1.68\text{Nm}/^\circ$ (52.02%) stiffer than the 3mm, non-reinforced AFO and had comparable stiffness to a 4mm non-reinforced AFO ($4.92\text{Nm}/^\circ$ to $5.03\text{Nm}/^\circ$), whilst being only 1.71g heavier. Furthermore, the Von Mises stress within the AFO was reduced alongside buckling in the coronal plane. Therefore, the initial design process could be considered a success, as it produced a reinforcement design which achieved the desired AFO mechanical performance whilst considering clinical and user requirements, such as minimising overall device thickness and mass. Furthermore, whilst it should be remembered that a revised clinical threshold of 4.19° was applied to the 5-year-old AFO data, to account for the fact that the FE model was only validated up to $\approx 85\%$ of the peak dorsiflexion moment in gait (Section 5.3), the deflection of the optimal X-Bar design was linear under the applied 15Nm torque. Therefore, the predicted behaviour would result in adequate mechanical properties under 100% peak dorsiflexion moment in gait ($\approx 17.9\text{Nm}/^\circ$), as long as this does not exceed the yield stress of the device.

Consequently, the next stage in the development of the reinforcement is to test its scalability to larger paediatric AFO sizes. The design can be scaled as the dimensions of the X-Bar reinforcement were defined anthropometrically or based on measurements from orthopaedic lasts. However, it should not be assumed that the dimensions of the optimal 5-year-old-sized design are directly translatable. This is because the peak external dorsiflexion moment in stance increases non-linearly with age (5-year-old = 17.9Nm, 10-year-old = 31.9Nm, 15-year-old = 54.2Nm), whilst the clinical threshold for a significant change in kinematics remains constant (5°). As a result, whilst the $1.68\text{Nm}/^\circ$

increase in stiffness provided by the X-Bar, was sufficient to reduce the maximum deflection of a 3mm PPH AFO for a 5-year-old to below the revised threshold (4.55° to 2.96°), this may not be the case when scaled to the size of a 10- or 15-year-old, which deflected 8.87° and buckled, respectively (Chapter 6). Consequently, the dimensions of the AFO and X-Bar will be tailored to each age group.

Given the secondary aim is to minimise the width of the AFO to aid footwear fit, it may seem logical to adjust the design of the X-bar, whilst maintaining a minimal, 3mm AFO. However, this is not appropriate as it would extend the length of the foot section, affecting footwear fit. Additionally, it may have detrimental effects on the gait biomechanics. During the first rocker, increasing the thickness of the posterior aspect of the AFO would create a positive heel which would position the GRF posterior to the knee and ankle, accelerating angular motion during loading response. Meanwhile, the increased posterior thickness may shift the position of the metatarsal heads beyond the rocker of the shoe, altering biomechanics during the third rocker. Finally, only changing the dimensions of the X-Bar may have detrimental effects on the overall mass of the device, as highlighted by the fact that for the 5-year-old-sized AFO, the 4mm non-reinforced AFO had a higher stiffness to mass ratio than any of the 3mm AFOs reinforced with the X-Bar design. As a result, there is a compromise to be found between the dimensions of the X-Bar and AFO.

7.5 Scaling the reinforcement to the older paediatric ages.

7.5.1 Methodology

Once the X-Bar reinforcement had been designed for the 5-year-old-sized AFO it was scaled to the larger AFO sizes. This was completed for the 10- and 15-year-old-sized AFO, using a two-step process. First, the appropriate thickness of the AFO and reinforcement was determined, to minimise the thickness of the AFO distal to the malleoli. The mechanical properties of a rigid AFO reinforced with an X-Bar with maximum arm width were evaluated. Initially, the thickness of the AFO and X-Bar was minimised

to 3mm. If this did not produce a device with the desired mechanical properties, the thickness of the X-Bar was increased to 4mm. Following this, if the stiffness was still inadequate, the thickness of the AFO was increased by 1mm, whilst the thickness of the X-Bar was reduced to 3mm. This process of alternatively increasing the thickness of the reinforcement, then the AFO continued until the maximum deflection of the AFO was less than 5° , when considering a 20% reduction in average AFO thickness.

Once the thickness had been determined, the second stage was to optimise the arm width of the X-Bar. To achieve this, the same process was performed as for the 5-year-old-sized AFO, where the width was increased in fifths from the minimum position (the malleolus width proximal to the mid-point of the malleoli) to the strap height (60mm distal the AFO height), then extended to the full height of the AFO. The optimal design was then interpreted as the minimum arm width to satisfy the criteria for maximum deflection at the reduced AFO thickness.

Across both steps the AFO designs were modelled as before and the age-matching FE models, validated in Section 5.3, were used to evaluate the mechanical properties. Finally, the data from the FE simulations were analysed as outlined earlier (Section 7.4).

7.5.2 Scaled X-Bar Design

Before the scaling process could be conducted, it was necessary to scale the X-Bar design to the larger paediatric AFO sizes. For the older ages, the X-Bar followed the same design as the one developed in the previous section (Section 7.4), with a full-length rear reinforcement, heel cup and arms which supported the mediolateral aspects of the AFO shell proximal to the malleoli. However, the dimensions changed relative to the anthropometric data or measurements taken from age-appropriate orthopaedic footwear lasts.

In the 10-year-old-sized AFO, the rear reinforcement extended the full length of the AFO height, equal to 300mm, and had a width of 30mm, taken to be the width of the heel tab from measurements from an orthopaedic shoe last. The heel cup extended from 70mm proximal to the heel on the posterior border to 45mm from the heel along the

distal border, equal to the coordinates of the mid-point of the malleoli apices in the sagittal plane. The arms began at 100mm proximal to the heel, and 30mm proximal to the mid-point of the malleoli, where 30mm was equal to the malleoli diameter measured from the positive mould. The width of the arms was increased by 28mm to the height of the strap, 140mm proximal to the starting height. Finally, the arms were 200mm wide, when extended to the top of the AFO (Figure 7.13).



Figure 7.13: 10-year-old-sized AFO X-Bar Reinforcement Design

Alternatively, for the 15-year-old-sized AFO, the rear reinforcement extended 355mm proximal to the heel and was 35mm wide. Meanwhile, the heel cup ran from a height of 85mm to a depth of 55mm. The arms were extended from 110mm, 35mm proximal to the mid-point of the malleoli, in 37mm increments to the strap height 185mm proximal. Finally, the maximum arm width was 245mm, which spanned to the top of the AFO (Figure 7.14).

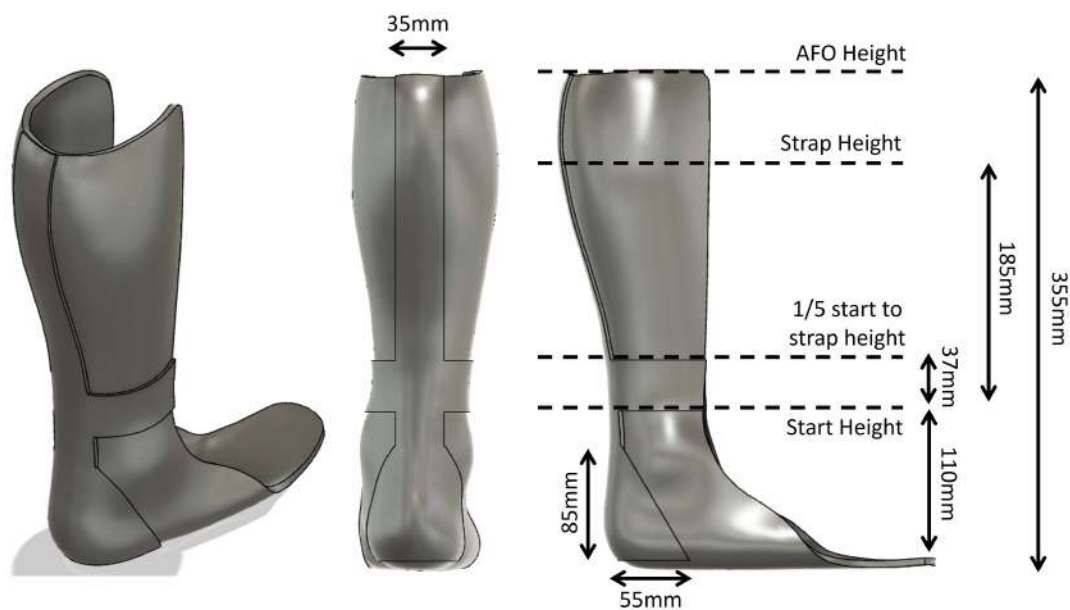


Figure 7.14: 15-year-old-sized AFO X-Bar Reinforcement Design

7.5.3 Stage 1: Determining the appropriate AFO and X-Bar thickness

10-year-old-sized AFO Results

For the 10-year-old-sized AFO, applying a 3mm X-Bar with maximum arm width (200mm), to a 3mm AFO, produced comparable mechanical properties to the 4mm non-reinforced AFO (Figure 7.15), with stiffness of $4.96\text{Nm}/^\circ$ and a maximum deflection of 4.57° (Table 7.8). Furthermore, increasing the thickness of the X-Bar, from 3mm to 4mm, resulted in a further $0.95\text{Nm}/^\circ$ ($\approx 12\%$) increase in stiffness. However, when considering the 20% reduction in average AFO thickness, neither the 3mm nor 4mm X-Bar could reinforce the 3mm AFO to reduce maximum deflection under the clinical threshold.

Alternatively, a 4mm thick AFO with a 3mm X-Bar with maximum arm width, restricted maximum deflection to 3.14° , whilst the deflection, at the 20% reduced AFO thickness, was also $<5^\circ$ (Figure 7.15). The stiffness of this device was $1.89\text{Nm}/^\circ$ ($\approx 24\%$) higher than the 3mm AFO with a 4mm X-Bar. Meanwhile, it was only 11.43g heavier, giving it a more favourable mass-to-stiffness ratio of $0.0260\text{Nm}/^\circ/\text{g}$ versus $0.0217\text{Nm}/^\circ/\text{g}$.

Increasing the thickness of the non-reinforced AFO by 3mm to 4mm resulted in a

3.02Nm/° in stiffness, whilst a 2.84Nm/° was seen when the thickness of the AFO, reinforced with the 3mm X-Bar, was increased similarly.

Table 7.8: Mechanical properties between AFO and X-Bar thickness for the 10-year-old-sized AFO.

AFO Thickness / mm	X-Bar Thickness / mm	Stiffness / Nm/°	Max Deflection / °	Mass / g	Δ% in stiffness vs 3mm non-reinforced
3	None	3.84	8.87	184.32	-
	3	6.96	4.57	317.79	81.38
	4	7.91	4.02	364.59	106.10
4	None	6.86	4.58	249.03	78.61
	3	9.80	3.14	376.02	115.42

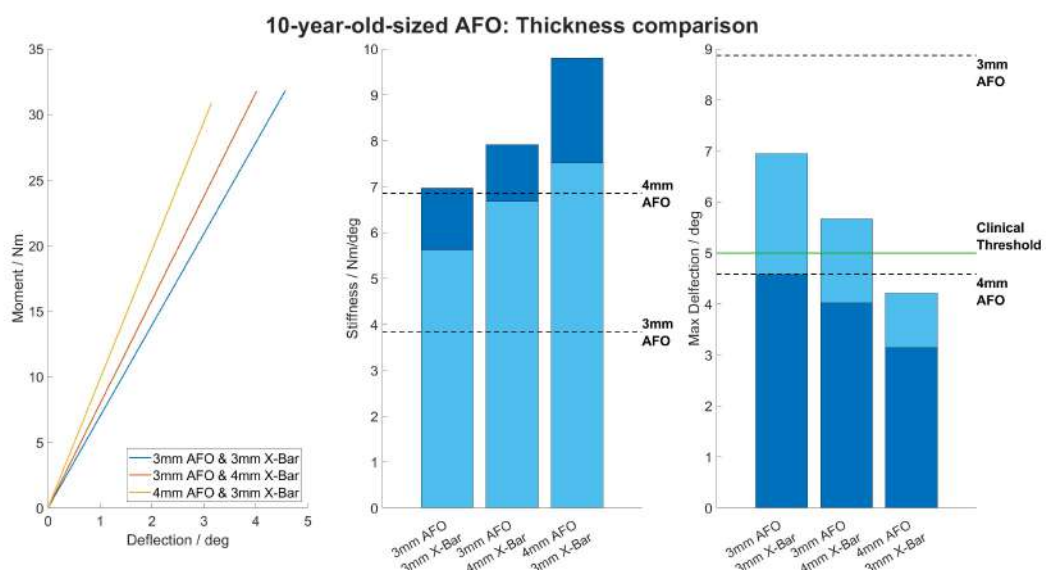


Figure 7.15: Determining optimal AFO and X-Bar thickness for the 10-year-old-sized AFO. Dark blue bars = mechanical properties at 100% thickness. Light blue bars = mechanical properties at 80% thickness.

15-year-old-sized AFO Results

For the 15-year-old-sized AFO, neither reinforced 3mm thick AFOs produced adequate mechanical properties, with maximum deflection below the clinical threshold. Alternatively, for the 4mm thick AFOs, the 3mm and 4mm X-Bar achieved the desired mechanical properties, comparable to or better than the 5mm non-reinforced AFO. However, after reducing the thickness by 20%, neither deflected less than the clinical threshold. Finally, the 5mm thick AFO with a 3mm X-Bar achieved the desired properties when accounting for the thickness lost during manufacturing (Figure 7.16).

When increasing the thickness of the AFO from 3mm to 4mm, resulted in a $3.47 \pm 0.28 \text{ Nm}/^\circ$ increase in stiffness across the different reinforcement conditions, whilst increasing thickness to 5mm resulted in a further $4.04 \pm 0.17 \text{ Nm}/^\circ$ (Table 7.9). Alternatively, increasing the thickness of the X-Bar from 3 to 4mm, stiffened the AFO by $0.62 \pm 0.17 \text{ Nm}/^\circ$.

Table 7.9: Mechanical properties of AFO and X-Bar thickness for the 15-year-old-sized AFO.

AFO Thick-ness / mm	X-Bar Thick-ness / mm	Stiffness / Nm/°	Max Deflection / °	Mass / g	Δ% in stiffness vs 3mm non-reinforced
3	None	4.68	-	244.98	-
	3	9.93	7.82	424.35	112.01
	4	10.43	6.29	486.72	122.73
4	None	8.18	6.79	330.30	74.62
	3	13.49	4.04	513.54	188.14
	4	14.24	3.75	577.08	204.01
5	None	12.38	4.33	417.60	164.46
	3	17.36	3.04	604.53	270.75

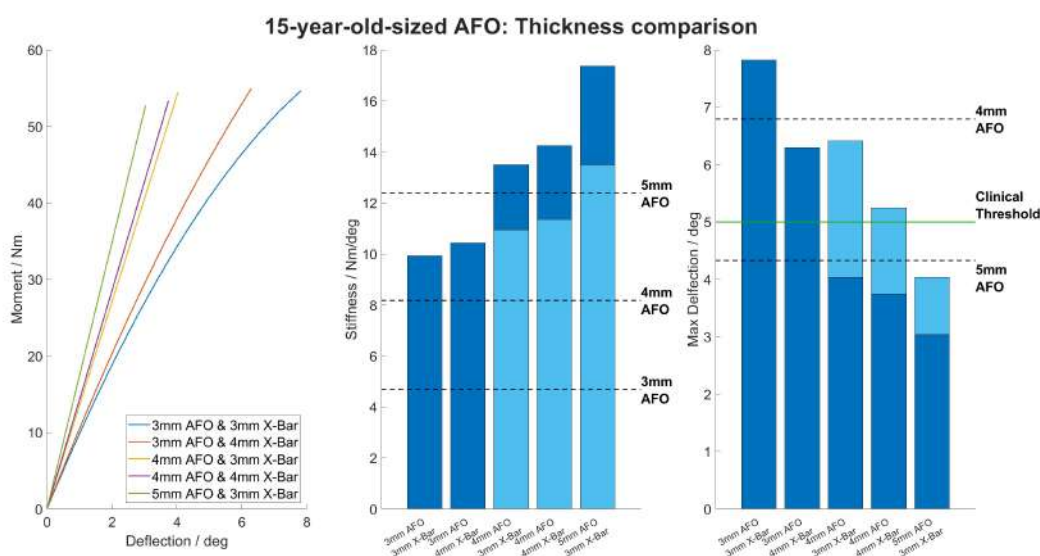


Figure 7.16: Determining optimal AFO and X-Bar thickness for the 15-year-old-sized AFO. Dark blue bars = mechanical properties at 100% thickness. Light blue bars = mechanical properties at 80% thickness.

Discussion

Although the secondary aim when reinforcing the rigid AFO was to minimise overall thickness, the primary objective was to ensure sufficient mechanical properties, whilst

compensating for loss of thickness due to the manufacturing process. When considering the results from the previous study (Chapter 6), where buckling of the 3mm 10- and 15-year-old-sized AFOs was evident, it was unlikely that a 3mm AFO and 3mm X-Bar would produce sufficient stiffness for these ages, as it had for the 5-year-old-sized model. This was confirmed by these results, which indicated that for a 10-year-old-sized, a 4mm thick AFO was necessary and for the 15-year-old-sized, a 5mm AFO.

Furthermore, for the 3mm, 10-year-old-sized AFO, increasing the thickness of the X-Bar by 1mm, increased the AFO stiffness by $0.95\text{Nm}/^\circ$, whilst increasing the AFO thickness by the same amount saw a $2.84\text{Nm}/^\circ$ rise. Assuming AFO stiffness increased linearly with X-Bar thickness, a 6mm X-Bar would be required to achieve the same increase in stiffness. Meanwhile, for the 15-year-old-sized AFO, increasing the thickness of the AFO from 3 to 4mm was ≈ 5.5 times more effective at increasing stiffness than the same increase in X-Bar thickness. However, it also suggests there may be a non-linear relationship between stiffness and AFO thickness, as the difference in stiffness between the 4mm and 5mm AFOs was, on average, $0.57\text{Nm}/^\circ$ greater than seen between a 3mm and 4mm AFO. This supports the importance of choosing the appropriate thickness for the AFO, as highlighted in Chapter 6, and confirms that increasing the thickness of the X-Bar alone is not appropriate to meet the specifications outlined for the AFO designs.

7.5.4 Stage 2: Optimising the Design of the X-Bar

10-year-old-sized AFO Results

Reducing the width of the X-Bar arm produced a similar trend as seen with the 5-year-old-sized AFO (Figure 7.17). Narrowing the arm length from the maximum height (200mm) to the strap height (140mm) resulted in a $0.1\text{Nm}/^\circ$ reduction in stiffness, after which reducing the arm width by 20% (28mm) demonstrated a fairly linear decrease in stiffness of $0.46 \pm 0.02\text{Nm}/^\circ$, when excluding the difference between the 84mm and 112mm arm width, which was only $0.22\text{Nm}/^\circ$, likely due to measurement error (Table 7.10).

Furthermore, with an AFO thickness equal to the pre-draped sheet, all the conditions produce adequate mechanical properties (maximum deflection $< 5^\circ$). However, when con-

sidering the 20% reduction in AFO thickness, only the reinforcements with arms wider than 60% the distance between the minimum position and the strap height (84mm), achieved acceptable mechanical properties.

Table 7.10: Mechanical properties between X-Bar arm widths for the 10-year-old-sized AFO

Reinforcement Length / mm	Stiffness / Nm/°	Max Deflection / °	Mass / g	Δ% in stiffness vs non-reinforced
None	6.86	4.58	249.03	-
28	8.11	3.79	288.81	18.26
56	8.58	3.57	299.52	25.22
84	9.02	3.40	311.85	31.61
112	9.24	3.32	326.07	34.77
140	9.70	3.17	341.64	41.46
200	9.80	3.14	376.02	43.00

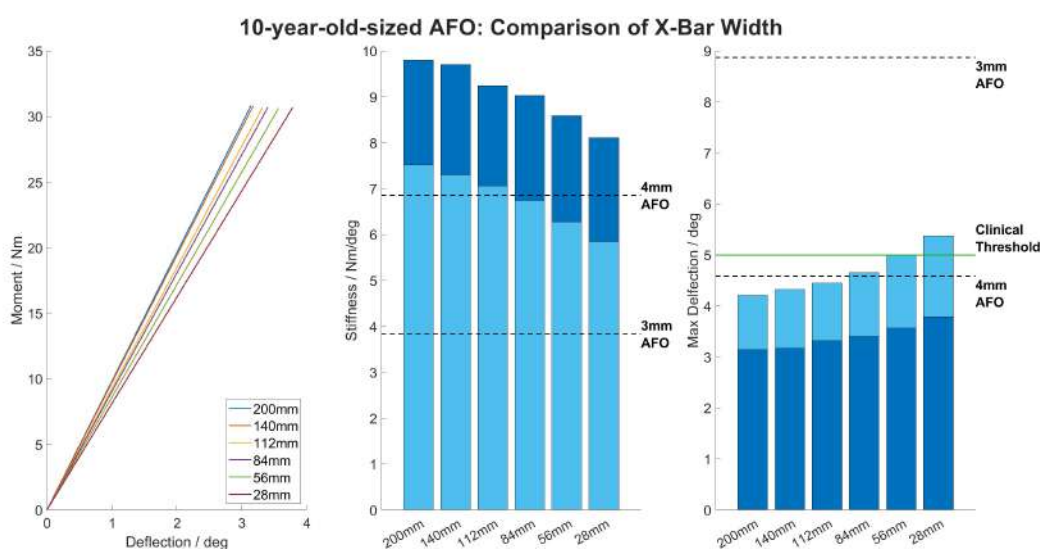


Figure 7.17: Comparison of X-Bar arm width for the 10-year-old-sized AFO. Dark blue bars = mechanical properties at 100% thickness. Light blue bars = mechanical properties at 80% thickness.

Once the optimal design for the X-Bar had been determined, the effect of the reinforcement on Von Mises stress distribution and coronal plane deformation was analysed. Like with the 5-year-old-sized AFO, the Von Mises stress was lower in the AFO reinforced with the X-Bar coupled with a reduction in coronal plane deformation of 0.98mm to 1.109mm (Figure 7.18, 7.19).

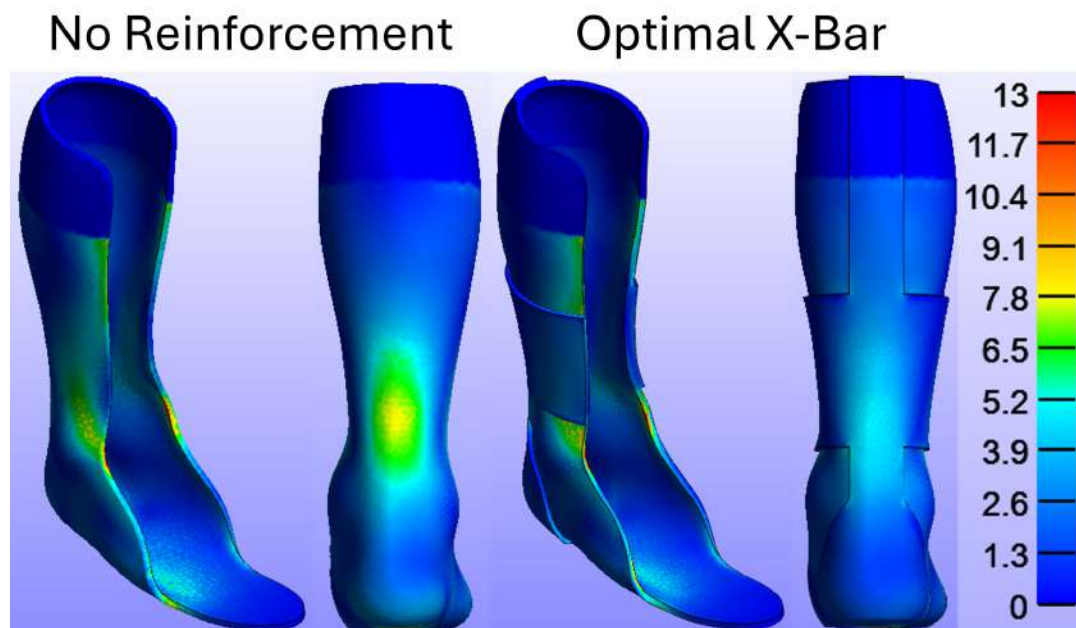


Figure 7.18: Effect of the optimised X-Bar reinforcement on the Von Mises stress distribution in a 10-year-old-sized 4mm PPH AFO with anterior trim lines. Von Mises stress was measured in MPa. The range of the colour bar has been manually adjusted.

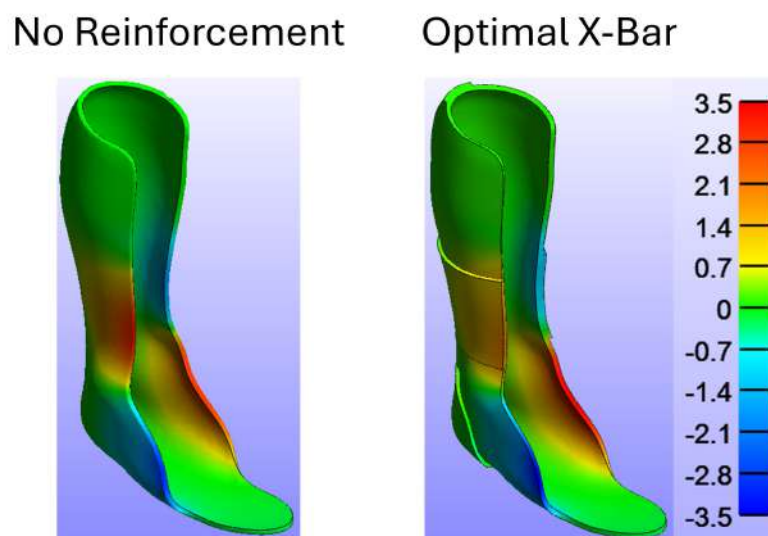


Figure 7.19: Effect of the optimised X-Bar reinforcement on the coronal plane deformation in a 10-year-old-sized 4mm PPH AFO with anterior trim lines. Deformation was measured in mm. The range of the colour bar has been manually adjusted.

15-year-old-sized AFO Results

Again, a similar trend was seen when changing the arm width of the X-Bar in the 15-year-old-sized AFO, however, the plateau in stiffness occurred earlier (Figure 7.20). Increasing the arm width from 37mm to 111mm, 37mm increments, produced a fairly linear increase in stiffness of $0.90 \pm 0.05 \text{ Nm}/^\circ$, after which the rate of increase decreased,

with only a $0.16\text{Nm}/^\circ$ difference between arm widths 148mm and 245mm (Table 7.11). Furthermore, whilst all X-Bar conditions demonstrated $<5^\circ$ maximum deflection at the idealised AFO thickness, only an arm width of 74mm (2/5 strap height) and above satisfied this criteria with an AFO with thickness 80% the pre-draped sheet.

Table 7.11: Mechanical properties between X-Bar arm widths for the 15-year-old-sized AFO

Reinforcement Length / mm	Stiffness / $\text{Nm}/^\circ$	Max Deflection / $^\circ$	Mass / g	$\Delta\%$ in stiffness vs non-reinforced
None	12.38	4.33	417.60	-
37	15.00	3.49	481.77	21.11
74	15.84	3.30	498.15	27.92
111	16.79	3.148	517.77	35.59
148	17.20	3.06	540.81	38.88
185	17.28	3.03	565.74	39.56
245	17.36	3.04	604.53	40.19

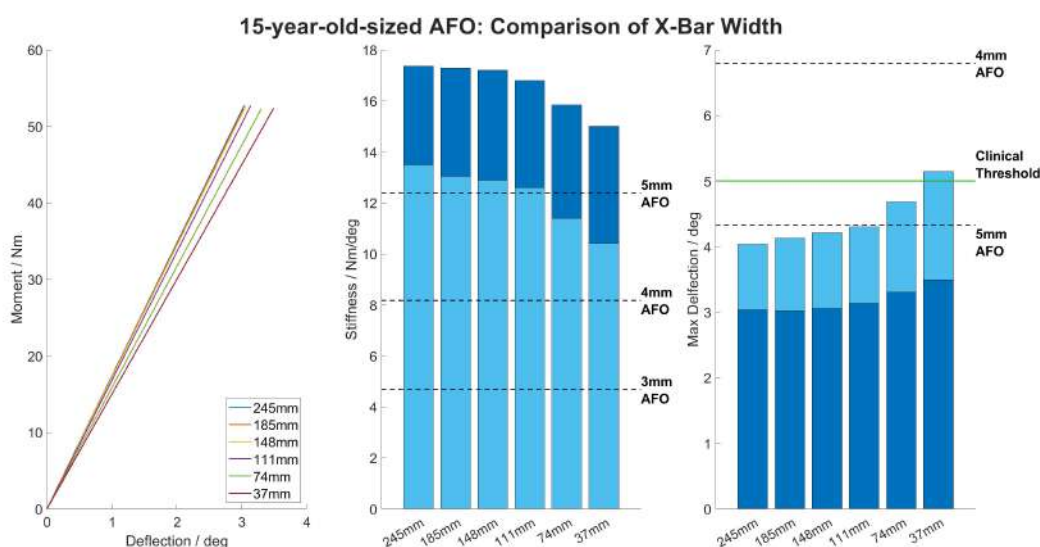


Figure 7.20: Comparison of X-Bar arm widths for the 15-year-old-sized AFO. Dark blue bars = mechanical properties at 100% thickness. Light blue bars = mechanical properties at 80% thickness.

Finally, the effects of the optimal X-Bar on Von Mises stress distribution and coronal plane deformation were analysed. As before, the Von Mises stress was lower in the AFO reinforced with the X-Bar, whilst coronal plane deformation was reduced by 0.76mm to 0.61mm (Figure 7.18, 7.19).

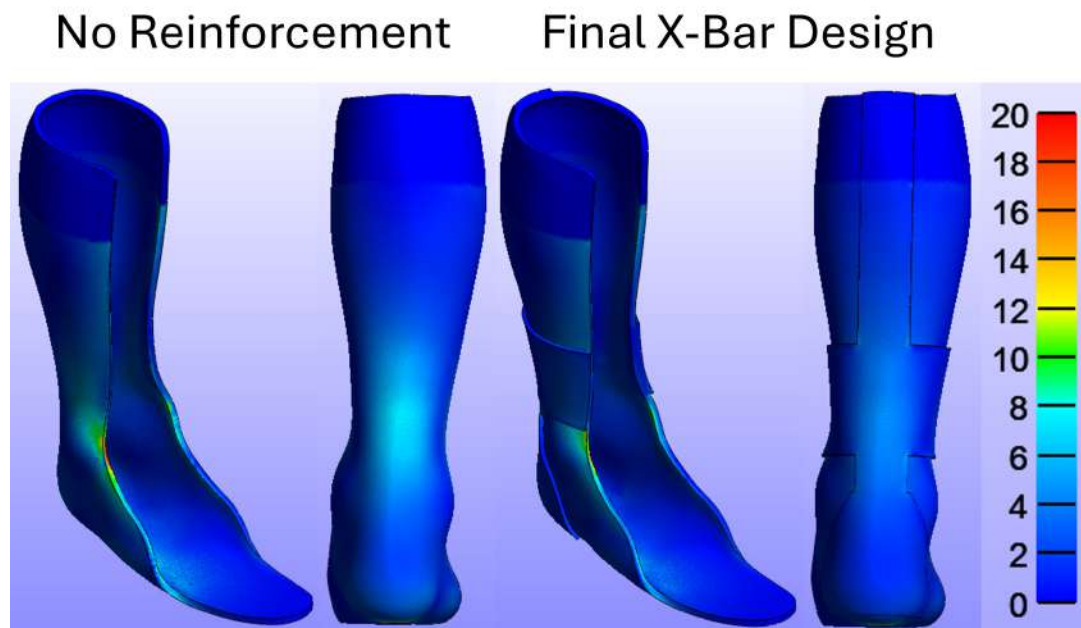


Figure 7.21: Effect of the optimised X-Bar reinforcement on the Von Mises stress distribution in a 15-year-old-sized 4mm PPH AFO with anterior trim lines. Von Mises stress was measured in MPa. The range of the colour bar has been manually adjusted.

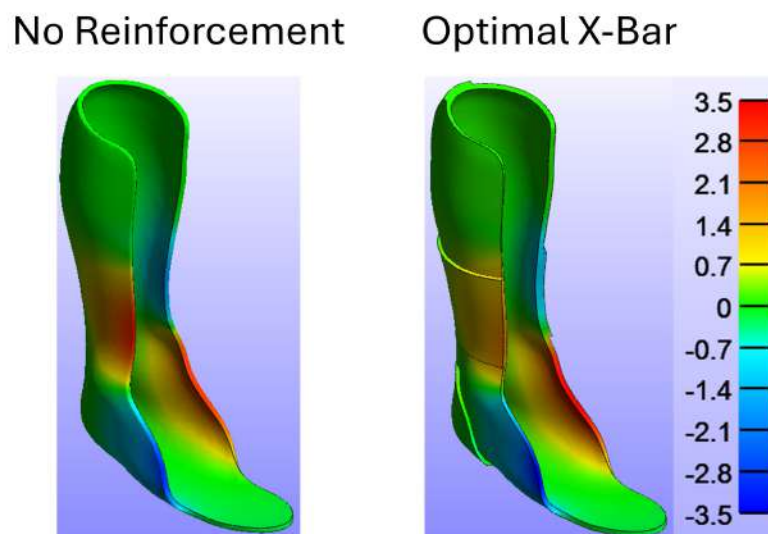


Figure 7.22: Effect of the optimised X-Bar reinforcement on the coronal plane deformation in a 15-year-old-sized 4mm PPH AFO with anterior trim lines. Deformation was measured in mm. The range of the colour bar has been manually adjusted.

Discussion

Increasing the arm width of the X-Bar in the 10- and 15-year-old-sized AFOs followed a similar trend to the one presented in the 5-year-old model. Initially, there was a near linear relationship between stiffness and arm width, before the rate of increase plateaued as the arms extended proximally, suggesting that increasing the thickness of the proximal

AFO has little effect on stiffness. For the 5-year-old-sized and 10-year-old-sized AFOs this plateau occurred at the height of the strap, whilst for the 15-year-old-sized AFO this occurred at 3/5 of the distance between the minimum arm position and the strap height. When comparing the Von Mises stress distribution in the non-reinforced, 5mm, 15-year-old-sized AFO to 3mm 5-year-old-sized and 4mm 10-year-old-sized AFOs, the area and level of stress in the proximal, anterior mediolateral regions of the AFO was lower (Figure 7.23). As a result, this would suggest the 5mm thick AFO was inherently more resistant to this mode of deformation so the X-Bar had less impact. Furthermore, if the measurement error in the 112mm width condition was not present, the plateau in 10-year-old-sized AFO stiffness started at 4/5 the strap height, supporting this rationale.

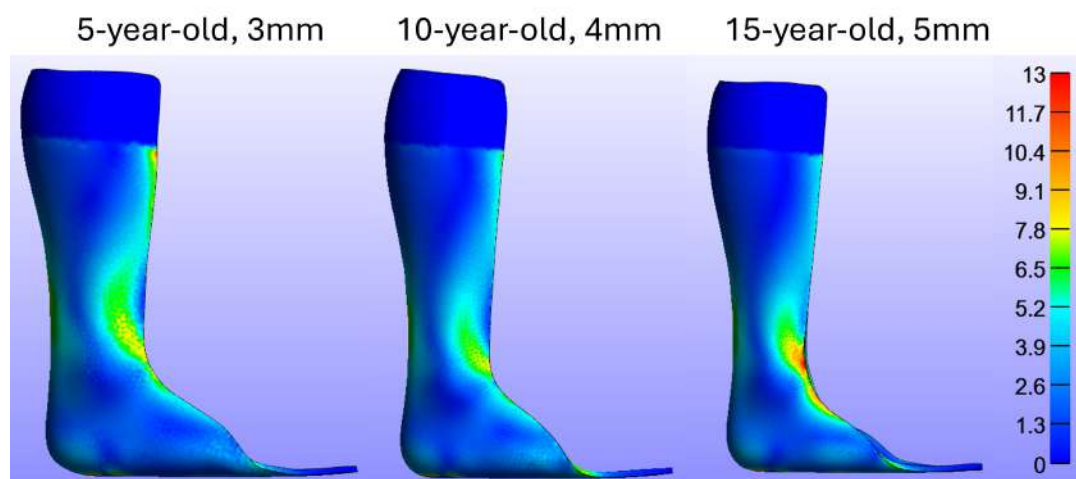


Figure 7.23: Comparisons of Von Mises stress distribution in the medial side of the non-reinforced, baseline AFOs for the three age groups. The range of the colour bar has been manually adjusted.

Overall, the process demonstrated that the X-Bar design could be scaled to the larger AFO sizes. Whilst the X-Bar did not provide sufficient additional stiffness for a 3mm thick AFO to be used in the older cohorts, pragmatically this was unlikely given the level of buckling shown in the previous study (Chapter 6). Instead, for the 10 and 15-year-old-sized AFOs, the X-Bar provided a method of ensuring the device had adequate mechanical properties whilst accounting for the thinning during the vacuum-forming process, without increasing the thickness of the pre-draped sheet. As a result, it produced narrower devices, with a similar mass to a thicker AFO with no reinforcement (5mm 10-year-old AFO = 299.25g, 6mm 15-year-old = 506.7g). Therefore, the specifications for the AFO design were still met.

7.6 Chapter Discussion

AFO reinforcements have tended to focus on the malleoli regions, due to the high stress and buckling that occurs in these areas[101], [212], [232]. The most common type is ribbing reinforcement, whose effects are optimised when placed anterior to the malleoli[193]. However, this challenges clinical practice where they are typically placed posterior to the malleoli to allow post-drape modifications to improve the fit of the device[293]. Meanwhile, ribbing widens the AFO impacting footwear fit. As a result, mediolateral reinforcements can cause conflict with the needs of both the clinician and user[190], [267]–[269], [271], [274]. Therefore, this study aimed to develop a novel reinforcement which targetted the posterior and proximal to the malleoli aspects of the AFO shell, aligning closer to the stakeholder requirements.

The final optimised X-Bar designs for the 5-, 10-, and 15-year-old-sized AFO, demonstrated a $1.68\text{Nm}/^\circ$ (52%), $2.16\text{Nm}/^\circ$ (31%) and $3.46\text{Nm}/^\circ$ (27.92%) increase in stiffness, respectively, when compared to non-reinforced AFOs of the same thickness. The findings aligned with the impact achieved using ribbing[193], [206] and mediolateral carbon-fibre inserts[206]. Furthermore, existing posterior AFO reinforcements include the chevron type proposed by Novacheck et al.[203], which was used to reinforce adult and paediatric PPC and PPH flexible AFOs. From the graphical data presented, the chevron reinforcement had a mixed effect on stiffness, with detrimental impacts seen for the adult sizes, which may have been caused by variations in AFO thickness which was not recorded. However, for the paediatric size it resulted in a $\approx 0.22\text{Nm}/^\circ$ ($\approx 56\%$) and $\approx 0.1\text{Nm}/^\circ$ ($\approx 18\%$) increase in stiffness for the PPC and PPH AFOs respectively. Meanwhile, Fatone et al. compared the stiffness of paediatric AFOs, three of which incorporated a posterior Y-shaped reinforcement. However, the impact of the reinforcement could not be isolated as the additional AFOs design factors were not controlled. As a result, the findings of this study validate the use of reinforcements that target areas of the AFO outside the malleoli region and develop the limited knowledge base surrounding their design.

Additionally, this was one of the first studies to attempt to design a rigid AFO with clinically acceptable mechanical properties. Hovorka et al. also took a similar approach,

however, they focused purely on the mechanical performance of the device, leading to a design which could not be translated into clinical practice[237]. It was also the first to try to compensate for the thinning of the AFO during the vacuum-forming process. Adopting this approach demonstrated that setting an appropriate AFO thickness was key to achieving the desired mechanical properties. For each age group, the thickness of the AFO increased by 1mm, whilst the contribution of the X-bar to overall device stiffness reduced. Furthermore, for the 15-year-old child, a 5mm thick AFO was required. This is supported by Chatzistergos et al., who predicted a 5.1mm sheet of PPC would be needed to compensate for the loss of AFO thickness during manufacturing and produce an AFO which did not buckle for adults[193]. Consequently, it challenges clinical practice regarding the thickness of AFOs used in paediatric populations.

However, the fact that a 5mm PPH AFO was required for the 15-year-old, suggests the X-Bar reinforcement had only limited success in minimising the thickness of the AFO to facilitate footwear fit. This was achieved for the 5-year-old child, arguably the most important, as smaller shoe sizes have the least space to accommodate an AFO. Nevertheless, it highlights the limitations of using PPH to reinforce rigid AFOs. The X-Bar was designed from PPH to reduce cost and utilise current manufacturing techniques. However, its stiffness-to-mass ratio limits the increase in stiffness it can provide without incurring potentially significant increases in mass and thickness. Alternatively, ribbing used across the malleoli does not increase the mass. Therefore, applying this technique to other areas of the device could be explored, however the aesthetics of this could be questioned. Additionally, materials with a higher stiffness-to-mass ratio, such as carbon fibre, may be more beneficial. Carbon fibre inserts have been laminated into the malleoli region of AFOs[120], [200], whilst it is also used in the soles of footwear to create a rigid sole. Finally, Badescu et al. highlighted the viability of reinforcing AFOs with metal wires through computational analysis, which decreased the maximum principal stress and deformation[255].

Consequently, there is scope for further development of the reinforcement design. However, supplementary studies are also required to help refine the design criteria used to inform this process. Firstly, the 20% reduction in average thickness was based on limited

evidence from two previous studies[205], [213]. Although Convery et al. investigated the between-clinic and technician variability in AFO thickness, both studies only considered 3mm AFOs made from a single positive mould. Furthermore, the measurements were taken from a limited number of locations (Convery et al. = four[205], Lunsford et al. = 10[213]). Therefore, this estimation of the average reduction in thickness is fairly crude. To improve this, further investigation into the thinning of polypropylene AFOs is required. This should consider all the factors which could influence variability, including polypropylene type and thicknesses, the shape of the positive mould and the manufacturing conditions, and adopt the method for measuring AFO thickness presented in this thesis, to observe fluctuations in thickness across the entire AFO shell.

Similarly, determining a clinically significant change in AFO mass would be beneficial. Throughout the design process, attempts were made to minimise the mass of the AFO, with the final X-Bar reinforcements increasing the mass of the AFOs for the 5-, 10- and 15-year-old by 40.1g, 62.82g and 80.55g respectively. However, whilst anecdotal links have been made between AFO mass and fatigue in children with CP by users and clinicians[268], [270], [271], [274], this relationship has never been studied. Additionally, AFO mass may also influence biomechanics during swing and the 1st rocker, where a heavier device could influence the momentum of the limb. Therefore, it was difficult to evaluate whether these increases in mass are clinically significant.

However, future research should include experimental verification of computational analysis, as performed by Chatzistergos et al.[193]. Firstly, this would provide valuable insight into how feasible the reinforcement was to manufacture. The X-Bar was intended to be laminated onto the AFO during vacuum forming. However, how practical this is, remains unknown, particularly given the reinforcement would need to be placed with a reasonable level of accuracy. Furthermore, whilst the simulations accounted for the thinning of the AFO during vacuum-forming, the X-Bar could be similarly affected. Finally, the verification process should include an analysis of the reinforcement's performance in walking trials. This is required to determine if a maximum deflection of $<5^\circ$ during static testing, translates to limiting ankle dorsiflexion by the same amount during dynamic loading in gait. Furthermore, it would be beneficial to understand how the device

impacts biomechanics across the lower limb, in all three planes and outside the second rocker of gait.

7.7 Conclusions

Overall, the study was successful in designing a novel reinforcement for rigid AFOs demonstrating that stiffening areas outside the malleoli region is a viable option. However, it highlighted potential limitations of using PPH to reinforce AFOs, suggesting other materials, with a higher stiffness-to-mass ratio, or designs would be more suitable in larger AFO sizes. Furthermore, the study introduced design specifications which incorporated the mechanical and clinical requirements for AFO design. Therefore, it is recommended that future studies aiming to optimise the design of rigid AFOs for clinical purposes, adopt similar specifications. However, further refinement of criteria, such as the amount of thinning during the vacuum forming process and the clinical significance of a change in AFO mass, would be beneficial.

Chapter 8

Thesis Discussion

Chapter Overview

The final chapter discusses the main findings of the thesis and evaluates how successfully the aims were met. In doing so, it demonstrates the novelty of the work conducted, and how it has broadened the scientific output. It then considers the limitations of the work, mainly associated with the use of FE analysis, before proposing several areas for future work.

8.1 Summary of main findings

A main issue with the OSKAR is that it does not provide guidance on how to design rigid AFOs for children with CP, with sufficient mechanical properties to facilitate biomechanical optimisation. As a result, literature reviews were conducted to assess the current understanding of the relationship between AFO design factors and the device's mechanical properties, revealing a limited body of evidence. Furthermore, it was found that stakeholders' requirements, such as the clinician, parent and user, may dictate what a clinically acceptable design looks like. Therefore, the thesis aimed to investigate the relationship between rigid AFO design factors and the stiffness of the device and move towards an optimised design for paediatric rigid AFOs.

To achieve these aims, FE analysis was determined as the most appropriate method to quantify AFO mechanical properties. As a result, FE models, which simulated the loading placed on an AFO during the second rocker, were developed and validated against experimental data collected using a test rig. The test rig utilised MOCAP so that it had the potential to be applied in both research and specialist clinical settings. As a result, it was the first example to demonstrate high within-session and test-retest reliability when using this technology. Once developed, FE analysis was used to conduct further primary research.

First, the effects of the four design factors, which influence AFO stiffness, were investigated within AFOs designed for a 5-, 10- and 15-year-old. Furthermore, the conditions tested were aligned to clinical practice through discussion with practising orthotists. This study represents the first to consider the combined effects of all four AFO design factors and a range of paediatric AFO sizes. Furthermore, as part of the AFO modelling process an anthropometric definition for rigid AFO trim lines was presented, which was the first attempt at defining a standard trim line for rigid AFOs. This study supported the consensus that AFO stiffness increases with material rigidity, thickness and anterior placement of the trim lines. However, more interestingly, it found that thickness and the depth of the trim line at the malleoli were the biggest contributors to AFO stiffness. Furthermore, the results challenged aspects of rigid AFO prescription, for example, the use of 3mm AFOs in paediatric populations, the use of through the malleoli trim lines

and the posterior to the malleoli placement of ribbed reinforcements.

Following this, these findings were applied to optimise the design of rigid AFOs for the three ages using a novel reinforcement. First, the reinforcement was designed for the 5-year-old-sized AFO, before the design was scaled to the larger sizes. This process was directed by a set of design specifications, which outlined a clear definition of adequate mechanical properties and additional design criteria relating to the use and provision of the device. As a result, it was the first attempt to optimise the design of paediatric rigid AFOs for clinical application, by considering both the mechanical and stakeholder requirements of the design. This resulted in a prototype reinforcement referred to as the X-Bar, which demonstrated the viability of reinforcing the posterior and proximal to the malleoli areas of the AFO. Furthermore, it was the first study to compensate for the thinning during the vacuum-forming process.

As a result, the work has significantly contributed to the current understanding of the relationships between rigid AFO design factors and the stiffness of the device and has moved towards an optimised design for paediatric rigid AFOs. Furthermore, a novel test rig, reinforcement, and approach to rigid AFO design were outlined in this thesis. Therefore, it can be concluded that both the aims of the thesis and the descriptors for a PhD have been successfully met.

8.2 Thesis Limitations

The main limitations of the work relate to the methodologies used. Firstly, the decision was made to model the paediatric AFOs by scaling them from an adult AFO, to remove the need to recruit a child from each age group. As discussed in Section 5.1, the transformation matrix was based on anthropometric data for the 50th percentile of typically developing individuals, presented by Snyder et al.[286], [287], chosen as it was as the most complete set of anthropometric data available. As a result, the measures used to define the transformation matrix were restricted to those included in this data set, meaning assumptions were made on the shape of the lower leg. This may have led to a slight distortion in the shape of the AFOs which would be more pronounced, the smaller

the AFO. It would likely affect the shank section of the AFO as its shape is more defined by soft tissues than the foot, however, it is unknown what impact this would have on stiffness. Alternatively, assuming the ankle is a circle may lead to widening the malleoli prominences, which has been shown to decrease the stiffness of AFOs[101]. Additionally, the AFO morphologies represent the 50th percentile of each age group, therefore they do not account for variations within these populations which could impact the behaviour of the AFOs.

Furthermore, this method of modelling the AFOs meant that only idealised conditions were tested within the FE simulations. In practice, impairments such as equinovarus and valgus, planovalgus, tibial torsion and femoral anteversion, common in children with CP, would alter the shape of the AFO and the planes about which, the AFO is loaded. Consequently, the effect of these patient-specific impairments on the mechanical performance of the AFO designs was not investigated. Previously, Sumihira et al. found that 10° of internal and external rotation had a limited effect on AFO mechanical properties during plantar and dorsiflexion[196]. However, the devices buckled under a less than 10Nm dorsiflexion moment and appeared to undergo torsion whilst deforming caused by loading through a single point.

Furthermore, a maximum deflection of 5° was used as the criteria for clinically adequate material properties[237], [292], with the applied moments based on the 50th percentile mass for each age group[286], [287]. However, higher than typical rates of obesity are seen in children with CP[294], [295], whilst atypical gait patterns such as apparent equinus and crouch gait, characterised by excessive knee flexion in stance, are amongst the most common[41]. Both would increase the peak dorsiflexion moment in stance, by increasing body weight and the GRF lever arm, respectively. As a result, the FE analysis does not account for these fluctuations in applied load.

Finally, children with CP display variability in the speed, symmetry, and kinematics of gait[50], [51], [296]. Therefore, questions could be raised over how well the static loading conditions used in the FE model represent the variable, dynamic loading placed on an AFO during gait, reaffirming the need for experimental validation. Collectively,

these assumptions limit the direct clinical relevance of the data produced in these studies. Instead, the observations provide the rationale for future work which could impact clinical practice, including experimental evaluation of rigid AFO design within relevant populations. This was planned as the final stage of the thesis, however, time constraints and issues with recruitment meant this was not possible.

8.3 Future Work

Having reflected on the successes and limitations of the thesis, several opportunities for further research have been identified. Firstly, the findings of both primary research studies highlighted the importance of thickness on the stiffness of vacuum-formed AFOs. As a result, OSKAR would benefit from the development of a tool which could be used to determine the appropriate thickness based on an individual's characteristics. To achieve this, a wider range of AFO morphologies and loading conditions should be inputted into the FE models, to evaluate their performance and formulate thresholds for the mechanical properties of AFOs manufactured from different materials and thicknesses. Ideally, these would be patient-specific. However, this would involve recruiting individuals with CP. Alternatively, the anthropometric data published by Snyder et al. includes measurements for the 5% and 95% percentile[286], [287]. Therefore, this data could be used to predict the upper and lower ranges for AFO mechanical properties for each age group. Furthermore, given the importance of thickness, there is a need to fully understand the effects of the vacuum-forming process on AFO thickness and establish a standard methodology which limits this.

Additionally, as discussed in Section 7.6, experimental verification of the X-Bar reinforcement, including mechanical bench testing, performance during walking trials and stakeholder feedback, should be prioritised. This would involve an initial proof-of-concept in a small sample of typically developing children, before applying the design in a larger cohort of children with CP. As a result, it would provide insight into how feasible the reinforcement is to manufacture and whether its predicted behaviour under static loading translates to significant clinical benefits when considering patient-specific morphologies and dynamic loading conditions. Ultimately, this is required to establish whether there

is value in the continued development of the design.

Assuming the X-Bar design is found to have clinical value, a more thorough assessment of its influence on mechanical properties and behaviour would be required. This should include properties such as hysteresis and the fatigue of the AFO across its life-cycle. To achieve this, both the rig and FE model would need to be developed to accommodate the assessment of these properties. In terms of the rig, this would require an automated loading system, similar to the ones used by Ielpai et al.[248] and Totah et al.[231]. Alternatively, FE analysis would require a viscoelastic material model, like the one explored by Ielpai et al.[232]. These developments to the rig and FE models would also allow further comparison of PPC and PPH, which is required to make recommendations on the most appropriate material to use clinically.

Alternatively, the second study demonstrated limitations to PPH reinforcements due to the material's stiffness-to-mass ratio. As a result, there may be a benefit in investigating the effects of carbon-fibre reinforcements, which have a high stiffness-to-mass ratio and therefore may allow thinner devices to be created. However, this line of research could also be expanded beyond vacuum-formed AFOs. 3D printing custom foot orthoses have been trialled, with the benefits of reducing waste and lead times. As 3D printing technology evolves, it will become a viable option for manufacturing AFOs alongside alleviating the restrictions on AFO design, associated with vacuum-forming. Firstly, it would widen the available materials that could be used to manufacture the devices, with several studies already evaluating these[232], [250], [253], [260]. Furthermore, it would allow topology optimisation to be used during the design process. Topology optimisation is widely used in mechanical and civil engineering, to determine the optimal material layout for a structure, via FE analysis, given the boundary and loading conditions of the FE model[297]. Previously, the free-form shapes it produces could not be manufactured via vacuum forming, however, 3D printing overcomes this issue. As a result, this may lead to the development of AFOs with variable thickness and perforations, with the benefits of easier donning, better compatibility with footwear, reduced mass, and increased thermal comfort.

In any case, future developments of rigid AFOs would benefit from refinement of the design specifications. As discussed in Section 7.6, this should involve establishing criteria for a clinically significant change in AFO deflection and mass, and for vacuum-formed devices, the amount of thinning that occurs during production. However, additional quantitative research, beyond the scope of previous research[190], [267]–[274], would also improve this process. Firstly, consultation with technicians would provide greater insight into the manufacturing limitations on AFO and reinforcement designs, particularly regarding footwear design, which was difficult to account for within this thesis. Furthermore, it may highlight variations across the industry which could impact AFO mechanical properties. Lastly, focus groups with clinicians and users evaluating the aesthetics and barriers to novel reinforcement designs would benefit the design process.

8.4 Concluding Remarks

This thesis provides the most thorough evaluation of the mechanical properties of paediatric, rigid AFOs, available. It has built on previous work by assessing all four design factors in a range of paediatric-sized AFOs and taken research one step further, by considering the functional, user and clinician requirements, to optimise AFO design. Furthermore, it was particularly successful in linking AFO mechanical properties to clinical practice, something that has largely been negated in previous research.

Additionally, it has highlighted the need for further research into AFO design to support clinical practice. For short-term clinical impact, the focus should be on developing guidelines for selecting appropriate AFO thickness, depending on the characteristics of the individual. However, in the longer term, reinforcements offer the most viable option to optimise AFO design to meet functional and user requirements. Therefore, continued effort in evaluating the performance of current designs, and developing novel solutions is required. This work should adopt and enhance the framework established in this thesis, to ensure the findings can be translated back to clinical practice.

8.5 Clinical Implications

Polypropylene thickness and trim line position were the biggest contributors to AFO stiffness. Therefore trim lines should be as anterior to the malleoli as possible whilst still allowing donning. Furthermore, careful consideration of the thickness is needed, with results questioning the use of 3mm polypropylene for children aged >10 years and suggesting >4.5mm polypropylene should be considered for ages >15 years, which may challenge current practice. Additionally, PPH should be preferred to PPC as it has greater rigidity and may allow for a thinner device. However, the failure of PPH was not considered. Meanwhile, posterior to the malleoli ribbing is ineffective, and instead should be placed anterior to the malleoli as demonstrated by Chatzistergos et al.[193]. Furthermore, whilst reinforcing areas outside of the malleoli region were shown to be viable, they were less effective than optimally placed ribbing.

However, clinicians should be aware of the impact that manufacturing can have on AFO mechanical properties. Firstly, polypropylene thinning of 20% significantly reduced AFO stiffness, whilst the technician's interpretation of the trim line and ribbing position could also be detrimental. Therefore, without manufacturing standards, clinicians must ensure they are satisfied with the devices they receive. AFO thickness in the malleoli region should be checked using digital callipers, whilst visual inspections of the position of the trim line and ribbing should be conducted.

Lastly, it is important to emphasise the clinical impacts of rigid AFO design. OSKAR, uses rigid AFOs to provide support and control during weight-bearing activities and correct the GRF alignment to promote full knee and hip extension during stance[16], [17]. Therefore, rigid AFOs facilitate typical musculoskeletal development and provide motor learning opportunities, ultimately increasing an individual's activity and participation[78]. However, this depends on the stiffness of the rigid AFO and its ability to control the ankle and shank. Instead, a poorly designed, rigid AFO, exhibiting excessive flexibility, may cause harm to the individual, increasing the risk of falls and allowing muscle contractures and bony deformities to progress. Not to mention, the additional costs and delays in starting treatment incurred when manufacturing a replacement device. Therefore, the key findings from this thesis should be adopted during prescribing AFOs.

Bibliography

- [1] C. Morris, R. Bowers, K. Ross, P. Stevens, and D. Phillips, "Orthotic management of cerebral palsy: Recommendations from a consensus conference," *NeuroRehabilitation*, vol. 28, pp. 37–46, 2011. DOI: 10.3233/NRE-2011-0630.
- [2] NHS Scotland, "Use of ankle-foot orthoses following stroke," NHS Scotland, Tech. Rep., 2009, pp. 1–56.
- [3] K. Van Naarden Braun, N. Doernberg, L. Schieve, D. Christensen, A. Goodman, and M. Yeargin-Allsopp, "Birth prevalence of cerebral palsy: A population-based study," *Pediatrics*, vol. 137, no. 1, Jan. 2016. DOI: 10.1542/peds.2015-2872.
- [4] A. Kakooza-Mwesige, C. Andrews, S. Peterson, F. W. Mangen, A. C. Eliasson, and H. Forsberg, "Prevalence of cerebral palsy in Uganda: a population-based study," *The Lancet Global Health*, vol. 5, no. 12, e1275–e1282, Dec. 2017. DOI: 10.1016/S2214-109X(17)30374-1.
- [5] M. Oskoui, F. Coutinho, J. Dykeman, N. Jetté, and T. Pringsheim, *An update on the prevalence of cerebral palsy: A systematic review and meta-analysis*, Jun. 2013. DOI: 10.1111/dmcn.12080.
- [6] T. F. Winters, J. R. Gage, and R. Hicks, "Gait patterns in spastic hemiplegia in children and young adults," *Journal of Bone and Joint Surgery*, vol. 69, no. 3, pp. 437–441, 1987. DOI: 10.2106/00004623-198769030-00016.
- [7] D. H. Sutherland and J. R. Davids, "Common Gait Abnormalities of the Knee in Cerebral Palsy," *Clinical Orthopaedics and Related Research*, vol. 288, pp. 139–147, 1993.
- [8] J. Rodda and H. K. Graham, "Classification of gait patterns in spastic hemiplegia and spastic diplegia: a basis for a management algorithm," *European Journal of*

- Neurology*, vol. 8, pp. 98–108, 2001. DOI: 10.1046/J.1468-1331.2001.00042.X.
- [9] J. M. Rodda, H. K. Graham, L. Carson, M. P. Galea, and R. Wolfe, “Sagittal gait patterns on spastic diplegia,” *Research Physiotherapist J Bone Joint Surg [Br]*, vol. 86, pp. 251–259, 2004. DOI: 10.1302/0301-620X.86B2.
- [10] R. Scehenker, W. J. Coster, and S. Parush, “Neuroimpairments, activity performance, and participation in children with cerebral palsy mainstreamed in elementary schools,” *Developmental Medicine & Child Neurology*, vol. 47, no. 12, pp. 808–814, Dec. 2005. DOI: 10.1111/J.1469-8749.2005.TB01085.X.
- [11] A. Mutlu, A. Livanelioglu, and M. K. Gunel, “Reliability of Ashworth and Modified Ashworth Scales in children with spastic cerebral palsy,” *BMC Musculoskeletal Disorders*, vol. 9, no. 1, pp. 1–8, Apr. 2008. DOI: 10.1186/1471-2474-9-44/TABLES/5.
- [12] E. Beckung and G. Hagberg, “Neuroimpairments, activity limitations, and participation restrictions in children with cerebral palsy,” *Developmental Medicine & Child Neurology*, vol. 44, no. 5, pp. 309–316, 2002. DOI: 10.1111/j.1469-8749.2002.tb00816.x.
- [13] B. H. Lee, “Relationship between gross motor function and the function, activity and participation components of the international classification of functioning in children with spastic cerebral palsy,” *Journal of Physical Therapy Science*, vol. 29, no. 10, pp. 1732–1736, 2017. DOI: 10.1589/jpts.29.1732.
- [14] M. Wingstrand, G. Hägglund, and E. Rodby-Bousquet, “Ankle-foot orthoses in children with cerebral palsy: a cross sectional population based study of 2200 children,” *BMC Musculoskeletal Disorders*, vol. 15, no. 1, p. 327, Dec. 2014. DOI: 10.1186/1471-2474-15-327.
- [15] D. Pratt, D. Tollafield, G. Johnson, and C. Peacock, “Foot Orthoses,” in *Biomechanical Basis of Orthotic Management*, P. Bowker, D. Condie, D. Bader, and D. Pratt, Eds., 7th, Oxford: Butterworth-Heinemann, 1993, ch. 6, pp. 70–98, ISBN: 0750613807.

- [16] E. Owen and S. Mcsp, "From Stable Standing to Rock and Roll Walking (Part 2) Designing, Aligning and Tuning Orthoses for Standing Stepping and Gait," Tech. Rep., 2014, pp. 4–16.
- [17] E. Owen, "From Stable Standing to Rock and Roll Walking (Part 1) The Importance of Alignment , Proportion and Profiles," *APCP Journal*, vol. 5, no. 1, pp. 7–18, 2014.
- [18] P. B. Butler and A. V. Nene, "The Biomechanics of Fixed Ankle Foot Orthoses and their Potential in the Management of Cerebral Palsied Children," *Physiotherapy (United Kingdom)*, vol. 77, no. 2, pp. 81–88, 1991. DOI: 10.1016/S0031-9406(10)63580-8.
- [19] T. Cook and B. Cozzens, "The Effects Of Heel Height And Ankle-Foot-Orthosis Configuration On Weight Line Location: A Demonstration Of Principles | O&P Virtual Library," *Orthotics and Prosthetics*, vol. 30, no. 4, pp. 43–46, 1976.
- [20] P. Rosenbaum, A. Leviton, M. Goldstein, *et al.*, "Definition and classification of cerebral palsy," Tech. Rep. 3, 2007, p. 166. DOI: 10.1111/j.1469-8749.2007.00166.x.
- [21] M. Stavsky, O. Mor, S. A. Mastrolia, S. Greenbaum, N. G. Than, and O. Erez, "Cerebral Palsy—Trends in Epidemiology and Recent Development in Prenatal Mechanisms of Disease, Treatment, and Prevention," *Frontiers in Pediatrics*, vol. 0, p. 21, Feb. 2017. DOI: 10.3389/FPED.2017.00021.
- [22] D. Strauss and R. Shaville, "Life expectancy of adults with cerebral palsy," *Developmental Medicine & Child Neurology*, vol. 40, no. 6, pp. 369–375, Jun. 1998. DOI: 10.1111/J.1469-8749.1998.TB08211.X.
- [23] F. Miller, "Etiology, Epidemiology, Pathology and Diagnosis," in *Cerebral Palsy*, New York: Springer, 2005, ch. 1.2, pp. 27–50, ISBN: 0-387-20437-7.
- [24] WHO, "International Classification of Functioning, Disability and Health (ICF)," Tech. Rep., 2001.
- [25] V. Schiariti, E. Longo, A. Shoshmin, *et al.*, "Implementation of the International Classification of Functioning, Disability, and Health (ICF) Core Sets for Children and Youth with Cerebral Palsy: Global Initiatives Promoting Optimal Function-

- ing,” *International Journal of Environmental Research and Public Health*, vol. 15, no. 9, Sep. 2018. DOI: 10.3390/IJERPH15091899.
- [26] WHO, “Towards a Common Language for Functioning, Disability and Health: ICF,” Tech. Rep., 2002.
- [27] A. du Plessis, “MECHANISMS AND MANIFESTATIONS OF NEONATAL BRAIN INJURY,” in *The Identification and Treatment of Gait Problems in Cerebral Palsy*, H. Hart, Ed., 2nd, London: Mac Keith Press, 2009, ch. 2.1, pp. 67–88, ISBN: 978-1-898683-65-0.
- [28] R. Baker, P. Thomason, and J. Rodda, “Physical examination,” in *Measuring Walking: Handbook of Clinical Gait Analysis*, H. Hart, Ed., 11th, London: Mac Keith Press, 2013, ch. 8, pp. 100–119, ISBN: 978-1-908316-66-0.
- [29] J. Y. Zhou, E. Lowe, K. Cahill-Rowley, G. B. Mahtani, J. L. Young, and J. Rose, “Influence of impaired selective motor control on gait in children with cerebral palsy,” *Journal of Children’s Orthopaedics*, vol. 13, no. 1, p. 73, Feb. 2019. DOI: 10.1302/1863-2548.13.180013.
- [30] A. Shortland, N. Fry, A. McNee, and M. Gough, “Muscle structure and function in cerebral palsy,” in *The Identification and Treatment of Gait Problems in Cerebral Palsy*, H. Hart, Ed., 2nd ed., London: Mac Keith Press, 2009, ch. 2.5, pp. 130–146, ISBN: 978-1-898683-65-0.
- [31] C. Cans, “Surveillance of cerebral palsy in Europe: a collaboration of cerebral palsy surveys and registers,” *Developmental Medicine & Child Neurology*, vol. 42, no. 12, pp. 816–824, Dec. 2000. DOI: 10.1111/J.1469-8749.2000.TB00695.X.
- [32] L. Albright, “Basal ganglia injury and resulting movement disorders,” in *The Identification and Treatment of Gait Problems in Cerebral Palsy*, H. Hart, Ed., 2nd, London: Mac Keith Press, 2009, ch. 2.3, pp. 99–106, ISBN: 978-1-898683-65-0.
- [33] NICE, “Spasticity in under 19s: management Clinical guideline,” NICE, Tech. Rep., Jul. 2012.

- [34] W. Peacock, "The pathophysiology of spasticity," in *The Identification and Treatment of Gait Problems in Cerebral Palsy*, 2nd ed., Mac Keith Press, 2009, ch. 2.2, pp. 89–98. DOI: 10.1046/j.1468-1331.2002.0090s1003.x.
- [35] E. Sellier, M. J. Platt, G. L. Andersen, I. Krägeloh-Mann, J. D. L. Cruz, and C. Cans, "Decreasing prevalence in cerebral palsy: a multi-site European population-based study, 1980 to 2003," *Developmental Medicine & Child Neurology*, vol. 58, no. 1, pp. 85–92, Jan. 2016. DOI: 10.1111/DMCN.12865.
- [36] WHO, "WHO Motor Development Study: windows of achievement for six gross motor development milestones.," *Acta paediatrica*, vol. suppl 450, pp. 86–95, Apr. 2006. DOI: 10.1111/J.1651-2227.2006.TB02379.X.
- [37] O. A. Klochkova, A. L. Kurenkov, and V. M. Kenis, "Development of contractures in spastic forms of cerebral palsy: Pathogenesis and prevention," *Pediatric Traumatology, Orthopaedics and Reconstructive Surgery*, vol. 6, no. 1, pp. 58–66, Mar. 2018. DOI: 10.17816/ECOGEN6158-66-7049.
- [38] M. A. Mathewson and R. L. Lieber, "Pathophysiology of Muscle Contractures in Cerebral Palsy," *Physical medicine and rehabilitation clinics of North America*, vol. 26, no. 1, p. 57, Feb. 2015. DOI: 10.1016/J.PMR.2014.09.005.
- [39] J. Gage and M. Schwartz, "CONSEQUENCES OF BRAIN INJURY ON MUSCULOSKELETAL DEVELOPMENT," in *The Identification and Treatment of Gait Problems in Cerebral Palsy*, J. Gage, M. Schwartz, S. Koop, and T. Novacheck, Eds., 2nd ed., London: Mac Keith Press, 2009, ch. 2.4, pp. 107–129.
- [40] J. Gage and M. Schwartz, "Normal Gait," in *The Identification and Treatment of Gait Problems in Cerebral Palsy*, J. Gage, M. Schwartz, S. Koop, and T. Novacheck, Eds., 2nd, London: Mac Keith Press, 2009, ch. 1.3, pp. 31–64, ISBN: 978-1-898683-65-0.
- [41] E. Papageorgiou, A. Nieuwenhuys, I. Vandekerckhove, A. Van Campenhout, E. Ortibus, and K. Desloovere, "Systematic review on gait classifications in children with cerebral palsy: An update," *Gait & Posture*, vol. 69, pp. 209–223, Mar. 2019. DOI: 10.1016/J.GAITPOST.2019.01.038.

- [42] S. R. Simon, S. D. Deutsch, R. M. Nuzzo, *et al.*, "Genu recurvatum in spastic cerebral palsy. Report on findings by gait analysis.," *Journal of Bone and Joint Surgery - Series A*, vol. 60, no. 7, pp. 882–894, Oct. 1978. DOI: 10.2106/00004623-197860070-00002.
- [43] D. Sutherland, "The development of mature gait," *Gait & Posture*, vol. 6, no. 2, pp. 163–170, Oct. 1997. DOI: 10.1016/S0966-6362(97)00029-5.
- [44] S. Chakraborty, A. Nandy, and T. M. Kesar, "Gait deficits and dynamic stability in children and adolescents with cerebral palsy: A systematic review and meta-analysis," *Clinical Biomechanics*, vol. 71, pp. 11–23, Jan. 2020. DOI: 10.1016/J.CLINBIOMECH.2019.09.005.
- [45] M. Abel and D. Damiano, "Strategies for Increasing Walking Speed in Diplegic Cerebral... : Journal of Pediatric Orthopaedics," *Journal of Pediatric Orthopaedics*, vol. 16, no. 6, pp. 753–758, 1996.
- [46] C. J. Kim and S. M. Son, "Comparison of Spatiotemporal Gait Parameters between Children with Normal Development and Children with Diplegic Cerebral Palsy," *Journal of Physical Therapy Science*, vol. 26, no. 9, p. 1317, Sep. 2014. DOI: 10.1589/JPTS.26.1317.
- [47] D. H. Kim, D. H. An, and W. G. Yoo, "Validity and reliability of ankle dorsiflexion measures in children with cerebral palsy," *Journal of back and musculoskeletal rehabilitation*, vol. 31, no. 3, pp. 465–468, 2018. DOI: 10.3233/BMR-170862.
- [48] X. Wang and Y. Wang, "Gait analysis of children with spastic hemiplegic cerebral palsy," *Neural Regeneration Research*, vol. 7, no. 20, p. 1578, Jul. 2012. DOI: 10.3969/J.ISSN.1673-5374.2012.20.008.
- [49] M. Galli, V. Cimolin, C. Rigoldi, N. Tenore, and G. Albertini, "Gait patterns in hemiplegic children with Cerebral Palsy: Comparison of right and left hemiplegia," *Research in Developmental Disabilities*, vol. 31, no. 6, pp. 1340–1345, Nov. 2010. DOI: 10.1016/J.RIDD.2010.07.007.
- [50] S. M. Brændvik, T. Gøihl, R. S. Braaten, and B. Vereijken, "The Effect of Increased Gait Speed on Asymmetry and Variability in Children With Cerebral Palsy," *Frontiers in Neurology*, vol. 10, p. 1399, Jan. 2019. DOI: 10.3389/FNEUR.2019.01399.

- [51] L. A. Prosser, R. T. Lauer, A. F. VanSant, M. F. Barbe, and S. C. Lee, "Variability and symmetry of gait in early walkers with and without bilateral cerebral palsy," *Gait & posture*, vol. 31, no. 4, p. 522, Apr. 2010. DOI: 10.1016/J.GAITPOST.2010.03.001.
- [52] S. M. Bruijn, M. Millard, L. van Gestel, P. Meyns, I. Jonkers, and K. Desloovere, "Gait stability in children with cerebral palsy," *Research in developmental disabilities*, vol. 34, no. 5, p. 1689, May 2013. DOI: 10.1016/J.RIDD.2013.02.011.
- [53] J. B. Tracy, D. A. Petersen, J. Pigman, *et al.*, "Dynamic stability during walking in children with and without cerebral palsy," *Gait & posture*, vol. 72, p. 182, Jul. 2019. DOI: 10.1016/J.GAITPOST.2019.06.008.
- [54] S. Wist, L. Carcreff, S. M. Bruijn, *et al.*, "Gait stability in ambulant children with cerebral palsy during dual tasks," *PLOS ONE*, vol. 17, no. 6, e0270145, Jun. 2022. DOI: 10.1371/JOURNAL.PONE.0270145.
- [55] K. Sharifmoradi, M. Kamali, and A. Tahmasebi, "Dynamic Balance During Gait in Children With Spastic Diplegic Cerebral Palsy Versus Normal Children," *Physical Treatments - Specific Physical Therapy Journal*, vol. 8, no. 1, pp. 9–16, Apr. 2018. DOI: 10.32598/PTJ.8.1.9.
- [56] R. Rethwilm, H. Böhm, M. Haase, D. Perchthaler, C. U. Dussa, and P. Federolf, "Dynamic stability in cerebral palsy during walking and running: Predictors and regulation strategies," *Gait & Posture*, vol. 84, pp. 329–334, Feb. 2021. DOI: 10.1016/J.GAITPOST.2020.12.031.
- [57] M. J. Kurz, D. J. Arpin, and B. Corr, "Differences in the dynamic gait stability of children with cerebral palsy and typically developing children," *Gait & Posture*, vol. 36, no. 3, pp. 600–604, Jul. 2012. DOI: 10.1016/J.GAITPOST.2012.05.029.
- [58] R. Palisano, P. Rosenbaum, S. Walter, D. Russell, E. Wood, and B. Galuppi, "Development and reliability of a System , Function in Children With Cerebral Palsy," *Developmental medicine and child neurology*, vol. 39, no. 4, pp. 214–223, 1997.

- [59] R. J. Palisano, P. Rosenbaum, D. Bartlett, and M. H. Livingston, "Content validity of the expanded and revised Gross Motor Function Classification System," *Developmental Medicine and Child Neurology*, vol. 50, no. 10, pp. 744–750, 2008. DOI: 10.1111/J.1469-8749.2008.03089.X.
- [60] P. Rosenbaum, S. Walter, S. Hanna, *et al.*, "Prognosis for gross motor function in cerebral palsy: creation of motor development curves," *JAMA*, vol. 288, no. 11, pp. 1357–1363, Sep. 2002. DOI: 10.1001/JAMA.288.11.1357.
- [61] L. K. Brunton, E. G. Condliffe, G. Kuntze, *et al.*, "More Than Just Adolescence: Differences in Fatigue Between Youth With Cerebral Palsy and Typically Developing Peers," *Annals of Rehabilitation Medicine*, vol. 45, no. 3, p. 197, 2021. DOI: 10.5535/ARM.20250.
- [62] L. K. Brunton, "Descriptive Report of the Impact of Fatigue and Current Management Strategies in Cerebral Palsy," *Pediatric Physical Therapy*, vol. 30, no. 2, pp. 135–141, 2018. DOI: 10.1097/PEP.0000000000000490.
- [63] D. Ghatamaneni, S. Kohli, S. Peters, J. MacDermid, and L. Brunton, "Prevalence of fatigue in adolescents and adults with cerebral palsy: a systematic review and meta-analysis," *Fatigue: Biomedicine, Health and Behavior*, vol. 11, no. 2-4, pp. 157–175, 2023. DOI: 10.1080/21641846.2023.2245585.
- [64] M. Nardon, F. Ruzzante, L. O'Donnell, A. Adami, S. Dayanidhi, and M. Bertucco, "Energetics of walking in individuals with cerebral palsy and typical development, across severity and age: A systematic review and meta-analysis," *Gait & Posture*, vol. 90, pp. 388–407, Oct. 2021. DOI: 10.1016/J.GAITPOST.2021.09.190.
- [65] L. Wiart, J. Darrah, and G. Kembhavi, "Stretching with children with cerebral palsy: What do we know and where are we going?" *Pediatric Physical Therapy*, vol. 20, no. 2, pp. 173–178, Jun. 2008. DOI: 10.1097/PEP.0B013E3181728A8C.
- [66] S. P. Das and G. S. Ganesh, "Evidence-based Approach to Physical Therapy in Cerebral Palsy," *Indian Journal of Orthopaedics*, vol. 53, no. 1, p. 20, Jan. 2019. DOI: 10.4103/ORTHO.IJORTHO{_}241{_}17.
- [67] J. R. Fox and W. Lovegreen, "Lower Limb Orthoses," in *Atlas of Orthoses and Assistive Devices*, Fifth Edit, Elsevier Inc., 2019, ch. 22, pp. 239–246. DOI: 10.1016/b978-0-323-48323-0.00022-6.

- [68] E. Owen, "When to use lower limb orthoses in cerebral palsy," *Paediatrics and Child Health (United Kingdom)*, vol. 30, no. 8, pp. 275–282, 2020. DOI: 10.1016/j.paed.2020.05.001.
- [69] T. F. Novacheck, G. Kroll, and A. Rasmussen, "Orthoses for Cerebral Palsy," in *Atlas of Orthoses and Assistive Devices*, J. Webster and M. Douglas, Eds., 5th ed., Philadelphia: Elsevier, Jan. 2019, ch. 33, pp. 337–349, ISBN: 978-0-323-48323-0.
- [70] J. C. Maas, A. J. Dallmeijer, P. A. Huijting, *et al.*, "A randomized controlled trial studying efficacy and tolerance of a knee-ankle-foot orthosis used to prevent equinus in children with spastic cerebral palsy," <http://dx.doi.org/10.1177/0269215514542355>, vol. 28, no. 10, pp. 1025–1038, Jul. 2014. DOI: 10.1177/0269215514542355.
- [71] J. Stockman, G. Eggertsdóttir, M. S. Gaston, *et al.*, "Ankle-foot orthoses among children with cerebral palsy: a cross-sectional population-based register study of 8,928 children living in Northern Europe," *BMC Musculoskeletal Disorders*, vol. 24, no. 1, pp. 1–7, 2023. DOI: 10.1186/s12891-023-06554-z.
- [72] I. Multani, J. Manji, T. Hastings-Ison, A. Khot, and K. Graham, *Botulinum Toxin in the Management of Children with Cerebral Palsy*, Aug. 2019. DOI: 10.1007/s40272-019-00344-8.
- [73] P. Ertzgaard, C. Campo, and A. Calabrese, "Efficacy and safety of oral baclofen in the management of spasticity: A rationale for intrathecal baclofen," *Journal of Rehabilitation Medicine*, vol. 49, no. 3, pp. 193–203, Mar. 2017. DOI: 10.2340/16501977-2211.
- [74] S. R. Ward, V. B. Minamoto, K. P. Suzuki, J. B. Hulst, S. N. Bremner, and R. L. Lieber, "Recovery of Rat Muscle Size but Not Function More Than One-Year after a Single Botulinum Toxin Injection," *Muscle & nerve*, vol. 57, no. 3, p. 435, Mar. 2018. DOI: 10.1002/MUS.25707.
- [75] J. Valentine, K. Stannage, V. Fabian, *et al.*, "Muscle histopathology in children with spastic cerebral palsy receiving botulinum toxin type A," *Muscle & Nerve*, vol. 53, no. 3, pp. 407–414, Mar. 2016. DOI: 10.1002/MUS.24763.

- [76] G. Molenaers and K. Desloovere, "Pharmacologic Treatment with Botulinum Toxin," *The Identification & Treatment of gait problems in cerebral palsy*, pp. 363–80, 2009.
- [77] T. Novacheck, "Orthopaedic treatment of muscle contractures," in *The Identification and Treatment of Gait Problems in Cerebral Palsy*, H. Hart, Ed., 2nd, London: Mac Keith Pres, 2009, ch. 5.5, pp. 445–472, ISBN: 978-1-898683-65-0.
- [78] E. Owen, M. Rahlin, and K. J. Kane, "Content Validity of a Collaborative Goal-Setting Pictorial Tool for Children Who Wear Ankle-Foot Orthoses: A Modified Delphi Consensus Study," *JPO Journal of Prosthetics and Orthotics*, vol. 36, no. 2, pp. 89–98, Apr. 2024. DOI: 10.1097/JPO.0000000000000462.
- [79] ISO, "ISO 8549-3-2020: Prosthetic and Orthotic Vocabulary: Part 3 Terms Relating to Orthoses," Geneva, Tech. Rep., 2020.
- [80] G. F. Kogler, M. Bridges, J. E. Hilliard, and K. K. Chui, "Materials and technology," in *Orthotics and Prosthetics in Rehabilitation*, Elsevier, Jan. 2019, pp. 144–163, ISBN: 9780323609135. DOI: 10.1016/B978-0-323-60913-5.00006-4.
- [81] N. Eddison, A. Healy, D. Buchanan, and N. Chockalingam, "Standardised classification system for bespoke thermoplastic ankle foot orthoses," *Foot*, vol. 53, no. March, p. 101924, 2022. DOI: 10.1016/j.foot.2022.101924.
- [82] E. Owen and K. Bjornson, "Fact Sheet: Ankle-Foot Orthoses and Footwear for Children with Cerebral Palsy - Selecting Optimal Designs," Tech. Rep., 2020, pp. 1–10.
- [83] L. Everaert, E. Papageorgiou, A. Van Campenhout, L. Labey, and K. Desloovere, "The influence of ankle-foot orthoses on gait pathology in children with cerebral palsy: A retrospective study," *Gait & Posture*, vol. 100, pp. 149–156, Feb. 2023. DOI: 10.1016/J.GAITPOST.2022.11.063.
- [84] T. Goihl, D. F. Rusaw, K. Roeleveld, and S. M. Brændvik, "Provision of ankle foot orthoses for children with cerebral palsy in Norway," *Journal of Rehabilitation and Assistive Technologies Engineering*, vol. 11, Jan. 2024. DOI: 10.1177/20556683241276804.

- [85] B. Meadows, R. Bowers, and E. Owen, "Biomechanics of the Hip, Knee, and Ankle," in *Atlas of Orthoses and Assistive Devices*, J. Webster and M. Douglas, Eds., vol. 5, Philadelphia: Elsevier, Jan. 2019, ch. 18, pp. 207–215, ISBN: 978-0-323-48323-0.
- [86] S. A. Rethlefsen and R. M. Kay, "Transverse plane gait problems in children with cerebral palsy," *Journal of Pediatric Orthopaedics*, vol. 33, no. 4, pp. 422–430, 2013. DOI: 10.1097/BPO.0b013e3182784e16.
- [87] J. B. Webster and B. J. Darter, "Principles of Normal and Pathologic Gait," *Atlas of Orthoses and Assistive Devices*, pp. 49–62, Jan. 2019. DOI: 10.1016/B978-0-323-48323-0.00004-4.
- [88] J. Perry and J. Burnfield, "Fundamentals," in *Gait Analysis: Normal and Pathological Function*, 2nd ed., Slack Incorporated, 2010, ch. 1, pp. 1–49, ISBN: 978-1-55642-766-4.
- [89] E. Owen, "How should we define the rockers of gait and are there three or four?" *Gait & Posture*, vol. 30, no. 1974, S49, 2009. DOI: 10.1016/j.gaitpost.2009.08.074.
- [90] T. Theologis, *Lever arm dysfunction in cerebral palsy gait*, Nov. 2013. DOI: 10.1007/s11832-013-0510-y.
- [91] P. B. Butler, N. Thompson, and R. E. Major, "Improvement in Walking Performance of Children With Cerebral Palsy: Preliminary Results," *Developmental Medicine & Child Neurology*, vol. 34, no. 7, pp. 567–576, 1992. DOI: 10.1111/j.1469-8749.1992.tb11487.x.
- [92] D. J. Bregman, A. Rozumalski, D. Koops, V. de Groot, M. Schwartz, and J. Harlaar, "A new method for evaluating ankle foot orthosis characteristics: BRUCE," *Gait & Posture*, vol. 30, no. 2, pp. 144–149, Aug. 2009. DOI: 10.1016/J.GAITPOST.2009.05.012.
- [93] S. Ounpuu, J. R. Gage, and R. B. Davis, "Three-dimensional lower extremity joint kinetics in normal pediatric gait," *Journal of Pediatric Orthopaedics*, vol. 11, no. 3, pp. 341–349, 1991. DOI: 10.1097/01241398-199105000-00012.

- [94] T. Ellexson, C. Nawrockli, and D. Schober, "Normal Kinetic Patterns of the Lower Extremities During Natural Walking in Children Aged Six to Ten," Ph.D. dissertation, Grand Valley State, 1995.
- [95] T. Cupp, D. Oeffinger, C. Tylkowski, and S. Augsburger, "Age-Related Kinetic Changes in Normal Pediatrics : Journal of Pediatric Orthopaedics," *Journal of Pediatric Orthopaedics*, vol. 19, no. 4, pp. 475–478, 1999.
- [96] B. Stansfield, S. Hillman, E. Hazlewood, *et al.*, "Sagittal Joint Kinematics, Moments, and Powers Are Predominantly Characterized by Speed of Progression, Not Age, in Normal Children," *Journal of Pediatric Orthopaedics*, vol. 21, no. 3, pp. 403–411, 2001.
- [97] M. Van der Linden, A. Kerr, E. Hazlewood, S. Hillman, and J. Robb, "Kinematic and Kinetic Gait Characteristics of Normal Children Walking at a Range of Clinically Relevant Speeds," *Journal of Pediatric Orthopaedics*, vol. 22, no. 6, pp. 800–806, 2002.
- [98] V. L. Chester, M. Tingley, and E. N. Biden, "A comparison of kinetic gait parameters for 3–13 year olds," *Clinical Biomechanics*, vol. 21, no. 7, pp. 726–732, Aug. 2006. DOI: 10.1016/J.CLINBIOMECH.2006.02.007.
- [99] K. J. Ganley and C. M. Powers, "Gait kinematics and kinetics of 7-year-old children: a comparison to adults using age-specific anthropometric data," *Gait & Posture*, vol. 21, no. 2, pp. 141–145, Feb. 2005. DOI: 10.1016/J.GAITPOST.2004.01.007.
- [100] D. J. Oeffinger, S. Augsburger, and T. Cupp, "Pediatric kinetics: Age related changes in able-bodied populations," *Gait & Posture*, vol. 5, no. 2, pp. 155–156, Apr. 1997. DOI: 10.1016/S0966-6362(97)83380-2.
- [101] W. Golay, T. Lunsford, B. Lunsford, and J. Greenfield, "The Effect of Malleolar Prominence on Polypropylene AFO Rigidity and Buckling," *Journal of Prosthetics and Orthotics*, vol. 1, no. 4, pp. 231–241, 1989.
- [102] T. Lunsford and B. Contoyannis, "Materials Science," in *Atlas of Orthoses and Assistive Devices*, J. B. Webster and M. Douglas, Eds., 5th ed., Philadelphia: Elsevier, 2019, ch. 2, pp. 7–41.

- [103] C. Ibeh, "Polypropylene," in *Thermoplastic materials: Properties, Manufacturing Methods and Applications*, 1, Taylor & Francis, 2011, ch. 10, pp. 193–260, ISBN: 9781420093841.
- [104] E. Owen, *The importance of being earnest about shank and thigh kinematics especially when using ankle-foot orthoses*, Sep. 2010. DOI: 10.3109/03093646.2010.485597.
- [105] E. Owen, "A PROPOSED CLINICAL ALGORITHM FOR DORSIFLEXION FREE AFOFCS BASED ON CALF MUSCLE LENGTH, STRENGTH, STIFFNESS AND SKELETAL ALIGNMENT," in *American Academy of Orthotist and Prosthetists*, 2015.
- [106] Owen E, "PROPOSED CLINICAL ALGORITHM FOR DECIDING THE SAGITTAL ANGLE OF THE ANKLE IN AN ANKLE-FOOT ORTHOSIS FOOTWEAR COMBINATION," *Gait & Posture*, S38–S39, 2005.
- [107] E. Owen, R. Bowers, and B. C. Meadows, "TUNING OF AFO FOOTWEAR COMBINATIONS FOR NEUROLOGICAL DISORDERS TUNING OF AFO FOOTWEAR COMBINATIONS FOR NEUROLOGICAL DISORDERS," in *International Society for Prosthetics and Orthotics (ISPO) 11th World Congress, Hong Kong, 2004*, pp. 278–279.
- [108] N. Eddison and N. Chockalingam, *The effect of tuning ankle foot orthoses-footwear combination on the gait parameters of children with cerebral palsy*, Apr. 2013. DOI: 10.1177/0309364612450706.
- [109] V. Inman, H. Ralston, and F. Todd, *Human Walking*, 1st. Baltimore: Williams and Wilkins, 1981.
- [110] A. Karas and D. Hoy, "Compensatory Midfoot Dorsiflexion in the Individual with," *Journal of Prosthetics & Orthotics*, vol. 14, no. 2, pp. 82–93, 2002.
- [111] M. A. Johanson, A. Dearment, K. Hines, *et al.*, "The effect of subtalar joint position on dorsiflexion of the ankle/rearfoot versus midfoot/forefoot during gastrocnemius stretching," *Foot and Ankle International*, vol. 35, no. 1, pp. 63–70, 2014. DOI: 10.1177/1071100713513433.

- [112] A. H. Hansen and D. S. Childress, "Effects of shoe heel height on biologic rollover characteristics during walking," *Journal of Rehabilitation and Development*, vol. 41, no. 4, pp. 547–554, 2004.
- [113] E. Owen, S. Fatone, and A. Hansen, "Effect of walking in footwear with varying heel sole differentials on shank and foot segment kinematics:" *Prosthetics & Orthotics International*, vol. 42, no. 4, pp. 394–401, Sep. 2017. DOI: 10.1177/0309364617728119.
- [114] E. Owen, D. Williams, S. Walmsley, and Courtney, "Counterintuitive but true: Plantarflexion alignments in walking AFOs can increase calf muscle length," *Journal of American Academy of Orthotists & Prosthetists*, vol. 32, no. 2, pp. 25–29, 2020.
- [115] K. Kane and K. Musselman, "Effects of solid ankle-foot orthoses with individualised ankle angles on gait for children with cerebral palsy and equinus," *Journal of Pediatric Rehabilitation Medicine*, vol. 13, no. 2, pp. 169–183, 2020.
- [116] N. Eddison, N. Chockalingam, and S. Osborne, "Ankle foot orthosis–footwear combination tuning: An investigation into common clinical practice in the United Kingdom," *Prosthetics and Orthotics International*, vol. 39, no. 2, pp. 126–133, Feb. 2015. DOI: 10.1177/0309364613516486.
- [117] N. Eddison, M. Mulholland, and N. Chockalingam, "Do research papers provide enough information on design and material used in ankle foot orthoses for children with cerebral palsy? A systematic review," *Journal of Children's Orthopaedics*, vol. 11, no. 4, p. 263, 2017. DOI: 10.1302/1863-2548.11.160256.
- [118] N. Eddison, A. Healy, R. Needham, and N. Chockalingam, "The effect of tuning ankle foot orthoses-footwear combinations on gait kinematics of children with cerebral palsy: A case series," *Foot*, vol. 43, no. November 2019, p. 101660, 2020. DOI: 10.1016/j.foot.2019.101660.
- [119] K. C. Jagadamma, F. J. Coutts, T. H. Mercer, *et al.*, "Optimising the effects of rigid ankle foot orthoses on the gait of children with cerebral palsy (CP) – an exploratory trial," *Disability and rehabilitation. Assistive technology*, vol. 10, no. 6, pp. 445–451, Nov. 2015. DOI: 10.3109/17483107.2014.908244.

- [120] B. Carse, R. Bowers, B. C. Meadows, and P. Rowe, "The immediate effects of fitting and tuning solid ankle-foot orthoses in early stroke rehabilitation," *Prosthetics and Orthotics International*, vol. 39, no. 6, pp. 454–462, Dec. 2015. DOI: 10.1177/0309364614538090.
- [121] T. Kobayashi, M. S. Orendurff, G. Hunt, *et al.*, "The effects of alignment of an articulated ankle-foot orthosis on lower limb joint kinematics and kinetics during gait in individuals post-stroke," *Journal of Biomechanics*, vol. 83, pp. 57–64, Jan. 2019. DOI: 10.1016/j.jbiomech.2018.11.019.
- [122] T. Gibson, R. S. Jeffery, and A. M. O. Bakheit, "Comparison of three definitions of the mid-stance and mid-swing events of the gait cycle in children," *Disability and Rehabilitation*, vol. 28, no. 10, pp. 625–628, 2006. DOI: 10.1080/09638280500276448.
- [123] E. Owen, "SHANK ANGLE TO FLOOR MEASURES OF TUNED 'ANKLE-FOOT ORTHOSIS FOOTWEAR COMBINATIONS' USED WITH CHILDREN WITH CEREBRAL PALSY, SPINA BIFIDA AND OTHER CONDITIONS.," *Gait & Posture*, vol. 16, no. Supp1, S132–S133, 2002.
- [124] E. Pratt, S. Durham, and D. Ewins, "Preliminary evidence for techniques used to optimally align (tune) fixed ankle-foot orthoses in children," *Journal of Prosthetics and Orthotics*, vol. 23, no. 2, pp. 60–63, Apr. 2011. DOI: 10.1097/JPO.0b013e3182173325.
- [125] S. Hutchins, P. Bowker, N. Geary, and J. Richards, "The biomechanics and clinical efficacy of footwear adapted with rocker profiles—Evidence in the literature," *The Foot*, vol. 19, no. 3, pp. 165–170, Sep. 2009. DOI: 10.1016/J.FOOT.2009.01.001.
- [126] S. Kamis, G. Leisman, and E. Carmeli, "Detecting the presence of leg length discrepancy based on gait deviations and functional measurement of leg length during walking," *BMJ Case Reports*, vol. 2017, 2017. DOI: 10.1136/bcr-2017-219645.
- [127] M. Aiona, K. P. Do, K. Emara, R. Dorociak, and R. Pierce, "Gait patterns in children with limb length discrepancy," *Journal of pediatric orthopedics*, vol. 35, no. 3, pp. 280–284, Apr. 2015. DOI: 10.1097/BPO.0000000000000262.

- [128] M. Vitale, J. Choe, A. Sesko, *et al.*, "The effect of limb length discrepancy on health-related quality of life: is the '2 cm rule' appropriate?" *Journal of Pediatric Orthopaedics Biomechanics*, vol. 15, no. 1, pp. 1–5, Jan. 2006.
- [129] S. Khamis and E. Carmeli, "The effect of simulated leg length discrepancy on lower limb biomechanics during gait," *Gait & Posture*, vol. 61, pp. 73–80, Mar. 2018. DOI: 10.1016/J.GAITPOST.2017.12.024.
- [130] S. Fatone, S. A. Gard, and B. S. Malas, "Effect of Ankle-Foot Orthosis Alignment and Foot-Plate Length on the Gait of Adults With Poststroke Hemiplegia," *Archives of Physical Medicine and Rehabilitation*, vol. 90, no. 5, pp. 810–818, May 2009.
- [131] R. Didevara, G. Aminian, and A. Daryabor, "The Effect of Ankle Angle and Foot-plate Length of Ankle-Foot Orthoses on Spatiotemporal Parameters and Knee Joint Angle in Post-Stroke Hemiplegic Gait Razieh," *Function and Disability Journal*, vol. 2, no. 1, pp. 37–45, Mar. 2019.
- [132] A. Aboutorabi, M. Arazpour, M. Ahmadi Bani, H. Saeedi, and J. S. Head, *Efficacy of ankle foot orthoses types on walking in children with cerebral palsy: A systematic review*, Nov. 2017.
- [133] J. P. Betancourt, P. Eleeh, S. Stark, and N. B. Jain, "Impact of Ankle-Foot Orthosis on Gait Efficiency in Ambulatory Children with Cerebral Palsy: A Systematic Review and Meta-analysis," *American Journal of Physical Medicine and Rehabilitation*, vol. 98, no. 9, pp. 759–770, Sep. 2019. DOI: 10.1097/PHM.0000000000001185.
- [134] R. Bowers and K. Ross, "A review of the effectiveness of lower limb orthoses used in cerebral palsy," Copenhagen, Tech. Rep. September, 2009, ch. 8, pp. 235–297.
- [135] B. C. Conner, N. M. Remec, C. M. Michaels, C. W. Wallace, E. Andrisevic, and Z. F. Lerner, "Relationship between ankle function and walking ability for children and young adults with cerebral palsy: a systematic review of deficits and targeted interventions," *Gait & posture*, vol. 91, p. 165, Jan. 2022. DOI: 10.1016/J.GAITPOST.2021.10.024.

- [136] E. M. Figueiredo, G. B. Ferreira, R. C. Maia Moreira, R. N. Kirkwood, and L. Fetters, "Efficacy of ankle-foot orthoses on gait of children with cerebral palsy: Systematic review of literature," *Pediatric Physical Therapy*, vol. 20, no. 3, pp. 207–223, Sep. 2008. DOI: 10.1097/PEP.0B013E318181FB34.
- [137] J. J. Gordo, P. Pascoal-Faria, A. Mateus, P. Morouço, V. Schiriati, and S. Amado, "Biomechanical Outcomes Related with Gait in Children with Cerebral Palsy Using Ankle-Foot Orthotic-A Systematic Review," 2019. DOI: 10.4028/www.scientific.net/AMM.890.301.
- [138] M. Lintanf, J. S. Bourseul, L. Houx, M. Lempereur, S. Brochard, and C. Pons, *Effect of ankle-foot orthoses on gait, balance and gross motor function in children with cerebral palsy: a systematic review and meta-analysis*, Sep. 2018. DOI: 10.1177/0269215518771824.
- [139] C. Morris and D. Bartlett, "Gross Motor Function Classification System: impact and utility," *Developmental Medicine & Child Neurology*, vol. 46, no. 1, pp. 60–65, Feb. 2007. DOI: 10.1111/J.1469-8749.2004.TB00436.X.
- [140] H. P. Neto, L. A. C. Grecco, M. Galli, and C. S. Oliveira, "Comparison of articulated and rigid ankle-foot orthoses in children with cerebral palsy: A systematic review," *Pediatric Physical Therapy*, vol. 24, no. 4, pp. 308–312, 2012. DOI: 10.1097/PEP.0B013E318268A4FC.
- [141] D. Ricardo, M. R. Raposo, E. B. Cruz, *et al.*, "Effects of ankle foot orthoses on the gait patterns in children with spastic bilateral cerebral palsy: A scoping review," *Children*, vol. 8, no. 10, pp. 1–21, 2021. DOI: 10.3390/children8100903.
- [142] E. Pourhosseingholi, B. Farahmand, A. Bagheri, M. Kamali, and M. Saeb, "Efficacy of different techniques of AFO construction for hemiplegia patients: A systematic review," *Medical Journal of the Islamic Republic of Iran*, vol. 33, no. 1, p. 50, 2019. DOI: 10.34171/MJIRI.33.50.
- [143] P. Firouzeh, L. K. Sonnenberg, C. Morris, and L. Pritchard-Wiart, "Ankle foot orthoses for young children with cerebral palsy: a scoping review," *Disability and Rehabilitation*, vol. 43, no. 5, pp. 726–738, Feb. 2021. DOI: 10.1080/09638288.2019.1631394.

- [144] B. Ivanyi, M. Schoenmakers, N. Van Veen, K. Maathuis, F. Nollet, and M. Nederhand, "The effects of orthoses, footwear, and walking AIDS on the walking ability of children and adolescents with spina bifida: A systematic review using International Classification of Functioning, Disability and Health for Children and Youth (ICF-CY) as a ref," *Prosthetics and Orthotics International*, vol. 39, no. 6, pp. 437–443, Dec. 2015. DOI: 10.1177/0309364614543550.
- [145] R. Teplicky, M. Law, and D. Russell, "The Effectiveness of Casts, Orthoses, and Splints for Children with Neurological Disorders," *Infants & Young Children*, vol. 15, no. 1, pp. 42–50, Jul. 2002.
- [146] T. M. Esterhuizen and L. Thabane, "Con: Meta-analysis: some key limitations and potential solutions," *Nephrol Dial Transplant*, vol. 31, pp. 882–885, 2016. DOI: 10.1093/ndt/gfw092.
- [147] E. Ridgewell, F. Dobson, T. Bach, and R. Baker, *A systematic review to determine best practice reporting guidelines for AFO interventions in studies involving children with cerebral palsy*, Jun. 2010. DOI: 10.3109/03093641003674288.
- [148] K. Kolaski, L. Romeiser Logan, K. D. Goss, and C. Butler, "Quality appraisal of systematic reviews of interventions for children with cerebral palsy reveals critically low confidence," *Developmental Medicine and Child Neurology*, pp. 1–11, 2021. DOI: 10.1111/dmcn.14949.
- [149] H. Arksey and L. O'Malley, "Scoping studies: Towards a methodological framework," *International Journal of Social Research Methodology: Theory and Practice*, vol. 8, no. 1, pp. 19–32, Feb. 2005. DOI: 10.1080/1364557032000119616.
- [150] A. C. Tricco, E. Lillie, W. Zarin, *et al.*, "PRISMA extension for scoping reviews (PRISMA-ScR): Checklist and explanation," *Annals of Internal Medicine*, vol. 169, no. 7, pp. 467–473, Oct. 2018. DOI: 10.7326/M18-0850.
- [151] D. Levac, H. Colquhoun, and K. K. O'Brien, "Scoping studies: Advancing the methodology," *Implementation Science*, vol. 5, no. 1, p. 69, Sep. 2010. DOI: 10.1186/1748-5908-5-69.
- [152] N. Eddison, N. Chockalingam, A. Healy, R. Needham, and V. Unnithan, "Exploratory Investigation into Energy Expenditure Using Tuned versus Nontuned Ankle-Foot Orthoses-Footwear Combinations in Children with Cerebral Palsy,"

- Journal of Prosthetics and Orthotics*, vol. 32, no. 1, pp. 14–23, Jan. 2020. DOI: 10.1097/JPO.0000000000000275.
- [153] P. Meyns, Y. L. Kerkum, M. A. Brehm, J. G. Becher, A. I. Buizer, and J. Harlaar, “Ankle foot orthoses in cerebral palsy: Effects of ankle stiffness on trunk kinematics, gait stability and energy cost of walking,” *European Journal of Paediatric Neurology*, vol. 26, pp. 68–74, May 2020. DOI: 10.1016/J.EJPN.2020.02.009.
- [154] A. J. Ries and M. H. Schwartz, “Ground reaction and solid ankle–foot orthoses are equivalent for the correction of crouch gait in children with cerebral palsy,” *Developmental Medicine & Child Neurology*, vol. 61, no. 2, pp. 219–225, Feb. 2019. DOI: 10.1111/DMCN.13999.
- [155] Y. L. Kerkum, A. I. Buizer, J. C. van den Noort, J. G. Becher, J. Harlaar, and M.-A. Brehm, “The Effects of Varying Ankle Foot Orthosis Stiffness on Gait in Children with Spastic Cerebral Palsy Who Walk with Excessive Knee Flexion,” *PLOS ONE*, vol. 10, no. 11, e0142878, 2015. DOI: 10.1371/journal.pone.0142878.
- [156] H. Dalvand, L. Dehghan, A. Feizi, S. A. Hosseini, and S. Amirsalari, “The impacts of hinged and solid ankle-foot orthoses on standing and walking in children with spastic diplegia,” *Iranian Journal of Child Neurology*, vol. 7, no. 4, pp. 12–19, 2013. DOI: 10.22037/ijcn.v7i4.3558.
- [157] K. Kane and J. Barden, “Comparison of ground reaction and articulated ankle-foot orthoses in a child with lumbosacral myelomeningocele and tibial torsion,” *Journal of Prosthetics and Orthotics*, vol. 22, no. 4, pp. 222–229, Oct. 2010. DOI: 10.1097/JPO.0B013E3181F919A4.
- [158] K. C. Jagadamma, F. J. Coutts, T. H. Mercer, *et al.*, “Effects of tuning of ankle foot orthoses-footwear combination using wedges on stance phase knee hyperextension in children with cerebral palsy Preliminary results,” *Disability and Rehabilitation: Assistive Technology*, vol. 4, no. 6, pp. 406–413, 2009. DOI: 10.3109/17483100903104774.
- [159] M. A. Brehm, J. Harlaar, and M. Schwartz, “Effect of ankle-foot orthoses on walking efficiency and gait in children with cerebral palsy,” *Journal of Rehabilita-*

- tion Medicine*, vol. 40, no. 7, pp. 529–534, Jul. 2008. DOI: 10.2340/16501977-0209.
- [160] S. Hayek, Y. Hemo, S. Chamis, *et al.*, “The effect of community-prescribed ankle-foot orthoses on gait parameters in children with spastic cerebral palsy,” *Journal of Children’s Orthopaedics*, vol. 1, no. 6, p. 325, 2007. DOI: 10.1007/S11832-007-0055-Z.
- [161] C. E. Buckon, S. S. Thomas, S. Jakobson-Huston, M. Moor, M. Sussman, and M. Aiona, “Comparison of three ankle—foot orthosis configurations for children with spastic diplegia,” *Developmental Medicine & Child Neurology*, vol. 46, no. 9, pp. 590–598, Sep. 2004. DOI: 10.1111/j.1469-8749.2004.tb01022.x.
- [162] H. White, J. Jenkins, W. Neace, C. Tylkowski, and J. Walker, “Clinically prescribed orthoses demonstrate an increase in velocity of gait in children with cerebral palsy: A retrospective study - ProQuest,” *Developmental Medicine and Child Neurology*, vol. 44, no. 4, pp. 227–232, Apr. 2002.
- [163] C. E. Buckon, S. S. Thomas, S. Jakobson-Huston, M. M. CPO, M. Sussman, and M. Aiona, “Comparison of three ankle-foot orthosis configurations for children with spastic hemiplegia,” *Developmental Medicine & Child Neurology*, vol. 43, no. 6, pp. 371–378, Jun. 2001. DOI: 10.1111/J.1469-8749.2001.TB00224.X.
- [164] C. M. Duffy, M. Graham, A. P. Cosgrove, H. K. Graham, and A. P. Cosgrove, “The Influence of Ankle-Foot Orthoses on Gait and Energy Expenditure in Spina Bifida,” *Journal of Pediatric Orthopaedics*, vol. 20, no. 3, pp. 356–361, May 2000. DOI: 10.1097/01241398-200005000-00016.
- [165] M. Galli, M. Crivellini, E. Fazzi, and F. Motta, “Energy Consumption and Gait Analysis in Children with Myelomeningocele,” *Functional Neurology*, vol. 15, no. 3, pp. 171–175, 2000.
- [166] D. Freeman, M. Orendurff, and M. Moor, “Case study: improving knee extension with floor-reaction ankle-foot orthoses in a patient with myelomeningocele and 20 degree knee flexion contractures.,” *Journal of Prosthetics & Orthotics*, vol. 11, no. 3, pp. 63–68, 1999.

- [167] S. Rethlefsen, K. Robert, S. Dennis, M. Forstein, and V. Tolo, "The Effects of Fixed and Articulated Ankle-Foot Orthoses on Gait Patterns in Subjects with Cerebral Palsy," *Journal of Pediatric Orthopaedics*, vol. 19, no. 4, pp. 470–474, Jul. 1999.
- [168] J. Thomson, S. Ounpuu, R. Davis, and P. DeLuca, "The Effects of Ankle-Foot Orthoses on the Ankle and Knee in Persons with Myelomeningocele: An Evaluation Using Three-Dimensional Gait Analysis.," *Journal of pediatric orthopaedics*, vol. 19, no. 1, pp. 27–33, Jan. 1999.
- [169] M. F. Abel, G. A. Juhl, C. L. Vaughan, and D. L. Damiano, "Gait Assessment of Fixed Ankle-Foot Orthoses in Children With Spastic Diplegia," *Archives of Physical Medicine and Rehabilitation*, vol. 79, pp. 126–133, 1998.
- [170] R. Brunner, G. Meier, and T. Ruepp, "Comparison of a Stiff and a Spring-Type Ankle-Foot Orthosis to Improve Gait in Spastic Hemiplegic Children," *Journal of Pediatric Orthopaedics*, vol. 18, no. 6, pp. 719–726, 1998.
- [171] S. A. Radtka, S. R. Skinner, D. M. Dixon, and M. E. Johanson, "A comparison of gait with solid, dynamic, and no ankle-foot orthoses," *Physical Therapy*, vol. 77, no. 4, p. 395, 1997.
- [172] E. A. Middleton, G. R. B. Hurley, and J. S. McIlwain, "The role of rigid and hinged polypropylene ankle-foot-orthoses in the management of cerebral palsy: a case study," *Prosthetics & Orthotics International*, vol. 12, no. 3, pp. 129–135, Jun. 1988. DOI: 10.3109/03093648809079396.
- [173] D. Totah, M. Menon, C. Jones-Hershinow, K. Barton, and D. H. Gates, *The impact of ankle-foot orthosis stiffness on gait: A systematic literature review*, Mar. 2019. DOI: 10.1016/j.gaitpost.2019.01.020.
- [174] D. Bregman, M. v. d. Krogt, V. d. Groot, J. Harlaar, M. Wisse, and S. Collins, "The effect of ankle foot orthosis stiffness on the energy cost of walking: A simulation study," *Clinical Biomechanics*, vol. 26, no. 9, pp. 955–961, Nov. 2011. DOI: 10.1016/J.CLINBIOMECH.2011.05.007.
- [175] H. E. Ploeger, N. F. Waterval, F. Nollet, S. A. Bus, and M. A. Brehm, "Stiffness modification of two ankle-foot orthosis types to optimize gait in individuals with non-spastic calf muscle weakness-A proof-of-concept study," *Journal of Foot and*

- Ankle Research*, vol. 12, no. 1, pp. 1–12, Aug. 2019. DOI: 10.1186/S13047-019-0348-8/TABLES/4.
- [176] E. Vasiliauskaite, A. Ielapi, M. D. Beule, *et al.*, “A study on the efficacy of AFO stiffness prescriptions,” <https://doi.org/10.1080/17483107.2019.1629114>, vol. 16, no. 1, pp. 27–39, 2019. DOI: 10.1080/17483107.2019.1629114.
- [177] Y. Bahar-Özdemir, C. Ünal-Ulutatar, D. Karali-Bingül, and E. Karadag-Saygi, “Efficacy of foot-ankle orthosis on balance for children with hemiplegic cerebral palsy: An observational study,” *Turkish Journal of Physical Medicine and Rehabilitation*, vol. 67, no. 3, p. 336, 2021. DOI: 10.5606/TFTRD.2021.5175.
- [178] D. A. Sanad, “Moderate effect of ankle foot orthosis versus ground reaction ankle foot orthosis on balance in children with diplegic cerebral palsy,” *Prosthetics and Orthotics International*, vol. 46, no. 1, pp. 2–6, Feb. 2022. DOI: 10.1097/PXR.000000000000060.
- [179] N. Rao and A. S. Aruin, “Role of ankle foot orthoses in functional stability of individuals with stroke,” *Disability and Rehabilitation: Assistive Technology*, vol. 11, no. 7, pp. 595–598, Oct. 2016. DOI: 10.3109/17483107.2015.1027300.
- [180] J. Laidler, “The Impact of Ankle-foot Orthoses on Balance in Older Adults: a Scoping Review,” *Canadian Prosthetics & Orthotics Journal*, vol. 4, no. 1, Jan. 2021. DOI: 10.33137/CP0J.V4I1.35132.
- [181] E. Dursun, N. Dursun, and D. Alican, “Ankle-foot orthoses: effect on gait in children with cerebral palsy,” *Disability and Rehabilitation*, vol. 24, no. 7, pp. 345–347, May 2002. DOI: 10.1080/0963820110090724.
- [182] M. Nevisipour and C. F. Honeycutt, “The impact of ankle-foot-orthosis (AFO) use on the compensatory stepping response required to avoid a fall during trip-like perturbations in young adults: Implications for AFO prescription and design,” *Journal of biomechanics*, vol. 103, p. 109703, Apr. 2020. DOI: 10.1016/J.JBIOMECH.2020.109703.
- [183] D. L. DAMIANO, “Meaningfulness of mean group results for determining the optimal motor rehabilitation program for an individual child with cerebral palsy,” *Developmental medicine and child neurology*, vol. 56, no. 12, p. 1141, Dec. 2014. DOI: 10.1111/DMCN.12505.

- [184] P. B. Butler, S. E. Farmer, C. Stewart, P. W. Jones, and M. Forward, "The effect of fixed ankle foot orthoses in children with cerebral palsy," *Disability and Rehabilitation*, vol. 2, no. 1, pp. 51–58, 2009. DOI: 10.1080/17483100600662009.
- [185] K. C. Jagadamma, E. Owen, F. J. Coutts, *et al.*, "The effects of tuning an Ankle-Foot Orthosis Footwear Combination on kinematics and kinetics of the knee joint of an adult with hemiplegia," *Prosthetics and Orthotics International*, vol. 34, no. 3, pp. 270–276, Sep. 2010. DOI: 10.3109/03093646.2010.503225.
- [186] B. T. Nguyen, N. A. Baicoianu, D. B. Howell, K. M. Peters, and K. M. Steele, "Accuracy and repeatability of smartphone sensors for measuring shank-to-vertical angle," *Prosthetics and Orthotics International*, vol. 44, no. 3, pp. 172–179, Jun. 2020. DOI: 10.1177/0309364620911314.
- [187] L. M. Oudenhoven, Y. L. Kerkum, A. I. Buizer, and M. M. van der Krogt, "How does a systematic tuning protocol for ankle foot orthosis–footwear combinations affect gait in children in cerebral palsy?" *Disability and Rehabilitation*, 2021. DOI: 10.1080/09638288.2021.1970829/SUPPL{_}FILE/IDRE{_}A{_}1970829{_}SM8705.DOCX.
- [188] Y. L. Kerkum, H. Houdijk, M. A. Brehm, *et al.*, "The Shank-to-Vertical-Angle as a parameter to evaluate tuning of Ankle-Foot Orthoses," *Gait and Posture*, vol. 42, no. 3, pp. 269–274, Sep. 2015. DOI: 10.1016/j.gaitpost.2015.05.016.
- [189] N. Eddison, A. Healy, R. Needham, and N. Chockalingam, "Shank-to-Vertical Angle in Ankle-Foot Orthoses: A Comparison of Static and Dynamic Assessment in a Series of Cases," *Journal of Prosthetics and Orthotics*, vol. 29, no. 4, pp. 161–167, Oct. 2017. DOI: 10.1097/JPO.000000000000141.
- [190] N. Eddison, A. Healy, and N. Chockalingam, "Does user perception affect adherence when wearing biomechanically optimised ankle foot orthosis – footwear combinations: A pilot study," *The Foot*, vol. 43, Jun. 2020. DOI: 10.1016/J.FOOT.2019.101655.
- [191] B. Stansfield, S. Hillman, E. Hazlewood, *et al.*, "Normalized Speed, Not Age, Characterizes Ground Reaction For... : Journal of Pediatric Orthopaedics," *Journal of Pediatric Orthopaedics*, vol. 21, no. 3, pp. 395–402, 2001.

- [192] M. Nagaya, "Shoehorn-type ankle-foot orthoses: Prediction of flexibility," *Archives of Physical Medicine and Rehabilitation*, vol. 78, no. 1, pp. 82–84, Jan. 1997. DOI: 10.1016/S0003-9993(97)90015-0.
- [193] P. E. Chatzistergos, N. Eddison, E. Ganniari-Papageorgiou, and N. Chockalingam, "A quantitative analysis of optimum design for rigid ankle foot orthoses: The effect of thickness and reinforcement design on stiffness," *Prosthetics & Orthotics International*, vol. Publish Ah, pp. 1–9, 2023. DOI: 10.1097/pxr.0000000000000247.
- [194] S. Fatone, E. Owen, F. Gao, G. Shippen, M. S. Orendurff, and K. Bjornson, "Comparison of Sagittal Plane Stiffness of Nonarticulated Pediatric Ankle-Foot Orthoses Designed to be Rigid," *Journal of Prosthetics & Orthotics*, vol. 0, no. 0, 2021.
- [195] T. Go, Y. Agarie, H. Suda, Y. Maeda, J. Katsuhira, and Y. Ehara, "Effect of trim line on stiffness in dorsi- and plantarflexion of posterior leaf spring ankle-foot orthoses," *Journal of Physical Therapy Science*, vol. 34, no. 4, p. 284, 2022. DOI: 10.1589/JPTS.34.284.
- [196] W. Sumihira, T. Otani, Y. Kobayashi, and M. Tanaka, "Computational modelling of ankle-foot orthosis to evaluate spatially asymmetric structural stiffness: Importance of geometric nonlinearity," *Proceedings of the Institution of Mechanical Engineers, Part H: Journal of Engineering in Medicine*, vol. 236, no. 9, pp. 1357–1364, 2022. DOI: 10.1177/09544119221114199.
- [197] H. K. Surmen and Y. Z. Arslan, "Evaluation of various design concepts in passive ankle-foot orthoses using finite element analysis," *Engineering Science and Technology, an International Journal*, vol. 24, no. 6, pp. 1301–1307, 2021. DOI: 10.1016/j.jestch.2021.03.004.
- [198] P. R. Kubasad, V. A. Gawande, S. R. Todeti, Y. D. Kamat, and N. Vamshi, "Design and analysis of a passive ankle foot orthosis by using transient structural method," *Journal of Physics: Conference Series*, vol. 1706, no. 1, 2020. DOI: 10.1088/1742-6596/1706/1/012203.

- [199] H. K. Surmen, N. E. Akalan, M. C. Fetvacı, and Y. Z. Arslan, "A novel dorsal trimline approach for passive-dynamic ankle-foot orthoses," *Journal of Mechanical Engineering*, vol. 64, no. 3, pp. 185–194, 2018. DOI: 10.5545/SV-JME.2017.4987.
- [200] F. Gao and G. G. Bedard, "Effects of materials, reinforcement, and heat treatment on thermoplastic solid ankle-foot orthosis mechanical properties: A preliminary study," *Journal of Prosthetics and Orthotics*, vol. 25, no. 3, pp. 143–150, 2013. DOI: 10.1097/JPO.0b013e31829c163d.
- [201] J. A. Ramsey, "Development of a method for fabricating polypropylene non-articulated dorsiflexion assist ankle foot orthoses with predetermined stiffness:" *Prosthetics & Orthotics International*, vol. 35, no. 1, pp. 55–69, Jan. 2011. DOI: 10.1177/0309364610394477.
- [202] S. A. Bielby, T. J. Warrick, D. Benson, *et al.*, "Trimline severity significantly affects rotational stiffness of ankle-foot orthosis," *Journal of Prosthetics and Orthotics*, vol. 22, no. 4, pp. 204–210, 2010. DOI: 10.1097/JPO.0b013e3181f9082e.
- [203] T. F. Novacheck, C. Beattie, A. Rozumalski, G. Gent, and G. Kroll, "Quantifying the Spring-Like Properties of Ankle-Foot Orthoses (AFOs)," *JPO Journal of Prosthetics and Orthotics*, vol. 19, no. 4, pp. 98–103, Oct. 2007. DOI: 10.1097/JPO.0b013e31812e555e.
- [204] A. Polliack, C. Swanson, S. Landsberger, and D. McNeal, "Development of a Testing Apparatus for Structural Stiffness... : JPO: Journal of Prosthetics and Orthotics," *Journal of Prosthetics and Orthotics*, vol. 13, no. 3, pp. 74–82, 2001.
- [205] P. Convery, R. J. Greig, R. S. Ross, and S. Sockalingam, "A three centre study of the variability of ankle foot orthoses due to fabrication and grade of polypropylene," *Prosthetics and Orthotics International*, vol. 28, no. 2, pp. 175–182, Jun. 2004. DOI: 10.1080/03093640408726702.
- [206] R. E. Major, P. J. Hewart, and A. M. Macdonald, "A new structural concept in moulded fixed ankle foot orthoses and comparison of the bending stiffness of four constructions," *Prosthetics and Orthotics International*, vol. 28, no. 1, pp. 44–48, Jun. 2004. DOI: 10.3109/03093640409167924.

- [207] W. DeToro, "Plantarflexion Resistance of Selected Ankle-Foot Orthoses: A Pilot Study of Commonly Prescribed Prefabricated and Custom-Molded Alternatives," *Journal of Prosthetics and Orthotics*, vol. 13, no. 2, pp. 39–44, 2001.
- [208] R. Singerman, D. J. Hoy, and J. M. Mansour, "Design Changes in Ankle-Foot Orthosis Intended to Alter Stiffness Also Alter Orthosis Kinematics," *JPO Journal of Prosthetics and Orthotics*, vol. 11, no. 3, pp. 48–56, 1999. DOI: 10.1097/00008526-199907000-00003.
- [209] T. Sumiya, Y. Suzuki, and T. Kasahara, "Stiffness control in posterior-type plastic ankle-foot orthoses: Effect of ankle trimline Part 2: Orthosis characteristics and orthosis/patient matching:" *Prosthetics & Orthotics International*, vol. 20, no. 2, pp. 132–137, Jun. 1996. DOI: 10.3109/03093649609164431.
- [210] S. Yamamoto, S. Miyazaki, and T. Kubota, "Quantification of the effect of the mechanical property of ankle-foot orthoses on hemiplegic gait," *Gait & Posture*, vol. 1, no. 1, pp. 27–34, Mar. 1993. DOI: 10.1016/0966-6362(93)90040-8.
- [211] F. Gao, W. Carlton, and S. Kapp, "Development of a motorized device for quantitative investigation of articulated AFO misalignment," *2010 4th International Conference on Bioinformatics and Biomedical Engineering, iCBBE 2010*, pp. 1–4, 2010. DOI: 10.1109/ICBBE.2010.5514982.
- [212] T. M. Chu, N. P. Reddy, and J. Padovan, "Three-dimensional finite element stress analysis of the polypropylene, ankle-foot orthosis: static analysis," *Medical Engineering & Physics*, vol. 17, no. 5, pp. 372–379, Jul. 1995. DOI: 10.1016/1350-4533(95)97317-I.
- [213] T. R. Lunsford, T. Ramm, and J. A. Miller, *Viscoelastic properties of plastic pediatric afos*, 1994. DOI: 10.1097/00008526-199400610-00002.
- [214] T. Kobayashi, A. K. Leung, and S. W. Hutchins, "Techniques to measure rigidity of ankle-foot orthosis: A review," *Journal of Rehabilitation Research and Development*, vol. 48, no. 5, pp. 565–576, 2011. DOI: 10.1682/JRRD.2010.10.0193.
- [215] A. Ielapi, M. Forward, and M. D. Beule, "Computational and experimental evaluation of the mechanical properties of ankle foot orthoses: A literature review:" *Pros*, vol. 43, no. 3, pp. 339–348, Jan. 2019. DOI: 10.1177/0309364618824452.

- [216] T.-M. Chu and R. Feng, "Determination of stress distribution in various ankle-foot orthoses: Experimental stress analysis," *Journal of Prosthetics & Orthotics*, vol. 10, no. 1, pp. 11–16, 1998.
- [217] E. Papi, J. Maclean, R. J. Bowers, and S. E. Solomonidis, "Determination of loads carried by polypropylene ankle-foot orthoses: A preliminary study," *J Engineering in Medicine*, vol. 229, no. 1, pp. 40–51, 2015. DOI: 10.1177/0954411914566630.
- [218] G. Tanino, Y. Tomita, S. Mizuno, *et al.*, "Development of an ankle torque measurement device for measuring ankle torque during walking," *Journal of Physical Therapy Science*, vol. 27, no. 5, p. 1477, May 2015. DOI: 10.1589/JPTS.27.1477.
- [219] S. Miyazaki, S. Yamamoto, T. Kubota, J. Ztok, and M. Prosthetic, "Effect of ankle-foot orthosis on active ankle moment in ..patients with hemiparesis," *Medical and Biological Engineering and Computing*, vol. 35, pp. 381–385, 1997.
- [220] S. Yamamoto, M. Ebina, S. Miyazaki, H. Kawai, and T. Kubota, "Development of a New Ankle-Foot Orthosis with Dorsiflexion Assist, Part 1: Desirable Characteristics of Ankle-Foot Orthoses for Hemiplegic Patients," *Journal of Prosthetics & Orthotics*, vol. 9, no. 4, pp. 174–179, 1997. DOI: 10.1097/00008526-199700940-00009.
- [221] S. Yamamoto, M. Ebina, S. Kubo, T. Hayashi, Y. Akita, and Y. Hayakawa, "Development of an Ankle-Foot Orthosis with Dorsiflexion Assist, Part 2: Structure and Evaluation," *Jounral of Prosthetics and Orthotics*, vol. 11, no. 2, pp. 24–28, 1999.
- [222] S. Yamamoto, A. Hagiwara, T. Mizobe, O. Yokoyama, and T. Yasui, "Development of an ankle-foot orthosis with an oil damper," *Prosthetics and Orthotics International*, vol. 29, no. 3, pp. 209–219, 2005. DOI: 10.1080/03093640500199455.
- [223] Y. Kim, T. C. Bulea, and D. L. Damiano, "Children with cerebral palsy have greater stride-to-stride variability of muscle synergies during gait than typically developing children: implications for motor control complexity," *Neurorehabilitation and neural repair*, vol. 32, no. 9, p. 834, Sep. 2018. DOI: 10.1177/1545968318796333.

- [224] A. Brégou Bourgeois, B. Mariani, K. Aminian, P. Y. Zambelli, and C. J. Newman, "Spatio-temporal gait analysis in children with cerebral palsy using, foot-worn inertial sensors," *Gait & Posture*, vol. 39, no. 1, pp. 436–442, Jan. 2014. DOI: 10.1016/J.GAITPOST.2013.08.029.
- [225] L. W. Beckers, E. A. Rameckers, R. J. Smeets, *et al.*, "Barriers to recruitment of children with cerebral palsy in a trial of home-based training," *Contemporary Clinical Trials Communications*, vol. 15, p. 100371, Sep. 2019. DOI: 10.1016/J.CONCTC.2019.100371.
- [226] D. Kilicel, F. De Crescenzo, G. Pontrelli, and M. Armando, "Participant Recruitment Issues in Child and Adolescent Psychiatry Clinical Trials with a Focus on Prevention Programs: A Meta-Analytic Review of the Literature," *Journal of Clinical Medicine*, vol. 12, no. 6, p. 2307, Mar. 2023. DOI: 10.3390/JCM12062307/S1.
- [227] G. Rogati, P. Caravaggi, A. Leardini, *et al.*, "A novel apparatus to assess the mechanical properties of Ankle-Foot Orthoses: Stiffness analysis of the Codivilla spring," *Journal of Biomechanics*, vol. 142, p. 111239, Sep. 2022. DOI: 10.1016/J.JBIOMECH.2022.111239.
- [228] C. Sheehan and E. Figgins, "A comparison of mechanical properties between different percentage layups of a single-style carbon fibre ankle foot orthosis," *Prosthetics & Orthotics International*, vol. 41, no. 4, pp. 364–372, Jun. 2016. DOI: 10.1177/0309364616652015.
- [229] B. Klasson, P. Convery, and S. Raschke, "Test apparatus for the measurement of the flexibility of ankle-foot orthoses in planes other than the loaded plane," *Prosthetics and Orthotics International*, vol. 22, no. 1, pp. 45–53, 1998. DOI: 10.3109/03093649809164456.
- [230] P. Cappa, F. Patanè, and G. Di Rosa, "A continuous loading apparatus for measuring three-dimensional stiffness of ankle-foot orthoses," *Journal of Biomechanical Engineering*, vol. 127, no. 6, pp. 1025–1029, 2005. DOI: 10.1115/1.2049313.

- [231] D. Totah, M. Menon, D. H. Gates, and K. Barton, "Design and evaluation of the SMAApp: A stiffness measurement apparatus for ankle-foot orthoses," *Mechatronics*, vol. 77, p. 102572, Aug. 2021. DOI: 10.1016/J.MECHATRONICS.2021.102572.
- [232] A. Ielapi, N. Lammens, W. Van Paepegem, *et al.*, "A validated computational framework to evaluate the stiffness of 3D printed ankle foot orthoses," *Computer Methods in Biomechanics and Biomedical Engineering*, vol. 22, no. 8, pp. 880–887, 2019. DOI: 10.1080/10255842.2019.1601712.
- [233] T. Kobayashi, A. K. Leung, and S. W. Hutchins, "Design of a manual device to measure ankle joint stiffness and range of motion," *Prosthetics and Orthotics International*, vol. 35, no. 4, pp. 478–481, 2011. DOI: 10.1177/0309364611425696.
- [234] K. Z. Takahashi and S. J. Stanhope, "Estimates of stiffness for ankle-foot orthoses are sensitive to loading conditions," *Journal of Prosthetics and Orthotics*, vol. 22, no. 4, pp. 211–219, Oct. 2010. DOI: 10.1097/JP0.0B013E3181F46822.
- [235] S. I. Ringleb, T. Armstrong, L. J. Berglund, H. B. Kitaoka, and K. R. Kaufman, "Stiffness of the arizona ankle-foot orthosis before and after modification for gait analysis," *Journal of Prosthetics and Orthotics*, vol. 21, no. 4, pp. 204–207, 2009. DOI: 10.1097/JP0.0b013e3181bfb28e.
- [236] T. Sumiya, Y. Suzuki, and T. Kasahara, "Stiffness control in posterior-type plastic ankle-foot orthoses: Effect of ankle trimline. Part 1: A device for measuring ankle moment," *Prosthetics and Orthotics International*, vol. 20, no. 2, pp. 129–131, Jun. 1996. DOI: 10.3109/03093649609164430.
- [237] C. F. Hovorka, G. F. Kogler, Y.-H. Chang, and R. Gregor, "Material properties and application of biomechanical principles provide significant motion control performance in experimental ankle foot orthosis-footwear combination," *Clinical Biomechanics*, vol. 82, pp. 105–285, Feb. 2021. DOI: 10.1016/J.CLINBIOMECH.2021.105285.
- [238] T. Kobayashi, A. K. Leung, Y. Akazawa, H. Naito, M. Tanaka, and S. W. Hutchins, "Design of an automated device to measure sagittal plane stiffness

- of an articulated ankle-foot orthosis," *Prosthetics and Orthotics International*, vol. 34, no. 4, pp. 439–448, Dec. 2010. DOI: 10.3109/03093646.2010.495370.
- [239] F. Gao, W. Carlton, and S. Kapp, "Effects of joint alignment and type on mechanical properties of thermoplastic articulated ankle-foot orthosis," *Prosthetics and Orthotics International*, vol. 35, no. 2, pp. 181–189, Jun. 2011. DOI: 10.1177/0309364611409617.
- [240] P. Bowker, D. Pratt, and W. Wallace, *Biomechanical basis of orthotic management*, 7th ed., P. Bowker, D. Condie, D. Bader, and D. Pratt, Eds. Oxford: Butterworth-Heinemann, 1993, ISBN: 9780750613804.
- [241] J. Muscolino, "Joints of the Lower Extremity," in *Kinesiology, The Skeletal System and Muscular Function*, K. White, Ed., 2nd ed., St Louis: Elsevier, 2011, ch. 8, pp. 303–317, ISBN: 978-0-323-06944-1.
- [242] R. S. Ross, R. J. G. Eig, and P. Convery, "Comparison of bending stiffness of six different colours of copolymer polypropylene," *Prosthetics and Orthotics International*, vol. 23, pp. 63–71, 1999.
- [243] G. Rogati, P. Caravaggi, and A. Leardini, "Design principles, manufacturing and evaluation techniques of custom dynamic ankle-foot orthoses: a review study," *Journal of Foot and Ankle Research*, vol. 15, no. 1, pp. 1–12, 2022. DOI: 10.1186/s13047-022-00547-2.
- [244] B. F. Mentiplay, M. Banky, R. A. Clark, M. B. Kahn, and G. Williams, "Lower limb angular velocity during walking at various speeds," *Gait & Posture*, vol. 65, pp. 190–196, Sep. 2018. DOI: 10.1016/J.GAITPOST.2018.06.162.
- [245] S. Yamamoto, M. Ebina, M. Iwasaki, S. Kubo, H. Kawai, and T. Hayashi, "Comparative Study of Mechanical Characteristics of Plastic AFOs," *Journal of Prosthetics and Orthotics*, vol. 5, no. 2, pp. 47–5, Apr. 1993.
- [246] D. Totah, K. Barton, and D. H. Gates, "The effect of rotational speed on ankle-foot orthosis properties," *Journal of Biomechanics*, vol. 123, p. 110483, Jun. 2021. DOI: 10.1016/J.JBIOMECH.2021.110483.

- [247] B. R. Shuman, D. Totah, D. H. Gates, F. Gao, A. J. Ries, and E. Russell Esposito, "Comparison of five different methodologies for evaluating ankle-foot orthosis stiffness," *Journal of NeuroEngineering and Rehabilitation*, vol. 20, no. 1, pp. 1–9, Dec. 2023. DOI: 10.1186/S12984-023-01126-7/FIGURES/4.
- [248] A. Ielapi, E. Vasiliauskaite, M. Hendrickx, *et al.*, "A novel experimental setup for evaluating the stiffness of ankle foot orthoses," *BMC Research Notes*, vol. 11, no. 1, pp. 1–7, Sep. 2018. DOI: 10.1186/S13104-018-3752-4/TABLES/1.
- [249] R. Pidaparti, *Engineering Finite Element Analysis*, ISBN: 9783031795695.
- [250] R. K. Chen, L. Chen, B. L. Tai, Y. Wang, A. J. Shih, and J. Wensman, "Additive manufacturing of personalized ankle-foot orthosis," *Transactions of the North American Manufacturing Research Institution of SME*, vol. 42, no. January, pp. 381–389, 2014.
- [251] R. Uning, N. A. Abu Osman, and R. B. Abdul Rahim, "3D finite element analysis of ankle-foot orthosis on patients with unilateral foot drop: A preliminary study," *IFMBE Proceedings*, vol. 21 IFMBE, no. 1, pp. 366–369, 2008. DOI: 10.1007/978-3-540-69139-6{_}93.
- [252] D. Zou, T. He, M. Dailey, *et al.*, "Experimental and computational analysis of composite ankle-foot orthosis," *Journal of Rehabilitation Research and Development*, vol. 51, no. 10, pp. 1525–1536, 2014. DOI: 10.1682/JRRD.2014-02-0046.
- [253] M. C. Faustini, R. R. Neptune, R. H. Crawford, and S. J. Stanhope, "Manufacture of passive dynamic ankle-foot orthoses using selective laser sintering," *IEEE Transactions on Biomedical Engineering*, vol. 55, no. 2, pp. 784–790, Feb. 2008. DOI: 10.1109/TBME.2007.912638.
- [254] G. Gomes, I. Lourenco, J. Oliveira, *et al.*, "Structural reinforcements on AFO's: A study using computer-aided design and finite element method," *ENBENG 2017 - 5th Portuguese Meeting on Bioengineering, Proceedings*, Mar. 2017. DOI: 10.1109/ENBENG.2017.7889432.
- [255] M. Badescu, C. Purcar, and D. Badescu, "Ankle Foot Orthoses with Wire Insertion," *Applied Mechanics and Materials*, vol. 371, pp. 554–558, 2013. DOI: 10.4028/www.scientific.net/AMM.371.554.

- [256] S. Syngellakis, M. A. Arnold, and H. Rassoulian, "Assessment of the non-linear behaviour of plastic ankle foot orthoses by the finite element method," *Proceedings of the Institution of Mechanical Engineers, Part H: Journal of Engineering in Medicine*, vol. 214, no. 5, pp. 527–539, 2000. DOI: 10.1243/0954411001535561.
- [257] S. Syngellakis and M. A. Arnold, "Modelling considerations in finite element analyses of ankle foot orthoses," *WIT Transactions on Ecology and the Environment*, vol. 160, pp. 183–194, 2012. DOI: 10.2495/DN120171.
- [258] A. Anbuvalanraj, S. Karuppudaiyan, and S. Roy, "Effects of trimline cut in ankle foot orthosis: An experimental and finite element analysis," *Journal of Orthopaedics*, vol. 56, pp. 63–69, Oct. 2024. DOI: 10.1016/J.JOR.2024.05.004.
- [259] K. Krukoniš, K. Daunoravičienė, J. Griškevičius, and A. Kilikevičius, "Method for ankle foot orthotics' mechanical assessment: A pilot study," *Mechanika*, vol. 23, no. 5, pp. 723–727, 2017. DOI: 10.5755/j01.mech.23.5.15765.
- [260] R. Raj, A. R. Dixit, K. Łukaszewski, *et al.*, "Numerical and Experimental Mechanical Analysis of Additively Manufactured Ankle–Foot Orthoses," *Materials*, vol. 15, no. 17, 2022. DOI: 10.3390/ma15176130.
- [261] M. Bischoff, K.-U. Bletzinger, W. A. Wall, and E. Ramm, "Models and Finite Elements for Thin-Walled Structures," *Encyclopedia of Computational Mechanics*, Aug. 2004. DOI: 10.1002/0470091355.ECM026.
- [262] A. Faux-Nightingale, M. Kelemen, and C. Stewart, "Ankle-foot orthosis adherence in children and adolescents with cerebral palsy: A scoping review," *Prosthetics and Orthotics International*, vol. 46, no. 4, pp. 351–356, Aug. 2022. DOI: 10.1097/PXR.0000000000000095.
- [263] E. Swinnen and E. Kerckhofs, "Compliance of patients wearing an orthotic device or orthopedic shoes: A systematic review," *Journal of Bodywork and Movement Therapies*, vol. 19, no. 4, pp. 759–770, 2015. DOI: 10.1016/j.jbmt.2015.06.008.
- [264] M. Schwarze, L. Horoba, J. Block, *et al.*, "Wearing Time of Ankle-Foot Orthoses with Modular Shank Supply in Cerebral Palsy: A Descriptive Analysis in a Clin-

- ically Prospective Approach,” *Rehabilitation Research and Practice*, vol. 2019, 2019. DOI: 10.1155/2019/2978265.
- [265] P. Dajpratham, C. Pongakkasira, P. Terachinda, W. Phutthakumnerd, and S. Pattaraporn, “Patient Compliance and Factors Related to Usage of Plastic Ankle-Foot Orthoses by Chronic Stroke Patients,” *Journal of Rehabilitation Medicine*, vol. 32, no. 1, pp. 29–33, 2022.
- [266] S. King, R. Teplicky, G. King, and P. Rosenbaum, “Family-Centered Service for Children with Cerebral Palsy and Their Families: A Review of the Literature,” *Seminars in Pediatric Neurology*, vol. 11, no. 1, pp. 78–86, 2004. DOI: 10.1016/j.spn.2004.01.009.
- [267] N. Zaino, M. Yamagami, D. Gaebler-Spira, K. Steele, K. Bjornson, and H. Feldner, ““That’s frustrating”: Perceptions of ankle foot orthosis provision, use, and needs among people with cerebral palsy and caregivers,” *Prosthetics and Orthotics International*, vol. 00, no. 00, 2022. DOI: 10.1111/dmcn.15243.
- [268] A. W. Heinemann, A. Deutsch, S. Fatone, *et al.*, “Patient and clinician perspectives on quality-of-care topics for users of custom ankle-foot orthoses,” *American Journal of Physical Medicine and Rehabilitation*, vol. 99, no. 6, pp. 540–549, Jun. 2020. DOI: 10.1097/PHM.0000000000001373.
- [269] D. Lahoud, C. H. Teng, E. Nusem, J. Burns, C. Wrigley, and T. L. Cheng, “Content analysis of child user and carer perspectives of ankle-foot orthoses,” *Prosthetics and Orthotics International*, p. 030 936 462 095 290, Sep. 2020. DOI: 10.1177/0309364620952906.
- [270] F. Holtkamp, E. Wouters, J. Van Hoof, Y. Van Zaalen, and M. Verkerk, “Use of and Satisfaction with Ankle Foot Orthoses,” *Clinical Research on Foot & Ankle*, vol. 03, no. 01, 2015. DOI: 10.4172/2329-910x.1000167.
- [271] C. Bayón, M. v. Hoorn, A. Barrientos, E. Rocon, J. P. Trost, and E. H. Asseldonk, “Perspectives on ankle-foot technology for improving gait performance of children with Cerebral Palsy in daily-life: requirements, needs and wishes,” *Journal of NeuroEngineering and Rehabilitation*, vol. 20, no. 1, pp. 1–16, 2023. DOI: 10.1186/s12984-023-01162-3.

- [272] A. Näslund, M. Tamm, A. K. Ericsson, and L. von Wendt, "Dynamic ankle-foot orthoses as a part of treatment in children with spastic diplegia—parents' perceptions.," *Physiotherapy research international : the journal for researchers and clinicians in physical therapy*, vol. 8, no. 2, pp. 59–68, Jun. 2003. DOI: 10.1002/pri.273.
- [273] M. Ribeiro Volpini Lana, J. Pimenta Maia, A. A. Horta, S. Teixeira da Fonseca, and M. Guimarães Assis, "'What if it were like this?' Perception of mothers of children with cerebral palsy about the ankle-foot orthosis of their children: A qualitative study," *Child: Care, Health and Development*, vol. 47, no. 2, pp. 252–260, 2021. DOI: 10.1111/cch.12840.
- [274] A. W. Heinemann, S. Fatone, S. L. LaVela, *et al.*, "Orthotists' and physical therapists' perspectives on quality of care indicators for persons with custom ankle-foot orthoses," *Assistive Technology*, vol. 33, no. 4, pp. 206–216, Jul. 2021. DOI: 10.1080/10400435.2019.1610814.
- [275] K. Kane, P. Manns, J. Lanovaz, and K. Musselman, "Clinician perspectives and experiences in the prescription of ankle-foot orthoses for children with cerebral palsy," *Physiotherapy Theory and Practice*, vol. 35, no. 2, pp. 148–156, 2019. DOI: 10.1080/09593985.2018.1441346.
- [276] S. B. Kaiser, C. M. Freeman, S. B. Wingate, *et al.*, "STIGMATA AND NEGOTIATED OUTCOMES: MANAGEMENT OF APPEARANCE BY PERSONS WITH PHYSICAL DISABILITIES," 1985.
- [277] D. J. Macfarlane and J. L. Jensen, "Factors in Diabetic Footwear Compliance," *Journal of the American Podiatric Medical Association*, vol. 93, no. 6, pp. 485–491, Nov. 2003. DOI: 10.7547/87507315-93-6-485.
- [278] A. Driano, L. Staheli, and L. Staheli, "Psychosocial Development and Corrective Shoewear Use in Childhood," *Journal of Pediatric Orthopaedics*, vol. 18, no. 3, pp. 346–349, 1998.
- [279] J. M. Orlando, B. Li, B. Bodt, and M. A. Lobo, "Users' Perceptions About Lower Extremity Orthotic Devices: A Systematic Review," *Archives of Physical Medicine and Rehabilitation*, vol. 104, no. 4, pp. 645–655, Apr. 2023. DOI: 10.1016/J.APMR.2022.10.010.

- [280] B. O'Connor, C. Kerr, N. Shields, and C. Imms, "A systematic review of evidence-based assessment practices by allied health practitioners for children with cerebral palsy," *Developmental Medicine & Child Neurology*, vol. 58, no. 4, pp. 332–347, Apr. 2016. DOI: 10.1111/DMCN.12973.
- [281] B. O'Connor, C. Kerr, N. Shields, and C. Imms, "Understanding allied health practitioners' use of evidence-based assessments for children with cerebral palsy: a mixed methods study," *Disability and Rehabilitation*, vol. 41, no. 1, pp. 53–65, Jan. 2017. DOI: 10.1080/09638288.2017.1373376.
- [282] V. Knox, P. Vuoskoski, and A. Mandy, "Use of outcome measures in children with severe cerebral palsy: A survey of U.K. physiotherapists," *Physiotherapy Research International*, vol. 24, no. 4, Oct. 2019. DOI: 10.1002/pri.1786.
- [283] K. J. Kane, J. L. Lanovaz, and K. E. Musselman, "Physical Therapists' Use of Evaluation Measures to Inform the Prescription of Ankle-Foot Orthoses for Children with Cerebral Palsy," *Physical & Occupational Therapy In Pediatrics*, vol. 39, no. 3, pp. 237–253, May 2019. DOI: 10.1080/01942638.2018.1463586.
- [284] N. Eddison, M. Gandy, P. Charlton, and N. Chockalingam, "Prescription practices for rigid ankle-foot orthoses among UK orthotists," *Prosthetics and Orthotics International*, vol. 46, no. 6, pp. 566–568, 2022. DOI: 10.1097/PXR.000000000000134.
- [285] *Patient & Public — NIHR School for Primary Care Research.*
- [286] R. Snyder, "Physical characteristics of children as related to death and injury for consumer product safety design," *Applied Ergonomics*, vol. 7, no. 2, p. 112, 1976. DOI: 10.1016/0003-6870(76)90178-2.
- [287] R. G. Snyder, L. W. Schneider, C. L. Owings, H. M. Reynolds, D. Golomb, and M. Schork, "Anthropometry of Infants, Children, and Youths to Age 18," pp. 208–315, 1977.
- [288] U. Della Croce and P. Bonato, "A novel design for an instrumented stairway," *Journal of Biomechanics*, vol. 40, no. 3, pp. 702–704, Jan. 2007. DOI: 10.1016/J.JBIOMECH.2006.01.020.

- [289] D. A. Winter, R. K. Greenlaw, and D. A. Hobson, "Television-computer analysis of kinematics of human gait," *Computers and Biomedical Research*, vol. 5, no. 5, pp. 498–504, 1972. DOI: 10.1016/0010-4809(72)90056-0.
- [290] D. A. Winter, H. G. Sidwall, and D. A. Hobson, "Measurement and reduction of noise in kinematics of locomotion," *Journal of Biomechanics*, vol. 7, no. 2, pp. 157–159, 1974. DOI: 10.1016/0021-9290(74)90056-6.
- [291] T. K. Koo and M. Y. Li, "A Guideline of Selecting and Reporting Intraclass Correlation Coefficients for Reliability Research," *Journal of Chiropractic Medicine*, vol. 15, no. 2, p. 155, Jun. 2016. DOI: 10.1016/J.JCM.2016.02.012.
- [292] J. L. McGinley, R. Baker, R. Wolfe, and M. E. Morris, *The reliability of three-dimensional kinematic gait measurements: A systematic review*, Apr. 2009. DOI: 10.1016/j.gaitpost.2008.09.003.
- [293] D. R. Clark and T. R. Lunsford, "Reinforced lower-limb orthosis-design principles," *Orthotics and Prosthetics*, vol. 32, no. 2, pp. 35–45, 1978.
- [294] D. Kiernan, C. Nikolopoulou, and K. Brady, "Prevalence of overweight and obesity in Irish ambulant children with cerebral palsy," *Irish Journal of Medical Science*, vol. 190, no. 1, pp. 225–231, Feb. 2021. DOI: 10.1007/S11845-020-02294-4/TABLES/2.
- [295] K. Brady, D. Kiernan, and A. Marron, "The progression of BMI status over time in Irish ambulant children with cerebral palsy," *Irish Journal of Medical Science*, vol. 191, no. 2, pp. 793–799, Apr. 2022. DOI: 10.1007/S11845-021-02635-X/TABLES/2.
- [296] A. Tabard-Fougère, D. Rutz, A. Pouliot-Laforte, *et al.*, "Are Clinical Impairments Related to Kinematic Gait Variability in Children and Young Adults With Cerebral Palsy?" *Frontiers in Human Neuroscience*, vol. 16, Mar. 2022. DOI: 10.3389/FNHUM.2022.816088.
- [297] J. ZHU, H. ZHOU, C. WANG, L. ZHOU, S. YUAN, and W. ZHANG, "A review of topology optimization for additive manufacturing: Status and challenges," *Chinese Journal of Aeronautics*, vol. 34, no. 1, pp. 91–110, Jan. 2021. DOI: 10.1016/J.CJA.2020.09.020.

Appendix A

PPIE semi-structured interview questions

The following are the semi-structured questions used to lead discussions with the clinical advisory group.

Questions regarding the design of the rigid AFOs

1. What properties of rigid AFOs influence the stiffness of the device?
2. What materials are paediatric rigid AFOs typically manufactured from?
3. Is there any rationale for determining which material is appropriate?
4. Are there any limitations on the materials used?
5. What is the range of material thickness typically used for paediatric rigid AFOs?
6. Is there any rationale for determining the appropriate thickness?
7. Are there any limitations on the thickness of materials used?
8. Can you describe the trim line you would prescribe for a “rigid AFO”?
9. How is this trim line related to the manufacturer?
10. Are there any rationale/limitations for the design of trim lines used?
11. Can you describe any reinforcements you would use in rigid AFOs?
12. What is the rationale for using each of these reinforcement designs?
13. Are there any limitations to any of these reinforcement designs?
14. Of all the design features of rigid AFOs that have been discussed today, which has the biggest influence on AFO stiffness?

Appendix B

Test Rig ISPO World Congress 2023

Poster Presentation

Introduction & Aims

Sagittal ankle stiffness, measured in Nm° , is a key property of ankle-foot orthoses (AFOs), underpinning their ability to control ankle motion[1]. However, despite recommendations[2], AFO stiffness is rarely reported[3] limiting valid meta-analysis and the inferences into design and performance.

Bench testing is the favoured option for measuring stiffness[4,5], although there only a limited number of test rigs which have been assessed for repeatability. These vary in clinical applicability due to technological demands, cost and size[6-9].

Additionally, buckling (mediolateral widening) at the ankle, is the main mode of AFO deformation[10]. However, the significance of this behaviour is poorly understood as no rig currently measures it.

Therefore the aim was to design a test rig capable of repeatably measuring the sagittal dorsiflexion ankle stiffness of polypropylene AFOs. The rig must accommodate a range of AFO sizes and be applicable within both research and highly specialised clinical practice. Additionally, the rig should measure hysteresis and buckling at the ankle of AFOs.

Test Rig Design

The surrogate limb consists of a uniaxial hinge, acting as a simplified ankle joint, with a non-deformable steel pole and footplate replicating the shank and foot respectively.

The location of the hinge joint can be adjusted in both the horizontal and vertical direction, according to anthropometric data[11] and previous work by Bregman et al[8], to align with the ankle joint centre.

The AFO is mounted beneath the surrogate limb with full foot contact, replicating flat-foot to heel-rise, with the AFO foot axis aligned to the hinge. The proximal AFO is secured to the shank via the standard AFO strapping around a clamping ring, the size of which is interchangeable.

A manual, discrete load is applied to the shank, generating an external dorsiflexing moment about the ankle, via a pulley system and hanging weights. This is increased and decreased incrementally, to assess stiffness and hysteresis.

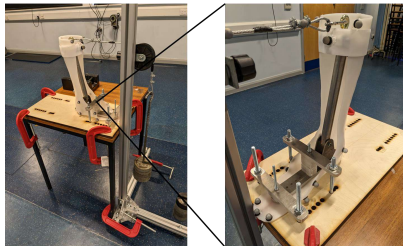


Fig 1. Test rig with enlarged insert of an AFO mounted within the surrogate limb

The rig incorporates 3-dimensional motion tracking, similar to that already utilised within specialist, 3-dimensional gait analysis clinics.

The AFO is modelled into shank and virtual foot segments via a 14 retro-reflective marker array, based on the CAST array[12], whilst the loading cable is modelled using markers placed at either end.

AFO deflection is measured as the angle between the shank and virtual foot in the sagittal plane whilst mediolateral widening at the ankle is determined from the coronal plane positional data of the malleoli markers.

Additionally, the angle between the loading cable and shank (θ in Fig 3), in the sagittal plane, is recorded to derive the moment arm at each weight increment.

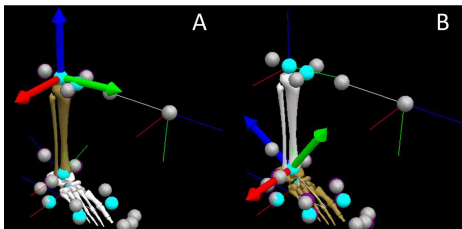


Fig 2. Visual3D image of the AFO model highlighting both the shank and foot segments

Repeatability Methodology and Data Analysis

Three polypropylene AFOs (1:Adult, 2:15 yrs) were loaded/unloaded to 14kg in 2kg increments, in 3-second intervals, generating a maximum dorsiflexion moment of approximately 40Nm° . One assessor tested each AFO 3 times across 2 sessions on the same day. Between sessions the AFO was dismantled from the rig and all markers removed.

During loading, 3-dimensional motion tracking (13 opto-electric cameras (QUALYSIS, Sweden), was used to measure the deflection of the shank and positional data of the malleoli markers. All motion tracking data was processed using Visual3Dx64 (C-Motion, US).

The dorsiflexion moment applied at the each weight increment was derived using the equation in Fig 3. A moment versus deflection scatter graph was then plotted and linear regression applied to the loading curve to determine the dorsiflexion stiffness. Hysteresis was calculated as the area between the loading and unloading curves. Integrals were calculated in excel then converted to radians so that energy was given in joules. Finally, mediolateral widening was calculated as the percentage change in malleoli width.

For dorsiflexion stiffness, hysteresis and buckling at the ankle, the within- and between-session ICCs are calculated using a two-way mixed effects model for absolute agreement using SPSSv27(IBM, US). The SEM was calculated using the equation $\text{SEM} = \sqrt{(\text{SD}_{\text{AFO1}} + \text{SD}_{\text{AFO2}} + \text{SD}_{\text{AFO3}})/N}$

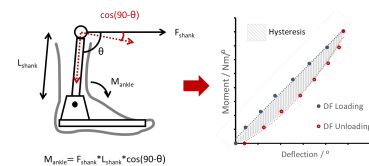


Fig 3. Diagram highlighting the derivation of the ankle moment then plotting of the moment versus deflection graph used to determine stiffness and hysteresis

Repeatability Results

Tab 1. Within- and between-session ICCs and SEM derived for ankle stiffness, hysteresis and buckling at the ankle

	Within-session		Between-session	
	ICC	SEM	ICC	SEM
Stiffness / Nm°	0.99	0.37	0.95	0.82
Hysteresis / J	0.87	2.61	0.83	3.39
Buckling / %	0.85	0.52	0.50	1.27

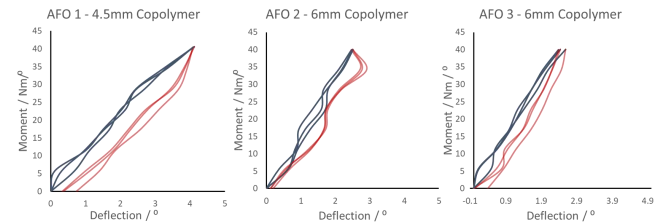


Fig 4. Session 1 moment versus deflection graphs for the 3 polypropylene AFOs

Discussion

The primary aim of developing a rig that measures AFO ankle stiffness was achieved. Within- and between-session ICCs were excellent and comparable to existing designs[6-8]. Although SEMs were higher than previously reported, the percentage error they equated to (within= $\approx 2-5\%$, between= $\approx 5-10\%$) is similar [6,9].

This is only the second paper to present repeatability data on hysteresis. The ICCs were lower than reported using an automated loading system[7], whilst the SEMs were comparable. This may highlight the limitations of manual, discrete loading which has a more variable, non-physiological loading rate.

This is the first test rig to monitor mediolateral widening at the ankle. Only moderate between-session ICCs were measured, whilst the within- and between-session SEMs represented percentage errors of $\approx 8-43\%$ and $\approx 18-103\%$ respectively. This may reflect the relative size of the measurement system error ($\approx 0.5\text{mm}$) to marker displacement (mean max displacement $\approx 2\text{mm}$), potentially highlighting the need for a more sensitive tool.

References

- 1 Totah et al, Gait and Posture, 2019
- 2 Ridgwell et al, Prosthet Orthot Int, 2010
- 3 Eddison et al, J Child Orthop, 2017
- 4 Ielapi, BMC Res Notes, 2018
- 5 Kobayashi et al, JRRD, 2011
- 6 Ielapi et al, BMC Res Notes, 2018
- 7 Totah et al, Mechatronics, 2021
- 8 Bregman et al, Gait & Posture, 2009
- 9 Novacheck et al, J Prosthet Orthot, 2007
- 10 Golay, J Prosthet Orthot, 1989
- 11 Tilley, 1993
- 12 Cappozzo, Clin Biomech, 1995

Acknowledgements

This work was supported by the UK Engineering and Physical Sciences Research Council (EPSRC) grant EP/S02249X/1 for the Centre for Doctoral Training in Prosthetics and Orthotics



Lead Author Contact Information

Sean Donald

s.donald4@edu.salford.ac.uk

University of Salford

PhD Student, P&O CDT

MEng Biomedical Engineering

Conflict of Interest

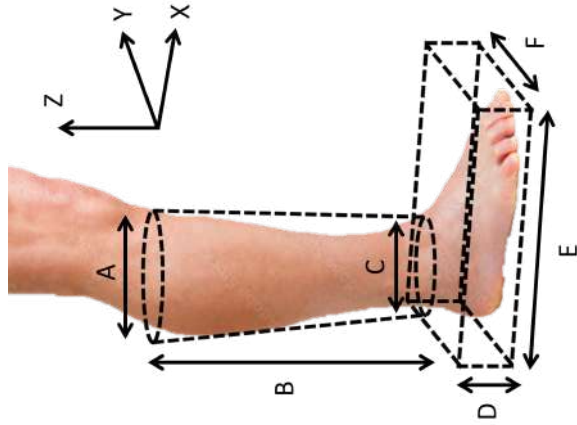
The author declares there is no conflict of interest

Appendix C

AFO Transformation Matrices

Table C.1: AFO Scaling Method based on anthropometric data from Snyder et al.[286], [287]

Anthropometric Measure	Measurement / mm				Scaling Factor		
	Adult	5yr	10yr	15yr	5yr	10yr	15yr
A	382	219	284	347	0.57	0.72	0.87
B	495	262	378	445	0.53	0.73	0.86
C	225	153	185	218	0.68	0.82	0.94
D	66	43	57	68	0.65	0.80	0.95
E	26	170	223	249	0.65	0.83	0.95
F	107	68	86	97	0.64	0.78	0.89



Appendix D

The validity of measuring AFO thickness from 3D scans

D.1 Introduction

The FE models used in this thesis predict the mechanical behaviour of AFOs modelled with a uniform thickness. During the validation process, the mechanical properties computed by these models are compared to experimental data, collected through bench testing. Therefore, the uniform thickness of the modelled AFOs should reflect the thickness of the manufactured AFOs, tested in the rig.

Previously, the thickness of the AFO inputted into FE models has been based on measurements taken in the malleoli region[193], as this is a known area of high stress, or based on measurement from several "key" locations[256], [257]. However, vacuum-formed AFOs have a non-uniform thickness due to stretching of the heated polypropylene sheet during manufacture. As a result, measurements taken in a limited number of locations may not be representative of the true variation in the manufactured AFO's thickness. This is especially true when measurements are taken using traditional devices such as digital calipers or micrometers, which restrict the locations which can be measured, to the vicinity of the trim line edge.

As a result, an alternative approach to measuring AFO thickness has been proposed. This method utilises 3-dimensional scanning technology to generate STLs of the inner and outer surface of the AFO, before measuring the distance between the vertices of the two meshes to estimate thickness. As a result, it has the potential to reduce assessor bias and allows the thickness of the entire AFO to be analysed. However, as the thickness is determined as the distance between the closest nodes on each mesh, the accuracy of the measurements may be affected by the size of the STL mesh. Therefore, the following study has been conducted with the aim of demonstrating the validity of using this novel method for measuring the thickness of AFOs.

D.2 Methodology

D.2.1 Experimental Procedure

One AFO from each age-group, manufactured for the test rig repeatability study (Section 5.2), was chosen at random for use in this study, so the influence of AFO size could be studied. The AFOs selected were the 5-year-old 3mm PPC AFO, the 10-year-old 4.5mm PPC AFO and the 15-year-old, 5mm PPH AFO.

An STL of the inner surface of each of these AFOs was generated using a 3D scanner (FreeScan UE Pro, Shinning 3D, China). These were then imported to Fusion (v2.0.20470, Autodesk, USA), where they were converted into a surface and thickened by 3mm, resulting in a solid part with known thickness, before being converted back into an STL with a uniform mesh.

To determine the effects of STL mesh element size on the accuracy of thickness measurements, the size of the elements in the STL mesh was increased, using the remesh tool and decreasing the density value by 0.1 from 1.0 to 0.1. At each mesh density, the inner and outer surfaces of the AFO were separated and saved as separate STLs. This process resulted in a total of 60 STLs, consisting of a pair of inner and outer surface STLs, for the ten mesh density conditions for each of the three AFOs.

Once the meshes had been created, a custom script in MATLAB (v2024a, MathWorks, USA) was used to determine the thickness of the three AFOs at each mesh density. The custom script converted the inner and outer surface STLs into point clouds, containing the X-Y-Z co-ordinates of the STL nodes. It then applied the "findNearestNeighbour" function to each of the points in the inner surface point cloud, returning the index and Euclidean distance between the reference node and its nearest neighbour on the outer surface point cloud, based on a kd-tree search algorithm.

D.2.2 Data Analysis

For the three AFO sizes, the mean and standard deviation AFO thickness, at the ten mesh densities, was taken across all the data points. Following this, the percentage error for each measurement tool was calculated, taking 3mm to be the actual AFO thickness. Finally, graphs comparing the change in AFO thickness and percentage error with increasing element size were created.

D.3 Results

For the 5-year-old AFO, thickness ranged from $3.023\pm 0.023\text{mm}$ to $3.792\pm 0.536\text{mm}$, whilst percentage measurement error increased from 0.78% to 26.39%. Meanwhile, for the 10-year-old AFO, AFO thickness ranged from $3.026\pm 0.026\text{mm}$ to $3.876\pm 0.555\text{mm}$, whilst percentage measurement error increased from 0.86% to 29.19%. Finally, for the 15-year-old AFO, AFO thickness ranged from $3.029\pm 0.026\text{mm}$ to $3.937\pm 0.574\text{mm}$, whilst percentage measurement error increased from 0.96% to 31.25%.

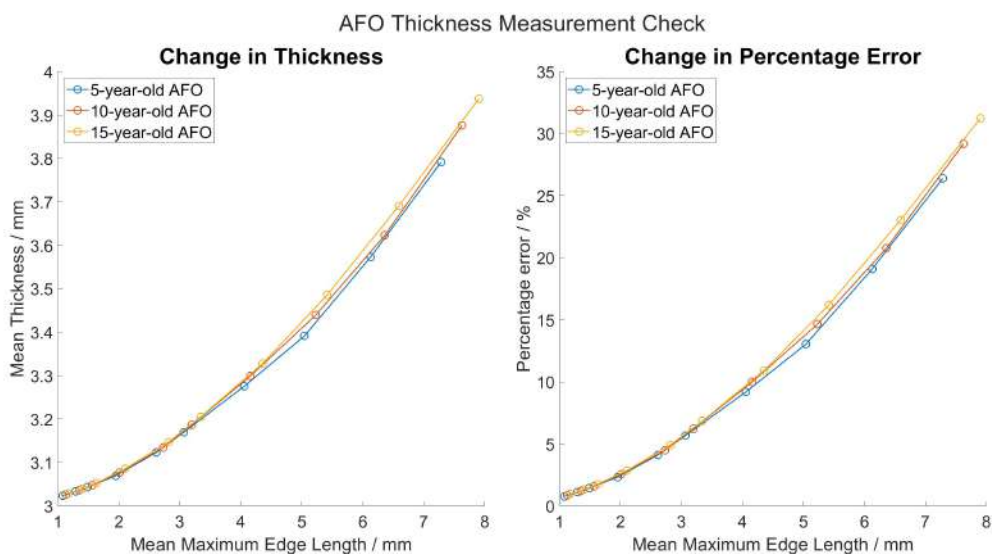


Figure D.1: Change in AFO thickness and percentage measurement error with STL element size.

D.4 Discussion

AFO thickness and percentage measurement error increased exponentially with the maximum edge length of the elements in the STL mesh (Figure D.1). This is due to two

reasons. Firstly, STL meshes are made up of 2-dimensional tetrahedral elements. Therefore, they cannot conform to the curvature of the AFO, which means as the element size increases, the AFO will be thickened. Secondly, as the element size increases, the number of nodes decrease. Therefore, the distance between nodes on the inner and outer surface may be extended as the nodes on each mesh are not normal to each other. Additionally, AFO size did not affect the accuracy of the measurement technique, demonstrated by the fact the curves for all three sizes followed the same trajectory. Although there were slight differences between the three AFOs, these were due to the fact that the maximum edge length at each mesh density increased with AFO size.

Previously, digital calipers have been used to measure the thickness of AFOs[193]. When measuring objects with flat surfaces, digital calipers generally have an accuracy of $\pm 0.02\text{mm}$. However, given their curved morphology, this will likely increase when measuring AFO thickness as it is difficult to place the teeth of the calipers flush to the surface. Alternatively, the accuracy of micrometers is an order of ten higher. However, these can be expensive, especially if purchasing micrometers with rounded ends to overcome the issue with digital calipers. Furthermore, both restrict measurements of AFO thickness to the trim line edge. The absolute error of the proposed technique was comparable to the accuracy of a digital micrometer at the lowest mesh density, whilst assessing the thickness of the whole AFO. As a result, is a valid technique for measuring AFO thickness, when the maximum edge length of $\approx 1\text{mm}$.

D.5 Conclusion

The new technique for measuring AFO had comparable accuracy to digital calipers when the maximum edge length of the STL is $\approx 1\text{mm}$. Therefore, it is a valid method for measuring AFO thickness.

Appendix E

Test rig Visual 3D marker model

No.	Marker	No.	Marker
1	WirePulley	14	ShankMed3
2	WireAFO	15	ShankMed4
3	RigEyeBolt	16	ShankPost1
4	RigTopR	17	ShankPost2
5	RigTopL	18	ShankPost3
6	RigPivotR	19	ShankPost4
7	RigPivotL	20	MalLat
8	ShankLat1	21	MalMed
9	ShankLat2	22	MalPost
10	ShankLat3	23	Heellat
11	ShankLat4	24	HeelMed
12	ShankMed1	25	Heel
13	ShankMed2	26	Toe

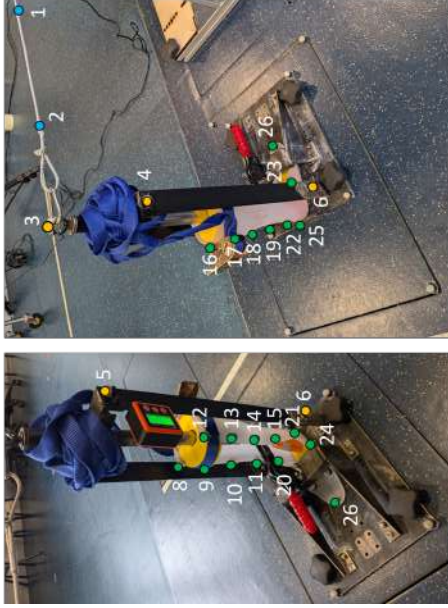


Figure E.1: Marker array used to model the test rig. Green = AFO. Yellow = Test Rig. Blue = Steel Cable.

Table E.1: Test Rig Visual 3D marker model

Segment	Origin	X-Axis	Y-Axis	Z-Axis	Tracking Markers
AFO Shank	Mid-point of MedShank1 & LatShank1	Origin → LatShank1	Cross-product of X & Z-Axis	Mid-point of MedMal → Mid-point of MedShank1 & LatShank1	All MedShank, LatShank & PostShank markers
AFO Foot	Mid-point of MedMal & LatMal	Origin → LatMal	Origin → Toe (radius = 0.1m)	Cross-product of X & Y-Axis	Heel, Toe, LatMal, MedMal, LatHeel & MedHeel
Rig Frame	RigEyeBolt (radius = 0.01m)	Origin → RigPivotL	Cross-product of X & z-Axis	Mid-point of RigPivotR & RigPivotL → origin	RigTopR & RigTopL
Wire Cable	WirePulley (radius = 0.1m)	Origin → LatShank1	RigEyeBolt → WirePulley	Cross-product of X & Y-Axis	Calibration markers

Appendix F

Polypropylene Material Testing

F.1 Introduction

To develop a valid FE, it is recommended that the inputted material properties are determined experimentally. In this case, PPC and PPH were modelled as isotropic elastic materials, deemed suitable as the model will only simulate static testing across one cycle. Under these conditions, the viscoelastic properties exhibited by these materials is negligible and therefore isotropic properties can be assumed. As a result, tensile testing of both PPC and PPH was conducted to determine elastic modulus and yield stress, according to ISO standards 527-1:2019, 527-2:2012 and 2818:2018.

F.2 Methodology

F.2.1 Experimental Procedure

Using a CNC router (AXYZ, UK), three tests specimens were then milled from 6x 2100x 1220mm, natural PPC and PPH sheets (Algeos, UK), according to the dimensions of the 1B specimen type, ISO527-2:2019 (Figure F.1a). As the materials are assumed to be isotropic, specimens were cut in the longitudinal direction only. Following milling, the surface of the specimens was checked for damage and faults, which may cause notch effects, and any burrs formed during milling were removed and edges finished with abrasive paper (grain size 220). After, gauge and gripping length were marked on the surface of the specimens using a permanent marker, 50mm and 115mm about the centre point respectively (Figure F.1b). Finally, specimens were conditioned at $23^{\circ}\text{C} \pm 2^{\circ}\text{C}$ and 50% relative humidity, for 16hrs, prior to testing.

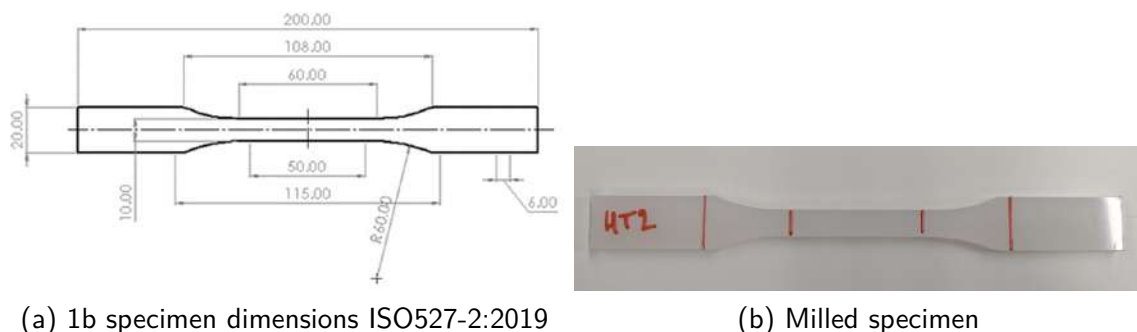
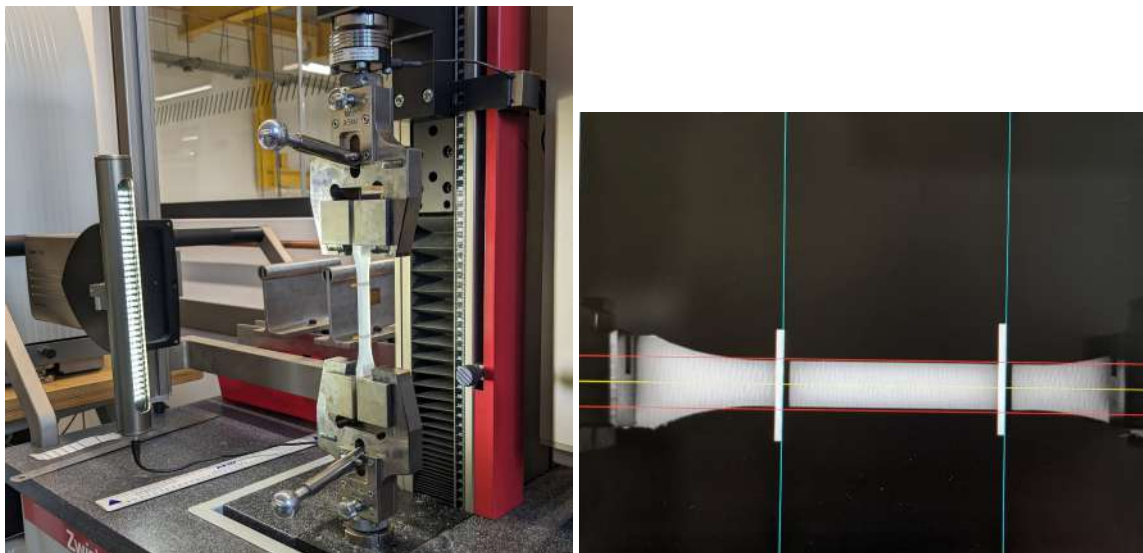


Figure F.1: Dog Bone specimens used to determine the tensile properties of polypropylene

The tensile material properties of the specimens were measured using a tensile tester

(ZwickRoell, 2.5kN, Germany). The in-built load cells (Xforce, ZwickRoell, Germany) measured stress whilst a VideoXtens optical extensometer (ZwickRoell, Germany) measured the longitudinal strain. Before loading the specimens, their width, and thickness were measured using digital callipers. Measurements were taken at three locations along the gauge length and inputted into the TestXpert workspace. Specimens were then loaded into the tensile tester so that the longitudinal axis aligned with the direction of extension through the centre line of the grips, whilst maintaining a gripping length of 115mm and ensuring no slippage (Figure F.2a). The optical extensometer was then calibrated to the gauge length before testing was carried out at $1\text{mm}/\text{min} \pm 0.2\text{mm}/\text{min}$ until failure (Figure F.2b).



(a) Test specimen loaded in tensile test machine. (b) Calibration of the optical extensometer to the gauge length of the specimen

Figure F.2: Tensile tester set-up

F.2.2 Data Analysis

The calculated yield stress longitudinal stress and strain data were exported to MATLAB (Version, MathWorks, USA) from all the specimens. The elastic modulus for each specimen was then calculated as the gradient of the linear region of the resultant stress-strain curve. Finally, the mean elastic modulus and yield stress were taken across the three repeats.

F.2.3 Results

The stress-strain curves for the two materials are presented in Figure F.3. The mean elastic modulus and yield stress are presented in Table F.1.

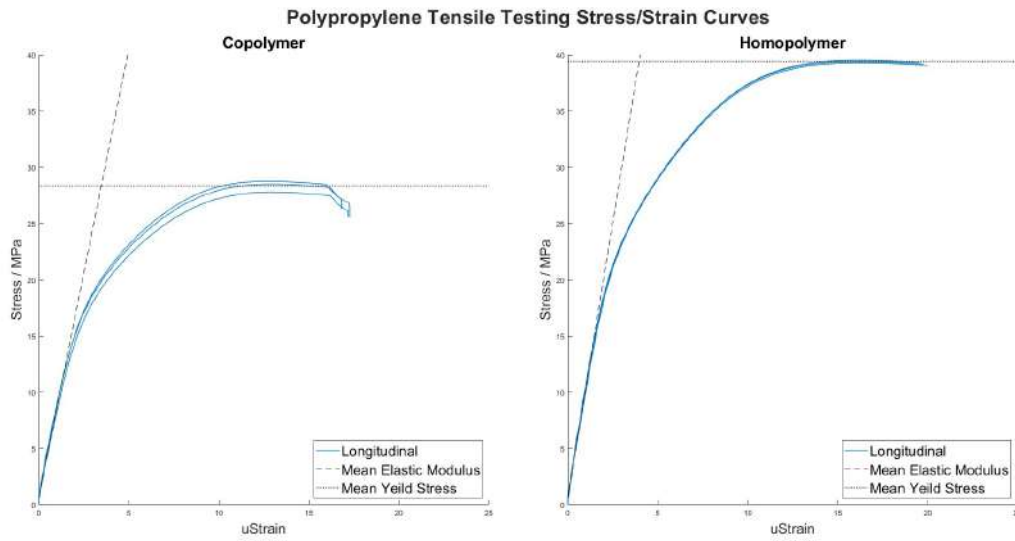


Figure F.3: Stress-Strain curves for copolymer and homopolymer polypropylene

Table F.1: Polypropylene tensile material properties

Material	Elastic Modulus / MPa	Yield Stress / MPa
Copolymer	796.96	28.33
Homopolymer	979.46	39.40

Appendix G

Variation in manufactured AFO Thickness

G.1 5-year-old, 3mm, PPC AFO

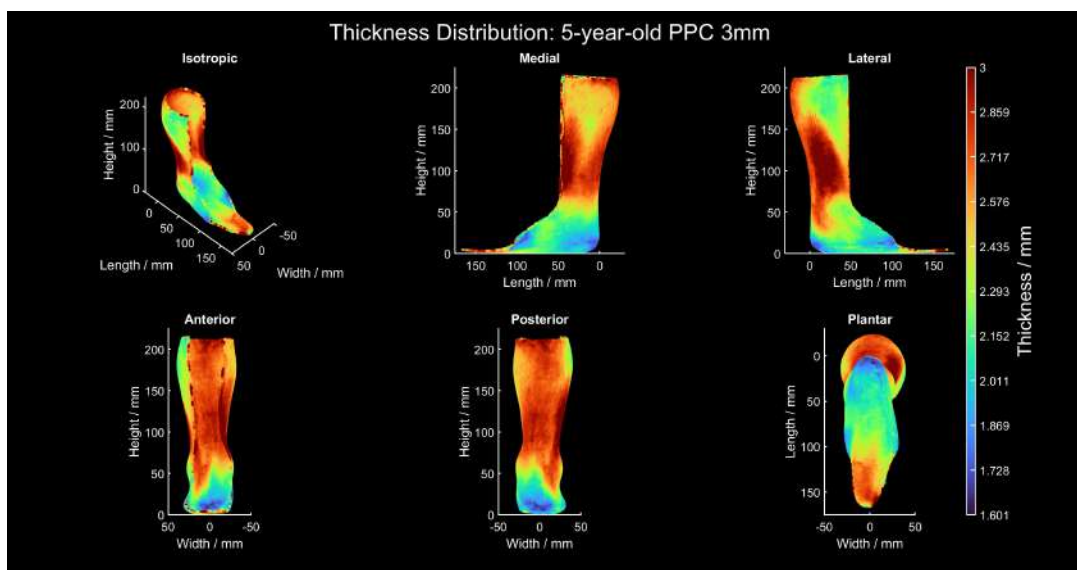


Figure G.1: Variation in thickness of the 5-year-old, 3mm, PPC AFO manufactured for the rig repeatability and FE validity studies.

G.2 5-year-old, 3mm, PPH AFO

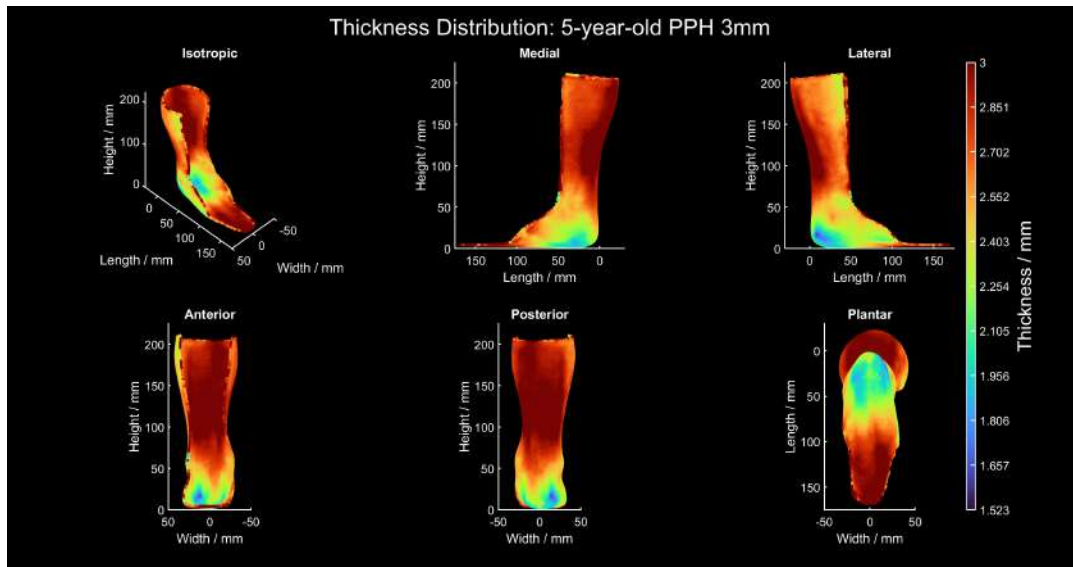


Figure G.2: Variation in thickness of the 5-year-old, 3mm, PPH AFO manufactured for the rig repeatability and FE validity studies.

G.3 10-year-old, 4.5mm, PPC AFO

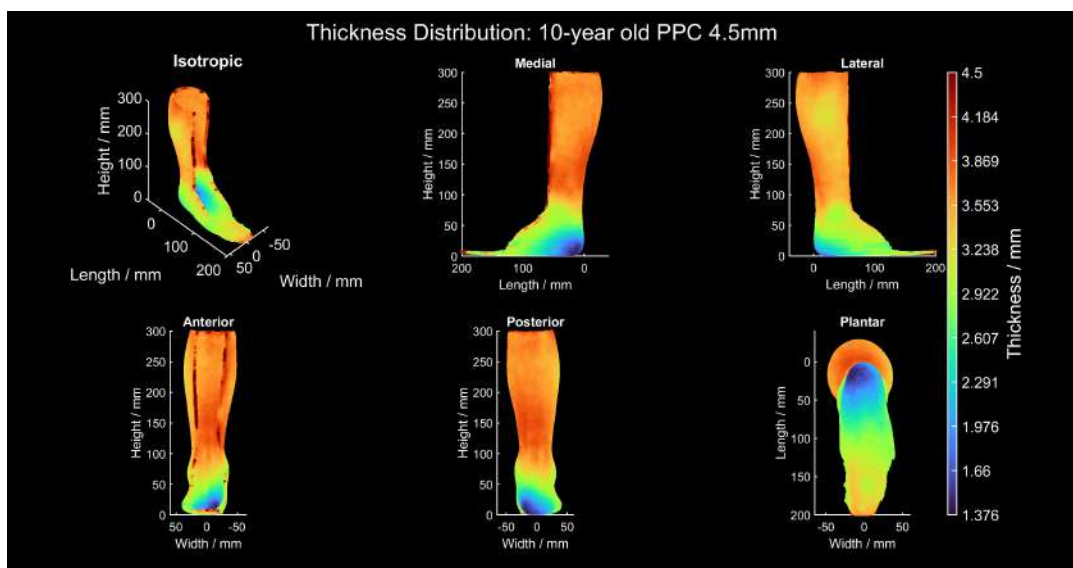


Figure G.3: Variation in thickness of the 10-year-old, 4.5mm, PPC AFO manufactured for the rig repeatability and FE validity studies.

G.4 10-year-old, 5mm, PPH AFO

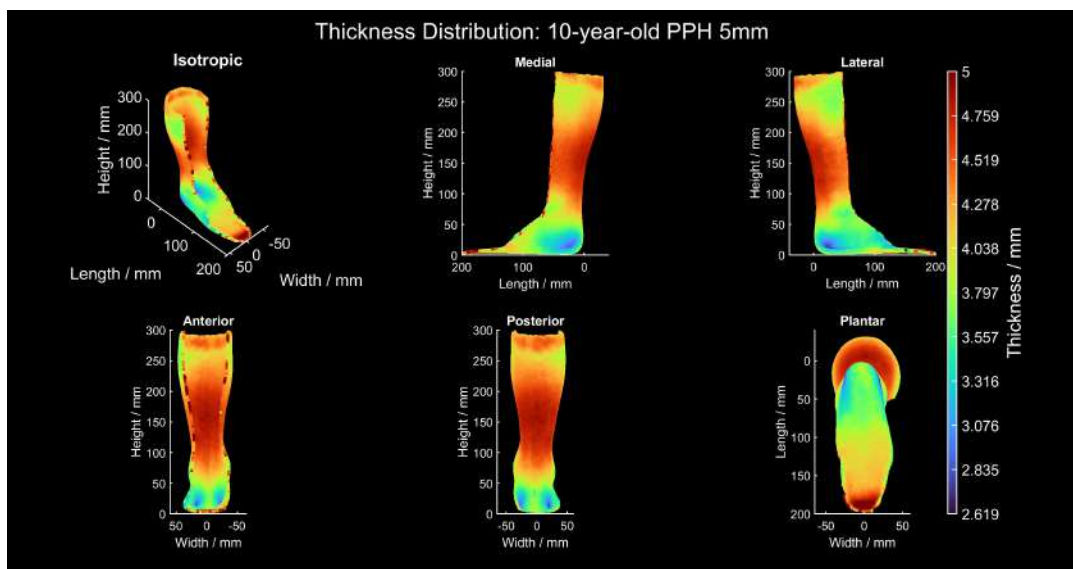


Figure G.4: Variation in thickness of the 10-year-old, 5mm, PPh AFO manufactured for the rig repeatability and FE validity studies.

G.5 15-year-old, 4.5mm, PPC AFO

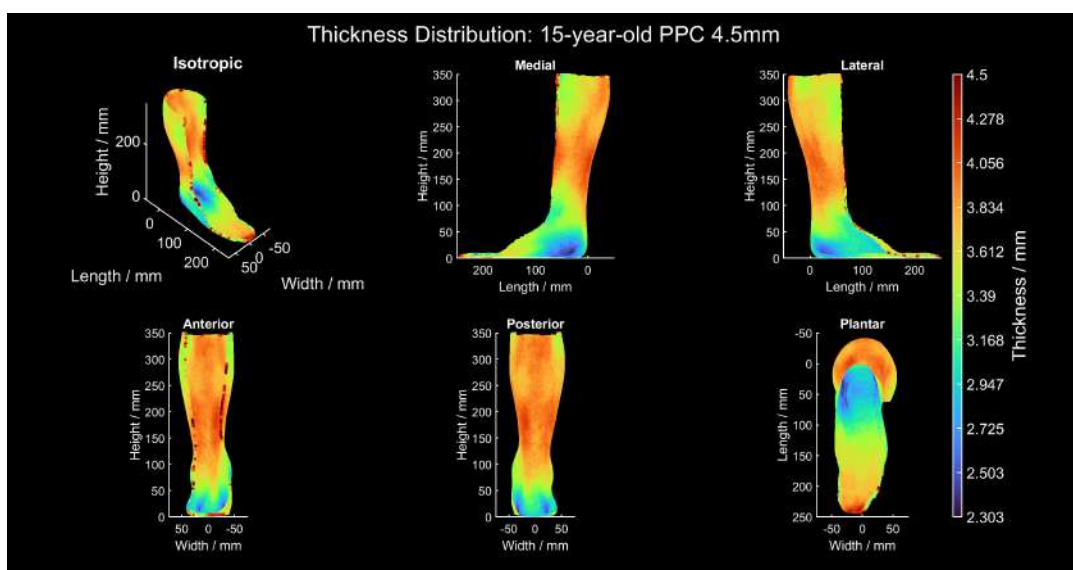


Figure G.5: Variation in thickness of the 15-year-old, 4.5mm, PPC AFO manufactured for the rig repeatability and FE validity studies.

G.6 5-year-old, 3mm, PPC AFO

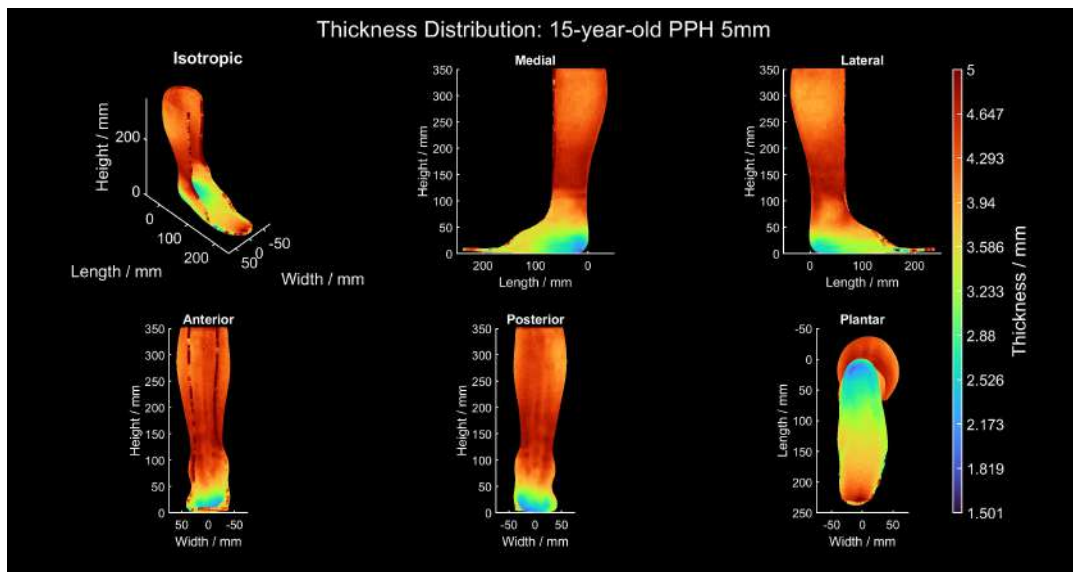


Figure G.6: Variation in thickness of the 15-year-old, 5mm, PPH AFO manufactured for the rig repeatability and FE validity studies.

Appendix H

Comparison of 15-year-old PPC 4.5mm thickness measured across repeat scans

Table H.1: Mean thickness of the 15-year-old 4.5mm PPC AFO

Scan no.	Material Thickness / mm	Mean AFO thickness / mm	$\Delta\%$ in thickness
Scan 1	4.5	3.577	-21.92
Scan 2	4.5	3.5297	-21.56

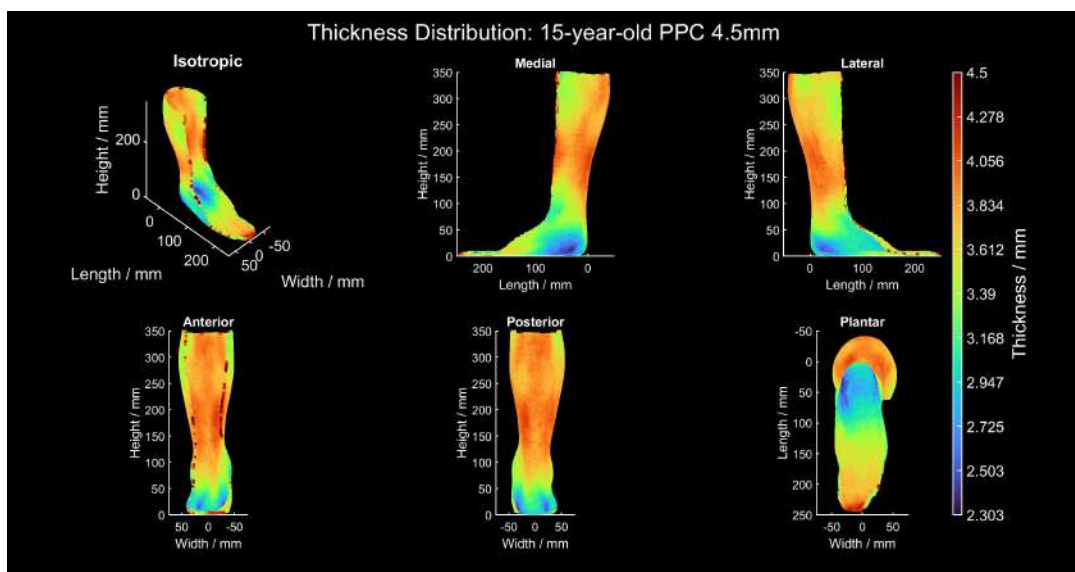


Figure H.1: Scan 1: Variation in thickness of the 15-year-old, 4.5mm, PPC AFO

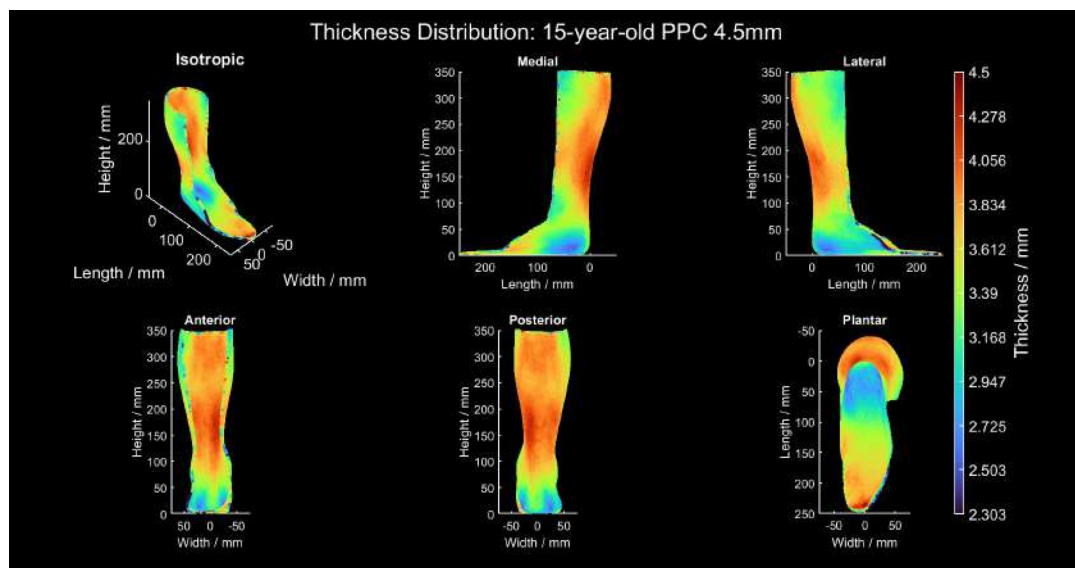


Figure H.2: Scan 2: Variation in thickness of the 15-year-old, 4.5mm, PPC AFO

Appendix I

The effects of ribbing placement on the mechanical properties of rigid AFOs

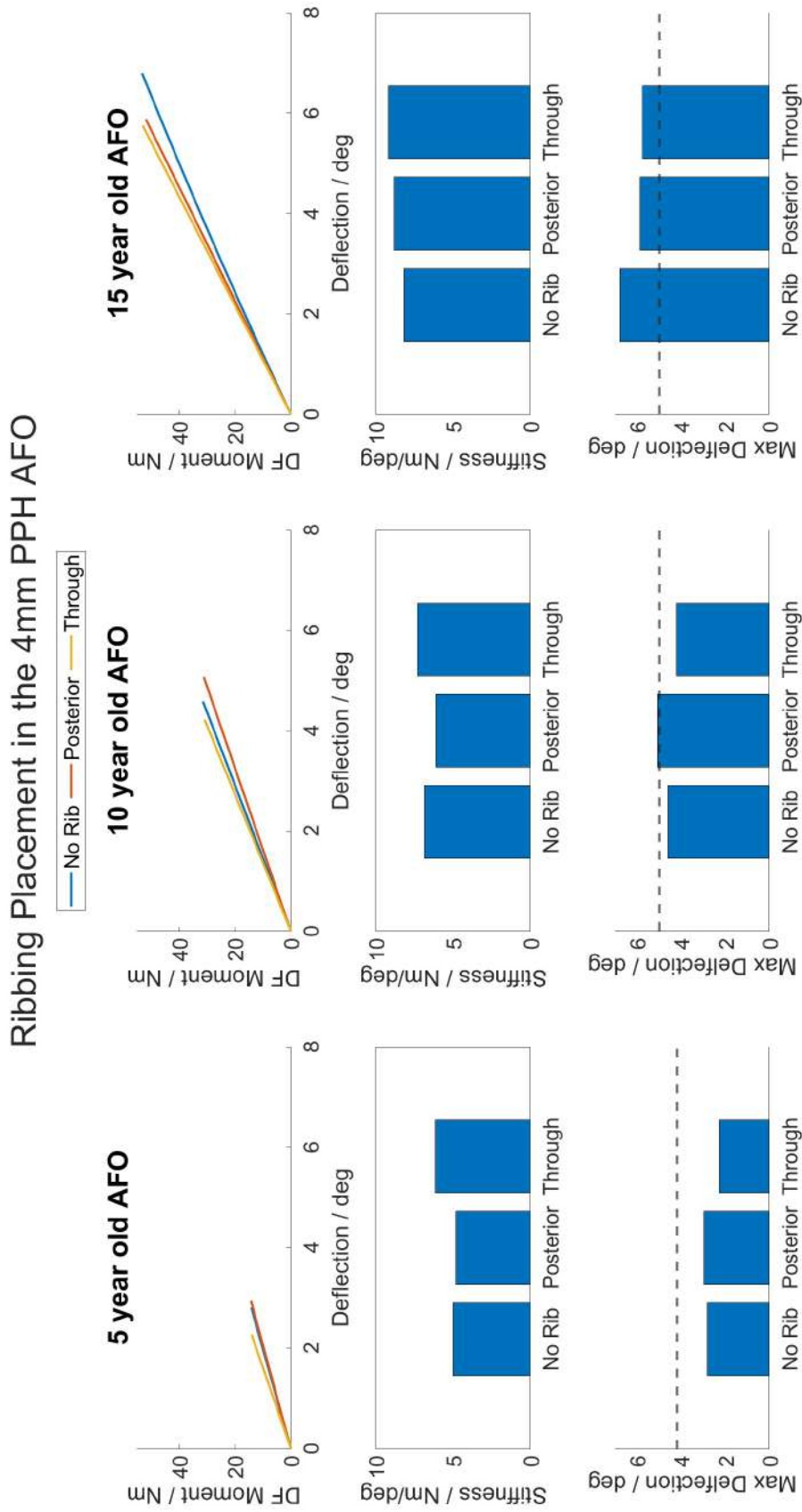


Figure I.1: Comparison of 4mm PPH AFO mechanical properties between ribbing placement.

Appendix J

Calculation of AFO thinning during the vacuum-forming process

Data from Convery et al., 2004, Prosthetics and Orthotics International, 28, 175-182

3 centres manufacture, 8, 3mm paediatric rigid AFOs from the same mould

		Thickness / mm			Reduction / mm					
		Site A	Site B	Site C	Site A	Site B	Site C	Av. Reduction	STDEV	% reduction
PPC	Sole	2.27	2.37	2.04	0.74	0.64	0.97	0.78	0.14	26.11%
	MedMal	2.35	2.38	2.11	0.66	0.63	0.9	0.73	0.12	24.33%
	LatMal	2.43	2.29	2.32	0.58	0.72	0.69	0.66	0.06	22.11%
	ProxCalf	2.82	2.73	2.63	0.19	0.28	0.38	0.28	0.08	9.44%
PPH	Sole	2.37	2.3	2.14	0.61	0.68	0.84	0.71	0.10	23.67%
	MedMal	2.32	2.29	2.24	0.66	0.69	0.74	0.70	0.03	23.22%
	LatMal	2.39	2.27	2.36	0.59	0.71	0.62	0.64	0.05	21.33%
	ProxCalf	2.79	2.73	2.65	0.19	0.25	0.33	0.26	0.06	8.56%

Average reduction for the 3mm PPC AFOs = 20.50%

Average reduction for the 3mm PPH AFOs = 19.19%

Data from Convery et al., 2004, Prosthetics and Orthotics International, 28, 175-182

3, 3mm rigid AFOs made from the same mould

		Thickness / mm			Reduction / mm					
		AFO 1	AFO 2	AFO 3	AFO 1	AFO 2	AFO 3	Mean	STDEV	% reduction
Proximal Calf (25cm from top)	A	2.92	2.82	2.84	0.28	0.38	0.36	0.340	0.043	10.63%
Medial Malleolus	B	2.79	2.57	2.74	0.41	0.63	0.46	0.500	0.094	15.63%
	C	2.49	2.36	2.54	0.71	0.84	0.66	0.737	0.076	23.02%
	D	2.49	2.31	2.39	0.71	0.89	0.81	0.803	0.074	25.10%
	E	2.29	2.31	2.34	0.91	0.89	0.86	0.887	0.021	27.71%
LatMal Lateral Malleolus	F	2.92	2.59	2.67	0.28	0.61	0.53	0.473	0.141	14.79%
	G	2.79	2.31	2.59	0.41	0.89	0.61	0.637	0.197	19.90%
	H	2.67	2.34	2.46	0.53	0.86	0.74	0.710	0.136	22.19%
	I	2.57	2.29	2.41	0.63	0.91	0.79	0.777	0.115	24.27%
Sole (35mm from end)	J	2.57	2.44	2.54	0.63	0.76	0.66	0.683	0.056	21.35%

Average reduction for the 3mm PPC AFOs = 20.46%